



저작자표시-비영리-변경금지 2.0 대한민국

이용자는 아래의 조건을 따르는 경우에 한하여 자유롭게

- 이 저작물을 복제, 배포, 전송, 전시, 공연 및 방송할 수 있습니다.

다음과 같은 조건을 따라야 합니다:



저작자표시. 귀하는 원저작자를 표시하여야 합니다.



비영리. 귀하는 이 저작물을 영리 목적으로 이용할 수 없습니다.



변경금지. 귀하는 이 저작물을 개작, 변형 또는 가공할 수 없습니다.

- 귀하는, 이 저작물의 재이용이나 배포의 경우, 이 저작물에 적용된 이용허락조건을 명확하게 나타내어야 합니다.
- 저작권자로부터 별도의 허가를 받으면 이러한 조건들은 적용되지 않습니다.

저작권법에 따른 이용자의 권리는 위의 내용에 의하여 영향을 받지 않습니다.

이것은 [이용허락규약\(Legal Code\)](#)을 이해하기 쉽게 요약한 것입니다.

[Disclaimer](#)

이학박사학위논문

옥신 신호전달 과정의  
새로운 전사조절 메커니즘 규명

**Characterization of novel transcription-regulatory  
mechanisms in auxin signaling processes**

2018년 8월

서울대학교 대학원

생명과학부

최희승

## **Abstract**

# **Characterization of novel transcription-regulatory mechanisms in auxin signaling processes**

**Hee-Seung Choi**

**School of Biological Sciences**

**The Graduate School**

**Seoul National University**

Plants make use of hormones as signaling molecules for development and adaptation to the environment. Auxin is one of key hormones, and its signaling pathway finalizes into transcriptional changes of auxin-responsive genes. The auxin signaling pathway consists of a single step. Auxin causes the degradation of transcription repressors by gluing them to the F-box protein of a SCF-complex, resulting in transcriptional activation of auxin-responsive genes. In contrast to this simple signaling process, auxin is implicated in a vast spectrum of plant developmental and responsive processes. This suggests that much more diversified signaling mechanism underlie various auxin-mediated developmental processes.

Each auxin signaling component exists in multiple variant forms. This study aims to demonstrate that the molecular variants of auxin-signaling components harness the diversification and fine-tuning of auxin responses in the transcription level.

In this study, the *Arabidopsis* (*Arabidopsis thaliana*) root hair single cell system was adopted as a primary biological assay system to assess auxin-signaling activity. Because the root hair is a protrusion from the root epidermal cell and its growth is proportional to internal auxin concentration or signaling activity, it provides a cell-autonomous system for the auxin signaling pathway. In addition, the root hair is easy to observe and to estimate its phenotype as a one-dimensional parameter.

Auxin/Indole-Acetic Acids (Aux/IAAs) are major transcription repressors in auxin signaling which recruit TOPLESS (TPL)/TPL-Related (TPR) co-repressors to the Auxin Response Factor (ARF) transcription factor on a target auxin-responsive gene. However, gain-of-function and stabilized *aux/iaa* mutations, considered to constitutively repress auxin responses, sometimes unusually promote auxin responses. The first part of this study embarked on this enigmatic problem in auxin signaling. This study demonstrated that Aux/IAAs can be classified into two groups, one with higher and the other with lower affinity to TPL/TPRs, and that a dose change of low affinity Aux/IAAs can result in a transient repressor-to-activator activity switch most likely by altering the TPL/TPR density in the target gene. This study suggests a novel transcription-regulatory model demonstrating the dose-dependent activity switch of a transcription repressor. It is conceivable that

the dose-dependent behavior of Aux/IAAs may contribute to fine-tuning of auxin-responsive transcription and responses.

ARFs are DNA-binding transcription factors for auxin-responsive genes and divided into two subgroups, activators (aARFs) and repressors (rARFs). While aARFs fit well the known auxin signaling pathway, the action mechanism of rARFs has been poorly understood. In the second part of this study, I investigated the molecular and biological roles of putative TPL/TPR-interacting motifs in a rARF (ARF2). The results showed that these putative TPL/TPR-interacting motifs of ARF2 are required for its interaction with TPL/TPRs and ARF2-mediated repressive functions in auxin responses.

Although auxin has long been implicated in root hair growth, the underlying molecular mechanism has remained to be elucidated. The third part addresses how aARFs directly and cooperatively work on the key master transcription factor for root hair growth. A previous study in my laboratory identified ROOT HAIR DEFECTIVE SIX-LIKE 4 (RSL4) as the master transcription factor that directly regulates root hair-specific genes required for root hair growth and morphogenesis. Here, I demonstrated that aARFs enhance root hair growth by directly binding to the auxin-response elements (AREs) on the regulatory region of *RSL4* and cooperatively working with RHD6, another *RSL4*-regulating transcription factor from the developmental pathway.

The root hair has been used as a useful model system for cell fate determination, morphogenesis, tip growth, and nutrient acquisition. However, the

ecological or physical role of root hairs so far has not been studied. To assess the role of root hairs in holding water and soil and thus in seedling survival, I examined the relationship between root hair length, root's holding capacity for water and soil, and the survival rate of *Arabidopsis* seedlings. Root's water and soil holding capacity and seedling survival rates showed a positive correlation with the root hair length, indicating that root hairs contribute for soil holding and hydrated conditions around the root and for sustaining seedlings' life upon sudden soil disruption.

In summary, my thesis study addresses the novel transcription-regulatory mechanism by the repressors (dose-dependent transcriptional switch) in auxin signaling, the functional analysis of uncharacterized auxin-signaling components (rARFs), the molecular mechanism of auxin in root hair growth, and the ecological role of root hairs. This study would help to expand our scope in gene transcription regulation not simply in auxin signaling but also in general gene regulation researches and opening a new scope into the role of root hairs in physical environments around the plant.

**Keywords:** *Arabidopsis thaliana*, Auxin, Auxin/Indole-Acetic Acid (Aux/IAA), Auxin Response Factor (ARF), Auxin signaling, Protein interaction, Root hair, Transcriptional regulation, Transcription factor

**Student Number:** 2010-23127

# Contents

Abstract .....	i
Table of contents .....	
v	
List of figures .....	xiii
List of tables .....	
xxi	
Abbreviations .....	xxiii
<b>Chapter I. General introduction</b> .....	
1	
1.1 Transcriptional regulation in plant development and response to environment .....	
2	
1.2 Various function of auxin in plant development .....	
4	
1.3 Multiple homologs of auxin signaling components.....	5
1.3.1 DNA-binding transcription factors; ARFs .....	
6	

1.3.2	Auxin co-receptor proteins; TIR1/AFBs .....	8
1.3.3	Another co-receptors, Aux/IAs that function as major repressors in auxin signaling .....	9
1.3.4	Co-repressor, TPL/TPRs .....	10
1.4	Questions in the present auxin signaling model .....	11
1.4.1	Different phenotypes of mutants from the same clade of auxin- signaling factors .....	12
1.4.2	The uncharacterized mechanism of repressor ARFs .....	15
1.4.3	Target gene-selecting mechanism of activator ARFs .....	17
1.5	The root hair system as a model to study auxin-signaling pathway .....	19

<b>Chapter II. Dose-dependent transcriptional activation by competition between Aux/IAA homologs .....</b>	<b>21</b>
--	-----------

2.1	Abstract .....	22
2.2	Introduction .....	22
2.3	Materials and methods .....	25
2.3.1	Accession numbers .....	25
2.3.2	Plant materials and growth conditions .....	26
2.3.3	Observation of root hairs .....	26
2.3.4	RNA isolation and quantitative reverse transcriptase (qRT)-PCR analysis .....	27
2.3.5	Observation of reporter gene expression and evaluation of promoter activity .....	27
2.3.6	Transgene constructs .....	28
2.3.7	Protein lysate preparation and immunoblots .....	30
2.3.8	<i>In vitro</i> pull-down assay and analysis protein signal intensity .....	31

2.3.9	Microscale thermophoresis .....	32
2.3.10	RNA sequencing .....	33
2.3.11	Model of the TPL-Aux/IAA interaction .....	34
2.4	Results .....	39
2.4.1	Opposite root hair phenotypes between gain-of-function <i>aux/iaa</i> mutants .....	39
2.4.2	A similar phenotypes in root hair-specific expressed <i>aux/iaas</i> GOF transformants .....	39
2.4.3	The difference in promoter activities of <i>ProE7</i> , <i>ProSHY2</i> , and <i>ProAXR2</i> .....	41
2.4.4	Native SHY2 has a positive effect of root hair growth .....	46
2.4.5	Transcriptional activity of SHY2 depends on its dose in a cell .....	46
2.4.6	Introducing a DEX-inducible system to reduce variations between transgenic lines .....	56
2.4.7	RNA sequencing results of <i>shy2-1:GFP:GR</i> lines in different DEX	

concentrations .....	
65	
2.4.8 axr2-1 does not act in a dose-dependent manner .....	
66	
2.4.9 Analysis of domain I of Aux/IAs .....	
68	
2.4.10 The roles of domain I and PB1 domain in Aux/IAs .....	
72	
2.4.11 AXR2 has a stronger affinity with TPL than SHY2 in pull-down assay .....	
79	
2.4.12 CG-motif Aux/IAs have stronger affinity with TPL than RG- motif Aux/IAs in MST .....	
79	
2.4.13 Modeling the differential affinity between TPL-Aux/IAs .....	
81	
2.5 Discussion .....	87

<b>Chapter III. Transcriptional repression mechanism of repressor ARFs in auxin signaling .....</b>	
<b>93</b>	

3.1	Abstract .....	94
3.2	Introduction .....	95
3.3	Materials and methods .....	100
3.3.1	Accession numbers .....	100
3.3.2	Plant materials and growth conditions .....	100
3.3.3	Construction of transgenes .....	101
3.3.4	Observation of biological parameters .....	102
3.3.5	RNA isolation and quantitative reverse transcriptase(qRT)-PCR analysis .....	103
3.3.6	Yeast two-hybrid assays .....	103
3.3.7	<i>In vitro</i> pull-down assay .....	104
3.4	Results I .....	108
3.4.1	In the root hair system, rARFs facilitate repression activity, and	

specifically overexpressed rARF results in short root hair phenotypes .....	108
3.4.2 ARF2 has two putative TPL/TPR binding motifs in the middle domain. ....	108
3.4.3 The repressive function of ARF2 in root hair growth .....	110
3.4.4 Mutations of the putative TPL/TPR-binding motifs suppress ARF2-mediated inhibition of root hair growth and <i>RSL4</i> expression. ....	111
3.4.5 Both EAR and RLFGI motifs are necessary for ARF2 to interact with TPL .....	114
3.4.6 The repressive motifs of ARF2 are required for the native function of ARF2 .....	119
3.5 Results II .....	128
3.5.1 Auxin does not enhance the rARF activity in root hair growth ....	128
3.5.2 The function of PB1 domain in ARF9 .....	128

3.5.3	The phyllotaxis defect in <i>arf9-1</i> loss-of-function mutants .....	133
3.6	Discussion .....	137
<b>Chapter IV. Transcriptional regulation of <i>RSL4</i> through cooperation between <i>RHD6</i> and <i>aARF</i> .....</b>		
<b>141</b>		
4.1	Abstract .....	142
4.2	Introduction .....	143
4.3	Materials and methods .....	146
4.3.1	Accession numbers .....	147
4.3.2	Plant materials and growth conditions .....	147
4.3.3	Construction of transgenes .....	148
4.3.4	Observation of biological parameters .....	149
4.3.5	Observation of reporter gene expression and evaluation of promoter activity .....	149

4.3.6 RNA isolation and quantitative reverse transcriptase (qRT)-PCR analysis .....	150
4.3.7 Preparation of fusion proteins and EMSA .....	150
4.3.8 ChIP and qPCR analysis .....	151
4.3.9 GUS histochemical analysis .....	153
4.4 Results .....	155
4.4.1 The relationship between root hair growth and <i>RSL4</i> expression	155
4.4.2 Root hair specifically overexpressed <i>aARFs</i> promote root hair growth by activating <i>RSL4</i> expression .....	155
4.4.3 Overexpressed <i>aARFs</i> in <i>rhb6-3</i> mutant could not restore root hair growth .....	158
4.4.4 Overexpressed <i>RHD6</i> in the auxin-defect mutant ( <i>axr2-1</i> GOF) recovered root hair growth .....	166

4.4.5	Key cis-elements in the <i>RSL4</i> promoter .....	166
4.4.6	RSL1,RSL4, and RHD6 bind to RHE in the <i>RSL4</i> promoter .....	176
4.4.7	RHD6 is required for aARF's binding to ARE .....	179
4.4.8	RHD6 affects the chromatin status of proximal region of the <i>RSL4</i> promoter .....	184
4.5	Discussion .....	188
<b>Conclusion of chapter I ~ IV .....</b>		<b>194</b>
<b>Chapter V. Ecological role of root hairs .....</b>		<b>199</b>
5.1	Abstract .....	199
5.2	Introduction .....	199
5.3	Materials and methods .....	200
5.3.1	Accession numbers .....	200
5.3.2	Plant materials and growth conditions .....	

201	
5.3.3 Observation of biological parameters .....	
201	
5.3.4 Measurements of root dehydration and soil holding .....	
201	
5.4 Results and discussion .....	
203	
Reference .....	
210	
초 록 .....	224
감사의 글 .....	228

# List of figures

## Chapter I

- Figure 1.** The auxin signaling pathway in the nucleus. .... 7
- Figure 2.** A phylogenetic tree showing auxin signaling components sequences in Arabidopsis. .... 13

## Chapter II

- Figure 3.** SHY2 positively but AXR2 and AXR3 negatively regulate root hair growth. .... 40
- Figure 4.** Root hair lengths of the independent transgenic lines including *ProE7:SHY2* or *ProE7:shy2-1* in WT or *shy2-1* background. .... 42
- Figure 5.** SHY2 positively and AXR2 and AXR3 negatively regulate root hair growth. .... 45
- Figure 6.** SHY2 positively regulates root hair growth. .... 47
- Figure 7.** Both root hair length and the *SHY2* transcript level in root hair-specific *SHY2-RNAi* lines showed a repressed aspect compared to wild-type plants or *shy2-1* mutants. .... 49

<b>Figure 8.</b> <i>shy2-1</i> expression levels inversely correlate with root hair growth, in contrast to <i>axr2-1</i> and <i>axr3-1</i> . .....	51
<b>Figure 9.</b> <i>shy2-1</i> expression levels inversely correlate with the expression of root hair-related and auxin-responsive genes. ....	53
<b>Figure 10.</b> <i>shy2-1</i> shows a dose-dependent activation/repression switch for root hair growth and auxin-responsive gene expression. ....	57
<b>Figure 11.</b> <i>axr2-1</i> shows a repression activity of root hair growth in a dose-independent manner. ....	67
<b>Figure 12.</b> The TPL-binding EAR motif is implicated in determining the activator or repressor property of an Aux/IAA. ....	69
<b>Figure 13.</b> The TPL-binding EAR motif is implicated in determining the activator or repressor property of an Aux/IAA. ....	74
<b>Figure 14.</b> The role of PB1 domain of Aux/IAAs in root hair growth. ....	75
<b>Figure 15.</b> A model illustrating role of each domain of Aux/IAA. ....	76
<b>Figure 16.</b> Malfunctioning Aux/IAAs enhance root hair growth because they take away the opportunity of other Aux/IAAs to bind to TPL. ....	78

<b>Figure 17.</b> Differential affinity of SHY2 and AXR2 to TPL. ....	81
<b>Figure 18.</b> Differential affinity of Aux/IAAs to TPL. ....	83
<b>Figure 19.</b> A model illustrating the SHY2 dose-dependent switch of transcriptional activity and root hair growth. ....	85
<b>Figure 20.</b> A simulated model of the RG-motif Aux/IAA-dependent decision by changeable TPL recruitment. ....	89

### Chapter III

<b>Figure 21.</b> Most repressor ARFs include putative co-repressor-binding motifs. ....	96
<b>Figure 22.</b> Sequences of putative repressive motifs of ARFs. ....	99
<b>Figure 23.</b> Repressor ARFs inhibit root hair growth. ....	109
<b>Figure 24.</b> Mutations of TPL-binding motifs suppress the ARF2-mediated inhibition of root hair growth. ....	112
<b>Figure 25.</b> Root hair length of mutant <i>ARF2</i> -overexpressing lines and <i>ARF2</i> expression. ....	115

<b>Figure 26.</b> Transcription levels of <i>ARF2</i> and root hair length in single transgenic lines. ....	116
<b>Figure 27.</b> EAR and RLFGV motifs are required for the interaction of ARF2 with TPL/TPRs in the yeast cell. ....	118
<b>Figure 28.</b> RT-PCR analysis of the <i>ARF2</i> transcript in two <i>arf2</i> mutant alleles. ....	120
<b>Figure 29.</b> The repressive motifs are required for the ARF2-mediated regulation of the flowering time. ....	122
<b>Figure 30.</b> The determination of seed size by ARF2 requires its TPL/TPR-binding motifs. ....	124
<b>Figure 31.</b> Root hair phenotypes of <i>arf2</i> loss-of-function mutants. ....	126
<b>Figure 32.</b> A model illustrating the repressor ARF sets the threshold in auxin signaling transcription. ....	127
<b>Figure 33.</b> Root hair length of ARF-overexpressing lines in different concentration auxin media. ....	129
<b>Figure 34.</b> Root hair length of overexpressing rARFs and PB1 domain-deleted	

rARFs. .... 131

**Figure 35.** Transcription levels of *ARF9* and root hair length in single transgenic lines. .... 132

**Figure 36.** Effect of PB1 domain in ARF9 binding to ARE. .... 134

**Figure 37.** *arf9* loss-of-function plant affects phyllotaxis change of vegetative leaves. .... 136

## Chapter IV

**Figure 38.** Relative root hair length and *RSL4* expression level of various lines that have short, normal, or long root hair phenotypes. .... 156

**Figure 39.** Root hair-specific overexpression of *ARFs* enhances root hair growth and the *RSL4* expression. .... 159

**Figure 40.** Overexpression of ARFs enhances root hair growth in wild-type background in estradiol inducible system. .... 162

**Figure 41.** Overexpression of ARFs could not enhance root hair growth in the *rhd6-3* mutant background. .... 163

**Figure 42.** Root hair images of *ARFs:GFP* in *rhd6* lines under auxin-treated

conditions. ....	164
<b>Figure 43.</b> Root hair images of <i>pMDC7-ARFs:GFP</i> in <i>rhd6</i> lines under estradiol- and auxin-treated conditions. ....	165
<b>Figure 44.</b> Root hair images of <i>pMDC7-RHD6:GFP</i> transgenic lines in <i>axr2-1</i> background. ....	167
<b>Figure 45.</b> Root hair lengths of <i>pMDC7-RHD6:GFP</i> under <i>axr2-1</i> transgenic lines. ....	168
<b>Figure 46.</b> Deletion analysis of the promoter region of <i>RSL4</i> for <i>RSL4</i> expression. ....	169
<b>Figure 47.</b> Different expression intensities from sequentially deleted <i>RSL4</i> promoters in Arabidopsis. ....	171
<b>Figure 48.</b> Relative activities of deleted <i>RSL4</i> promoters by comparing GFP expression. ....	172
<b>Figure 49.</b> Root hair length of <i>RSL4</i> complementation lines. ....	174
<b>Figure 50.</b> Analyses of <i>RSL4</i> promoter region. ....	175
<b>Figure 51.</b> Relative activities of deleted <i>RSL4</i> promoters by comparing GFP	

expression. ....	177
<b>Figure 52.</b> RSL1, RHD6, and RSL4 Bind to the RHE. ....	178
<b>Figure 53.</b> ChIP analysis of RSL4:GFP binding to the RHE on the <i>RSL4</i> promoter region in four-day-old seedling roots. ....	180
<b>Figure 54.</b> Analyses of auxin response to the <i>RSL4</i> promoter region. ....	182
<b>Figure 55.</b> Chromatin immuno-precipitation (ChIP) analysis showing ARF5- binding to auxin response elements (AREs) on the <i>RSL4</i> promoter region. ....	183
<b>Figure 56.</b> ChIP analysis at the <i>RSL4</i> promoter region showed that ARF5 binding to AREs is interrupted in <i>rhb6-3</i> mutant. ....	185
<b>Figure 57.</b> ChIP analysis showing the level of H3K27me3 in the <i>RSL4</i> promoter region. ....	187
<b>Figure 58.</b> A model illustrating the developmental factor affects aARF's binding to ARE on the target gene promoter. ....	189
<b>Figure 59.</b> Expression pattern of <i>ProARF5:GUS</i> . ....	193

## Conclusions of chapter I ~ IV

**Figure 60.** The auxin and developmental signaling pathway in root hair growth. .... 196

## **Chapter V**

**Figure 61.** Root phenotypes of transgenic lines. .... 204

**Figure 62.** Seedlings' water retention ability depends on root hair length. 206

**Figure 63.** Soil holding ability of seedlings depends on root hair length. .. 207

**Figure 64.** The survival ratio is high for hairy root lines. .... 208

# List of tables

## Chapter II

**Table 1.** Absolute mRNA expression value of Aux/IAs from hair 9 tissue was derived from *Arabidopsis* eFP

browser. .... 35

**Table 2.** The assumed population of each oligomer in a cell. ....

35

**Table 3.** The primer list. ....

37

**Table 4.** The list of overlapping SHY2-u genes with up-regulated genes by auxin. ....

58

**Table 5.** The list of overlapping SHY2-d genes with down-regulated genes by auxin. ....

61

**Table 6.** The list of overlapping SHY2-u genes with RHE-containing

genes. ....

62

**Table 7.** The list of overlapping SHY2-d genes with RHE-containing

genes. ....

64

### **Chapter III**

**Table 8.** The primer list. ....

106

### **Chapter IV**

**Table 9.** The primer list. ....

154

# Abbreviations

<b>aARF</b>	Activator ARF
<b>rARF</b>	Repressor ARF
<b>ARF</b>	AUXIN RESPONSE FACTOR
<b>Aux/IAA</b>	AUXIN/INDOLE-3-ACETIC ACID
<b>ARE</b>	Auxin-response element
<b>ChIP</b>	Chromatin immunoprecipitation
<b>Col-0</b>	Columbia ecotype of Arabidopsis
<b>DBD</b>	DNA-binding domain
<b>DEX</b>	Dexamethasone
<b>EMSA</b>	Electrophoresis mobility shift assay
<b>GFP</b>	Green fluorescent protein
<b>GOF</b>	Gain-of-function
<b>GR</b>	Glucocorticoid receptor
<b>GUS</b>	$\beta$ -glucuronidase
<b>H3K27me3</b>	Trimethylation on lysine of histone 3
<b>IAA</b>	Indole-3-acetic acid
<b>kDa</b>	Kilodalton
<b>Kd</b>	Dissociant constant
<b>Ler</b>	Landsberg <i>erecta</i> ecotype of Arabidopsis
<b>LOF</b>	Loss-of-function
<b>MD</b>	Middle region domain
<b>MST</b>	Microscale thermophoresis
<b>PB1</b>	Phox and Bem1p
<b>PIN</b>	PIN-FORMED
<b>ProE7</b>	<i>EXPANSIN A7</i> promoter

<b><i>ProZmE7</i></b>	<i>Zea mays</i> <i>EXPANSIN A7</i> promoter
<b>qRT-PCR</b>	Quantitative real-time polymerase chain reaction
<b>RHD6</b>	ROOT HAIR DEFECTIVE6
<b>RHE</b>	Root hair-specific cis-element
<b><i>RHS</i></b>	<i>ROOT HAIR SPECIFIC</i> genes
<b>RNAi</b>	RNA interference
<b>RSL4</b>	ROOT HAIR DEFECTIV SIX-LIKE4
<b>TIR1/AFB</b>	TRANSPORT INHIBITOR RESISTANT 1/AUXIN SIGNALING F-BOX.
<b>TPL</b>	TOPLESS
<b>TPR</b>	TPL-RELATED
<b>Y2H</b>	Yeast two-hybrid-assay

## **Chapter I.**

### **General introduction**

# **1.1 Transcriptional regulation in plant development and response to environment**

Plants grow where they have been found. Thus, they must adapt themselves to environmental conditions for survival. To grow and survive, plants need to change their body, developing new organs throughout their whole life cycle even during the postembryonic phase (reviewed in Kaufmann et al., 2010). In the sequential course of these changes, the primary events are signal transduction and transcriptional regulation.

Many endogenous and environmental signals and associated genetic programs regulate the plastic growth of plants. Hormone responses are fundamental in these processes of plant growth. Plants have seven major hormones: auxin, cytokinin, gibberellin, brassinosteroid, abscisic acid, jasmonate, and ethylene. Although there are cross-talk pathways with multiple hormones or environmental and developmental signaling, a single hormone can also cause significant changes in plant development (Chapman and Estelle, 2009; Gray, 2004; Nemhauser et al., 2006). In the past few decades, many approaches have been used to find the connection between gene expression and hormone responses. A high-sensitivity analysis of transcripts revealed that hormone-mediated gene expression is a major part of hormone responses (Nemhauser et al., 2006). Another study of mutants defected in hormone processes has also contributed to the understanding of hormone-related gene expression (Goda et al., 2008).

Transcription is the first step of changing genetic information into functional proteins. It generates mRNA from DNA as a template, and this is an important part of the central mechanism of molecular biology. Multicellular organisms express genes when the protein is required to respond to developmental or environmental cues. Numerous experiments have been conducted to determine what factors control transcription. They discovered a vast range of factors involved in transcription, such as the transcription factor (TF), chromatin remodeler, polymerase, chaperone, acetyltransferase, and methyltransferase.

However, recent researchers have focused on revealing the relationship between factors rather than finding individual new factors. Advanced techniques have led us to observe dynamics in transcriptional regulation (reviewed in Coulon et al., 2013). Researchers showed that transcriptional protein complexes assemble and disassemble from the target site of the chromatin within seconds through photo-bleaching experiments (McNally et al., 2000). Other groups discovered that nucleosomes are removed at promoter regions and reassembled using a histone source from *trans* in ranges from minutes to hours through high-resolution microarray experiments (Dion et al., 2007; Schermer et al., 2005). Additionally, big data from genomic and system biology studies have helped us understand the complexity of transcriptional regulation (reviewed in Gaudinier and Brady, 2016).

In this thesis, I will address the regulatory complexity of the dynamics of transcription factors to understand the role of hormone signaling in plant molecular biology.

## **1.2 Various functions of auxin in plant development**

The concept of plant hormones began from observations of the relationship between morphogenesis and development. Darwin started modern research into the phototropism of grass coleoptiles and postulated the existence of hormones (Darwin, 1880). Indole-3-acetic acid (IAA or auxin) was the first to be identified and is an essential hormone for plant growth. It is transported throughout the plant by the phloem (Cambridge and Morris, 1996) and cell-to-cell by specific auxin transporters (Bennett et al., 1996; Blakeslee et al., 2007; Cho et al., 2007b; Ganguly et al., 2012; Geisler et al., 2005; Petrasek et al., 2006). The dynamic and differential auxin distribution results in various developmental processes. Auxin is involved in almost every developmental process, including cell enlargement, cell division, vascular tissue differentiation, root initiation, apical dominance, leaf senescence, fruit abscission, fruit setting, assimilate partitioning, fruit ripening, flowering, the growth of flower parts, and femaleness in dioecious flowers (reviewed in Davies, 2010).

For decades, discovering the function of auxin was a remarkable achievement. Embryogenesis is a critical process for establishing the plant body and axis. In the course of embryonic patterning, every step is required for the redirection of the auxin flow and local accumulation of auxin. This results in asymmetric, anticlinal, or periclinal cell division for new organ formation (Friml et al., 2003). Plants establish body organization during not only embryogenesis, but also during the postembryonic developmental stages. The auxin distribution pattern

is also changed dramatically at the postembryonic stage by the polar-localized transporter. The polar localization of auxin transporters establish various organ primordia and develop them into mature organs (Benková et al., 2003; Reinhardt et al., 2000). Even organ regeneration depends on auxin maxima (Xu et al., 2006).

Many studies have shown that auxin contributes to the development of vascular tissues. Vascular tissue patterning is an elaborate and highly ordered organization, especially the veins in leaves. Vascular strand formation is stimulated by auxin (Sachs, 1981), and pre-procambial cells accumulate a high level of auxin (Mattsson et al., 2003). Auxin activates auxin-responsive genes in leaves for patterning leaf veins. Taken together, these results suggest that auxin is a positional signal that regulates vascular development (Wenzel et al., 2007).

Plants respond differentially in different tissues in terms of tropistic stimulation. For example, plants react to gravity positively and negatively. Roots bend down to the earth, whereas shoots bend away from the earth. Auxin is undoubtedly the major hormone in the gravitropic response. It is involved in asymmetric plant growth by regulating cell elongation (reviewed in Davies, 2010; Tanaka et al., 2006). In support of this, many mutants that have defected the auxin transporter or auxin response factors, have shown an abnormal phenotype in phototropism and gravitropism (Bennett et al., 1996; Friml et al., 2002; Luschnig et al., 1998; Okushima et al., 2005b).

## **1.3 Multiple homologs of auxin signaling components**

Auxin rapidly induces the expression of various genes at the molecular level (Abel and Theologis, 1996). To understand the mechanism of auxin action in plants, I aim to clarify the links between signal transduction and downstream effects as differential gene expression. In this chapter, I describe the molecular mechanism of auxin signaling. The nuclear receptor, TRANSPORT INHIBITOR RESPONSE1/AUXIN F-BOX (TIR1/AFB)-mediated auxin-signaling mechanism in the nucleus has been well characterized (Mockaitis and Estelle, 2008). TIR1/AFBs are F-box proteins of the E3 ubiquitinase SCF complex, and auxin binding to the receptor enhances the interaction between TIR1/AFB and the substrate Auxin/Indole-Acetic-Acid (Aux/IAA), transcriptional repressors for auxin-responsive genes (Dharmasiri et al., 2005; Kepinski and Leyser, 2005). Ubiquitinated Aux/IAs undergo proteasome-mediated degradation, which makes Auxin Response Factors (ARFs), transcription factors binding to the auxin-response cis-element (ARE), free to act on the auxin-responsive genes (Chapman and Estelle, 2009; Guilfoyle and Hagen, 2007; Mockaitis and Estelle, 2008). The Aux/IAs recruit TPL/TPRs, and then TPL/TPRs continuously recruit histone deacetylases for transcriptional repressive activity (Wang et al., 2013). Thus, the transcriptional activity of ARFs depends on the Aux/IAs concentration in cells (Figure 1).

### **1.3.1 DNA-binding transcription factors; ARFs**

Auxin-response element (ARE) has been determined through the promoter analysis

of an auxin-responsive gene in soybean (Ulmasov et al., 1995). The ARFs are identified for transcriptional factor binding to ARE through Y2H assay (Ulmasov et

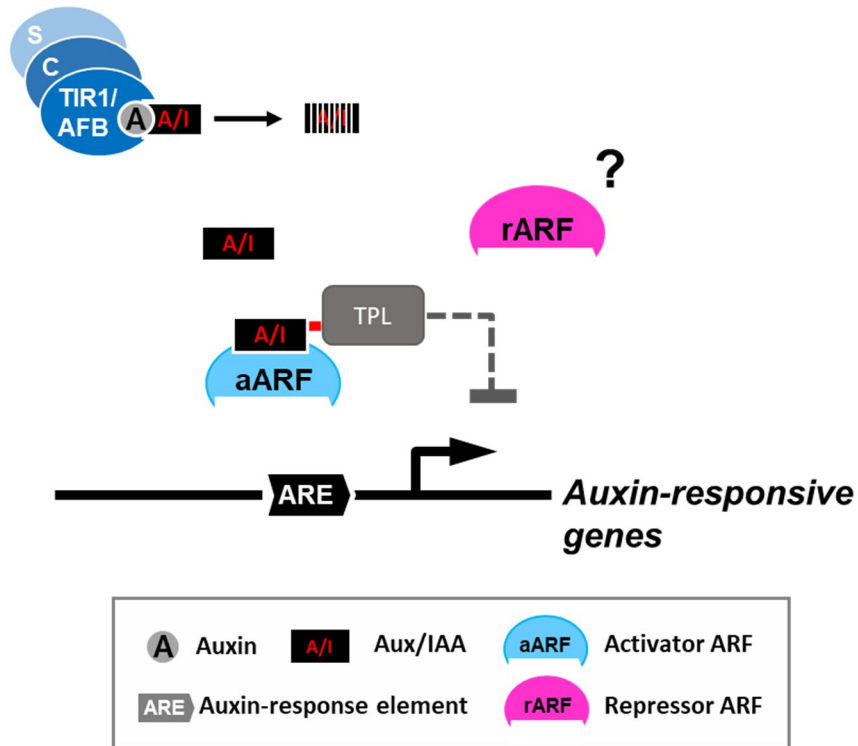


**Figure 1. The auxin signaling pathway in the nucleus.** Auxin leads to degradation of Aux/IAA by co-binding to TIR1/AFB (the F-box) and Aux/IAA. Aux/IAA functions as a repressor by interacting with aARF that binds to ARE-containing auxin-responsive genes and by recruiting TPL/TPR co-repressor to the

target gene. The action mechanism of rARF that is DNA-binding transcriptional repressor has been poorly understood.

al., 1997a). In the Arabidopsis genome, the ARFs bind to canonical AREs in the promoter of target genes (Goda et al., 2004; Nemhauser et al., 2004). In a recent crystal structural study, the ARF was homodimerized by its dimerization domain (DD) in DNA-binding domain. This homodimerization of ARF increases binding affinity to AREs (Boer et al., 2014). ARFs contain conserved C-terminal domains that are similar to Aux/IAA protein's PB1 domain. Finally, crystallographic data demonstrated that the C-terminal region of Arabidopsis ARF7 takes a PB1 domain for interaction with both ARF7 and IAA17 (Korasick et al., 2014). The heterotypic dimerization of ARF-Aux/IAA using the PB1 domain suppresses the transcriptional activity of ARFs (Tiwari, 2003; Tiwari et al., 2003). The region between the DBD and PB1 domains has been called the middle region domain (MD). Two groups based on the sequence of MD divide these ARFs, and MD determines the transcriptional activity (Tiwari et al., 2003; Ulmasov et al., 1999). In protoplast assays, the ARFs containing glutamine-rich MD activate transcription. Other ARFs are thought to be repressors (Guilfoyle and Hagen, 2007).

### 1.3.2 Auxin co-receptor proteins; TIR1/AFBs

TIR1/AFB is a component of the SCF<sup>TIR1/AFB</sup> complex and localizes in the nucleus (Abel et al., 1994). This complex catalyzes E3-ligase activity (Gray et al., 1999). All members of the TIR1/AFB protein family interact with auxin, and mutants of this protein family have shown auxin-related phenotypes. In addition, the mutants of the other components of the SCF<sup>TIR1/AFB</sup> complex, ARABIDOPSIS SKP1 HOMOLOG (ASK1), CULLIN 1 (CUL1), or RING-BOX 1 (RBX1), have also

shown auxin-defected phenotypes (Gilkerson et al., 2009; Gray et al., 1999; Gray et al., 2002; Gray et al., 2001). Crystal structure assay was performed using TIR1-ASK1, auxin, and the binding peptide of Aux/IAA (Tan et al., 2007). This result demonstrates that the leucine-rich-repeat domain of TIR1/AFB forms an auxin-binding pocket, and then auxin and the peptide of Aux/IAA interact with the leucine-rich-repeat domain. Researchers also showed that auxin stabilized the interaction between Aux/IAA peptide and TIR1/AFB (reviewed in Salehin et al., 2015).

1.3.3 Another co-receptors, Aux/IAAs that function as major repressors in auxin signaling

Aux/IAAs were discovered as early auxin-responsive genes with four conserved domains. They showed a transcriptional repression function in protoplast transfection assays (Tiwari et al., 2004; Tiwari et al., 2001). Aux/IAAs bind to co-repressors, TPL/TPRs for transcriptional repression. The TIR1/AFB binding sites are conserved among Aux/IAAs and these sequences act as a degron inducing protein degradation. The binding sequences are usually located in domain II. However, each Aux/IAA has a different interacting affinity with TIR1, which results in the differential stability of Aux/IAAs (Dreher et al., 2006). There are two conserved amino acids (Lysine and Arginine, KR motifs) between domains I and II. Aux/IAAs including KR motifs are easily degraded at a low level of auxin because of the high affinity to auxin and TIR1 (Calderon Villalobos et al., 2012; Dreher et al., 2006; Moss et al., 2015). This is due to the different binding affinity with TIR1

and Aux/IAAs. The different half-lives range from several minutes to 20 h (Dreher et al., 2006). A gain-of-function mutation in domain II stabilizes Aux/IAAs and increases its own protein level in a cell. Gain-of-function mutant lines showed auxin-resistant phenotypes at a variety of plant development stages (Fukaki et al., 2002; Nagpal et al., 2000; Reed, 2001; Tatematsu et al., 2004; Yang et al., 2004). This indicates that the Aux/IAA level is important in auxin responses.

The C-terminal domain of Aux/IAAs results in homo- or hetero-dimerization with Aux/IAAs or ARFs. (Tiwari et al., 2004). It has been suggested that the C-terminal domain of Aux/IAAs and ARFs might form a type I/II Phox and Bem1p (PB1). Proteins with the PB1 domain could form an oligomer (reviewed in Guilfoyle and Hagen, 2012). Crystal structural analysis supports this idea (Korasick et al., 2014). The interactome data from a high-throughput yeast two-hybrid experiment showed that Aux/IAAs prefer to bind ARFs rather than Aux/IAAs themselves, especially activator ARFs (Vernoux et al., 2011). Additionally, another research group proved that the interacting affinity between Aux/IAA and aARF is stronger than homo-oligomeric interaction. They showed the equilibrium dissociation constants (Kd) of homo-oligomerization (6.6  $\mu$ M for IAA17) and hetero-oligomerization (73 nM for IAA17 and ARF5) by using isothermal titration calorimetry (ITC).

#### 1.3.4 Co-repressor, TPL/TPRs

It is known that TOPLESS/TPL-RELATED (TPL/TPR) proteins, as co-repressors, interact with transcription complexes in hormonal signaling, meristem maintenance

process, and defense responses (Gallavotti et al., 2010; Kieffer et al., 2006; Pauwels et al., 2010; Szemenyei et al., 2008; Zhu et al., 2010). TPL consists of a complex with HISTONE DEACETYLASE 19 (HDA19). This complex facilitates the histone deacetylation of the target chromatin region and results in transcriptional repression (Ryu et al., 2014). However, transcriptional co-repressors cannot bind to DNA. Thus, they should be involved in DNA-binding transcriptional complex to suppress gene expression. Aux/IAAs also recruit the TPL family to inhibit the transcriptional activity of aARFs (Szemenyei et al., 2008). The ETHYLENERESPONSIVE ELEMENT BINDING FACTOR–ASSOCIATED REPRESSOR (EAR) or EAR-like repressor motifs of Aux/IAA enable TPL to access DNA binding as a transcriptional complex. These motifs are located in the N-terminal region (domain I) of Aux/IAA. The crystal structural assay demonstrates that the EAR motif of Aux/IAA binds to the CTLH region at the N-terminal of TPL (Ke et al., 2015).

## **1.4 Questions in the present signaling model**

Over the past decade, outstanding progress has been made in auxin signaling (reviewed in Mockaitis and Estelle, 2008; Weijers and Wagner, 2016). The course from auxin signal perception to differential gene expression consists of three protein families. The simple nuclear auxin-signaling pathway is implicated in a plethora of plant growth and developmental processes. The variety of auxin

responses is attributable at least partly to the multiplicity of auxin-signaling components and thus to the different expression pattern and the molecular property of each component member. The Arabidopsis genome has six TIR1/AFBs, 29 Aux/IAAs, and 23 ARFs (Figure 2). This is relatively large members of a group. Auxin signaling results in significant outputs altering the plant body with the transcriptional changes. Thus, it is strictly required for fine-tuning transcriptional regulation. However, the present signaling model is insufficient for understanding the mechanism of total auxin response. I have selected the following matters of importance. The first is different phenotypes of mutants from the same clade of auxin-signaling factors. The second is the undiscovered mechanism of repressor ARFs (rARFs). The third is the target gene-selecting mechanism of activator ARFs (aARFs). To solve these problems, I suggest that protein-protein interactions with signaling components or other transcription factors rule the properties of this auxin response pathway and discuss this from Chapters II to IV.

#### 1.4.1 Different phenotypes of mutants from the same clade of auxin-signaling factors

The first question is based on an observation. The members of each signaling component family show distinctive or sometimes even opposite effects in auxin responses. Typically, hypocotyl growth, lateral root formation, and root hair growth are considered positive auxin responses (Leopold, 1955; Masucci and Schiefelbein, 1994; Wilson et al., 1990). TIR1/AFBs have been thought to auxin receptor resulting in positive auxin response (Dharmasiri et al., 2005). However, AFB4 and

AFB5 mediate negative auxin signaling. Their loss-of-function mutants showed longer petioles and hypocotyl and increased the lateral root number (Greenham et al., 2011).

In the transient protoplast assay using the synthetic auxin-responsive

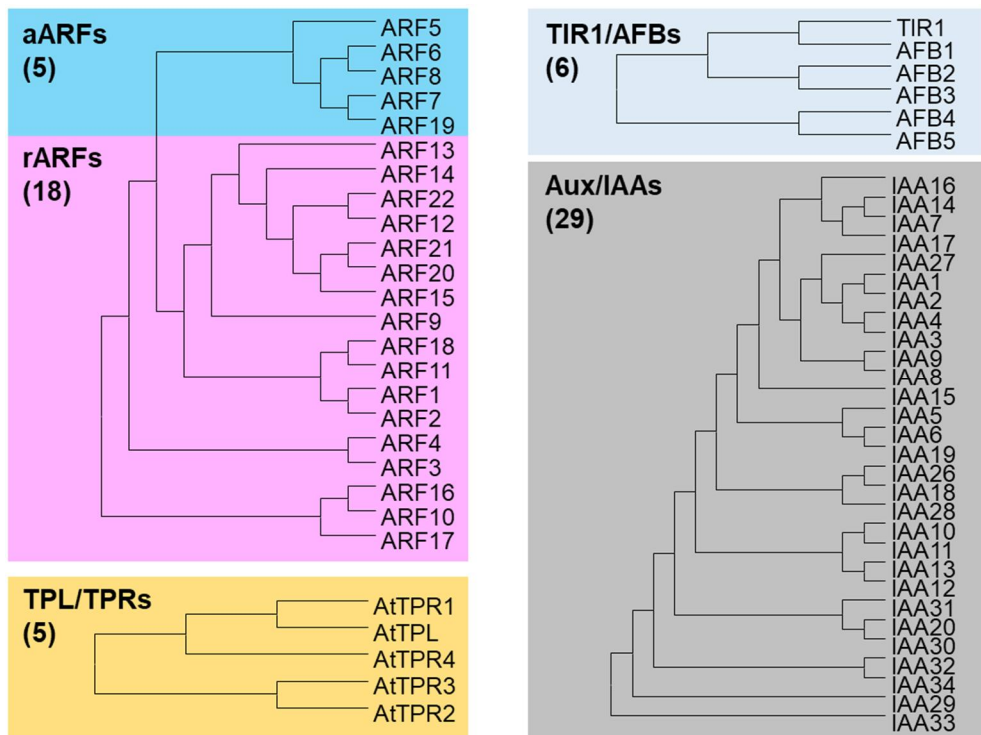


**Figure 2. A phylogenetic tree showing auxin signaling components sequences in Arabidopsis.** Phylogenetic analysis was performed by the Neighbor-Joining method with amino acid sequences using the MEGA4 software package (<http://www.megasoftware.net/mega4/mega.html>). The clade is highlighted with a red area (activator ARFs) blue area (repressor ARFs), green area (Aux/IAAs), and yellow area (TIR1/AFBs).

promoter (DR5)-reporter system, ARFs were classified as transcriptional activators and repressors, consistent with the existence of respective activation and repressor domains (Tiwari et al., 2003), although this simple dichotomic classification of ARFs is not always applicable in plants (Okushima et al., 2005b). Several studies have shown that even ARF5, as a known typical activator transcription factor in auxin response, could repress the expression of the target gene (Zhang et al., 2014; Zhao et al., 2010). Aux/IAAs have been known to act as transcriptional repressors in nuclear auxin signaling. Most *aux/iaa* gain-of-function mutants (GOF) remain for a longer time than wild-type Aux/IAAs and result in auxin-resistant phenotypes. However, some Aux/IAA homologs exhibit activator-like auxin phenotypes in a certain condition. For instance, the *shy2-2* (the GOF of IAA3), *slr1-1* (the GOF of IAA14), *iaa28-1* (the GOF of IAA28), and *msg2-1* (the GOF of IAA19) mutants showed few or no lateral roots that represented auxin-resistant phenotypes. However, *axr2-1* (the GOF of IAA7) mutation increased the lateral root number (Fukaki et al., 2002; Nagpal et al., 2000; Reed, 2001; Rogg et al., 2001; Tatematsu et al., 2004). The GOF mutants of Aux/IAAs (IAA7, IAA17, IAA3, and IAA6) generally represent a short hypocotyl (Nagpal et al., 2000; Rouse et al., 1998; Tian and Reed, 1999). The short hypocotyl is also an auxin-resistant phenotype. However, the *iaa18-1* GOF mutant showed contrary phenotypes as a longer hypocotyl in light-grown conditions (Ploense et al., 2009). Promoter swapping and complementation experiments between gain-of-function *aux/iaa* mutants also revealed molecular diversification among Aux/IAAs (Muto et al., 2007). The *bdl* (GOF mutant of IAA12) mutant showed embryonic and postembryonic phenotypes,

whereas the IAA3 GOF mutant or IAA3-expressed lines by promoter *BDL* had no embryonic phenotypes (Weijers et al., 2005).

As mentioned earlier, the present auxin-signaling model is not sufficient to interpret these contrary phenotypes. In particular, I will focus on studying the differential function of Aux/IAAs and discuss it in Chapter II.

#### 1.4.2 The uncharacterized mechanism of repressor ARFs

The second question raised concerns repressor ARFs (rARFs). In the course of auxin signaling, ARFs have a DNA-binding domain and work for sequence-specific transcription factors. Although several ARFs are categorized repressors (rARF), it is unclear how the rARF works as a repressor and what the function of plant development is.

In the past, researchers have not welcomed repressor study. Typically, the transcriptional activator research field is highlighted in the transcriptional regulation mechanism. Approximately 7% of the DNA sequences from a eukaryotic cell are transcribed to the RNA. Thus, it does not seem appropriate to selectively repress the remaining 93% of DNA sequences. However, apparently, large numbers of repressors still exist and play an important role in transcriptional regulation in the cell (reviewed in Johnson, 1995; Gray and Levine, 1996). To clearly express the required gene in the cell, a cooperative relationship between the activator and repressor is needed. The sequence-specific transcriptional repressor is as important as an activator in transcriptional regulation (Payankulam et al., 2010).

Aux/IAAs are transcription repressors in auxin signaling. The recruiting

co-repressor provides the transcriptional repressive force to Aux/IAAs. However, Aux/IAAs are passively involved in repression pathways because of the absence of DNA-binding ability. The transcriptional function of activator ARFs has inhibited through interaction with Aux/IAAs because their PB1 domain facilitates heterodimerization (Boer et al., 2014; Han et al., 2014; Korasick et al., 2014). Even though many rARFs also have PB1 domains, they showed no or a weak interaction with Aux/IAAs (Vernoux et al., 2011). Therefore, another mechanism is required to interpret the transcriptional repression manner of rARFs. There are many other repression methods. The repressor competes to bind DNA by excluding the chance of the binding of an activator or interfering with the activity of a DNA-bound activator (reviewed in Johnson et al., 1995). rARFs are available for these two repression mechanisms because rARFs can bind to DNA and interact with aARFs through the DNA-binding domain and PB1 domain, respectively. Some groups have suggested that rARFs work as repressors in an auxin-independent manner due to less binding affinity with Aux/IAAs. They might be competing with aARFs for binding to ARE (Okushima et al., 2005a; Richter et al., 2013; Vernoux et al., 2011). Other groups have suggested the possibility of directly recruiting co-repressors, TPL/TPRs. Several review papers mention that rARFs have (R/K)LFGxL or EAR motifs, which are TPL/TPRs binding motifs (Guilfoyle and Hagen, 2001; Lokerse and Weijers, 2009). Finally, a high-throughput yeast two-hybrid experiment identified TPL-interacting proteins among the transcription factors of Arabidopsis. A number of interacting proteins, including rARFs (ARF2, ARF9, and ARF18), have short repression domain sequences, such as RLFV or EAR motifs (Causier

et al., 2012a). If rARFs recruit a co-repressor and bind to aARF or directly to DNA, rARFs play an active part in transcriptional repression. However, this has been not verified, at least in *Arabidopsis*.

In spite of the importance of gene repression and the possibility of a repression mechanism, the gap in knowledge of rARFs has resulted in significant limitations in understanding auxin signaling. Thus, I consider this theme and suggest the repression mechanism in Chapter III.

#### 1.4.3 Target gene-selecting mechanism of activator ARFs

The raised third question is how aARFs find the correct target genes and regulate their expression from the numerous genes containing auxin response elements (AREs) in promoter regions. I could easily observe AREs in the promoter regions without the enough information of the functionality. However, I have no choice but to depend on computational data because there are not enough available DNA-binding data about activator ARFs, such as chromatin immunoprecipitation (ChIP)-seq assay. The researchers conducted microarray data and computational analysis together. They showed many AREs localized at 5'UTR of the putative target-gene promoters; these genes are usually up-regulated in auxin responses by confirming the pattern of auxin-responsive gene expression. Furthermore, it revealed that palindromic ARE is strongly related to auxin response, the same finding as that in previously published experimental data (Boer et al., 2014; Mironova et al., 2014; Ulmasov et al., 1999). Meanwhile, they also reported that a significant number of putative AxREs are false positive sites (Mironova et al., 2014). In addition, other

experimental data support the existence of null-function AREs. ARF7 selectively bound to AREs, not all AREs in the ChIP analysis (Chung et al., 2011).

In another bioinformatics analysis, it was reported that there are many other cis-elements near ARE sites, such as bZIP response elements (ZRE), Myb response elements (MRE), and bZIP-associated G-box related elements (GRE) (Berendzen et al., 2012). Recently, the analysis of genome-wide target, genetic, and biochemical interactions confirmed that several cis-elements were enriched near ARF6 target-binding sites. ARF6 regulates the hypocotyl length in a cooperative relationship with two transcription factors (PHYTOCHROME INTERACTING FACTOR 4 and BRASSINAZOLE RESISTANT 1) binding to those cis-elements (Oh et al., 2014). This cis-element enrichment tendency with ARE appeared from not only *Arabidopsis*, but also *Oryza sativa*, monocot plants (Berendzen et al., 2012). I could infer that the appropriate transmitting of auxin signal-mediating aARFs requires other hormonal or environmental transcription factors to select the real target genes.

It has been reported that aARFs interact with other transcription factors for transcription (Scacchi et al., 2010; Shin et al., 2007; Varaud et al., 2011). In particular, ARF5, an activator ARF, directly binds to transcriptional complexes, including BRM and SYD, which are SWI/SNF chromatin remodeling ATPase. This interaction enhances the ARF5 binding to DNA (Wu et al., 2015). Several studies represent that ARF transcriptional activity is connected to establishing a high-order complex (reviewed in Chandler, 2016).

Consequently, I suggest that aARFs interact with another transcription factor or chromatin remodeler for fine-tuning transcriptional regulation, such as selecting the correct target genes, determining the expression timing, and regulating the expression level. I will discuss this regulation in depth in Chapter IV.

## **1.5 The root hair system as a model to study auxin-signaling pathway**

The function of a gene is tightly connected to other specific tissue- or cell-type factors. Moreover, overall tissues and organs respond to auxin and auxin-signaling components are expressed in almost every cell. Therefore, it is difficult to determine the correct transcriptional activity of auxin-signaling factors from mutant phenotypes. Analyzing the auxin response in a single-cell assay system is helpful for validating the activation or repression role of a signaling factor.

A root hair is the protrusion of root epidermal cells, and its growth is positively regulated by auxin in a cell-autonomous manner (Cho et al., 2007b; Ganguly et al., 2010; Masucci and Schiefelbein, 1994, 1996; Pitts et al., 1998). In the auxin-signaling study, I will take advantage of the auxin-responsive single root hair cell system. Our lab has researched EXPANSIN A7 protein. It expresses in the root hair cell specifically, and its biological function is definitely related to root hair growth (Cho and Cosgrove, 2002; Kim et al., 2006; Lin et al., 2011).

Previously, our lab expressed several auxin-signaling factors in the root hair cells using the root hair-specific *EXPANSIN A7* promoter (*ProE7*). I readily observed a positive or negative auxin response in the root hair phenotypes depending on the functionality of the expressed factors. For example, auxin exporter-overexpressed lines driven by *ProE7* usually represented short-root-hair phenotypes because of the decreasing auxin level in the root hair cells (Ganguly et al., 2010). The overexpressed GOF of Aux/IAA driven by *ProE7* also showed short root hairs (Lee et al., 2016), whereas aARF- or TIR1-overexpressed lines driven by *ProE7* showed relatively long root hair phenotypes. This is similar to the auxin level increasing seedlings (Ganguly et al., 2010; Mangano et al., 2017).

Auxin has been considered a root hair elongation hormone, but the molecular mechanism has not been known. Recently, I showed that ARF5 directly binds to ARE in the ROOT HAIR DEFECTIVE SIX-LIKE4 (*RSL4*) promoter regions and increases *RSL4* expression in the mRNA level. *RSL4* is a key transcription factor that regulates root hair growth (Hwang et al., 2017; Vijayakumar et al., 2016; Won et al., 2009; Yi et al., 2010). Thus, I suggest that auxin regulates the root hair growth mediating *RSL4* expression and estimate the molecular function of auxin-signaling components for the *RSL4* expression intensity in hair cells.

## **Chapter II.**

### **Dose-dependent transcriptional activation by competition between Aux/IAA homologs**

## **2.1 Abstract**

Auxin affects the plant cell division, expansion, and differentiation of developmental growth. The members of the auxin-signaling component family show distinctive or sometimes even opposite effects in auxin responses. Here, I characterize the differential transcriptional activity between Aux/IAs by root hair system. Aux/IAs, such as IAA7/AXR2 and IAA17/AXR3, commonly inhibit target gene expression by recruiting a co-repressor, TPL. Interestingly, the different dose of IAA3/SHY2 leads to opposite transcriptional regulation and physiological change in root hair cells. The TPL-binding motif of SHY2 (RG-motif) is distinct from the motif of AXR2 or AXR3 (CG-motif), and dose-dependent transcriptional changes were identically observed from other RG-motif Aux/IAs. Experimental validation and modeling indicate that RG-motif is weaker than CG-motif regarding the interacting affinity with TPL. It results in fewer TPL to transcriptional complexes. I suggest that this mechanism is required for a sensitive auxin response and extend the view of transcriptional regulation to re-consider the role of the repressor.

## **2.2 Introduction**

Recently, researchers have discovered a difference from the classic viewpoint that transcription simply changes between on and off states. For a fine-tuned transcript level and therefore more biological usefulness, the co-transcription factor shifts

their transcriptional activity, rather than one-sided transcriptional changes (Reynolds et al., 2013).

There are many cases of bi-functional transcriptional regulation. To switch transcriptional direction, the chromatin status changes from open to closed, the activity of the transcription factor changes from a repressor to an activator, or the transcription factor replaces the co-factors as an activator or repressor.

Many chromatin-modifying proteins regarded as repressors appear in the promoter region of actively transcribed genes from the high-throughput data. For example, the Histone Deacetylase 1 (Hdac1) of zebrafish might carry out the transcriptional activation of target genes during embryogenesis in genome-wide transcriptome data (Harrison et al., 2011). Even though Hdac1 is a well-known function in transcriptional repression, chromodomain/helicase/DNA-binding domain CHD3 proteins PICKLE (PKL), a part of the HDAC complex, has been involved in transcriptional repression in previous studies. From principal components analysis, a double mutant of PKL and PKL homolog PKL2, *pkl pkl2*, showed up- and down-regulated target genes. It appears that PKL has a dual function. Following this paper, PKL can up-regulate target gene expression only in the absence of H3K27me3 (Aichinger et al., 2009). Genome-wide analyses show that one transcription factor has a dual function in gene regulation. PHYTOCHROME-INTERACTING FACTOR1 (PIF1), also known as PIL5, is a transcription factor involving seed germination. Chromatin immunoprecipitation-chip (ChIP-chip) and microarray analysis have shown that PIF1 regulates the

transcription of the target genes both positively and negatively by binding to the promoter of target genes (Oh et al., 2009). The Krüppel (Kr) repressor is essential in *Drosophila* organogenesis during later embryonic development (Licht et al., 1990). Kr regulates the transcription of the chloramphenicol acetyl transferase (CAT) reporter gene both positively and negatively in Schneider tissue culture cells (Sauer and Jäckle, 1993). A clade of four PLETHORA (PLT) homologs regulates the growth of the root primordium at three stages: stem cell programming, mitotic activity, and exit to differentiation (Galinha et al., 2007). The activity of PLT homologs depends on the dose at the root stem cell and neighboring stem cells.

In these variable situations, I found a similar phenomenon in the course of transmitting auxin signaling. Auxin signaling results in transcriptional changes and the consequent induce changes in the plant body in various environmental changes and developmental requirements. Aux/IAAs have been known to act as transcriptional repressors in nuclear auxin signaling. However, some Aux/IAA homologs exhibit activator-like auxin phenotypes in a certain condition. Because the mutant forms are resistant to degradation, the gain-of-function *aux/iaa* mutants are thought to cause auxin-defective phenotypes (Gray et al., 2001; Ramos et al., 2001). However, depending on the organ or tissue type, some of these dominant (or semi-dominant) Aux/IAA mutants show intriguing contrary phenotypes. Details are given in the general introduction parts. The opposite phenotypes among these mutants are shown even in a single cell level; *axr2-1* and *axr3-1* have no or much shorter root hairs, but *shy2-2* grows longer root hairs than the wild type (Knox et al., 2003; Leyser et al., 1996; Wilson et al., 1990). Considering that lateral and

adventitious root formation and root hair growth are stimulated by auxin, these stabilized Aux/IAA repressors are supposed to consistently inhibit these auxin-mediated root responses. If so, these results raise the question of how the transcriptional factor categorized as a repressor has been geared toward auxin response, such as the longer root hair phenotype of *shy2-2*.

Previously, it was revealed that the repression function of Aux/IAAs originated from domain I. Now, it has been shown that the EAR motifs of domain I recruit the TPL/TPRs to the chromatin (Causier et al., 2012a; Szemenyei et al., 2008). The EAR motif varies among Aux/IAAs, suggesting the molecular diversification of Aux/IAAs by this motif (Lokerse and Weijers, 2009; Tiwari et al., 2004; Tiwari et al., 2001).

I investigated the functional diversification of Aux/IAAs and demonstrated that SHY2/IAA3 contributes to root hair growth in a dose-dependent manner. Finally, our results suggest that SHY2 can act as either a transcriptional repressor or an activator depending on its dosage, a kind of phenomenon that has scarcely been found in the molecular function of a transcription regulator.

## **2.3 Materials and methods**

### **2.3.1 Accession numbers**

The accession numbers for the genes analyzed in this study are AT1G04240 (*SHY2*),

AT3G23050 (*AXR2*), At1G04250 (*AXR3*), AT3G23030 (*IAA2*), AT3G15540 (*IAA19*), AT2G23170 (*GH3.3*), AT4G27260 (*GH3.5*), At1G15750 (*TPL*), At4G33880 (*RSL2*), At1G27740 (*RSL4*), and AT1G12560 (*EXPA7*). *axr2-1* (CS3077), *axr3-1* (CS57504) were purchased from the *Arabidopsis* stock center (<http://www.arabidopsis.org/>).

### 2.3.2 Plant materials and growth conditions

*Arabidopsis* (*Arabidopsis thaliana*), Columbia ecotype, was used as the wild-type plant in this study. *Arabidopsis* seeds were cold-treated at 4 °C for 3 days prior to germination in the dark. *Arabidopsis* plants were transformed using *Agrobacterium tumefaciens* strain C58C1 (Bechtold and Pelletier 1998) and transformants were selected on hygromycin-containing (10 µg mL<sup>-1</sup>) phyto-agar plates. All T2 generation seeds for the measurement of root hair length were grown on agarose plates containing 4.3 g/L Murashige and Skoog (MS) nutrient mix (Sigma-Aldrich), 1 % Suc, 0.5 g/L MES (pH 5.7), KOH, and 0.8 % agarose. All seeds were cold treated at 4 °C for 3 d and germinated at 23 °C under 16-h-light/8-h-dark photoperiods. For all pharmacological experiments, 3-d-old seedlings of homozygous transformants were transferred to new plates and grown for an additional day, after which root hairs were observed.

### 2.3.3 Observation of root hairs

Observation of root hairs and estimations of root hair length were performed as described previously (Ganguly et al., 2010). For estimation of root hair length,

digital photographs of roots were taken using a stereomicroscope (Leica MZ FLIII and Leica DFC425 • C) at 40 X to 50 X magnifications. The hair length from 16 hairs protruding perpendicularly from each side of the root was measured by LAS application Suite V3.8.

### 2.3.4 RNA isolation and quantitative reverse transcriptase PCR (qRT-PCR) analysis

Total RNA was isolated from the roots of 4-d-old seedlings (25 for each line) using an RNeasy Plant Mini Kit (Qiagen). cDNA was synthesized as described previously (Lee and Cho, 2006). qRT-PCR analyses were performed using a TOPreal™ qPCR 2 x PreMIX (SYBR Green, Enzynomics) and a Chromo4™ Four-Color Real-Time Detector (Bio-Rad). Gene-specific signals were normalized relative to *Actin7*. Each reaction was performed in triplicate and each experiment was repeated three times using independent preparations of RNA. Primers are listed in Table 1

### 2.3.5 Observation of reporter gene expression and evaluation of promoter activity

The fluorescence from reporter proteins and organelle markers was observed by confocal laser scanning microscopy (LSM 510 and LSM 700; Carl Zeiss). GFP was detected using 488/505- to 530-nm. Fluorescence images were digitized using the Zeiss LSM image browser. Promoter activity was evaluated by quantifying the

GFP fluorescence using the histogram function of Adobe Photoshop (Adobe Systems) as described by Cho and Cosgrove (2002). For observation of DEX-inducible nuclear localization of *shy2-1* or *axr2-1* in *ProE7:shy2-1:GFP:GR* or *ProE7:axr2-1:GFP:GR* respectively, GFP signals in 5-8 nucleus of root hair cell in EXPA7 domain were detected.

### 2.3.6 Transgene constructs

The Arabidopsis *EXPA7* promoter *ProE7* (Cho and Cosgrove, 2002) was used for cloning all *Aux/IAA* transgenes. The binary vector *pCAMBIA1300-NOS* was used as the cloning vector. *ProE7p13M* was modified from *pCAMBIA1300* (Hyg+) and carries the *AtEXPA7* promoter at -480 bp from the transcription initiation site (Kim et al., 2006).

*ProE7:YFP*, *ProE7:GFP* and *ProE7:axr2-1* were as previously described (Lee and Cho, 2006; Cho et al., 2007a, Won et al., 2009).

For the *ProE7:SHY2* and *ProE7:shy2-1* constructs, genomic fragments of *SHY2* and *shy2-1* were obtained by PCR using genomic DNA of wild-type plants and *shy2-1* mutants as template and cloned into the *ProE7:axr2-1* vector replacing *axr2-1* regions. For *ProE7:SHY2:GFP* and *ProE7:shy2-1:GFP* constructs, a region of *GFP* gene was obtained by PCR using *pGPTV-GFP* vector and cloned into *ProE7:SHY2* and *ProE7:shy2-1* vectors.

For the *ProZmE7:shy2-1:GFP* construct, a promoter fragment of *ProZmE7* was obtained by PCR using the plasmid of *ProZmE7(-*

276/+46):*pC1300A* (Kim and Cho, 2006) as template and cloned into the *HindIII/XmaI* sites of the binary vector *pCAMBIA1300-NOS*. A fusion gene fragment of *shy2-1:GFP* was obtained by PCR using the plasmid of *ProE7:shy2-1:GFP* as a template and cloned into the *AvrII/XbaI* sites downstream of the *ProZmE7* region. For the *ProZmE7:axr2-1*, *ProZmE7:axr3-1*, *ProZmE7:iaa2-1*, *ProZmE7:slr-1*, *ProZmE7:axr5-1*, and *ProZmE7:msg2-1* constructs, genomic fragments of each gene was obtained by PCR using genomic DNA of gain-of-function mutants as template and replaced to *shy2-1:GFP* region of *ProZmE7:shy2-1:GFP* vector. For the *ProZmE7:iaa2-1C17R* and *ProZmE7:shy2-1R13C* constructs, amino acids of domain I of Aux/IAAs were substituted by PCR using genomic DNA as template and cloned into the *ProZmE7:shy2-1:GFP* vector replacing *shy2-1:GFP* region.

For the *ProSHY2:axr2-1*, *ProSHY2:axr3-1*, *ProSHY2:shy2-1:GFP*, *ProAXR2:axr2-1*, and *ProAXR2:shy2-1:GFP* constructs, full length of *SHY2* and *AXR2* promoters were obtained by PCR using the genomic DNA of Arabidopsis as template and cloned into *SalI/BamHI* sites and *HindIII/SalI* sites the binary vector *pCAMBIA1300-NOS*, respectively (*ProSHY2* vectors, *ProAXR2* vectors). Each gene fragment and *shy2-1:GFP* were obtained by PCR using the plasmid of *ProZmE7:aux/iaas* or the plasmid of *ProZmE7:shy2-1:GFP* as template and cloned into downstream *ProSHY2* vector or *ProAXR2* vector.

For the *ProE7:RNAi* constructs, RNAi target region of *SHY2* (*SHY2-RNAi1* and *SHY2-RNAi2*) were amplified by PCR using cDNA of Arabidopsis

seedlings as template and cloned into the *XhoI/KpnI* and *HindIII/XbaI* sites of the *pHannibal* vector to generate sense and antisense fragments. Next, the fragments of *SHY2-RNAi1* and *SHY2-RNAi2* were transferred into the *SalI/XbaI* sites of the binary vector *pCAMBIA1300-NOS*. For the *ProE7:Aux/IAAs:GFP:GR* constructs, the *GR* fragment was obtained by PCR and cloned into the *ProE7p13M* vector (*ProE7:GR*). The *Aux/IAAs:GFP* were obtained by PCR using the plasmid of *ProE7:Aux/IAAs:GFP* and cloned into the *PacI/MluI* sites downstream of the *ProE7* and upstream of the *GR* of *ProE7:GR* vector. For the *ProE7:Aux/IAAmImIIs* constructs, site-directed mutagenesis of the domain I of the Aux/IAA was performed by PCR. The genomic DNA of gain-of-function mutants and the plasmid of *ProE7:IAA7mlabmII* (Lee et al., 2016) were used as template. The PCR products of the *Aux/IAAmImIIs* were cloned into the *ProE7p13M* vector. For the *ProE7:Aux/IAAmIIΔPB1s* constructs, the N-terminal region of Aux/IAAs were obtained by PCR using the genomic DNA of gain-of-function mutants as template and cloned into the *ProE7:GFP* vector. For the *ProE7:Aux/IAAmImIIΔPB1s* constructs, the fragments of domain I and II mutated Aux/IAA were obtained by PCR using the plasmid of *ProE7:Aux/IAAmImIIs*.

For *Escherichia coli* expression of SHY2, AXR2, IAA2 series and TPL proteins in the *in vitro* pull down assay, the fragments of each gene was obtained by PCR using synthesized cDNA from Arabidopsis as template and cloned into *pGEX-4t-1* vector and *pET-30a-c(+)* vector. TPL proteins was amplified N-Terminal region (1 to 188 amino acids). For tagging both GST and His6 to Aux/IAAs, the GST fragment was obtained by PCR and cloned in-frame of *pET-30a-C(+)*-

*Aux/IAAs* with *XhoI* sites. All primers listed in Table 3.

### 2.3.7 Protein lysate preparation and immunoblots

All proteins were expressed in *E. coli* BL21DE3 by inducing with isopropyl b-D-1-thiogalactopyranoside (IPTG). Each protein has different induction conditions (TPL<sub>nt</sub> protein - 0.5 mM IPTG, 4 °C, 18 h; SHY2 protein - 0.2 mM IPTG, 22 °C, 5 h; AXR2 protein - 0.2 mM IPTG, 0.2 % glucose, 28 °C, 3 h). The lysate was then collected after induction using bacterial protein extraction reagent B-PER (Thermo Scientific Inc., USA) containing 0.2 mg/ml Lysozyme Solution (Sigma, USA), 1 unit/ml Recombinant DNase I (TAKARA BIO INC., Japan), Protease Inhibitor Cocktail (Santa Cruz Biotechnology, Tablet). *Aux/IAAs* were purified from glutathione resin by boiling 10 min with SDS 10 % solution.

An equal amount of each protein sample was separated by SDS-PAGE, transferred into a nitro-cellulose membrane (Amersham Biosciences, Corston, Bath, UK), and probed with 1/1000-diluted anti-HIS mouse IgG (MBL, Japan) and 1/2000-diluted Goat anti-Mouse IgG horseradish peroxidase (HRP)-conjugated (COLUMBIA BIOSCIENCES, USA). Chemiluminescence detection was performed with the two type of ECL western blotting substrates ECL Pico (LPS solution, Korea) and High-resolution ECL Femto-100 (LPS solution, Korea) in a Chemiluminescence imaging system (Davinch-Chem, Corebio, Korea).

### 2.3.8 *In vitro* pull-down assay and analysis protein signal intensity

Firstly, His-SHY2-GST or His-AXR2-GST were immobilized on glutathione resin for 2 h and then incubated with His6-TPL<sub>nt</sub> for 2 h at 4 °C. The glutathione resin was then washed five times with TBS buffer. Proteins were purified from glutathione resin by boiling 10 min with SDS 10 % solution.

The pull-down experiments were repeated three times with similar results. Measurement of protein signal intensity from western pictures was conducted as followed descriptions. At the western blot experiment, reliable quantification of target protein level requires measurement of the target and loading control proteins. As a loading control, TPL<sub>nt</sub> lysate sample has loaded all membranes. Aux/IAA signal intensity = (Aux/IAA western bands – Aux/IAA bands background) / loading control. TPL<sub>nt</sub> signal intensity = (TPL<sub>nt</sub> western bands – TPL<sub>nt</sub> bands background) / loading control. Four independent cultures were analyzed. The western signal intensity of His-AXR2-GST protein was weaker than His-SHY2-GST protein. High-resolution ECL was used for increase signal intensity of AXR2 protein. Western signal intensity was evaluated by using the histogram function of Adobe Photoshop (Adobe Systems).

### 2.3.9 Microscale thermophoresis

The TPL proteins were CY5 labeled for microscale thermophoresis (MST) by using the Monolith NT Protein Labeling Kit RED-NHS (NanoTemper Technologies, München, Germany), following the step of the manufacturer instructions. Briefly, 10 µM proteins were incubated with dye in labeling buffer (manufacturer supplied) in the dark at room temperature for 1 h. The excess dye

was removed using gel filtration columns (manufacturer supplied) and the proteins were eluted in 200  $\mu$ l of binding buffer (20 mM Tris-HCl, 100 mM NaCl, pH 8.0).

Thermophoresis was analyzed using the Monolith-NT.115<sup>pic</sup> (NanoTemper Technologies GmbH, Munich, Germany) with LED power 80 % and MST power 30 %. To determine the K<sub>d</sub> values of TPL to Aux/IAAs, the compounds were arrayed across a 16-point dilution series consisting of binding buffer conditions with 0.01 % Tween-20. The Aux/IAAs protein concentration was sequentially diluted. The concentration of the labeled TPL was kept constant at 50 nM. All samples and buffers were centrifuged at 13,000 rpm for 10 min before being loaded into standard capillaries.

### 2.3.10 RNA sequencing

Three-day-old *ProE7:GFP* (control) and *ProE7:shy2-1:GFP:GR* seedlings were grown on MS medium with hygromycin for selection. Then, we moved seedlings to new medium containing dexamethasone (DEX) 0.1 nM, 1  $\mu$ M or equivalent amount of ethanol solvent and keep it for one day. We used total RNA samples from the root (1 $\mu$ g) for preparing the library by Illumina TruSeq mRNA Sample Prep kit (Illumina, Inc., San Diego, Ca, USA). The sequencing was performed at MACROGEN Inc. (Seoul, Korea). The indexed libraries from two biological replicates were sequenced using the HiSeq2500 platform (Illumina, San Diego, USA) by the Macrogen Incorporated. The transcript counts in isoform level were calculated, and the relative transcript abundances were measured in FPKM (Fragments Per Kilobase of exon per Million fragments mapped) using Cufflinks.

We excluded transcripts with zeroed FPKM values more than one for total samples. We added 1 with FPKM value of the filtered transcript to facilitate log2 transformation. The data in Figure 10F. was sorted by fold enrichment. Firstly, I make a differentially expressed gene (DEG)-list for elimination DEX dependency. Those genes were determined with DEX 0.1 nM-Cont versus Mock-Cont and DEX 1  $\mu$ M-Cont versus Mock-Cont.

Secondly, the SHY2-response DEGs were determined with Dex 0.1 nM-SHY2 versus Mock-SHY2 and Dex 1  $\mu$ M-SHY2 versus Mock-SHY2. Results were imported into Microsoft Excel for filtering ( $|FC| > 1.2$  cut-off, raw.p  $< 0.05$ ) and generating Venn diagram. Then, we selected SHY2-response genes filtered DEX dependent genes.

### 2.3.11 Model of the TPL-Aux/IAA interaction

Here, I calculate the number of binding TPL with increasing concentration SHY2-AXR2 set or IAA2 series. Let  $C_{protein}$  denote the concentrations of proteins. In first set, the total Aux/IAA protein concentration ( $C_{total}$ ) is the sum of concentration of SHY2 ( $C_{shy2}$ ), AXR2 ( $C_{axr2}$ ), and the other Aux/IAs ( $C_{other}$ ). In Second set, I applied IAA2 ( $C_{IAA2}$ ), IAA2-C17R ( $C_{C17R}$ ) instead of SHY2 or AXR2. The fraction of monomer ( $f_1$ ) can be represented as the equation (2) based on a logarithmic relationship with the  $C_{total}$

$$C_{total} = C_{shy2} + C_{axr2} + C_{other} \quad (1)$$

$$f_1 = a * \ln(C_{total}) + b \quad (2)$$

Based on the result of the eight-state model (Han et al., 2014), here we set a and b as -0.153 and 0.9025 to calculate the  $f_1$  with given concentration of  $C_{total}$ . The initial values of  $C_{shy2}$  and  $C_{axr2}$  are 0.004 and 0.053 and the value of  $C_{other}$  is fixed to 0.8 following Table 2. In second set, the initial values of  $C_{IAA2}$  and  $C_{C17R}$  are 0.012 and the value of  $C_{other}$  is fixed to 0.8 following Table 2.

**Table 1.** Absolute mRNA expression value of Aux/IAs from hair 9 tissue was derived from *Arabidopsis* eFP browser.

Gene	IAA1/ AXR5	IAA2	IAA3/ SHY2	IAA4	IAA5	IAA6	IAA7/ AXR2	IAA8	IAA9	IAA10	IAA11	IAA12	IAA13
Expression value	339.74	58.22	18.07	1.34	188.02	13.9	235.98	228.1	237.22	69.07	28.11	1.06	3.96
% of Aux/IAs	7.6	1.2	0.4	0.03	4.21	0.31	5.28	5.1	5.31	1.54	0.62	0.02	0.08
Gene	IAA14/ SLR	IAA16	IAA17/ AXR3	IAA18	IAA19/ MSG2	IAA26	IAA27	IAA28	IAA29	IAA30	IAA31	IAA33	SUM
Expression value	140.24	236.74	1070.7	61.73	976.34	23.52	9.1	261.33	8.21	212.92	23.6	17.24	4464.5
% of Aux/IAs	3.14	5.3	23.98	1.38	21.86	0.52	0.2	5.85	0.18	4.76	0.52	0.38	100*

\* 100% [Aux/IAs] = 1

The total fraction of the oligomer is denoted by  $(1 - f_1)$ , and the fraction of each oligomer ( $f_i$ ) from dimer to octamer can be represented as equation (3).

$$f_i = (1 - f_1)p_i \quad (i = 2,3,4,5,6,7,8) \quad (3)$$

**Table 2.** The assumed population of each oligomer in a cell.

	Dimer ( $p_2$ )	Trimer ( $p_3$ )	Tetramer ( $p_4$ )	Pentamer ( $p_5$ )	Hexamer ( $p_6$ )	Heptamer ( $p_7$ )	Octamer ( $p_8$ )
Population (%)	21.70	18.57	15.93	13.55	11.67	9.912	8.53

The population of each oligomer ( $p_i$ ) is denoted in Table 3. We referred

the population of each oligomer to the monomer-oligomer equilibrium model (Han et al., 2014) and normalized that a constant ratio of each oligomer to the total concentration of oligomer regardless of monomer concentration. We have investigated the effect of oligomer population on TPL binding level and found out our constant ration of each oligomer is reasonable (data are not shown). Based on these assumptions, we calculate the artificial number of TPL-Aux/IAAs complexes. The number of binding TPL to Aux/IAAs is proportional to the concentration ratio of each protein, their dissociation coefficient, and the concentration of each oligomer. Therefore, the number of TPL binding to AXR2, SHY2, and other Aux/IAAs ( $N_{T_{axr2}}$ ,  $N_{T_{shy2}}$ , and  $N_{T_{other}}$ ) can be represented as following:

$$N_{T_{axr2}} = \sum_{i=1}^8 f_i \frac{i}{K_{axr2}} \frac{C_{axr2}}{C_{total}} N_{ARF} \quad (4)$$

$$N_{T_{shy2}} = \sum_{i=1}^8 f_i \frac{i}{K_{shy2}} \frac{C_{shy2}}{C_{total}} N_{ARF} \quad (5)$$

The dissociation coefficients of AXR, SHY, and other proteins, i.e.,  $K_{axr}$ ,  $K_{shy}$ , and  $K_{other}$ , are set to 0.86, 2.3, and 0.86, respectively. In second set, the dissociation coefficients of IAA2, IAA2-C17R, and other proteins, i.e.,  $K_{IAA2}$ ,  $K_{C17R}$ , and  $K_{other}$ , are set to 1.29, 2.35, and 0.86, respectively. Based on these equations, we calculated the number of TPL bond in the given AXR and SHY concentrations.

**Table 3.** The primer list

Subject		Primer name	Primer sequence (5' to 3')
qRT-PCR	ACTIN7	At-actin7F	GTGTGTCTTGTCCTTATCTGGTTCG
		At-actin7R	AATAGCTGCATTGTCACCCGATACT
	IAA19	RT-IAA19-F	GGTGACAACTGCGAAATAC
		RT-IAA19-R	CACTCGTCTACTCCTCTA
	SHY2 (transgene)	RT-SHY2+GFP F	CCAATACGCAAAACCGCCTCTC
		RT-SHY2+GFP R	CGCTCACTGCCCTTTC
	GH3.5	RT-GH3.5F2325	ATGGATTACGCAATCAGCTTGGAAGC
		RT-GH3.5R2504	CCACATCCATCTTAGTTACTCCCAC
	SHY2	Rt-SHY-F	GAAAGGCTCAGATTGTTGATGGC
		Rt-SHY-R	TCCTTGACCTCATGCTCAGATTC
	RSL4	RSL4_737F	AGA GAA GAT TAA CGA AAG GCT CAA
		RSL4_998R	CCA ATG GTG CGT ACA TCC ATA
GH3.3	GH3.3F2791RT	GTTGTGAAGAAATGGAACGTTCGAGGAGC	
	GH3.3R2980RT	CTTCTCAACGACGACGTTCTGCTGACC	
Transgene constructs	ProE7:AHK3	AHK3_SIF	TCGTGTGCGCAAGTGTGATGATGCTGTTCC
		AHK3_XbR	ACTACTACTCTAGATGCATAGGAGACACGAG
	ProE7:SHY2 /ProE7:shy2-1	SHY2_XbF	TATCTTCTAGACAATCTTGAAGAATAAG
		SHY2_XmR	TGAAGCCGGTAACTACACCACAGCCTA
	ProE7:SHY2:GFP /ProE7:shy2-1:GFP	GFP_HdF	TGAAAACTCCCTCTATATAGATTGCTC
		GFP_SIR	CTCGACGAGGATGGGCAC
	ProE7:ARR1	ARR1_SIF	TTGAGGTCGACCTACATAGAGAGAGG
		ARR1_PtR	TTTCTGCAATCAAAACCGAAATGTCGATG
	ProZmE7:axr2-1	AXR3_SmF	ACC CGG GAT GAT GGG CAG TGT CGAG
		AXR2_SmF	ACC CGG GAT GAT CGG CCAACT TAT G
	ProZmE7:iaa2-1	p33nosR	ACC GGC AAC AGG ATT CAATC
	ProAXR2:AXR2	AXR2_SIF	ATAGTCGACATGATCGGCACACTTATG
		AXR2_KnR	ATCAGGTACCCGTCATATGTTGATCA
	axr2-1	axr2-1F228Bm	CTTCGGATCTTCTTCTTCCCTCTTAC
		axr2-1R2303Kn	ATCAGGTACCCGTCATATGTTGATCA
	axr3-1	axr3-1F268Bm	AAGAGGATCCCAAGAAAGAAAGGTT
		axr3-1R2268Kn	AATGGTACCACAAGCTCTGCTCTTGCA
	GFP	ProEGFP F260Bm	TAGAGGATCCCGGTACAGGTCG
		ProEGFP R1056Kn	TAA TGG TAC CGA CCG GCG CTC AGT TG
		GFP_HdF	TGAAAACTCCCTCTATATAGATTGCTC
		GFP_SIR	CTCGACGAGGATGGGCAC
	GUS	ProBI121F5731Bm	TGAGGATCCCGGTGGTCAGT
		ProBI121R7626Kn	CTCGGTACCAATTCGAGGCAGT
	ProAXR2	ProAXR2_HdF	TATAAAGCTTGAACAACCGATCA
		ProAXR2_SIR	TATAGTCGACGTACTTGTAAATAGA
	ProSHY2	ProSHY2_SIF	TTTCTGCTGACTGCTACTATAGTAAATTC
		ProSHY2_BmR	AGA GGA TCC AAA GAAAGCTTTGTTAT
	ProZmE7	ProZmE7_HdF	CTACGAAGCTTCAAGAAGCCCA
		ProZmE7_XmR	CAT TAC CCG GGC TGT TTC C
	shy2-1	shy2-1F78Bm	TTC TGG ATC CAT TCT TGAAGAATAAGT
		shy2-1R2961Kn	TCTCGGTACCAAAGAACTCTATTTT
	ProSHY2:shy2-1	shy2-1F78Bm	TTC TGG ATC CAT TCT TGAAGAATAAGT
EGFPXb1031R		GAA TTC TAG AGT CGC GGC CGC TTT	
ProZmE7:shy2-1:GFP	shy2-1_AvF	TAG TCC TAG GGC AAT TCT TGAAGAAA	
	GFP_XbR	TCA GTT GGA ATT CTAGAG TCG C	
ProAXR2:shy2-1:GFP	shy2-1_SIF	ATAGTCGACATGATGAGTTTGTAAAC	
	GFP_KnR	ATCAGGTACCCGTCATATGTTGATCA	

**Table 3.** The primer list (continued)

Subject		Primer name	Primer sequence (5' to 3')
Transgene constructs	ProE7:SHY2-RNAi1	SHY2FKn-New	TTT TGG TAC CTA TCC TTG AAA GAGA
		SHY2FHd(i)-New	TTAAGC TTA TTA TCC TTG AAA GAGA
		SHY2FXb(i)-New	TCT CTA GAT CAG AAAACAGTT TCT TCT
	ProE7:SHY2-RNAi2	shy2F-3UT-XhF	TAT ATC TCG AGG ATA TAT CTT CAAGAAATC T
		shy2F-3UT-KpR	ACC AAT TGG GGT ACC CAT TTG AAT TTT ACC GAT G
		shy2R-3UT-HdF	GAAATC GAT AAG CTT CAT TTG AAT TTT ACC GAT G
		shy2R-3UT-XbR	TAT ATT CTA GAG ATA TAT CTT CAAGAAATC T
	Dex-inducible expression	SHY2_PacIF	CCG GTT AAT TAA TCA TGG ATG AGT TTG TTA AC
		EGF-MI-R	GCC ACG CGT CTT GTA CAG CTC GTC C
		GR_SpeIF	ACC ACT AGT GTA CGG TGG GGA TCC AAT TCA
	N-terminal SHY2	GR_SpeIR	ACC ACT AGT CTC AGT TAG GTC GAG TCATT
		SHY2_DIF	ATC GTC GAC ATG GAT GAG TTT GTT AAC C
		SHY2_DmlR	TAA TCC CAG CGC CAG CTC
	N-terminal AXR2	SHY2_DIIR	ATC GGC GCG CCC TAT TCT TCT TAC TCT GAA TGT TGT T
		AXR2_DF	ATG CGT CGA CGG ATG ATC GGC CAA CTT ATG
	SHY2DImII, SHY2DmlmII	AXR2_DIIR	ATC GGC GCG CCT CGT TCT TCC TGT AGT TCC TCA C
		SHY2-Sall-F	ATC GTC GAC ATG GAT GAG TTT GTT AAC C
	AXR2DImII, AXR2DmlmII	SHY2DII-AscR	ATC GGC GCG CCC TAT TCT TCT TAC TCT GAA TGT TGT T
		AXR2-Sall-F	ATG CGT CGA CGG ATG ATC GGC CAA CTT ATG
	IAA2, iaa2-1, IAA2-C17R, IAA2ml	AXR2DII-AscR	ATC GGC GCG CCT CGT TCT TCC TGT AGT TCC TCA C
		IAA2-Sm-F	TGA TCC CGG GGC AAT GGC GTA CGA GAA AGT
		IAA2-m1'x_R	GGT AAT CCA AGA GCT AGC TCT
		iaa2-1m294R	TCA CTG ATG GCC AAC CAA C
Proteins for pull-down assay	His-tagged TPL	IAA2-Sm-R	CAA ACC CGG GTC AGC TTC TCT GGA TCA TAA GG
		His-TPL-EcF	AAA GAA TTC ATG TCT TCT CTT AGT AGA G
	GST-tagged TPL	His-TPL-Nt-SIR	CAA AGT CGA CTC AAT TTT TAC AAA GCT G
		GST-Hd-F	AAA AAA GCT TTA ATG TCC CCT ATA CTA GGT
	HIS- or GST-tagged SHY2	GST-Xh-R(stop)	AAA ACT CGA GTC AGG AAC CAG ATC CGA TTT
		shy2-Kp1F	AAA AGG TAC CAT GGA TGA GTT TGT TAA CC
HIS- or GST-tagged SHY2	shy2-Bm567R	AAA AGG ATC CTA CAC CAC AGC CTA AAC CTT	
	axr2-Kp1F	AAA AGG TAC CAT GAT CGG CCA ACT TAT GAA	
Proteins for MST assay	GST-tagged SHY2	axr2-Bm729R	AAA AGG ATC CAG ATC TGT TCT TGC AGT ACT
		S2-GST-SI1F	CCG GGT CGA CTC ATG GAT GAG TTT GTT AAC
	GST-tagged AXR2	S2-GST-Nt1R	CGA TGC GGC CGC TCA TAC ACC ACA GCC TA
		axr2-1F228Bm	CTT CGG ATC CTT TCT TCT TCC CCT CTT AC
		axr2-GST-Nt1R	AGC TGC GGC CGC TCA AGA TCT GTT CTT GCA GTA

## 2.4 Results

### 2.4.1 Opposite root hair phenotypes between gain-of-function *aux/iaa* mutants

Aux/IAA inhibits auxin signaling as a transcription repressor. Gain-of-function (GOF) *aux/iaa* proteins are not degraded by auxin; thus, they are accumulated in a cell. Through analogy with the auxin inhibition condition, it was anticipated that GOF *aux/iaa* mutants would show a short-root-hair phenotype. Two GOF *aux/iaa* mutants, *axr2-1* and *axr3-1*, which are stabilized IAA7 and IAA17, seedlings grew considerably shorter root hairs or almost no root hairs compared with the control plant (Cont, *ProE7::GFP*), as previously reported (Knox et al., 2003; Leyser et al., 1996; Wilson et al., 1990). However, a similar stabilized IAA3 mutant, *shy2-1* (Soh et al., 1999), grew root hairs that were ~126% the length of the control plant (Figure 3). This raises challenging questions, such as whether certain Aux/IAAs are not necessarily repressors, but act as activators for auxin responses.

### 2.4.2 A similar phenotypes in root hair-specifically expressed *aux/iaas* GOF transformants

The difference in expression patterns might result in the opposite root hair phenotypes among stabilized Aux/IAA mutants. To explore this question, root hair-specific *EXPANSIN A7* promoter (*ProE7*; Cho and Cosgrove, 2002; Kim et al., 2006) was used to express stabilized Aux/IAAs in the root hair specifically.

*P r o E 7 : a x r 2 - l*

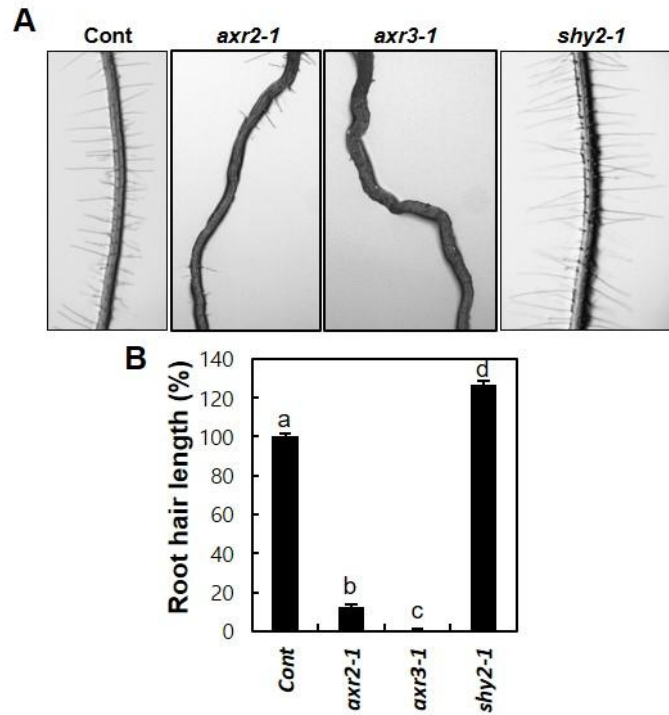


**Figure 3. SHY2 positively but AXR2 and AXR3 negatively regulate root hair growth.** (A) Root hair phenotypes of wild-type (Cont) and three gain-of-function *aux/iaa* mutants (*shy2-1*, *auxr2-1*, and *auxr3-1*). Scale bar is 500  $\mu$ m. (B) Root hair lengths of Cont and *aux/iaa* mutants. Data represent means  $\pm$  s.e. (n = 192–240 root hairs from independent lines). Statistically significant differences are denoted with different letters (one-way ANOVA with Tukey’s unequal N-HSD *post hoc* test,  $P < 0.05$ ).

(*axr2-1ox*) inhibits root hair growth (Won et al., 2009). This is similar to the root hair phenotype of the *axr2-1* GOF plant. It appears that that *axr2-1* completely blocked auxin signaling in the root hair cells (Figure 4A). Even *ProE7:shy2-1* (*shy2-1ox*) and *ProE7:SHY2* (*SHY2ox*) also showed almost complete inhibition of root hair growth, suggesting that the inhibition of root hair growth by *shy2-1* was not due to its mutation in the degron (Figure 4). These results indicated that *axr2-1*, *shy2-1*, and SHY2 have similar roles as repressors of root hair growth and auxin response. However, root hair phenotype of *shy2-1* GOF seedlings have already been observed the opposite. They had longer root hairs than those of the control plant (Figure 3). Thus, it was analyzed whether root hair expressing *shy2-1* and SHY2 still inhibited root hair growth in the *shy2-1* mutant background. Both stabilized and wild-type SHY2 in *shy2-1* GOF mutants almost completely or greatly suppressed root hair growth. These results intriguingly indicate that root hair specifically overexpressed SHY2 and either stabilized or wild-type proteins inhibited root hair growth, even though intrinsic stabilized SHY2 enhanced root hair growth (Figure 4).

#### 2.4.3 The difference in promoter activities of *ProE7*, *ProSHY2*, and *ProAXR2*

It was wondered whether SHY2 enhances root hair growth in a non-cell autonomous manner because root hair overexpressing SHY2 still maintained the property as a repressor, whereas *shy2-1* GOF appeared like an activator in root hair cell growth. This led to examine whether SHY2 indeed expresses in the root hair

cell. The expression pattern of shy2-1:GFP fusion proteins were analyzed under the

*S*

*H*

*Y*

2

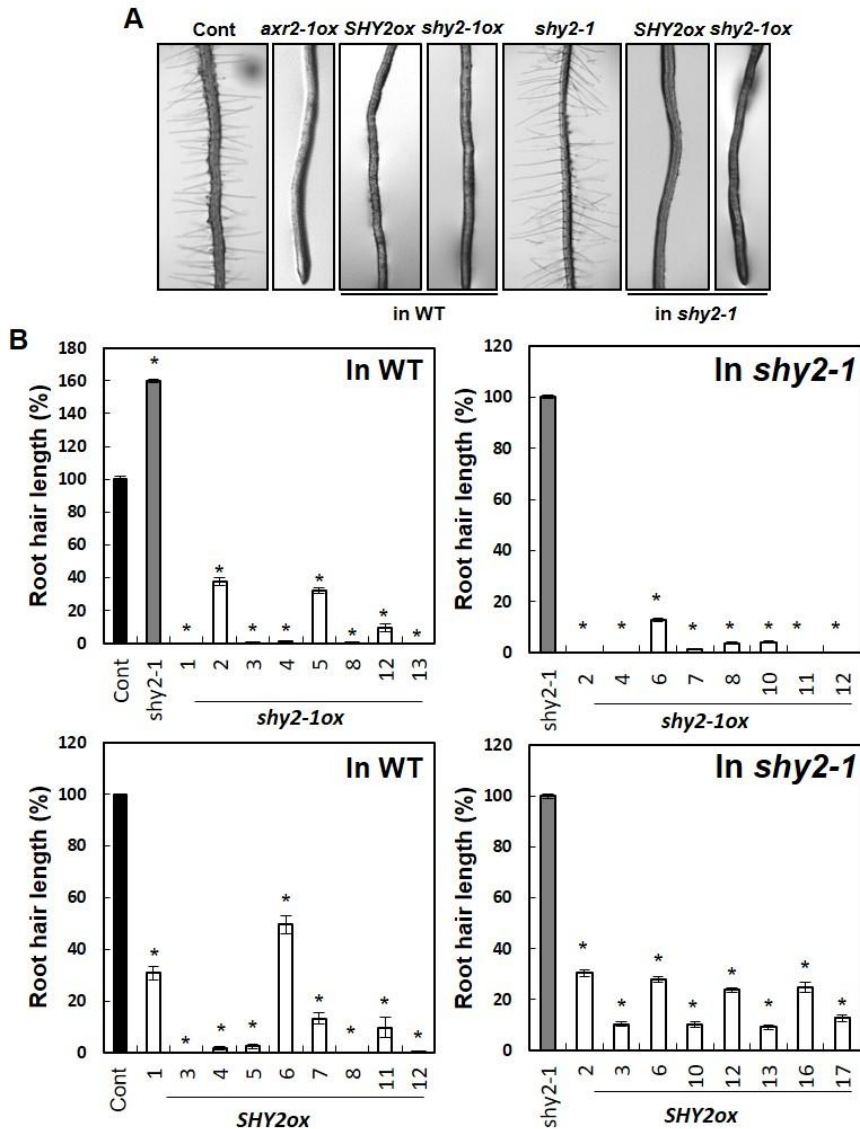


**Figure 4. Root hair lengths of the independent transgenic lines including *ProE7:SHY2* or *ProE7:shy2-1* in WT or *shy2-1* background. (A) Root hair phenotypes of control (Cont, *ProE7:GFP*) and root hair-specific overexpression lines of *axr2-1*, *shy2-1*, and *SHY2* (*axr2-1ox*, *ProE7:axr2-1*; *shy2-1ox*, *ProE7:shy2-1*; and *SHY2ox*, *ProE7:SHY2*) in wild-type (WT) background or *shy2-1* mutant. (B) Root hair lengths of control and *shy2-1*, and root hair-specific overexpression**

transformants (*shy2-1ox*, and *SHY2ox*) in WT and *shy2-1* backgrounds. Data represent means  $\pm$  s.e. (n = 160–700 root hairs form Cont, *shy2-1*, and independent lines). The values are relative to the control values and significantly different ( $*P < 0.0001$ ; Student's t test) from the control values or *shy2-1* values.

promoter (*ProSHY2*) in the root. For this construct under *ProSHY2*, the strongest expression was seen in the vascular tissue. However, albeit weaker than in the vasculature, obvious expression was observed in the root hair cells (Figure 5A). These expression and localization results suggest that SHY2 can hair-cell-autonomously affect root hair growth.

For the control of root hair cell expression, the *shy2-1:GFP* under *ProE7* was expressed. This promoter directly expressed *shy2-1:GFP* in the root hair cell nucleus (Figure 5A). Then, it was discovered that the intensity of *shy2-1:GFP* driven by *ProE7* was stronger than that driven by *ProSHY2*. I analyzed whether promoter intensity can affect the function of Aux/IAAs. The expression pattern of *shy2-1:GFP* under the *AXR2* promoter (*ProAXR2*) was also checked. The promoter strengths of these three promoters in the root hair cell were estimated by measuring the *shy2-1:GFP* fluorescence levels in the root hair cell nucleus. The expression ratio of *shy2-1:GFP* was approximately 10:1:3.5 for *ProE7:shy2-1-GFP*, *ProSHY2:shy2-1-GFP*, and *ProAXR2:shy2-1-GFP*, respectively (Figure 5B). Because the expression strength of *ProSHY2* in a root hair cell was considerably weaker than that of *ProE7* and *ProAXR2*, I hypothesize that the difference in promoter strength induces the opposite phenotypes between *shy2-1* GOF and *ProE7:shy2-1:GFP* and between *shy2-1* GOF and *axr2-1* GOF.

To further analyze the relationship between protein ability and promoter intensity, the stabilized forms of three Aux/IAAs using the *SHY2* promoter were

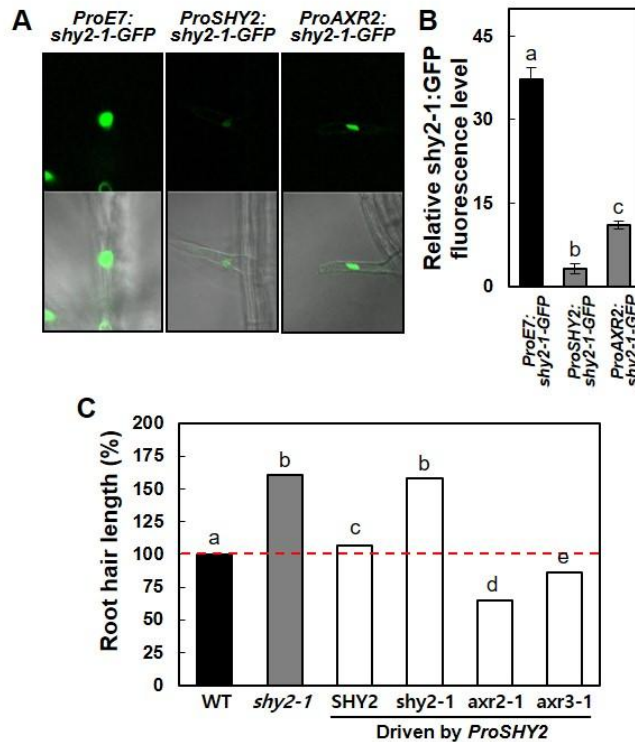


**Figure 5. SHY2 positively and AXR2 and AXR3 negatively regulate root hair growth.** (A) Nuclear localized *shy2-1:GFP* in root hair cells. (B) Relative levels of *shy2-1:GFP* fusion protein expressed under different promoters. The expression levels were estimated from the nuclear GFP signal intensity from 15 roots for each construct. Data represent means  $\pm$  s.e. ( $n = 10\text{--}25$  root hair cells from independent lines). Statistically significant differences are denoted with different letters (one-way ANOVA with Tukey's unequal N-HSD *post hoc* test,  $P < 0.05$ ). (C) Root hair lengths of WT, *shy2-1*, and *SHY2* and *aux/iaa* transformants. Wild-type *SHY2* and gain-of-function mutant genes (*shy2-1*, *axr2-1*, and *axr3-1*) were expressed under the *SHY2* promoter (*ProSHY2*) in the WT background. Data represent means  $\pm$  s.e. ( $n = 945\text{--}10,762$  root hairs from WT, mutant, and independent transgenic lines). Statistically significant differences are denoted with different letters (one-way ANOVA with Tukey's unequal N-HSD *post hoc* test,  $P < 0.05$ ). Hayeon Lee performed these experiments.

expressed. *ProSHY2:shy2-1* in the wild-type background recapitulated the root hair phenotype of the *shy2-1* mutant (Figure 5C). Introducing another copy of wild-type SHY2 with its own promoter also slightly enhanced root hair growth (Figure 5C). However, stabilized AXR2 and AXR3 under *ProSHY2* significantly inhibited root hair growth. In themselves, AXR2 and AXR3 proteins had stronger repression activity than the activity of SHY2. These results further support the idea that SHY2 is an activator but AXR2 and AXR3 are suppressors for root hair growth under *ProSHY2*. Nevertheless, SHY2 is not always an activator. It is likely that *shy2-1* and SHY2 driven by *ProE7* resulted in short root hair though SHY2 showed a weaker repression function than *shy2-1* (Figures 3 and 4C). This indicates again that the function of *shy2-1* or SHY2 is variable according to expression intensity, whereas *axr2-1* and *axr3-1* have a consistent repression function in root hair growth.

#### 2.4.4 Native SHY2 has a positive effect on root hair growth

To further support the idea that SHY2 cell-autonomously controls root hair growth and to demonstrate the molecular function of native SHY2 in root hair growth, I observed the root hair phenotype of *shy2-31* loss-of-function (LOF) and SHY2-RNA interference (RNAi) lines, which have a decreased SHY2 level. I analyzed the root hair phenotype of *shy2-31* LOF mutant in a Landsberg *erecta* (*Ler*) background (Knox et al., 2003). The *shy2-31* LOF showed significantly shorter root hair length than *Ler* or Col-0 (Figure 6). Additionally, I conducted root hair-specific RNAi of SHY2 using *ProE7*. I made two independent RNAi constructs and introduced them

into a wild-type or *shy2-1* mutant. Both RNAi1 and RNAi2 significantly decreased

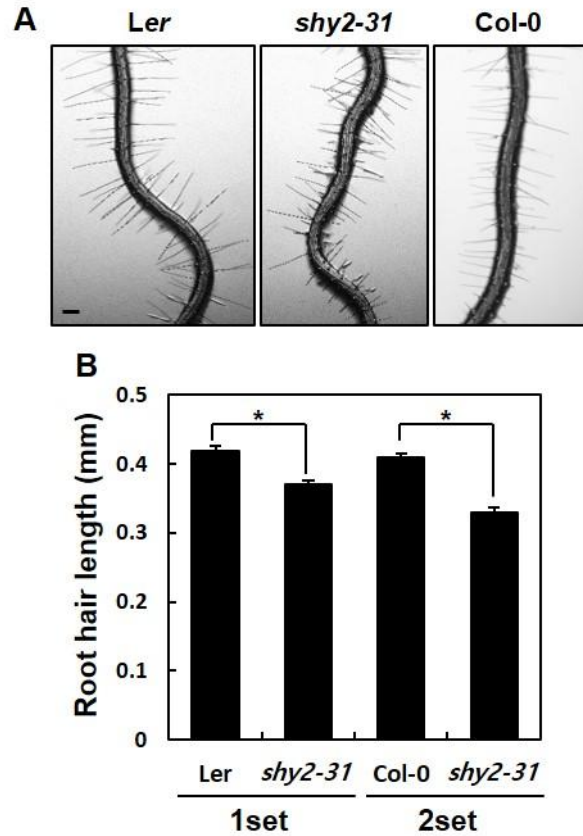


**Figure 6. SHY2 positively regulates root hair growth.** (A) Root hair phenotypes of Landsberg *erecta* (*Ler*), loss-of-function *shy2* mutant (*shy2-31*), and Columbia (*Col-0*). (B) Two sets of root hair length assay. Data represent means  $\pm$  s.e. ( $n = 269-295$  root hairs from 1set and  $n = 291-420$  root hairs from 2set). Differences are

significant ( $*P < 0.0001$ ). Scale bar is 100  $\mu\text{m}$ .

the *SHY2* transcript levels compared with those of their corresponding non-transgenic lines (Figure 7). Accordingly, *SHY2-RNAi* transformants in both wild-type and *shy2-1* backgrounds grew root hairs that were 16 to 32% (on average among independent lines for each construct) of the root hair length of the controls (Figure 7). Together with the root hair-expression pattern of native SHY2 (Figure 5A), this root hair-inhibition by root hair-specific *SHY2-RNAi* strongly suggests that the native SHY2, functioning in the root hair cell, is a positive effector for root hair growth. However, the question remains of how the SHY2 molecule can enhance root hair growth, but at the same time a high dose of SHY2 inhibits root hair growth.

#### 2.4.5 Transcriptional activity of SHY2 depends on its dose in a cell

*ProSHY2* and *ProAXR2* were able to drive *shy2-1* expression in the root hair cell, but these promoters did not have specificity to the root hair cell. To further specify the dose effect of *shy2-1* in the root hair cell, the stabilized *shy2-1* into the root hair cell was introduced using *ProZmE7*, the root hair-specific cis-elements (RHEs) including maize *EXPA7* promoter, but with a much weaker strength than *Arabidopsis ProE7* (Kim et al., 2006). If *shy2-1*, expressed by *ProSHY2* in the root hair cell at lower levels than that by *ProE7*, could enhance the root hair growth, the weak root hair-specific *ProZmE7*-driven *shy2-1* should phenocopy the *ProSHY2:shy2-1* transformant. *ProZmE7:shy2-1* transgenic lines showed varying phenotypes in root hair growth that were longer or shorter than or similar to the

wild type (Figure 8). On the other hand, all the *ProZmE7:axr2-1* and *ProZmE7:axr3-1* transgenic lines consistently grew shorter root hairs than the control plants (Figure 8). Because I

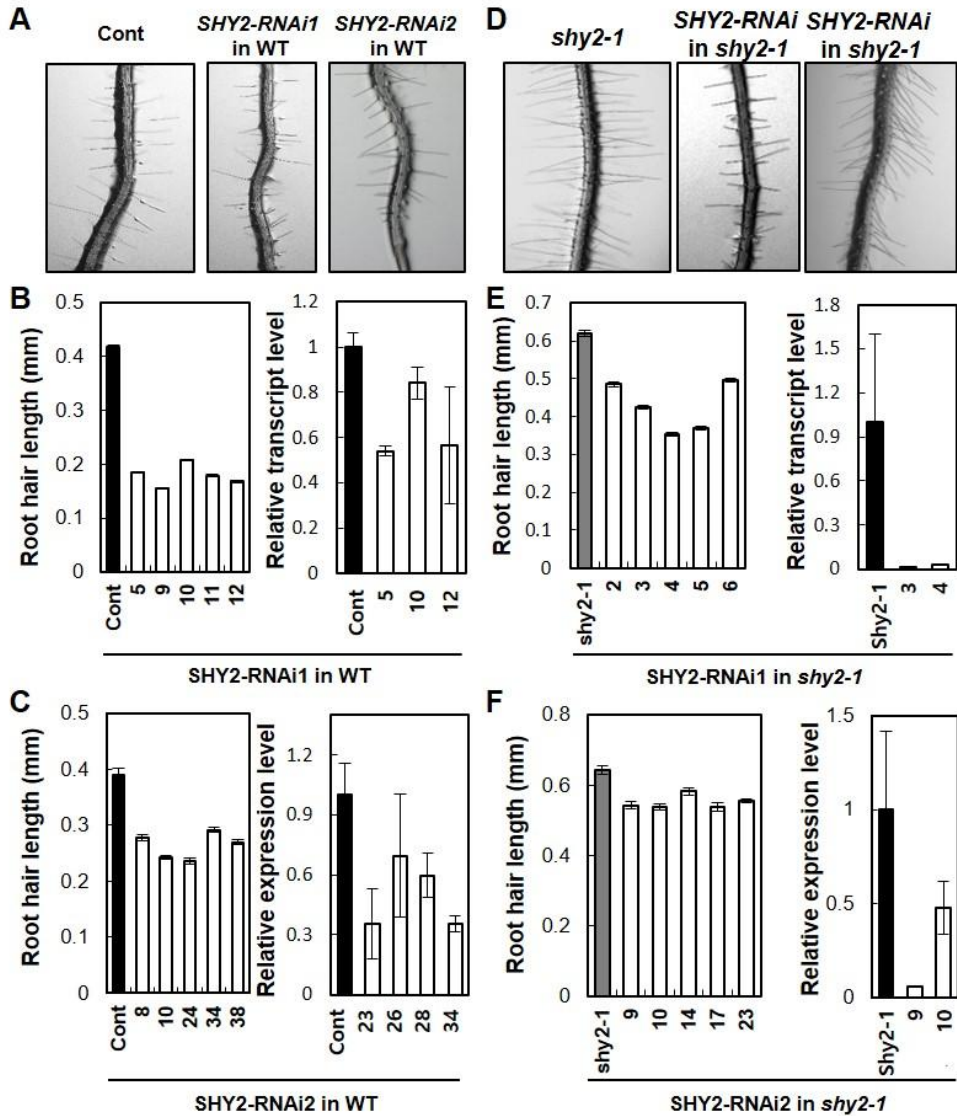


**Figure 7. Both root hair length and the *SHY2* transcript level in root hair-specific *SHY2-RNAi* lines showed a repressed aspect compared to wild-type plants or *shy2-1* mutants. (A) The root hair phenotypes of *ProE7::GFP* (Cont) and two type of root hair-specific RNA interference of *SHY2* transformants (*SHY2-RNAi1* and *SHY2-RNAi2*) in WT background. (B and C) Root hair lengths and *SHY2* transcript levels of *SHY2-RNAi1* and *SHY2-RNAi2* in WT background. Root**

hair data represent means  $\pm$  s.e. (n = 691–800 root hairs). (D) Root hair phenotypes of *shy2-1*, *SHY2-RNAi1*, and *SHY2-RNAi2* in *shy2-1* background. (E and F) Root hair lengths and *SHY2* transcript levels of *SHY2-RNAi1* and *SHY2-RNAi2* in *shy2-1* background. Root hair data represent means  $\pm$  s.e. (n = 213–495 root hairs). Transcript data represent means  $\pm$  s.d. from two independent experiments.

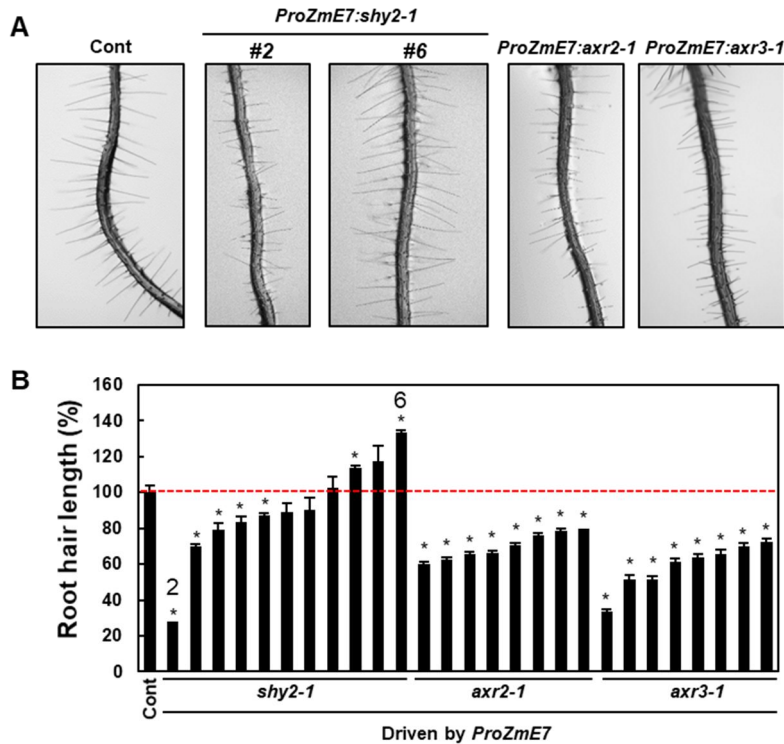


**Figure 8.** *shy2-1* expression levels inversely correlate with root hair growth, in contrast to *axr2-1* and *axr3-1*. (A) Representative root hair phenotype images of the control (Cont; *ProE7:YFP*), short- or long-haired *ProZmE7:shy2-1*, *ProZmE7:axr2-1*, and *ProZmE7:axr3-1* lines. (B) Relative root hair length of the control, and transgenic lines as described in (A). Data represent means  $\pm$  s.e. ( $n = 526\text{--}3,356$  root hairs from Cont,  $n = 502\text{--}2354$  root hairs from *ProZmE7:shy2-1*,  $n = 336\text{--}800$  root hairs from *ProZmE7:axr2-1*,  $n = 95\text{--}241$  root hairs from *ProZmE7:axr3-1*). Differences are significant ( $*P < 0.05$ ). Hayeon Lee and Min-Soo Lee performed these experiments.

hypothesized regarding the dose dependency of the SHY2 function for root hair growth, it was conceivable that the varying root hair lengths of the *ProZmE7:shy2-1* transformants could result from the different expression levels among different transgenic lines.

To test this possibility, two independent lines from long- and short-root-haired groups were selected (Figure 8). When analyzed by quantitative RT-PCR, the *shy2-1:GFP* transcript levels of the short-root-haired lines (#2) were considerably higher (~four-fold on average) than those of the long-haired lines (#6) (Figure 9A). The root hair-specific cell wall-loosening factor expansins (*EXPA7* in Arabidopsis and *OsEXPA17* and *30* in rice) were required for normal root hair tip growth in Arabidopsis and rice (Lin et al., 2011; ZhiMing et al., 2011), and the *EXPA7* expression was shown to be positively regulated by auxin signaling (Cho and Cosgrove, 2002; Won et al., 2009). The short-haired *ProZmE7:shy2-1* and long-haired lines expressed significantly lower and much higher levels of *EXPA7* than that of the wild type, respectively. The *ProE7:shy2-1* transformants also expressed much lower levels of *EXPA7* than that of the wild type (Figure 9B). These results also show a consistent correlation among *shy2-1* doses, root hair lengths, and *EXPA7* levels.

A recent study showed that RHD6-LIKE 4 (RSL4, a bHLH transcription factor) regulates *EXPA7* transcription. RSL4 is a developmental cue in root hair growth and mediates auxin and root hair growth (Hwang et al., 2017; Mangano et al., 2017; Yi et al., 2010). I tested whether *RSL4* expression was also regulated by

shy2-1 in a dose-dependent manner. First, the *RSL4* transcript level was considerably

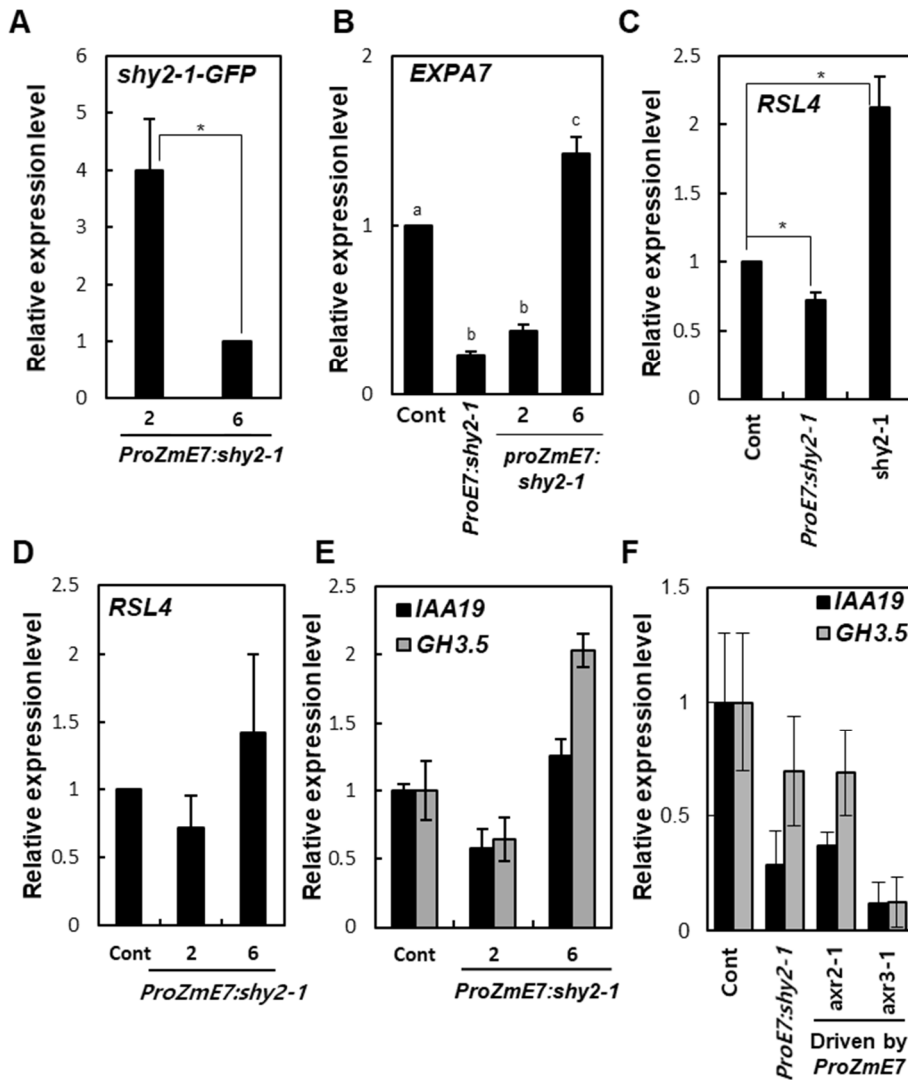


**Figure 9.** *shy2-1* expression levels inversely correlate with the expression of root hair-related and auxin-responsive genes. Quantitative RT-PCR analyses of *shy2-1:GFP* (A), *EXPA7* (B), root hair regulatory genes (*RSL4*, D) and auxin responsive genes (*IAA19* and *GH3.5*, E) transcripts of control and *ProZmE7:shy2-1* lines. Data represent means  $\pm$  s.e. from two independent experiments. Statistically significant differences are denoted with different letters (one-way ANOVA with Tukey's unequal N-HSD *post hoc* test,  $P < 0.05$ ). (C) Transcript level of *RSL4* of control, *ProE7:shy2-1:GFP*, and *shy2-1*. Data represent means  $\pm$  s.e. from four

independent experiments. The values are significantly different ( $*P < 0.05$ ) for the control value. (F) Transcript level of *IAA19* and *GH3.5* of control, *ProE7:shy2-1*, *ProZmE7:axr2-1*, and *ProZmE7:axr3-1*. Data represent means  $\pm$  s.e. from three independent experiments. Hayeon Lee and Min-Soo Lee contributed to these experiments.

increased in the long-haired *shy2-1* mutant, whereas it was reduced in the short-haired *ProE7:shy2-1* transformant (Figure 9C). In the *ProZmE7:shy2-1* transgenic background, the long-haired lines expressed more RSL4 transcripts than the short-haired lines (Figure 9D). This suggests that the SHY2-dependent regulation of *EXPA7* could be achieved by the SHY2-mediated modulation of RSL4, consistent with the previous model.

The *EXPA7* gene, with no auxin response element in its promoter region and regulated by RSL4, does not seem to be the primary target of auxin signaling. To determine whether the typical primary target genes in auxin response are modulated in a *shy2-1* dose-dependent manner, the transcript levels of *IAA19* and *Gretchen Hagen3-5 (GH3-5)* (Paponov et al., 2008) were quantitatively analyzed in long- or short-haired *ProZmE7:shy2-1* lines. Similarly, with the *EXPA7* and *RSL4* results, the expression of these primary auxin-responsive genes also showed an inverse relationship with the *shy2-1* dose (Figure 9E). Additionally, I analyzed the transcript levels of *IAA19* and *GH3-5* from *ProE7:shy2-1*, *ProZmE7:axr2-1*, and *ProZmE7:axr3-1* seedlings, the transgenic lines of which showed only short root hair (Figure 9F). In these short-haired lines, the down-regulated auxin-responsive genes indicate that a high dose of *shy2-1*, stabilized AXR2, and AXR3 repress auxin-responsive genes. This root hair-specific dose-effect analysis strongly supports the idea that SHY2 can mediate auxin signaling in the root hair either positively or negatively depending on its dose. These results again indicate that AXR2 and AXR3 play only a negative role in the auxin response in the root hair cell, whereas SHY2 has dose-dependent dual functions.

## 2.4.6 Introducing a DEX-inducible system to reduce variations between transgenic lines

Although *ProZmE7* specifically drives down-stream genes in a root hair cell, the expression intensity of the promoter is different between all independent lines. To sensitively distinguish the dose effect of *shy2-1* in a root hair cell, a dexamethasone (DEX)-inducible system (Lloyd et al., 1994; Park et al., 2002; Schena et al., 1991) was introduced. This system allowed the gradual expression of stabilized *shy2-1* into the root hair cell using *ProE7*. The fused glucocorticoid receptor, a steroid-binding domain, to *shy2-1:GFP* inactivated the function of *shy2-1* in the absence of ligand DEX by capturing it in the cytosol. The function of *shy2-1* as a transcription factor was activated in the presence of ligand DEX by permitting the nuclear localization of *shy2-1*. The level of *shy2-1:GFP:GR* in a root hair cell and the root hair cell length were tested. Following gradually increasing the DEX concentration from 0 to 1  $\mu\text{M}$ , the level of the GFP signal was stronger and each step showed a significantly different signal intensity (Figure 10A, C). In this experiment, I also measured the root hair length in each DEX concentration step (Figure 10B, D). The highest level of *shy2-1:GFP:GR* exhibited the shortest root hair compared with the root hair length of the lower DEX concentration step. This means that a high level of *shy2-1* in the cell resulted in short root hair (likely the root hair phenotype of *ProE7:shy2-1*). The root hair length from each DEX concentration step gradually decreased following increasing the DEX concentration, except the root hair from the 0.1 nM DEX step

(Figure 10D). Even though the relative GFP intensity of the 0.1 nM DEX step was

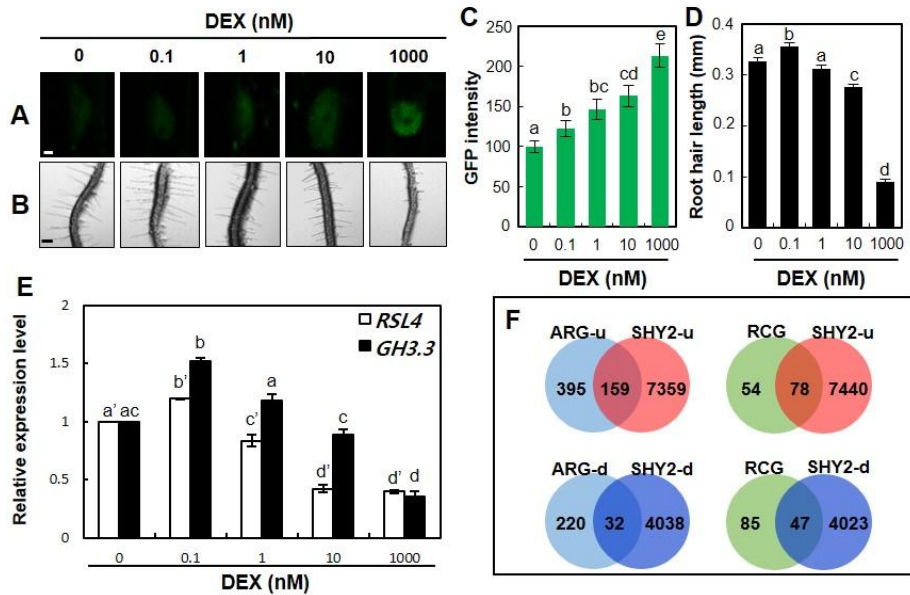


**Figure 10. *shy2-1* shows a dose-dependent activation/repression switch for root hair growth and auxin-responsive gene expression.** (A–D) Changes of nuclear *shy2-1*:GFP signal levels (A and C) and root hair length (B and D) of *ProE7:shy2-1:GFP:GR* transformants in different DEX induction conditions. Data represent means  $\pm$  s.e. ( $n = 89\text{--}110$  nuclei for each treatment [C] and  $332\text{--}400$  root hairs [D]). Scale bar is  $1\ \mu\text{m}$ . (E) Changes in the auxin-responsive gene (*RSL4* and *GH3.3*) expression of *ProE7:shy2-1:GFP:GR* transformants in different DEX induction conditions. Data represent means  $\pm$  s.e. ( $n =$  four RNA samples). Statistically significant differences are denoted with different letters (one-way ANOVA with Tukey's unequal N-HSD *post hoc* test,  $P < 0.05$ , C, D, E). (F) Venn diagrams showing numbers of *shy2-1*:GFP:GR-mediated up-regulated genes (SHY2-u) by  $0.1\ \text{nM}$  DEX and down-regulated genes (SHY2-d) by  $1,000\ \text{nM}$  DEX, and their overlapping gene numbers with up-(ARG-u) or down-(ARG-d) regulated genes by auxin and root hair-specific cis-element (RHE)-containing genes (RCG). The identification of differentially expressed genes was based on the criterion of the false discovery rate  $|FC| \geq 1.2$ . Min-Soo Lee contributed to these experiments.

Gene ID	Gene Symbol	Description	Fold change
AT5G66920	sks17	SKU5 similar 17	1.291195
AT5G65270	RABA4a	RAB GTPase homolog A4A	1.250846
AT5G63810	BGAL10	beta-galactosidase 10	1.319188
AT5G61010	EXO70E2	exocyst subunit exo70 family protein E2 (AT5G61010.1; AT5G61010.2)	1.302257
AT5G59370	ACT4	actin 4 (AT5G59370.1; AT5G59370.2)	1.255392
AT5G58620	MZN1.16	zinc finger (CCCH-type) family protein	1.542173
AT5G55050	K13P22.5	GDSL-like Lipase/Acylhydrolase superfamily protein	1.246435
AT5G54500	FQR1	flavodoxin-like quinone reductase 1 (AT5G54500.1; AT5G54500.2)	1.257387
AT5G53290	CRF3	cytokinin response factor 3	1.272981
AT5G52890	MXC20.12	AT hook motif-containing protein (AT5G52890.1; AT5G52890.2)	1.28099
AT5G51670	K10D11.2	Protein of unknown function (DUF668)	1.310845
AT5G51380	MFG13.9	RNI-like superfamily protein	1.303908
AT5G50300	AZG2	Xanthine/uracil permease family protein	1.806499
AT5G49170	K21P3.4	unknown protein	1.407549
AT5G48900	K19E20.1	Pectin lyase-like superfamily protein	1.305318
AT5G45280	K9E15.6	Pectinacetylterase family protein (AT5G45280.1; AT5G45280.2)	1.939167
AT5G44910	K21C13.9	Toll-Interleukin-Resistance (TIR) domain family protein	1.586851
AT5G44260	K9L2.1	Zinc finger C-x8-C-x5-C-x3-H type family protein	1.710705
AT5G40590	MNF13.11	Cysteine/Histidine-rich C1 domain family protein	1.694151
AT5G39580	MIJ24.50	Peroxidase superfamily protein (AT5G39580.1; AT5G39580.2)	1.520972
AT5G38710	MKD10.10	Methylenetetrahydrofolate reductase family protein	1.231816
AT5G27000	ATK4	kinesin 4	1.536093
AT5G26930	GATA23	GATA transcription factor 23	2.054949
AT5G25460	F18G18.200	Protein of unknown function, DUF642	1.771081
AT5G18470	T28N17.6	Curculin-like (mannose-binding) lectin family protein	1.290591
AT5G17340	MKP11.1	Putative membrane lipoprotein	1.635334
AT5G15160	BNQ2	BANQUO 2	1.697007
AT5G13460	IQD11	IQ-domain 11	1.220424
AT5G12940	T24H18.110	Leucine-rich repeat (LRR) family protein	1.419484
AT5G12050	F14F18.220	unknown protein	1.580913
AT5G07110	PRA1.B6	prenylated RAB acceptor 1.B6	1.290211
AT5G06860	PGIP1	polygalacturonase inhibiting protein 1	1.32103
AT4G39990	RABA4B	RAB GTPase homolog A4B	1.346898
AT4G39390	NST-K1	nucleotide sugar transporter-KT 1 (AT4G39390.1; AT4G39390.2; AT4G39390.3)	1.390564
AT4G38410	F22113.180	Dehydrin family protein	2.026826
AT4G37870	PCK1	phosphoenolpyruvate carboxykinase 1	1.216197
AT4G37450	AGP18	arabinogalactan protein 18	1.269476
AT4G36500	AP22.75	unknown protein	1.4309
AT4G32460	F8B4.160	Protein of unknown function, DUF642 (AT4G32460.1; AT4G32460.2)	1.796166
AT4G32350	F8B4.50	Regulator of Vps4 activity in the MVB pathway protein	1.261607
AT4G31910	F11C18.110	HXXXD-type acyl-transferase family protein	1.259775
AT4G30850	HHP2	heptahelical transmembrane protein2 (AT4G30850.1; AT4G30850.2)	1.331761
AT4G30420	F17I23.240	nodulin MtN21 /EamA-like transporter family protein	1.409844
AT4G30290	XTH19	xyloglucan endotransglucosylase/hydrolase 19	1.469902
AT4G30280	XTH18	xyloglucan endotransglucosylase/hydrolase 18	1.564124
AT4G30140	CDEF1	GDSL-like Lipase/Acylhydrolase superfamily protein	3.047638
AT4G30080	ARF16	auxin response factor 16	1.36841
AT4G25420	GA20OX1	2-oxoglutarate (2OG) and Fe(II)-dependent oxygenase superfamily protein	2.704396
AT4G22610	F7K2.190	Bifunctional inhibitor/lipid-transfer protein/seed storage 2S albumin superfamily protein	2.967628
AT4G22530	F7K2.110	S-adenosyl-L-methionine-dependent methyltransferases superfamily protein	1.546213
AT4G22470	F7K2.50	protease inhibitor/seed storage/lipid transfer protein (LTP) family protein	7.651837
AT4G19460	F24J7.20	UDP-Glycosyltransferase superfamily protein	1.288178
AT4G16670	DL4360W	Plant protein of unknown function (DUF828) with plant pleckstrin homology-like region	1.665666

**Table 4.** The list of overlapping SHY2-u genes with up-regulated genes by auxin.

**Table 4.** The list of overlapping SHY2-u genes with up-regulated genes by auxin

Gene ID	Gene Symbol	Description	Fold change
AT4G15160	DL3625W	Bifunctional inhibitor/lipid-transfer protein/seed storage 2S albumin superfamily protein (AT4G15160.1; AT4G15160.2)	1.698987
AT4G14560	IAA1	indole-3-acetic acid inducible	1.362186
AT4G13710	F18A5.100	Pectin lyase-like superfamily protein	1.208143
AT4G13210	F17N18.100	Pectin lyase-like superfamily protein	1.578373
AT4G12110	SMO1-1	sterol-4alpha-methyl oxidase 1-1	1.945542
AT4G09570	CPK4	calcium-dependent protein kinase 4	1.323458
AT4G08040	ACS11	1-aminocyclopropane-1-carboxylate synthase 11	2.339883
AT4G04990	C17L7.3	Protein of unknown function (DUF761)	1.212678
AT4G02410	T14P8.3	Concanavalin A-like lectin protein kinase family protein	1.237648
AT4G01870	T7B11.13	tolB protein-related	1.620064
AT4G00080	UNE11	Plant invertase/pectin methylesterase inhibitor superfamily protein	1.246845
AT3G62630	AT3G62630	Protein of unknown function (DUF1645)	1.359233
AT3G62110	AT3G62110	Pectin lyase-like superfamily protein	1.300837
AT3G61930	AT3G61930	unknown protein	1.679942
AT3G61160	AT3G61160	Protein kinase superfamily protein (AT3G61160.1; AT3G61160.2)	1.204879
AT3G58120	BZIP61	Basic-leucine zipper (bZIP) transcription factor family protein	1.230565
AT3G55740	PROT2	proline transporter 2 (AT3G55740.1; AT3G55740.2)	1.413744
AT3G55720	AT3G55720	Protein of unknown function (DUF620)	1.239733
AT3G54030	AT3G54030	Protein kinase protein with tetratricopeptide repeat domain	1.229969
AT3G50900	AT3G50900	unknown protein	1.45781
AT3G49700	ACS9	1-aminocyclopropane-1-carboxylate synthase 9	6.587971
AT3G46810	AT3G46810	Cysteine/Histidine-rich C1 domain family protein	1.31125
AT3G44720	ADT4	arogenate dehydratase 4	1.567775
AT3G42800	AT3G42800	unknown protein	1.490828
AT3G29360	AT3G29360	UDP-glucose 6-dehydrogenase family protein	1.425245
AT3G28180	CSLC04	Cellulose-synthase-like C4	1.413714
AT3G25900	HMT-1	Homocysteine S-methyltransferase family protein	1.473514
AT3G25290	AT3G25290	Auxin-responsive family protein (AT3G25290.1; AT3G25290.2)	1.66926
AT3G15370	EXPA12	expansin 12	1.642469
AT3G13380	BRL3	BRI1-like 3	1.507396
AT3G13000	MGH6.15	Protein of unknown function, DUF547	1.231604
AT3G12670	emb2742	CTP synthase family protein	1.306225
AT3G12610	DRT100	Leucine-rich repeat (LRR) family protein	1.547241
AT3G10870	MES17	methyl esterase 17	1.937517
AT3G07390	AlR12	auxin-responsive family protein	1.571635
AT3G04910	WNK1	with no lysine (K) kinase 1	1.278007
AT3G04570	AHL19	AT-hook motif nuclear-localized protein 19	1.354715
AT3G03170	T17B22.14	unknown protein	1.303516
AT3G02885	GASA5	GAST1 protein homolog 5	1.942483
AT2G47550	T30B22.15	Plant invertase/pectin methylesterase inhibitor superfamily	2.85384
AT2G47260	WRKY23	WRKY DNA-binding protein 23	1.369652
AT2G47140	F14M4.3	NAD(P)-binding Rossmann-fold superfamily protein	1.294546
AT2G46950	CYP709B2	cytochrome P450, family 709, subfamily B, polypeptide 2	1.220271
AT2G46740	F19D11.2	D-arabinono-1,4-lactone oxidase family protein	1.316832
AT2G45400	BEN1	NAD(P)-binding Rossmann-fold superfamily protein	1.219537
AT2G43870	F18O19.2	Pectin lyase-like superfamily protein	1.956365
AT2G43590	F18O19.30	Chitinase family protein	1.485995
AT2G42440	MHK10.16	Lateral organ boundaries (LOB) domain family protein	1.356373
AT2G41850	PGAZAT	polygalacturonase abscission zone A. thaliana	2.482996
AT2G41230	F13H10.22	unknown protein	1.872863
AT2G39800	P5CS1	delta1-pyrroline-5-carboxylate synthase 1 (AT2G39800.1; AT2G39800.2; AT2G39800.3; AT2G39800.4)	1.677469
AT2G39710	F17A14.9	Eukaryotic aspartyl protease family protein	1.581042
AT2G39700	EXPA4	expansin A4	1.26259
AT2G39130	T7F6.1	Transmembrane amino acid transporter family protein	1.306913
AT2G37940	AtIPCS2	Arabidopsis Inositol phosphorylceramide synthase 2	1.250817
AT2G35770	scpl28	serine carboxypeptidase-like 28	1.971361

(continued).

**Table 4.** The list of overlapping SHY2-u genes with up-regulated genes by auxin

Gene ID	Gene Symbol	Description	Fold change
AT2G35300	LEA18	Late embryogenesis abundant protein, group 1 protein	3.384003
AT2G35290	T4C15.4	unknown protein	1.245086
AT2G32610	CSLB01	cellulose synthase-like B1	1.602746
AT2G29440	GSTU6	glutathione S-transferase tau 6	1.830028
AT2G26480	UGT76D1	UDP-glucosyl transferase 76D1	2.323885
AT2G24300	T28I24.3	Calmodulin-binding protein (AT2G24300.1; AT2G24300.2)	1.477352
AT2G19990	PR-1-LIKE	pathogenesis-related protein-1-like	1.559498
AT2G18980	F19F24.18	Peroxidase superfamily protein	1.758502
AT2G18210	F8D23.2	unknown protein	1.595343
AT2G15490	UGT73B4	UDP-glycosyltransferase 73B4 (AT2G15490.1; AT2G15490.2; AT2G15490.3)	1.502406
AT2G04160	AIR3	Subtilisin-like serine endopeptidase family protein	1.762696
AT1G80840	WRKY40	WRKY DNA-binding protein 40	1.212456
AT1G78970	LUP1	lupeol synthase 1 (AT1G78970.1; AT1G78970.2)	1.491204
AT1G77690	LAX3	like AUX1 3	1.307595
AT1G77280	T14N5.13	Protein kinase protein with adenine nucleotide alpha hydrolases-like domain	1.424073
AT1G76160	sks5	SKU5 similar 5	1.223838
AT1G75640	F10A5.16	Leucine-rich receptor-like protein kinase family protein	1.784364
AT1G75500	WAT1	Walls Are Thin 1 (AT1G75500.1; AT1G75500.2)	1.30891
AT1G72230	T9N14.17	Cupredoxin superfamily protein	1.254568
AT1G68880	bZIP	basic leucine-zipper 8	1.384734
AT1G67750	F12A21.12	Pectate lyase family protein	1.417373
AT1G65310	XTH17	xyloglucan endotransglucosylase/hydrolase 17	1.234328
AT1G64980	F13O11.28	Nucleotide-diphospho-sugar transferases superfamily protein	1.305296
AT1G64405	AT1G64405	unknown protein	1.948096
AT1G64390	GH9C2	glycosyl hydrolase 9C2	1.839884
AT1G62045	AT1G62045	BEST Arabidopsis thaliana protein match is: ankyrin repeat family protein (TAIR:AT1G11740.1)	1.353269
AT1G52830	IAA6	indole-3-acetic acid 6	1.875027
AT1G49450	F13F21.11	Transducin/WD40 repeat-like superfamily protein	1.338192
AT1G49430	LACS2	long-chain acyl-CoA synthetase 2	1.490445
AT1G36940	T32E20.35	unknown protein (AT1G36940.1; AT1G36940.2)	1.478935
AT1G35140	PHI-1	Phosphate-responsive 1 family protein	1.618797
AT1G34110	F12G12.7	Leucine-rich receptor-like protein kinase family protein	1.405719
AT1G33260	T16O9.6	Protein kinase superfamily protein (AT1G33260.1; AT1G33260.2)	1.335858
AT1G30760	AT1G30760	FAD-binding Berberine family protein	2.455843
AT1G29430	F15D2.2	SAUR-like auxin-responsive protein family	1.247127
AT1G28130	GH3.17	Auxin-responsive GH3 family protein (AT1G28130.1; AT1G28130.2)	1.3221
AT1G23340	F26F24.22	Protein of Unknown Function (DUF239) (AT1G23340.1; AT1G23340.2)	1.202013
AT1G23080	PIN7	Auxin efflux carrier family protein (AT1G23080.1; AT1G23080.2; AT1G23080.3)	1.232223
AT1G22880	CEL5	cellulase 5 (AT1G22880.1; AT1G22880.2)	1.787322
AT1G22810	T22J18.2	Integrase-type DNA-binding superfamily protein	7.029307
AT1G22440	F12K8.21	Zinc-binding alcohol dehydrogenase family protein	1.36707
AT1G20190	EXPA11	expansin 11	1.461341
AT1G19050	ARR7	response regulator 7	1.394703
AT1G11545	XTH8	xyloglucan endotransglucosylase/hydrolase 8	1.304327
AT1G10460	GLP7	germin-like protein 7	1.445723
AT1G09350	GolS3	galactinol synthase 3	1.269991
AT1G06080	ADS1	delta 9 desaturase 1	1.403125
AT1G04680	T1G11.7	Pectin lyase-like superfamily protein	1.539409
AT1G03820	F21M11.27	unknown protein	1.252623
AT1G02900	RALF1	rapid alkalization factor 1	1.232028

(continued).

**Table 5.** The list of overlapping SHY2-d genes with down-regulated genes by

Gene ID	Gene Symbol	Description	Fold change
AT5G67400	RHS19	root hair specific 19	0.569505
AT5G57180	CIA2	chloroplast import apparatus 2 (AT5G57180.1; AT5G57180.2; AT5G57180.3)	0.309146
AT5G47610	MNJ7.20	RING/U-box superfamily protein	0.011171
AT5G35190	T25C13.70	proline-rich extensin-like family protein	0.606035
AT5G19890	F28I16.40	Peroxidase superfamily protein	0.372865
AT5G19800	T29J13.220	hydroxyproline-rich glycoprotein family protein	0.226257
AT5G15830	bZIP3	basic leucine-zipper 3	0.684346
AT5G06640	F15M7.17	Proline-rich extensin-like family protein	0.507105
AT5G06630	F15M7.16	proline-rich extensin-like family protein	0.502412
AT5G02230	T7H20.280	Haloacid dehalogenase-like hydrolase (HAD) superfamily protein (AT5G02230.1; AT5G02230.2)	0.586359
AT4G40090	AGP3	arabinogalactan protein 3	0.563652
AT4G30460	F17I23.200	glycine-rich protein	0.484616
AT4G28850	XTH26	xyloglucan endotransglucosylase/hydrolase 26	0.035138
AT4G25820	XTH14	xyloglucan endotransglucosylase/hydrolase 14	0.485626
AT4G25220	RHS15	root hair specific 15	0.205383
AT4G15630	DL3855W	Uncharacterised protein family (UPF0497)	0.278668
AT4G08410	T28D5.100	Proline-rich extensin-like family protein	0.617229
AT4G02270	RHS13	root hair specific 13	0.647589
AT3G62680	PRP3	proline-rich protein 3	0.608224
AT3G54590	HRGP1	hydroxyproline-rich glycoprotein	0.516585
AT3G54580	AT3G54580	Proline-rich extensin-like family protein	0.589818
AT3G49960	AT3G49960	Peroxidase superfamily protein	0.554464
AT3G46130	MYB48	myb domain protein 48 (AT3G46130.1; AT3G46130.2; AT3G46130.3; AT3G46130.4)	0.712507
AT3G23410	FAO3	fatty alcohol oxidase 3	0.710508
AT2G38170	CAX1	cation exchanger 1 (AT2G38170.1; AT2G38170.2; AT2G38170.3)	0.528799
AT2G32530	CSLB03	cellulose synthase-like B3	0.625753
AT2G24980	F27C12.10	Proline-rich extensin-like family protein	0.429758
AT2G20520	FLA6	FASCICLIN-like arabinogalactan 6	0.254848
AT1G72510	T10D10.2	Protein of unknown function (DUF1677) (AT1G72510.1; AT1G72510.2)	0.728789
AT1G68520	T26J14.9	B-box type zinc finger protein with CCT domain	0.085952
AT1G62560	FMO GS-OX3	flavin-monoxygenase glucosinolate S-oxygenase 3	0.373255
AT1G43160	RAP2.6	related to AP2 6	0.596887

auxin.

Gene ID	Gene Symbol	Description	Fold change
AT5G67400	RHS19	root hair specific 19	1.452042
AT5G61550	K11J9.12	U-box domain-containing protein kinase family protein	1.325592
AT5G61350	MFB13.1	Protein kinase superfamily protein	1.454905
AT5G59870	HTA6	histone H2A 6	1.331556
AT5G57540	XTH13	xyloglucan endotransglucosylase/hydrolase 13	1.823194
AT5G57530	XTH12	xyloglucan endotransglucosylase/hydrolase 12	2.065494
AT5G51270	MWD22.22	U-box domain-containing protein kinase family protein	1.331763
AT5G41730	MUF8.1	Protein kinase family protein	1.854852
AT5G40860	MHK7.9	unknown protein	1.522019
AT5G26080	T1N24.105	proline-rich family protein	1.429436
AT5G24880	F6A4.90	BEST Arabidopsis thaliana protein match is: calmodulin-binding protein-related (TAIR:AT5G10660.1)	1.484281
AT5G22410	RHS18	root hair specific 18	2.071957
AT5G18910	F17K4.160	Protein kinase superfamily protein	1.360599
AT5G07450	CYCP4;3	cyclin p4;3	1.461368
AT5G06640	F15M7.17	Proline-rich extensin-like family protein	1.477113
AT5G03640	F17C15.60	Protein kinase superfamily protein	1.38266
AT4G40090	AGP3	arabinogalactan protein 3	1.506803
AT4G35890	T19K4.20	winged-helix DNA-binding transcription factor family protein	1.223364
AT4G34580	COW1	Sec14p-like phosphatidylinositol transfer family protein	1.328753
AT4G29180	RHS16	root hair specific 16 (AT4G29180.1; AT4G29180.2)	1.544768
AT4G28850	XTH26	xyloglucan endotransglucosylase/hydrolase 26	3.102933
AT4G25820	XTH14	xyloglucan endotransglucosylase/hydrolase 14	1.277048
AT4G25790	F14M19.70	CAP (Cysteine-rich secretory proteins, Antigen 5, and Pathogenesis-related 1 protein) superfamily protein	1.717297
AT4G25220	RHS15	root hair specific 15	1.774109
AT4G22080	RHS14	root hair specific 14	1.680611
AT4G19680	IRT2	iron regulated transporter 2 (AT4G19680.1; AT4G19680.2)	2.099802
AT4G13390	T9E8.130	Proline-rich extensin-like family protein	1.520668
AT4G08410	T28D5.100	Proline-rich extensin-like family protein	1.585671
AT4G04900	RIC10	ROP-interactive CRIB motif-containing protein 10	1.369982
AT4G03330	SYP123	syntaxin of plants 123	1.322817
AT4G02270	RHS13	root hair specific 13	1.339333
AT4G01830	PGP5	P-glycoprotein 5	2.340504
AT4G01820	PGP3	P-glycoprotein 3	1.887504
AT4G00680	ADF8	actin depolymerizing factor 8	1.272535
AT3G62680	PRP3	proline-rich protein 3	1.654509
AT3G60280	UCC3	uclacyanin 3	2.315343
AT3G57570	AT3G57570	ARM repeat superfamily protein (AT3G57570.1; AT3G57570.2)	1.286851
AT3G24350	SYP32	syntaxin of plants 32 (AT3G24350.1; AT3G24350.2)	1.202409
AT3G18670	AT3G18670	Ankyrin repeat family protein	1.526844
AT3G10710	RHS12	root hair specific 12	1.311892
AT3G07070	F17A9.25	Protein kinase superfamily protein	1.600438
AT2G46860	PPa3	pyrophosphorylase 3	2.305642
AT2G45890	ROGGEF4	RHO guanyl-nucleotide exchange factor 4	1.338447
AT2G38500	T6A23.30	2-oxoglutarate (2OG) and Fe(II)-dependent oxygenase superfamily protein	1.60647
AT2G25240	T22F11.17	Serine protease inhibitor (SERPIN) family protein	1.242771
AT2G20520	FLA6	FASCICLIN-like arabinogalactan 6	3.454557
AT2G17670	T17A5.11	Tetratricopeptide repeat (TPR)-like superfamily protein (AT2G17670.1; AT2G17670.2)	1.301245
AT2G03720	MRH6	Adenine nucleotide alpha hydrolases-like superfamily protein	1.242062
AT2G02990	RNS1	ribonuclease 1	6.148966
AT1G70460	RHS10	root hair specific 10	1.417001
AT1G69240	MES15	methyl esterase 15	1.410314
AT1G63600	F2K11.4	Receptor-like protein kinase-related family protein	1.5193
AT1G63450	RHS8	root hair specific 8	1.613597
AT1G62980	EXPA18	expansin A18	1.60727
AT1G62440	LRX2	leucine-rich repeat/extensin 2	1.245905
AT1G59850	F23H11.17	ARM repeat superfamily protein	1.585513
AT1G54970	PRP1	proline-rich protein 1	3.600394
AT1G35670	CDPK2	calcium-dependent protein kinase 2	1.561319
AT1G35330	T9I1.10	RING/U-box superfamily protein	1.302065
AT1G34540	CYP94D1	cytochrome P450, family 94, subfamily D, polypeptide 1	1.846589

**Table 6.** The list of overlapping SHY2-*u* genes with RHE-containing genes.

**Table 6.** The list of overlapping SHY2-u genes with RHE-containing genes

Gene ID	Gene_Symbol	Description	Fold change
AT1G34510	F12K21.18	Peroxidase superfamily protein	2.324832
AT1G34330	F7P12.9	pseudogene, putative peroxidase, similar to anionic peroxidase Gl:559235 from ( <i>Petroselinum crispum</i> )	1.790688
AT1G31750	F5M6.24	proline-rich family protein	2.019973
AT1G30870	T17H7.19	Peroxidase superfamily protein	1.430199
AT1G30850	RSH4	root hair specific 4	1.288323
AT1G26940	T2P11.13	Cyclophilin-like peptidyl-prolyl cis-trans isomerase family protein	1.228086
AT1G25240	F4F7.37	ENTH/VHS/GAT family protein	1.938175
AT1G22880	CEL5	cellulase 5 (AT1G22880.1; AT1G22880.2)	1.787322
AT1G22620	ATSAC1	Phosphoinositide phosphatase family protein	1.26331
AT1G21130	T22I11.4	O-methyltransferase family protein (AT1G21130.1; AT1G21130.2)	1.264487
AT1G17180	GSTU25	glutathione S-transferase TAU 25	2.213754
AT1G16440	RSH3	root hair specific 3	1.310936
AT1G16370	OCT6	organic cation/carnitine transporter 6	2.457834
AT1G12950	RSH2	root hair specific 2	1.959822
AT1G12040	LRX1	leucine-rich repeat/extensin 1	1.338184
AT1G05990	RHS2	EF hand calcium-binding protein family	1.375171
AT1G05250	YUP8H12.14	Peroxidase superfamily protein	1.578702
AT1G05240	YUP8H12.15	Peroxidase superfamily protein	1.580042

(continued).

Gene ID	Gene Symbol	Description	Fold change
AT5G67400	RHS19	root hair specific 19	0.569505
AT5G61650	CYCP4;2	CYCLIN P4;2	0.319703
AT5G57540	XTH13	xyloglucan endotransglucosylase/hydrolase 13	0.577071
AT5G57530	XTH12	xyloglucan endotransglucosylase/hydrolase 12	0.615694
AT5G49700	K215.6	Predicted AT-hook DNA-binding family protein	0.454077
AT5G40860	MHK7.9	unknown protein	0.64622
AT5G26080	T1N24.105	proline-rich family protein	0.443616
AT5G19800	T29J13.220	hydroxyproline-rich glycoprotein family protein	0.226257
AT5G19790	RAP2.11	related to AP2 11	0.364037
AT5G18910	F17K4.160	Protein kinase superfamily protein	0.622337
AT5G06640	F15M7.17	Proline-rich extensin-like family protein	0.507105
AT4G40090	AGP3	arabinogalactan protein 3	0.563652
AT4G34580	COW1	Sec14p-like phosphatidylinositol transfer family protein	0.759525
AT4G30320	F17I23.340	CAP (Cysteine-rich secretory proteins, Antigen 5, and Pathogenesis-related 1 protein) superfamily protein	0.5783
AT4G28850	XTH26	xyloglucan endotransglucosylase/hydrolase 26	0.035138
AT4G25820	XTH14	xyloglucan endotransglucosylase/hydrolase 14	0.485626
AT4G25790	F14M19.70	CAP (Cysteine-rich secretory proteins, Antigen 5, and Pathogenesis-related 1 protein) superfamily protein	0.61221
AT4G25220	RHS15	root hair specific 15	0.205383
AT4G13390	T9E8.130	Proline-rich extensin-like family protein	0.51995
AT4G08410	T28D5.100	Proline-rich extensin-like family protein	0.617229
AT4G02270	RHS13	root hair specific 13	0.647589
AT4G01830	PGP5	P-glycoprotein 5	0.374169
AT4G01120	GBF2	G-box binding factor 2	0.675634
AT3G63380	AT3G63380	ATPase E1-E2 type family protein / haloacid dehalogenase-like hydrolase family protein	0.474397
AT3G62680	PRP3	proline-rich protein 3	0.608224
AT3G10710	RHS12	root hair specific 12	0.594925
AT3G01175	AT3G01175	Protein of unknown function (DUF1666)	0.794557
AT2G29450	GSTU5	glutathione S-transferase tau 5	0.045187
AT2G25240	T22F11.17	Serine protease inhibitor (SERPIN) family protein	0.688735
AT2G20520	FLA6	FASCICLIN-like arabinogalactan 6	0.254848
AT2G03980	F3C11.9	GDSL-like Lipase/Acylhydrolase superfamily protein	0.670866
AT2G03720	MRH6	Adenine nucleotide alpha hydrolases-like superfamily protein	0.739762
AT1G63600	F2K11.4	Receptor-like protein kinase-related family protein	0.486989
AT1G62980	EXPA18	expansin A18	0.785998
AT1G61080	T7P1.21	Hydroxyproline-rich glycoprotein family protein	0.262928
AT1G59850	F23H11.17	ARM repeat superfamily protein	0.327338
AT1G54970	PRP1	proline-rich protein 1	0.786771
AT1G34540	CYP94D1	cytochrome P450, family 94, subfamily D, polypeptide 1	0.143525
AT1G34510	F12K21.18	Peroxidase superfamily protein	0.190322
AT1G34330	F7P12.9	pseudogene, putative peroxidase, similar to anionic peroxidase Gl:559235 from ( <i>Petroselinum crispum</i> )	0.625354
AT1G31750	F5M6.24	proline-rich family protein	0.390419
AT1G26250	F28B23.9	Proline-rich extensin-like family protein	0.648826
AT1G25240	F4F7.37	ENTH/VHS/GAT family protein	0.254195
AT1G12560	EXPA7	expansin A7	0.643414
AT1G12040	LRX1	leucine-rich repeat/extensin 1	0.675783
AT1G05990	RHS2	EF hand calcium-binding protein family	0.437738
AT1G05340	YUP8H12.4	unknown protein	0.304013

**Table 7.** The list of overlapping SHY2-d genes with RHE-containing genes.



significantly higher than that of the 0 nM DEX step, its root hair length was longer than that of the 0 nM DEX step. This indicates that the slightly increasing level of *shy2-1* resulted in longer root hair, such as that of *shy2-1* GOF.

These results confirmed that SHY2 regulates root hair growth in a dose-dependent manner. The dose-dependent manner of SHY2 in root hair growth is also applied in transcriptional regulation. To assess whether this SHY2 capacity is able to regulate gene expression, the transcript level of *RSL4* and auxin-responsive genes, such as *GH3-3*, from transgenic lines grown in different DEX concentration media were analyzed. Similar results to those for the *ProZmE7:shy2-1* lines were found. The long-root-haired seedlings of the 0.1 nM DEX step increased the levels of *RSL4* and *GH3-3*, whereas the short-root-haired seedlings decreased the levels of both *RSL4* and *GH3-3* depending on DEX concentration (Figure 10E). It seems that the dose dependency of SHY2 capacity regulates not only root hair growth, but also affects root hair-related genes and auxin-responsive genes.

#### 2.4.7 RNA sequencing results of *shy2-1:GFP:GR* lines in different DEX concentrations

It has been suggested that Aux/IAAs function as transcriptional repressors (Tiwari et al., 2004; Tiwari et al., 2001). However, our root hair data reveal that SHY2 regulates root hair growth positively and negatively, suggesting that SHY2 may work as a bi-functional transcription factor. I have already confirmed the transcript level of *RSL4* and auxin-responsive genes. However, to explore the genome-wide transcriptional landscape controlled by SHY2, I conducted an RNA Sequencing

(RNA-Seq) experiment between *shy2-1:GFP:GR*-expressing lines at different DEX concentrations. I investigated the RNA-Seq data with published auxin-responsive genes or root hair-related genes. Firstly, RNA-Seq data was identified by differentially expressed genes (DEGs) based on the following criteria: a false discovery rate  $|FC| \geq 1.2$  from *shy2-1:GFP:GR*-mediated up-regulated genes (SHY2-u) by 0.1 nM DEX and down-regulated genes (SHY2-d) by 1000 nM DEX. I collected the represented auxin-responsive up-regulated genes (ARG-u) and down-regulated genes (ARG-d) (Goda et al., 2004; Lee et al., 2009; Nemhauser et al., 2004; Okushima et al., 2005b). The number of SHY2-u overlapping ARG-u was 159 and that of SHY2-d overlapping ARG-d was 32 (Figure 10F). This data indicated that SHY2 is able to up- and down- regulate the transcription of target genes in the auxin response. I also referred to the literature for the selection of the RHE-containing genes (RCGs; Hwang et al., 2017) that are required for root hair formation. Comparison with RCGs showed both SHY2-u and SHY2-d were involved in root hair growth (Figure 10F). The overlapping genes are listed in Tables 4 to 7. Venn diagrams of differently expressed genes demonstrate that SHY2 works as a bi-functional transcription factor for not only a few genes, but also overall transcription.

#### 2.4.8 *axr2-1* does not act in a dose-dependent manner

Next, a DEX-inducible system with *axr2-1:GFP* was used to further investigate whether *axr2-1* also has a dose-dependent capacity. The *ProE7:axr2-1:GFP:GR* lines showed short root hair without DEX (Figure 11E). It was presumed that *axr2-*

1:GFP:GR could repress root hair growth even with a low expression level because

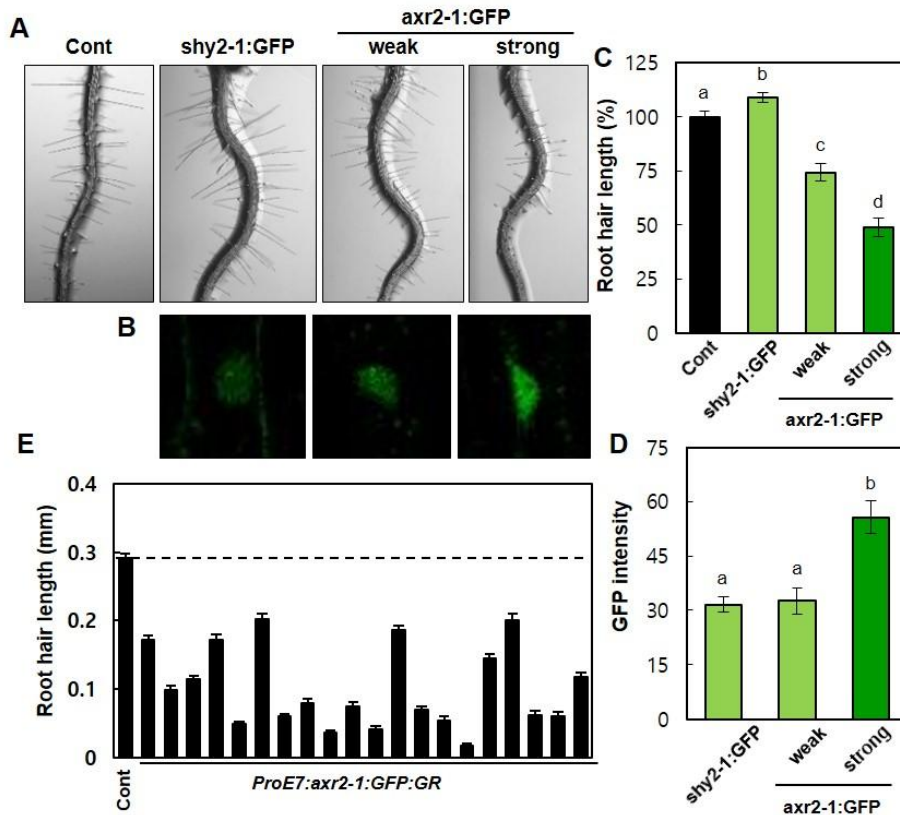


**Figure 11. *axr2-1* shows a repression activity of root hair growth in a dose-independent manner.** (A–D) Root hair length (A and C) and nuclear GFP signals (B and D) of control (Cont, *ProE7:GFP*), *ProE7:shy2-1:GFP:GR* (*shy2-1:GFP*), and *ProE7:axr2-1:GFP:GR* (*axr2-1:GFP*) lines in the DEX 0.1 nM induction condition. Two different induction lines (weak and strong) were analyzed for *axr2-1:GFP*. Data represent means  $\pm$  s.e. ( $n = 110\text{--}493$  root hairs [C] and 18–37 nuclei [D]). Scale bar is 100  $\mu\text{m}$  (A) and 1  $\mu\text{m}$  (B). Statistically significant differences are denoted with different letters (one-way ANOVA with Tukey’s unequal N-HSD *post hoc* test,  $P < 0.05$ ) (C and D). (E) Root hair length of *ProE7:axr2-1:GFP:GR* transformants without DEX induction. Data represent means  $\pm$  s.e. ( $n = 72\text{--}260$  root hairs from independent seedlings).

a small amount of GR-tagged protein could pass through the nucleus membrane without DEX. However, I treated DEX 0.1 nM for equal conditions with shy2-1:GFP:GR lines. There were two types of transgenic lines expressing axr2-1:GFP induced by DEX. One of them showed a similar signal intensity as shy2-1:GFP from the 0.1 nM DEX step. Another axr2-1:GFP line represented a strong GFP signal in a root hair cell (Figure 11B, D). The weak expression of axr2-1:GFP lines obviously showed short root hair (Figure 11A, C), indicating that axr2-1 consistently works as a repressor in root hair growth and denies following dose dependency.

#### 2.4.9 Analysis of domain I of Aux/IAAs

To demonstrate the differences between the functions of Aux/IAAs, I referred to two phylogenetic trees. The phylogenetic tree by Lokerse and Weijers represented two amino acids found at positions 2 and 4 of the EAR motif in domain I (x1 and x2, respectively). Lee et al. made the phylogenetic tree and divided it into four groups depending on the status of the EAR motif, such as the amount of Leucine or the number of motifs. The EAR motif is known as a binding motif with a co-repressor, TPL/TPRs (Causier et al., 2012a; Szemenyei et al., 2008). To attempt to understand the differences between Aux/IAAs, I created a phylogenetic tree and examined whether domain I of Aux/IAAs was necessary and sufficient for transcriptional repression (Figure 12A).

It was discovered that IAA7/AXR2 and IAA17/AXR3, whose GOF lines showed only the short-root-hair phenotype, contain two EAR motifs, and x1 and x2

of the first EAR motif are Cysteine and Glycine (CG-motif). Domain I of

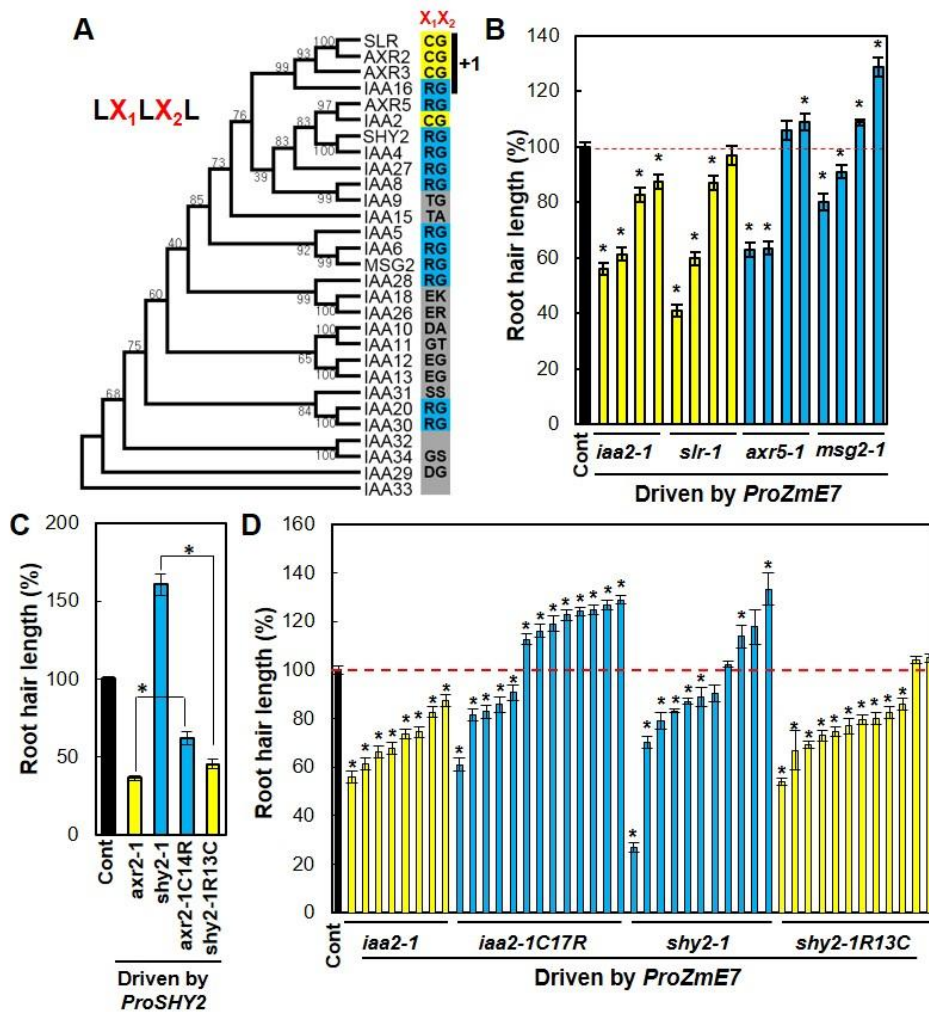


**Figure 12. The TPL-binding EAR motif is implicated in determining the activator or repressor property of an Aux/IAA.** (A) Phylogenetic relationship of the EAR motif ( $LX_1LX_2L$ ) of Arabidopsis Aux/IAAs.  $X_1$  and  $X_2$  are indicated in the second and fourth amino acids in the EAR motif, respectively. The amino acid sequence is represented in each color box (CG: yellow; RG: blue; others and no EAR motifs: gray). Four Aux/IAAs marked “+1” have an extra EAR motif for which sequences are different from the first motifs. (B) Relative root hair length of

control (Cont, *pE7:YFP*) and transformants expressing dominant mutant *aux/iaa* genes under a weak root hair-specific promoter (*ProZmE7*). Data represent means  $\pm$  s.e. (n = 192–512 root hairs) for independent lines. The values are significantly different ( $*P < 0.05$ , Student's *t*-test) from the control value. (C) Relative root hair length of the control (Cont, *pE7:YFP*) and transformants expressing dominant mutant *aux/iaa* genes and their EAR-motif-swapped versions under the *SHY2* promoter (*ProSHY2*). Data represent means  $\pm$  s.e. (n = 44–1,268 root hairs). Differences are significant ( $*P < 0.0001$ , Student's *t*-test). (D) Relative root hair length of control (Cont, *pE7:YFP*) and transformants expressing dominant mutant *aux/iaa* genes and their EAR-motif-swapped versions under *ProZmE7*. Data represent means  $\pm$  s.e. (n = 624–1,200 root hairs). The values are significantly different ( $*P < 0.001$ , Student's *t*-test) from the control value. Anindya Ganguly and Min-Soo Lee performed these experiments.

IAA3/SHY2 contains only one EAR motif, and x1 and x2 are Arginine and Glycine (RG-motif). To know whether the different status of the EAR motif causes the opposite phenotype expressed by Aux/IAAs, the root hair phenotype of several GOFs were further investigated. Which one was more critical for the regulation of root hair length, the number of motifs or the amino acid sequence was wondered. There are CG-motif Aux/IAAs, IAA2, and IAA14/SLR, and is likely that IAA7, IAA17, and IAA14 contain two EAR motifs, but IAA2 contains only one EAR motif. Regardless of the number of EAR motifs, almost all of the independent transgenic lines expressing IAA2 GOF (*iaa2-1*) and IAA14 GOF (*slr-1*) by *ProZmE7* had shorter root hair than the root hair length of the control line. Whereas transgenic lines expressing stabilized RG-motif Aux/IAAs, such as IAA1 GOF (*axr5-1*) and IAA19 GOF (*msg2-1*) by *ProZme7*, showed both shorter and significantly longer root hair phenotypes than the root hair of the control lines (Figure 12B). I can infer that the regulation force of positive and negative root hair growth comes from the sequence of the EAR motif by observing the root hair of RG-motif Aux/IAA.

To confirm this hypothesis, the domain I function using the substitution mutant form of the EAR motifs were analyzed. The mutated proteins, which were amino acids substituted by Cysteine to Arginine for the first EAR motif of *axr2-1* (*axr2-1C14R*) and Arginine to Cysteine for the EAR motif of *shy2-1* (*shy2-1R13C*), respectively, were expressed under *ProSHY2*. *ProSHY2:axr2-1C14R* lines showed longer root hair than *ProSHY2:axr2-1*, meaning that *axr2-1C14R* has less repression activity than *axr2-1*. *ProSHY2:shy2-1R13C* had shorter root hair than

not only *ProSHY2:shy2-1*, but also Cont (Figure 12C). This represents that the change of RG-

motif to CG-motif in SHY2 creates strong repression activity for root hair growth.

However, in spite of likely having the *shy2-1* RG-motif, *ProSHY2:axr2-1C14R* did not grow longer root hair than the control lines. This could be due to *axr2-1* having one more EAR motif in amino acid sequences (Figure 12A). For sophisticated evaluation of the repression activity between the CG-motif and RG-motif, I analyzed the *iaa2-1* and *shy2-1* because both Aux/IAs have one EAR motif in domain I (Figure 12A). The root hair length of *iaa2-1*, *shy2-1*, motif substituted *iaa2-1* (*iaa2-1C17R*), and *shy2-1R13C* expressed under *ProZmE7* were measured. Transgenic lines containing CG-motif, such as *ProZmE7:iaa2-1* and *ProZmE7:shy2-1R13C*, had relatively shorter root hair than those containing RG-motif, such as *ProZmE7:iaa2-1C17R* and *ProZmE7:shy2-1* (Figure 12D). It was found that the independent transgenic lines of *ProZmE7:iaa2C17R* and *ProZmE7:shy2-1* showed both shorter and longer root hair phenotypes than the control lines. These motif-swapping results confirmed that RG-motif has less repression activity than CG-motif (Figure 12C), and moreover, RG-motif Aux/IAs only regulate root hair growth positively and negatively (Figure 12D). Thus, I can infer that the opposite root hair phenotype is due to less repression activity from the RG-motif of Aux/IAs and differently expressed protein levels.

#### 2.4.10 The roles of domain I and PB1 domain in Aux/IAs

Before determining the reason for CG- and RG-motif differences in repression

activity, the effect of the EAR motif in root hair growth should be understood. To observe the effect of TPL in root hair growth, the TPL:GFP under *ProE7* was expressed. The root hair length is inversely proportional to the TPL:GFP signal intensity (Figure 13). Root hair growth is confirmed to be affected by TPL.

To demonstrate the difference in function between Aux/IAAs, I must mention one more property of Aux/IAA that interacts with ARFs. Aux/IAAs can bind to ARFs through the PB1 domain. I made four transgenic lines that are overexpressed in the N-terminal (domains I and II) deleted Aux/IAAs by *ProE7* (SHY2 $\Delta$ DI,II, AXR2 $\Delta$ DI,II, AXR3 $\Delta$ DI,II, and IAA2 $\Delta$ DI,II). They had longer root hair length than the control lines did (Figure 14B and C). The function of PB1 domains is indistinguishable in root hair growth, meaning that domains I and II are required for the repressive function of Aux/IAAs when recruiting TPL (Figure 15).

Additionally, I tested the function of full-length of Aux/IAAs with malfunctioning EAR motifs by substituting Leucine with Arginine in the EAR motif (Figure 14A). Root hair was specifically overexpressed in stabilized Aux/IAAs within the mutated EAR motif (IAA2mImII and SHY2mImII) and long root hair was shown by all independent transgenic lines (Figure 14D and E). Although Aux/IAAmImIIs can bind to ARFs, they did not work as a repressor in root hair growth. It seems like that they are not much different in domain II and the PB1 domain of IAA2 and SHY2 except in domain I. The root hair phenotype of *ProE7:Aux/IAAmImIIs*, which loses the function of recruiting TPLs, led to the conclusion that TPL is necessary for the transcriptional repression and inhibition of cell growth, at least in a root hair cell. Overexpressing Aux/IAAmImIIs may dilute

the concentration of normal Aux/IAs in a cell and then results in de-repressed root

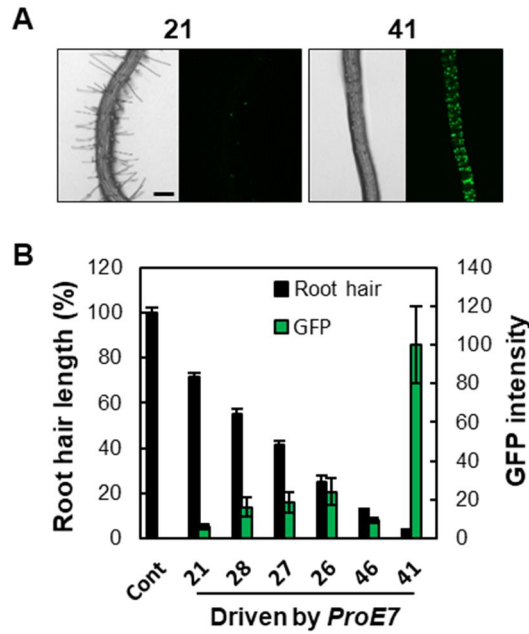


**Figure 13. The TPL-binding EAR motif is implicated in determining the activator or repressor property of an Aux/IAA.** (A) Root hair and TPL:GFP expression images of two independent *ProE7:TPL:GFP* lines. Scale bar is 100  $\mu\text{m}$  for all. (B) Root hair length and GFP intensity of control (Cont, WT) and independent *ProE7:TPL:GFP* lines. Data represent means  $\pm$  s.e. ( $n = 176\text{--}224$  root hairs). Min-Soo Lee performed these experiments.

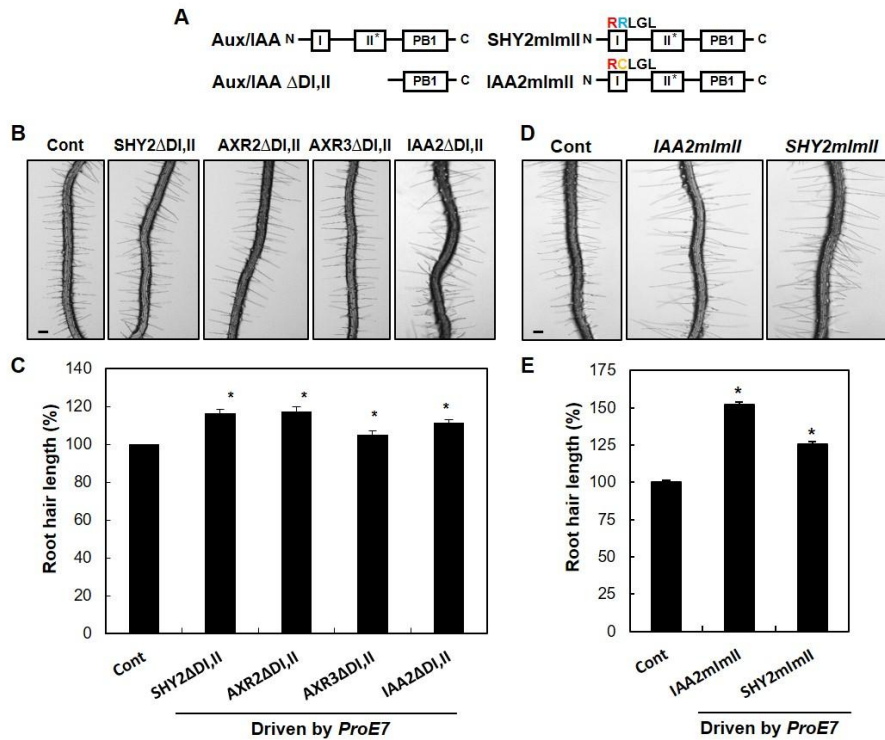


**Figure 14. The role of PB1 domain of Aux/IAAs in root hair growth.** (A) Schematic modular domain structure of deleted domain I and II AuxIAAs (Aux/IAA $\Delta$ DI,II) or mutated Aux/IAAs that are substitutions of Leu residue to Arg in the LxLxL motif (SHY2mImII and IAA2mImII). (B and C) Root hair images (B) and relative root hair lengths (C) of control (Cont, *ProE7::YFP*) and PB1 domain-expressing lines by *ProE7*. Data represent means  $\pm$  s.e. (n = 991–5,376 root hairs). (D and E) Root hair images (D) and relative root hair lengths (E) of control (Cont, *ProE7::YFP*) and IAA2mImII and SHY2mImII expressing lines by *ProE7*. Data represent means  $\pm$  s.e. (n = 272–1,088 root hairs from each transgenic plant). The values are significantly different (\* $P < 0.001$ , Student's *t*-test) from the control

value (C and E). Scale bar is 100  $\mu\text{m}$ . Min-Soo Lee contributed to these experiments.

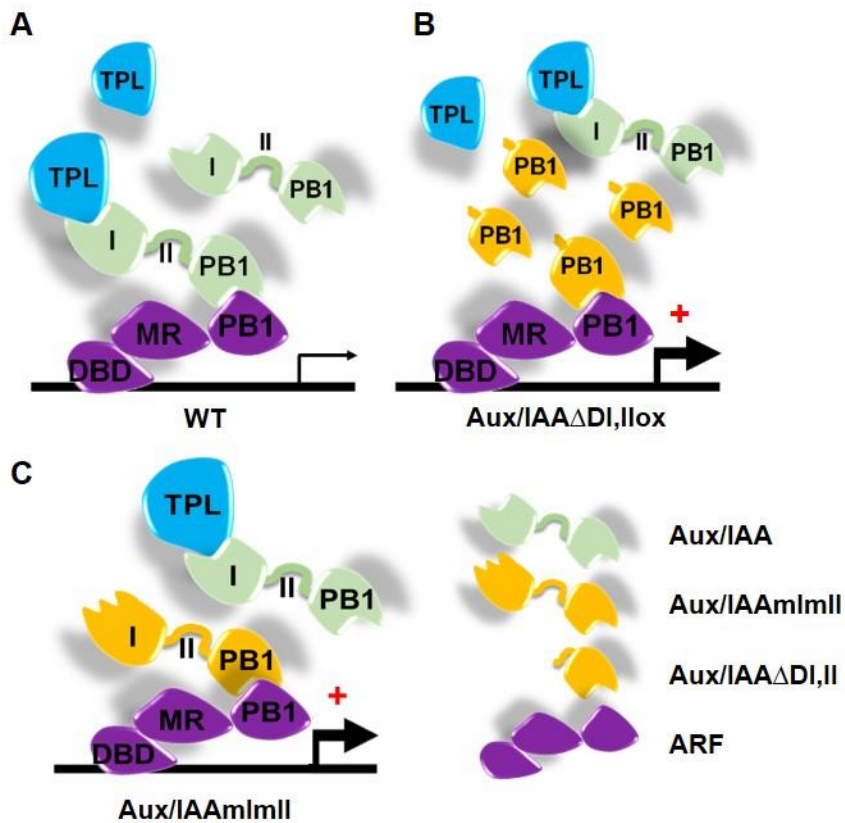


**Figure 15. A model illustrating role of each domain of Aux/IAA.** (A) Aux/IAs recruit TPL by domain I and bind to ARF by PB1 domain for regulation of auxin-responsive genes. (B) Intact Aux/IAs compete with domain I,II deleted Aux/IAs (Aux/IAA $\Delta$ DI,II) against the auxin response factor (ARF) and its results in overexpression of auxin-responsive genes in *ProE7:Aux/IAA  $\Delta$ DI,II* lines. (C) Intact Aux/IAs compete with domain I mutated Aux/IAs (Aux/IAAmImlII) against TPL and its results in overexpression of auxin-responsive genes in

*ProE7:Aux/IAAmImII* lines

hair cell growth (Figure 15C).

There are two types of malfunction-shy2-1 and axr2-1 proteins, which have a deleted C-terminal (PB1) domain, eliminating binding activity to ARFs (Guilfoyle and Hagen, 2012; Korasick et al., 2014). One group, Aux/IAAmII $\Delta$ PB1, had stabilized but PB1-deleted Aux/IAAs. The other group had an additionally mutated EAR motif that substituted Lysine to Arginine (Aux/IAAmImII $\Delta$ PB1) for the elimination of repression activity (Figure 16A). These mutants were expressed via *ProE7* and observed root hair length. *ProE7:Aux/IAAmII $\Delta$ PB1* lines showed longer root hairs than control lines, whereas *ProE7:Aux/IAAmImII $\Delta$ PB1* lines showed normal root hair length that was similar to control lines (Figure 16B, C). I interpret the above root hair data in two ways. Since transgenic lines did not decrease their root hair length, I suggest that PB1 domain-deleted Aux/IAAs lose their repression activity. Secondly, overexpressing Aux/IAAmII $\Delta$ PB1 and binding to TPL/TPRs but not ARFs showed increased root hair growth activity. From this result, I suggest that natural TPL is consumed by binding malfunction-Aux/IAA and is under the behavioral restriction of binding normal Aux/IAA for transcriptional repression (Figure 16D).

Previously, it was reported that most Aux/IAAs prefer to bind to activator ARFs (ARF5, 6, 7, 8 and 19) instead of repressor ARFs. Activator ARFs interact with both IAA3 and IAA7 without a big bias (Vernoux et al., 2011). The interaction between aARF and Aux/IAAs only results in transcriptional repression, not transcriptional activation. However, I need a story for dose-dependent bi-functional

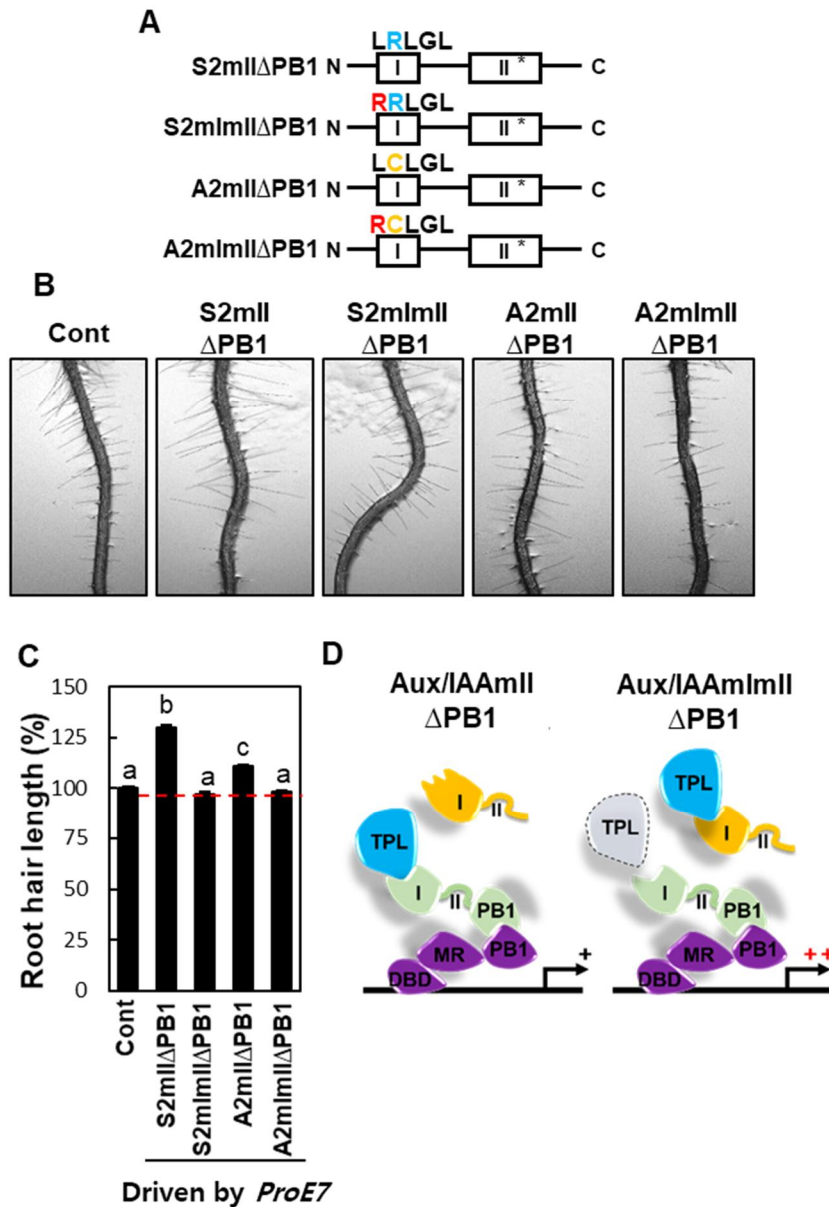


**Figure 16. Malfunctioning Aux/IAAs enhance root hair growth because they take away the opportunity of other Aux/IAAs to bind to TPL.** (A) Schematic modular domain structure of mutated Aux/IAAs. Two constructs consist of domain II mutated and PB1 domain deleted Aux/IAA (*AXR2mIIΔPB1* and *SHY2mIIΔPB1*). The other constructs are similar to the previous two, but they have additional

substitution mutations of Leu residue to Arg in the LxLxL motif to diminish the repressive function of Aux/IAA proteins (*AXR2mImII ΔPB1* and *SHY2mImII ΔPB1*). (B and C) Root hair images (B) and relative root hair length (C) of control (Cont, *ProE7:GFP*) and four transgenic lines under *ProE7* (*ProE7:AXR2mImIIΔPB1*, *ProE7:SHY2mImIIΔPB1*, *ProE7:AXR2mImIIΔPB1*, and *ProE7:SHY2mImIIΔPB1*). Data represent means ± s.e. (n = 1,318–2,369 root hairs). Statistically significant differences are denoted with different letters (one-way ANOVA with Tukey's unequal N-HSD *post hoc* test,  $P < 0.05$ ).

SHY2. To solve the problem of SHY2, it should be considered the differences in domain I between Aux/IAAs.

#### 2.4.11 AXR2 has a stronger affinity with TPL than SHY2 in a pull-down assay

Until now, I reasoned that repression activity for root hair growth was dependent on EAR motif and a dose of RG-motif Aux/IAAs. Consistent with the hypothesis that the activity of RG-motif Aux/IAAs is related to TPL, I conducted protein-protein interaction assays between TPL and Aux/IAAs. I first performed an immunoprecipitation pull-down assay using Aux/IAAs tagged with both GST and 6xHis as bait and TPL-N-terminal (TPLnt, 188 amino acids containing LiSH and CTLH) tagged with only 6xHis as prey. Using the *axr2-1* and *shy2-1* protein concentration gradient, we quantified the pulling-down of TPLnt via protein immunoblot analysis after normalization by the loading control. *shy2-1* also showed interaction with TPLnt, but *axr2-1* strongly interacted with TPLnt at a relatively low protein concentration. This experiment uncovered that *axr2-1*, CG-motif Aux/IAA, has a stronger interaction affinity with TPL than *shy2-1*, RG-motif Aux/IAA (Figure 17). However, *axr2-1* has two LxLxL motifs while *shy2-1* has only one. I thought that comparing the affinity between AXR2-TPL and SHY2-TPL was unfair because of the number of EAR motifs in domain I.

#### 2.4.12 CG-motif Aux/IAAs have a stronger affinity with TPL than RG-motif Aux/IAAs in MST

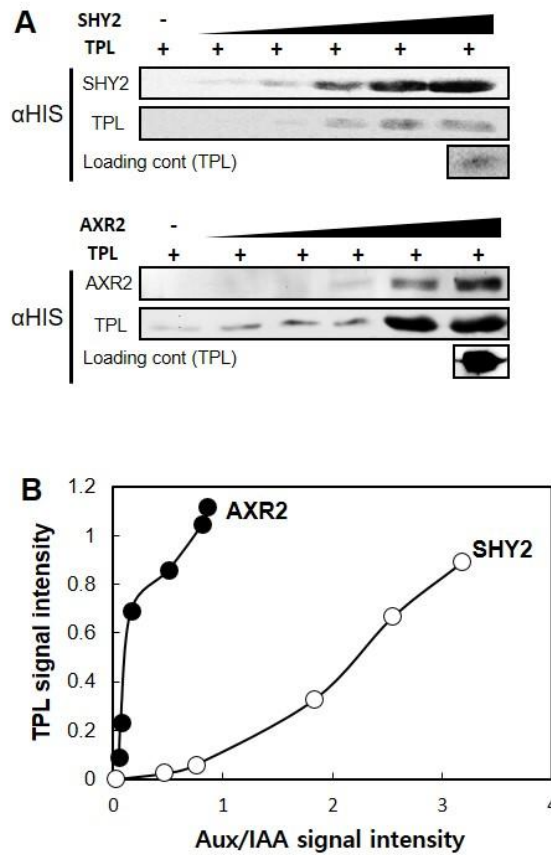


**Figure 17. Differential affinity of SHY2 and AXR2 to TPL.** (A) Immunoblot analyses of Aux/IAs (SHY2 and AXR2) and TPL after the pull-down of TPL with Aux/IAs. TPL was pulled down by different concentrations of Aux/IAs. His6-tagged TPL and Aux/IAs were detected with anti-His antibody. The same amount of TPL protein was counted to normalize the immunoblot intensities from different blots. Similar pull-down results were obtained from four independent experiments. (B) Quantification of the pull-down result from (A) reveals a higher affinity of AXR2 to TPL than that of SHY2. The quantification of TPL pulled down along Aux/IAA concentrations was performed as described in the method section.

This question was addressed quantitatively by microscale thermophoresis (MST) and through comparison with LxLxL motif-mutated IAA2 or IAA2. For the MST assay, only stabilized Aux/IAAs in the GOF form was used. Firstly, AXR2 was bound to TPLnt with  $K_d$   $0.86 \pm 0.25 \mu\text{M}$  (Figure 18A). The results showed a significantly lower affinity of SHY2 for the TPLnt (Figure 18B,  $K_d$   $2.3 \pm 1.61 \mu\text{M}$ ) coincident with the immunoblot data. The interacting affinity of IAA2 and TPLnt /showed higher values ( $K_d$   $1.29 \pm 0.43 \mu\text{M}$ ) than the affinity of EAR motif-mutated IAA2 and TPLnt (Figure 18C). However, the affinity between AXR2 and TPLnt is significantly higher than between IAA2 and TPLnt. The substituted EAR motif IAA2 (IAA2-1C17R)'s binding affinity with TPLnt is comparable to that observed between shy2-1 and TPLnt (Figure 18D, IAA2-1C17R,  $K_d$   $2.35 \pm 1.12 \mu\text{M}$ ). IAA2mI with a malfunctioning EAR motif has the lowest affinity with TPLnt (Figure 18E,  $K_d$   $4.35 \pm 1.82 \mu\text{M}$ ), and MST assay confirms that TPLnt has a higher affinity for the CG-motif Aux/IAAs compared to RG-motif Aux/IAAs, but there is still some interaction between TPL and RG-motif Aux/IAAs. Our results suggest that both the differential interacting affinity between Aux/IAAs and TPL and the differential concentration of Aux/IAAs in a root hair cell made a dose-dependent change in transcriptional activity for root hair growth.

#### 2.4.13 Modeling the differential affinity between TPL-Aux/IAAs

I performed modeling to reveal that the ratio of different Aux/IAAs determines TPL number at the transcriptional complex. These experimental observations led to the

reaction illustration of the dual effects of SHY2 on root hair growth. Aux/IAs are

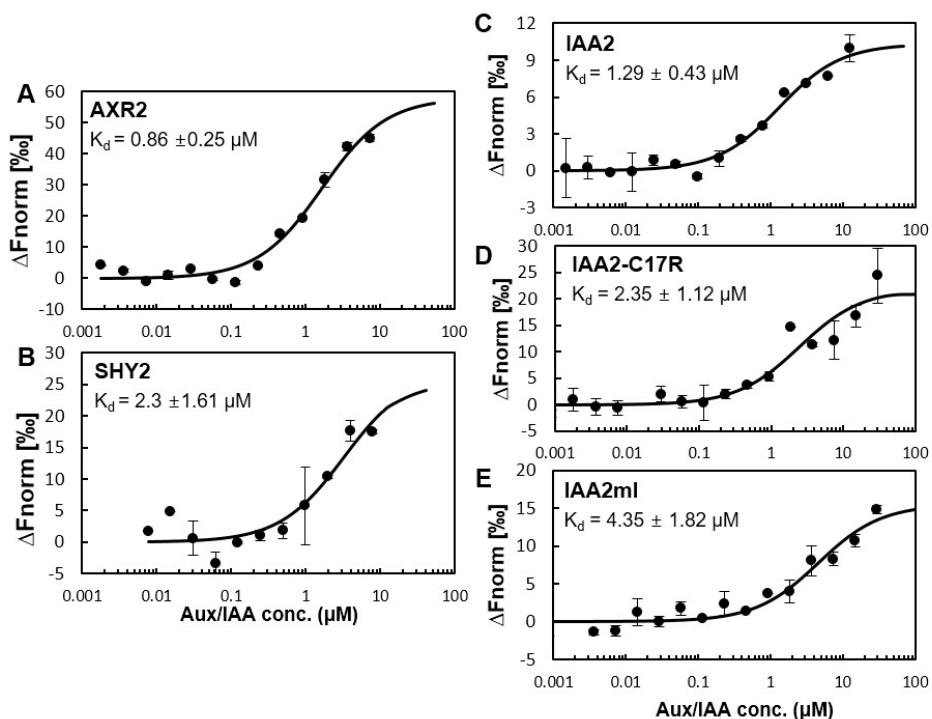


**Figure 18. Differential affinity of Aux/IAAs to TPL.** (A–E) *In vitro* binding analyses using MST (MicroScale Thermophoresis) between GST tagged Aux/IAAs (AXR2, SHY2, IAA2, IAA2-C17R, and IAA2ml) and TPL. IAA2-C17R is a mutated IAA2 by substituting Arg for the 17<sup>th</sup> Cys in the EAR motif. IAA2ml is a loss-of-EAR motif mutant by substituting Arg for the 1<sup>st</sup> Leu of the EAR motif. Data represent means  $\pm$  s.d. and F norm [%], the percentage of change in normalized fluorescence.



thought to conduct their repressive function through the recruitment of TPL using domain I and hetero-oligomerization with ARFs using PB1 domain (Han et al., 2014; Szemenyei et al., 2008), placing the transcription factor-complex with Aux/IAAs at the center. In the wild-type seedlings, the condition of the balanced low-level AXR2 and SHY2 and expression of RSL4 (auxin-responsive root hair master regulator) is maintained, and therefore, this transcription leads to a normal length of root hair (Figure 19B). The loss of the SHY2, as in *shy2-31*, causes only high TPL-affinity Aux/IAAs to exist, resulting in a relatively strong repression of RLS4 expression (Figure 19A). A small increase in SHY2 takes possession of the ARFs more than AXR2 does. In the *shy2-1* GOF situation, the transcriptional complex recruits less TPL because SHY2 occupies ARFs instead of AXR2. This complex has a weak interaction affinity with TPL (Figure 19C). However, a high level of SHY2, likely a SHY2ox line, makes a large hetero-oligomer with ARFs and may then recruit more TPL than a normal transcriptional complex. This results in strong repression of the expression of RSL4 as well as short root hair (Figure 19D).

After discovering the differential interaction affinity, I investigated the impact of this affinity on transcriptional regulation in root hair growth. Interaction analysis results lead to a model for the TPL-bound pattern in the root hair cell. Transcriptional regulation by TPL cooperates with several Aux/IAAs with different EAR motifs. I performed a mathematical study of this model and focused on the dose-dependent function of Aux/IAAs. It is almost impossible to obtain a precise understanding of all parameter spaces in auxin signaling. I assumed that other

auxin-

related factors are consistent, such as TPL, ARFs, and all Aux/IAs except SHY2

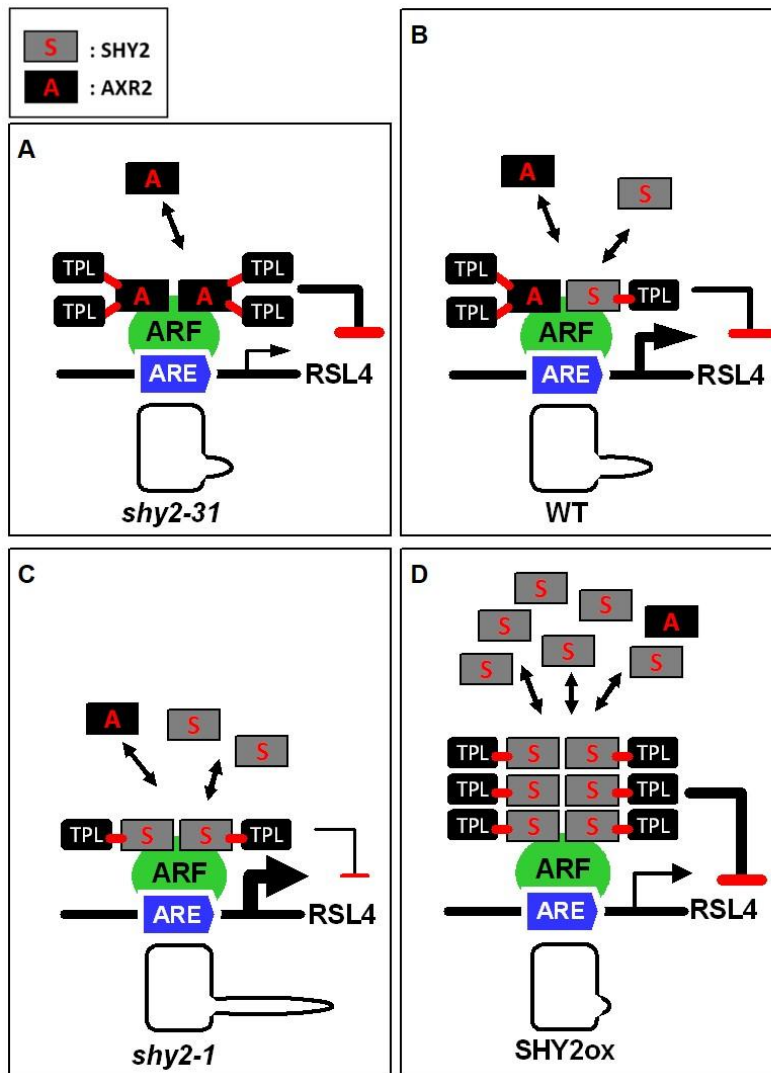


**Figure 19. A model illustrating the SHY2 dose-dependent switch of transcriptional activity and root hair growth.** A schematic model depicting how different transcriptional outputs result from varying SHY2 concentrations. In the condition of using wild-type (WT), a dose balance is maintained between Aux/IAAs with high (e.g. AXR2, A) or low (e.g. SHY2, S) affinity to TPL, resulting in WT-level expression of auxin-responsive root hair-forming genes. A loss of SHY2 as in *shy2-31* causes the existence of only high TPL-affinity

Aux/IAAs, resulting in the relatively strong repression of the target gene expression. A slight increase in the SHY2 dose as in *shy2-1* causes a replacement of high TPL-affinity Aux/IAAs (AXR2) by SHY2, resulting in less repression of the target gene expression. In SHY2 over-dosed conditions as in *SHY2ox* increased the multimerization of SHY2 and recruited more TPL, resulting in the strong repression of the target gene expression. (ARF, auxin response factor; ARE, auxin-response cis-element; RSL4, auxin-responsive root hair master regulator).

and AXR2, and focused on the behavior of the model depending on the interaction affinity between TPL and Aux/IAAs at different concentrations.

In addition to data on the TPL-Aux/IAAs relationship, I created a set of general considerations. Firstly, the pool of ARFs is consistent and sufficient to maintain gene regulation in wild-type root hair growing conditions. Secondly, the amount of TPL is large enough to bind with all Aux/IAAs in a cell. Thirdly, I set the level of Aux/IAA in a root hair cell. Usually, the Aux/IAAs decay rates are variable at different auxin concentrations. The half-life of Aux/IAAs varies over a wide range between several minutes and more than 20 h (Drecher et al., 2006). However, the TIR1 binding affinity of SHY2 ( $K_d = 16.97 \pm 3.43 \text{ nM}$ ) and AXR2 ( $K_d = 17 \pm 7.81 \text{ nM}$ ) is similar (Calderon Villalobos et al., 2012). Thus, I suggest that there is no effect of half-life in this model. The initial ratio of both RG-motif Aux/IAAs and CG-motif Aux/IAAs refer to the mRNA levels described in Arabidopsis e-FP browser (Winter et al., 2007; this level is described in the methods). In previous reports, the average protein concentration in a cell was about  $1 \mu\text{M}$ , ranging from  $2 \text{ nM}$  to  $30 \mu\text{M}$  (Ghaemmaghami et al., 2003; Lu et al., 2007). In the root hair growing condition, it is speculated that a high concentration of Aux/IAAs are not considered to be highly abundant in the cell. I assumed that the total concentration of Aux/IAAs is  $1 \mu\text{M}$ .

Finally, I performed a mathematical and numerical study of the model. This model allows for predicting the amount of TPL bound to the transcriptional complex through two independent systems, one involving the CG-motif Aux/IAAs

(AXR2 and IAA2) and the other RG-motif Aux/IAAs (SHY2 and IAA2-C17R). Based on these simulations, I traced the reciprocal number of bound TPL ( $1/N\_TPL$ ) in the changing Aux/IAA concentration. The  $1/N\_TPL$  increased following an increase in of RG-motif Aux/IAAs concentration, and then  $1/N\_TPL$  began to decrease. On the other hand,  $1/N\_TPL$  consistently decreased following the increase in CG-motif Aux/IAAs concentration (Figure 20A, B). I followed the population of the Aux/IAAs oligomer to the monomer-oligomer equilibrium model (Han et al., 2014), as described in the method because Aux/IAAs are homo-oligomeric proteins. I investigated the effect of oligomer population on TPL binding level and found out our constant ratio of each oligomer was reasonable. If I assume one oligomer proportion, the model does not fit our hypothesis (Figure 20C, D, E). In conclusion, I predicted that the differential expression of the CG-motif Aux/IAAs and RG-motif Aux/IAAs in a cell generates differences in recruiting TPL to the transcriptional complex and leads to differential transcriptional repression activity. SHY2 is mainly a transcriptional repressor, but it can be a transient activator at a certain concentration.

## 2.5 Discussion

The root hair data demonstrated that the gain-of-function *aux/iaa* mutants have different phenotypes in differential tissues. This may be caused by the differential expression pattern or the protein character. In this study, *ProE7:shy2-1:GFP:GR* transgenic plants grew longer or shorter root hair than the control line with

dependence on DEX concentration, resulting in a change in the shy2-1:GFP:GR

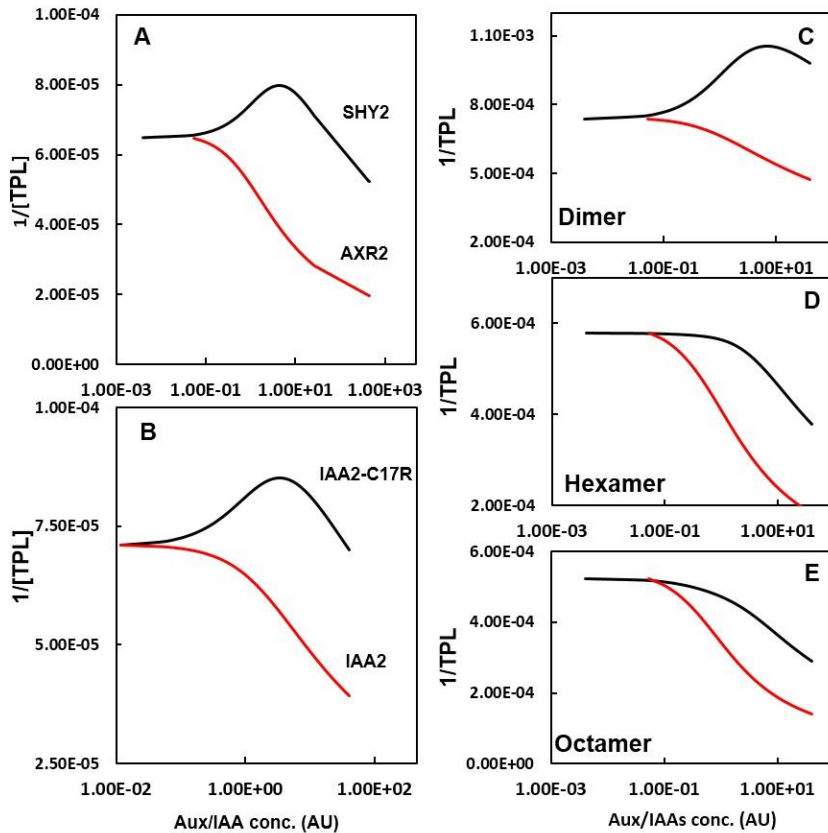


**Figure 20. A simulated model of the RG-motif Aux/IAA-dependent decision by changeable TPL recruitment.** (A and B) Computer simulations demonstrating varying transcriptional (and root hair growth) outputs ( $1/[TPL]$ ) according to increasing dose of Aux/IAAs. SHY2/IAA2-C17R and AXR2/IAA2 represent weak and strong TPL-affinity Aux/IAAs, respectively. Inverse concentration values of TPL ( $1/[TPL]$ ) recruited by Aux/IAAs were simulated for increasing the Aux/IAA dose. (C–E) Computer simulations demonstrate various transcriptional outputs ( $1/[TPL]$ ) according to formation of Aux/IAAs oligomerization. RG-motif Aux/IAA (black line) and CG-motif Aux/IAA (red line) represent weak and strong TPL-affinity Aux/IAAs, respectively. The oligomerization types of Aux/IAA proteins result in different pattern outputs, particularly RG-motif Aux/IAA (artificial unit, AU). Hoonyoung Park contributed to these experiments.

concentration of the nucleus. Whereas *ProE7:axr2-1:GFP:GR* transgenic lines consistently suppressed root hair growth, I hypothesized that the reason for the different function between Aux/IAAs is the RG-motif Aux/IAAs moderately interacting with TPL, resulting in the bi-functional transcriptional activity.

There are several transcription factors exchanging co-factors. The events of Aux/IAAs and other cases have similarities and differences. Overall, in other cases, transcription factors change their partners via co-transcription factors. For example, LEUNIG HOMOLOG (LUH) regulates a subset of genes both activated and repressed by PIF1. LUH binds to PIF1 as a co-regulator and accumulates in the promoter region of activated or repressed PIF1-target genes (Lee et al., 2015). The transcription pattern of target genes is similar for both mutant seeds of *pif1* and *luh*. A similar case is reported in myeloid leukemia (AML) patients. E proteins (E2a, HeLa E-box binding (HEB), E2-2, etc.) demonstrate a co-factor exchange mechanism. Many AML patients have *t* (8;21) chromosomal translocation, one of the most frequent chromosomal abnormalities, which highly increases the chance of a AML1-ETO fusion protein complex forming. High-level expressed AML1-ETO protein complex in Kasumi-1 cells inhibits transcriptional activation by binding to E proteins and then recruits HDAC-containing complexes in co-immunoprecipitation experiments in spite of E proteins regulating actively transcription by interacting with p300/CREB-binding protein (CBP) coactivators. All these different associations of E proteins happened because of the sequence similarity between the NHR1 region (TAFH domain) of ETO and 17-amino acid p300/CBP, which are the targets of E proteins (Zhang et al., 2004). In *Drosophila*

segmentation, the repressor Krüppel (Kr) interacts with several types of basal RNA polymerase II transcription machinery in co-immunoprecipitation experiments. By interacting with TFIIB, the monomeric Kr can act as a transcriptional activator. However, dimer-formed Kr interacting with TFIIE $\beta$  results in transcriptional repression at high concentrations of Kr (Sauer et al., 1995). Contrary to the above examples, our case does not change the cofactor. Interestingly, change only happens the protein level of Aux/IAAs. The change at the SHY2 level affects the activity of the transcriptional complex when interacting with other Aux/IAAs. Thus, the function of Aux/IAA only appears within the machinery of homologs. This phenomenon was first observed in hormone responses.

In this study, I confirmed only CG- and RG-motif Aux/IAAs. The proportion of CG- and RG motif Aux/IAAs was over 55% of the Arabidopsis Aux/IAAs. However, there are still other types of Aux/IAAs with differential sequences of amino acids in EAR motifs, such as TG, EA, EK, ER, DA, GT, EG, SS, GS, and DG (Figure 12). The differential sequence of the EAR motif has a different affinity for TPL/TPRs (Ke et al., 2015). Thus, I suggest that the various interacting relationships among the five TPL/TPRs and 29 Aux/IAAs will have unique transcriptional conditions that were unexpected before.

Even though the auxin concentration is the wild-type level, resulting in degradation of Aux/IAAs and positive auxin response in a cell, there are still Aux/IAAs not degraded by auxin. This small level of Aux/IAAs may work as a transcription factor for fine-tuning transcriptional regulation. Our results showed

the changing transcriptional pattern through a small dose of Aux/IAAs. Lavy and colleagues analyzed the effect of Aux/IAA on auxin response by eliminating all three Aux/IAAs of *Physcomitrella patens*. The plant-deleted Aux/IAAs (Aux/IAA-del) mutants showed a similar phenotype to plants grown in high auxin conditions or with more severe phenotypes. They also checked the targeted gene expression level in Aux/IAA-del mutants via RNA-Sequencing. Many up- or down-regulated genes in wild-type plants are more activated or suppressed in Aux/IAA-del mutants. A gene up-regulated 15 times in auxin-treated wild-type plants was up-regulated and expressed 430 times in the mutants. The authors mentioned that the knowledge of the Aux/IAA transcription ability is underestimated (Lavy et al., 2016).

We demonstrated how the different doses of Aux/IAAs that have a relatively weak interaction with TPL (SHY2 or RG-motif Aux/IAAs) induce phenotype variation. Although SHY2 is a repressor in auxin signaling, SHY2 could suppress the repressive function of other Aux/IAAs, such as CG-motif Aux/IAAs that have a strong interaction with TPL. A slightly increased SHY2 takes away the binding opportunity with TPL from CG-motif Aux/IAAs. If only CG-motif Aux/IAA is present in a cell, the auxin-responsive genes may be severely suppressed. These plants will require more auxin for auxin response. However, normal plants have RG-motif Aux/IAAs. RG-motif Aux/IAAs maintain a balance between repression and less-repression by modulating the level of TPL at the transcriptional complex. They need a small quantity of auxin, so this system may be necessary to enhance the efficiency of auxin signaling and to regulate fine-

tuning transcription. Likewise, protein-protein interaction enables the multifarious auxin response.

## **Chapter III.**

### **Transcriptional repression mechanism of repressor**

#### **ARFs in auxin signaling**

### 3.1 Abstract

Auxin signaling both positively and negatively affects target gene expression depending on conditions. Activator auxin response factors (aARFs) are released from Aux/IAA by auxin and consistently activate auxin-responsive genes. Although some auxin response factors are grouped as transcriptional repressors (rARF), the molecular mechanisms and biological functions have not been clearly defined. In our root hair system, the ARF2 and most rARFs (ARF1–4, 9–11, and 16) act as repressors and inhibit root hair growth; most have repressive motifs. First, this study shows the function of two putative co-repressor-binding motifs (EAR and RLFGI) of ARF2 in an auxin-independent manner. In particular, ARF2 contains both motifs in the middle domain and interacts with the co-repressor TPL and TPL homologs (TPRs) in the yeast two-hybrid assay. Both EAR and RLFGI motifs of ARF2 work as repressive motifs in regulating root hair growth, flowering time, and seed size that are deeply related *arf2* mutant phenotypes. Overall, these data suggest that the function of ARF2 directly recruiting TPL/TPRs is necessary to establish the repressive biological functions of rARF. Second, how rARFs exert their repression function in an auxin-dependent manner remains to be answered. Generally, Aux/IAAs prefer binding aARFs to binding rARF; this study examines how Aux/IAA suppresses the repressive function ability of ARF4 and ARF9, which are known Aux/IAA binding rARF. Wild-type ARF9 and mutant ARF9 in that it lost the ability to bind Aux/IAAs showed differential repressive activities. The function and role of ARF9 in auxin dependent manner should be further assessed.

## 3.2 Introduction

In *Arabidopsis*, the hormone response always changes the expression pattern of target genes whether categorized as upregulated or downregulated (Goda et al., 2008; Nemhauser et al., 2006). Besides, the number of genes up-regulated by exogenous hormone treatment is at an approximately similar level to the number of down-regulated genes (Goda et al., 2008). These results indicate that the repression mechanism is as important as gene activation.

One of the major transcription factors is AUXIN RESPONSE FACTOR (ARF), which binds to the auxin response cis-element (ARE) in the auxin-signaling pathway. ARFs are divided into three classes for land plants (Finet et al., 2012; Kato et al., 2015). Class A, including ARFs with a middle region (MD) where Gln is rich, are classified as transcriptional activators based on gene expression assays in protoplasts (Ulmasov et al., 1999). Class B and C ARFs are classified as repressor ARFs (rARFs) depending on their transcriptional activity and the molecular structure of MD, where Ser/Pro/Leu are rich (Guilfoyle and Hagen, 2001; Tiwari et al., 2003; Figure 21). Class C ARFs are targeted by *microRNA 160*.

The mechanism by which aARFs modulate the transcription of auxin-responsive genes has been well-characterized and is considered equivalent to the auxin-signaling pathway. Obviously, repressor ARFs have shown a repressive transcriptional function (Li et al., 2004b; Okushima et al., 2005b) in the protoplast assay. However, how rARFs exhibit the transcriptional repression activity remains to be determined.

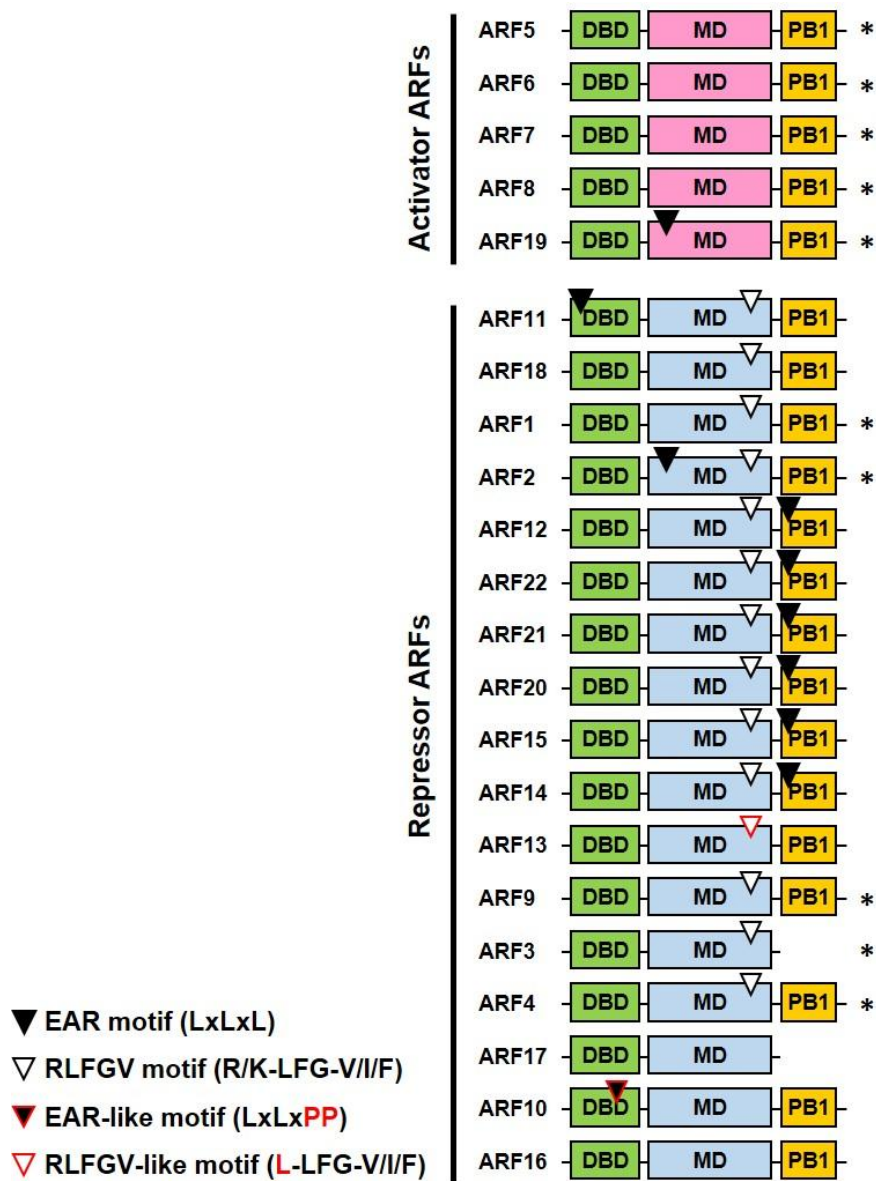


**Figure 21. Most repressor ARFs include putative co-repressor-binding motifs.**

Schematic domain structures of Arabidopsis ARF transcription factors (DBD, DNA binding and dimerization domain; MD, Middle region domain; PB1, Phox and Bem1 domain). EAR (or EAR-like) and RLFVG (RLFVG-like) indicate putative TPL/TPR-binding repressive motifs. Asterisks mark the ARFs whose activation/repression activities are experimentally determined.

The both of C-terminal domains of Aux/IAA and ARFs are Phox and Bem1p (PB1) domain, that are known as a protein-protein interacting domains (Guilfoyle and Hagen, 2012). The Aux/IAAs interact with the aARFs by using each PB1 domain and the consequent Aux/IAAs recruit TPL/TPRs by its repressive motif for transcription suppressing (Szemenyei et al., 2008; Ulmasov et al., 1997a; Ulmasov et al., 1997b). Removal of Aux/IAAs from aARFs in the presence of auxin results in the activation of auxin-responsive genes. However, rARF even have PB1 domain at the C-terminal region, *in vitro* experiments revealed that rARF does not prefer binding with Aux/IAAs (Piya et al., 2014; Vernoux et al., 2011). This indicated that rARFs may not borrow the repressive mechanism from Aux/IAAs, recruiting TPL/TPRs. Thus, rARFs require another repressive mechanism. rARF have still DNA-binding domain. It was suggested that rARF may compete against aARFs for DNA-binding sites or block activity of aARFs by hetero-dimerization between aARF and rARF

Transcription factors with TPL-binding motifs (LxLxL and R/K-LFG-V) work as transcriptional repressors in diverse pathways (Ikeda and Ohme-Takagi, 2009; Kagale et al., 2010; Ohta et al., 2001). Causier et al. showed that ARF2, ARF9, and ARF18 bind to TPL/TPRs in interactome data carried out on large-scale Y2H (Causier et al., 2012a). A review paper showed that rARFs and ARF19 have TPL-binding motifs. The authors analyzed R/K-LFG-V/I/F where the last site is extended as a hydrophobic amino acid rather than the more stringent R/K-LFG-V (Lokerse and Weijers, 2009). Thus, the alternative function of rARFs may directly recruit TPL/TPRs for gene repression. I have also shown the location and

sequences of TPL-binding motifs and putative binding motifs (Figure 21 and 21).

Out of the 18 loss-of-function rARF mutants, only *arf2* and *arf3* showed a clear phenotype. However, ARF3 has a truncated form protein without a PBI domain (Figure 21) currently ARF2 is the only canonical rARF. With the exception of ARF3, the *arf2* loss-of-function plant has obvious phenotypes in various developmental stages. Megaintegumenta (*mnt*), a mutant allele of ARF2, showed dramatically increased seed size and weight due to enlarged seed coats. Moreover, the mutant showed big epidermal cells in rosette leaves and long floral organs at stage 13 (Smyth et al., 1990), causing extra cell division and expansion in many organs (Schruff et al., 2006). Okushima et al. have shown that ARF2 is expressed in the peripheral zone of cotyledons, in the bottom part of the hypocotyl, and in the root vasculature of 3-day-old, light-grown seedlings via GUS expression under the *ARF2* promoter. The loss-of-function mutants of *arf2* (*arf2-6*, *arf2-7*, and *arf2-8*) have various phenotypes, such as long, thick, wavy inflorescence stems, large leaves, abnormal flower morphology, and late flowering under long-day conditions (Okushima et al., 2005b). In addition, *hls1* seedlings grown in dark conditions showed an increased level of the ARF2 protein, which worked as a transcriptional repressor of the DR5 synthetic reporter, an auxin-regulated reporter (Li et al., 2004a). Due to the various phenotypes of *arf2* mutant, ARF2 is regarded as a transition between hormones and environmental cues (Chandler, 2016). In this study, we chose ARF2 as a model for studying rARF, which has both EAR and RLFGV motifs (Figure 21). I investigated the TPL-binding motifs of ARF2, which consider the repressive force of rARFs in the developmental processes by

analyzing complementation experiments.

A	EAR motif (EAR-like)	B	RLFGV motif (RLFGV-like)
ARF19	SPSQQLQLQLLQKLQ	ARF11	VTSSCRLFGFDLTSK
ARF11	IKLQILQLWLKLIIV	ARF18	TNCSYRLFGFDLTSN
ARF2	MIHSGLSLKLHESPK	ARF1	NGNVCRFLFGFELVEN
ARF12	NGYDQLILELEKLF	ARF2	REGNCRFLFGIPLTNN
ARF22	NGYDQLILELEELFD	ARF12	TGTNFRFLGVTLDTP
ARF21	NGYDQLILELEKLF	ARF22	TGTNFRFLGVSLVTP
ARF20	NGYDQLILELEKLF	ARF21	AGTNFRFLGVTLDTP
ARF15	NGYDQLILELEKLF	ARF20	AVTNFRFLGVSLAIP
ARF14	NGYDQLILELEKLF	ARF15	AGTNFRFLGVSLATP
ARF10	ENDAVLGLTPPSSDG	ARF14	AVASFRLFGVSLATP
		ARF9	TTANYRFLGVSLATP
		ARF3	GSGRCRFLFGFPLTDE
		ARF4	ASSGCKLFGFSLPVE
		ARF13	ATTSCLLFGVDLTKV

**Figure 22. Sequences of putative repressive motifs of ARFs.** Sequence alignments of EAR (A) and RLFGV (B) motifs of ARFs. The motifs are highlighted in gray boxes. ARF10 and ARF13 include EAR-like and RLFGV-like motif, respectively.

Although, rARF does not favor that method of interacting with other auxin-signaling components, there are exceptions of ARF9 and ARF4. In yeast two-hybrid experiments, ARF9 interacts with two ARFs and sixteen Aux/IAAs (Vernoux et al., 2011) and ARF4 interacts with almost all Aux/IAAs (Piya et al., 2014). These two rARFs could recruit Aux/IAAs for transcriptional repression. However, whether they really work with Aux/IAAs for the repression of auxin-response genes is still unknown. I will address this topic in Results II of this chapter.

## **3.3 Materials and methods**

### **3.3.1 Accession numbers**

Sequence data and mutant information from this article can be found in the Arabidopsis Genome Initiative or GenBank/EMBL databases under the following accession numbers; AT5G62000 (*ARF2*), AT5G54510 (*GH3.6*), AT1G12560 (*EXPA7*), AT1G27740 (*RSL4*), AT1G15750 (*TPL*), AT1G80490 (*TRP1*), AT3G16830 (*TPR2*), AT5G27030 (*TPR3*), AT3G15880 (*TPR4*), CS24600 (*arf2-6*), and CS24601 (*arf2-7*).

### **3.3.2 Plant materials and growth conditions**

*Arabidopsis thaliana*, Columbia ecotype (Col-0), was used as a control and for transformation of transgene constructs unless otherwise stated. Arabidopsis plants

were transformed using *Agrobacterium tumefaciens* strain C58C1 (pMP90) by the inflorescence-dipping method. Transformed plants were selected on hygromycin-containing plates (30  $\mu\text{g ml}^{-1}$ ). All seeds were grown on agarose plates containing 4.3  $\text{g ml}^{-1}$  Murashige and Skoog (MS) nutrient mix (Duchefa, Netherlands), 1% sucrose, 0.5  $\text{g ml}^{-1}$  MES pH 5.7 with KOH, and 0.8% agarose. Seeds were cold treated before germination at 23°C under a 16 h/8 h light/dark photoperiod. For observation of root hairs, homozygous transformants were planted on antibiotic-free media, and T1 and T2 lines were planted on hygromycin containing media. Hygromycin did not significantly interfere with root hair development, as shown in the control *ProE7:YFP* (yellow fluorescence protein) transformants. Two control lines were adopted; WT for the *arf2-6* and *arf2-7* mutant analysis and *ProE7:YFP* (Lee and Cho, 2006; Ganguly et al., 2010) for the transformant analysis with hygromycin. Two *arf2* mutants were obtained from the Arabidopsis Biological Resource Center.

### 3.3.3 Construction of transgenes

To root hair-specifically overexpress ARFs using the root hairspecific *EXPA7* promoter (*ProE7*) for the *ProE7:ARFs* constructs, the ARFs sequences were obtained by PCR using Arabidopsis genomic DNA as the template and the primer sets listed in Supplementary Table 1. To generate root hair-specific overexpression lines for wild-type and mutant forms of *ARF2* (genomic wild-type *ARF2*, ma, mb, and mab), sequences were obtained by PCR using the primers listed in Supplementary Table 1. The modified binary vector, pCAMBIA 1300-NOS,

including *ProE7*, was used as the cloning vector to direct root hair-specific expression and to fuse with ARFs and mutant forms of *ARF2*. For the *arf2* mutant complementation experiments, *ProE7* was replaced by *ProARF2* in the *ProE7*-driven constructs for wild-type or mutant ARF2. For the *ProE7:ARF4ΔPBI*, *ProE7:ARF9ΔPBI*, and *ProE7:ARF10ΔPBI* constructs, the fragment of *ARFsΔPBI* were obtained by PCR using the primer sets listed in Table 1 and *ProE7:ARF4*, *ProE7:ARF9*, and *ProE7:ARF10Δ* as templates. For the *ProE7:ARF9mKmOPC*, the fragment of *ARF9mKmOPC* was obtained by mega-PCR using the primer sets listed in Table 1 and inserted into *ProE7-GFP* vector.

For the yeast two-hybrid (Y2H) constructs, cDNAs for fulllength TPL/TPRs, full length ARF2, and wild-type and mutant forms of ARF2 domains were PCR-amplified using the primer sets in Supplementary Table 1 and cloned into the binding domain (BD)-expressing *pGBKT7* or the activation domain (AD)-expressing *pGADT7* vector depending on the experimental design. All constructs were confirmed by nucleotide sequencing. For Arabidopsis transformation, the Agrobacterium-mediated floral dipping method was adopted. Transgene insertion in the Arabidopsis transformants was confirmed by PCR analysis using transgene-specific primers.

### 3.3.4 Observation of biological parameters

Root hair length was estimated as described in Lee and Cho (2006, 2009) with modifications. The 3-day-old seedling root was digitally photographed using a stereomicroscope (M205 FA, Leica, Heerbrugg, Switzerland) at 40X magnification.

The lengths of 9 consecutive hairs protruding perpendicularly from each side of the root, 18 hairs in total, were estimated using ImageJ 1.50b software (National Institutes of Health, United States). For the flowering time analysis, the emergence of a 1-cm-long inflorescence was considered as the bolting time. To estimate seed size, the seeds from control, mutants, or independent T1 transformants were harvested, dried for 2 weeks, digitally photographed under a stereomicroscope, and the seed area calculated using ImageJ 1.50b software. For the phyllotaxis analysis, the angle of rosette leaf were measured.

### 3.3.5 RNA isolation and quantitative reverse transcriptase (qRT)-PCR analysis

Total RNA was isolated from the roots of 4-day-old seedlings (25 for each line) using an RNeasy Plant Mini Kit (Qiagen). cDNA was synthesized as described previously (Lee and Cho, 2006). qRT-PCR analyses were performed using an amfiSure qGreen Q-PCR Master mix without ROX (Applied GenDEOT) and a Chromo4™ Four-Color Real-Time Detector (Bio-Rad). Gene specific signals were normalized by the *ACTIN7* transcript level. qRT-PCRs were performed in three technical replications per RNA sample with three independent RNA preparations. Primers used for quantitation were as in Supplementary Table 1.

### 3.3.6 Yeast two-hybrid assays

Yeast two-hybrid experiments were performed using the Matchmaker Yeast Two-Hybrid System (Clontech, Palo Alto, CA, United States) with the yeast strain

AH109 following the manufacturer's protocol. Direct interaction of two proteins was investigated by co-transformation of the plasmids into the yeast cell. Transformed cells were cultured in a SD2<sup>-</sup> medium (lacking Leu and Trp) at 30°C for 3 days. Single colonies were suspended in the SD2<sup>-</sup> medium, and serial 1:10 dilutions were plated in either SD2<sup>-</sup>, SD3<sup>-</sup> (lacking Leu, Trp and His), or SD4<sup>-</sup> (lacking Leu, Trp, His and Ade). 3-amino-triazole (0.2–0.5 mM) was included for cultivation in SD3<sup>-</sup>. Cell growth was observed 4–10 days after plating. Yeast cells containing *pGBKT7-p53* and *pGADT7-T*, which express *BD* with murine *p53* and *AD* with SV40 large T-antigen, respectively, were used as positive controls. The yeast cell line expressing human *lamin C* with *BD* fusion protein was used as a negative control.

### 3.3.7 *in vitro* pull-down assay

To produce, ARF9 and ARF9 $\Delta$ PB1 proteins, the gene-containing vectors were transformed into *E. coli* strain BL21 and the transgene expression was induced with 0.25mM isopropyl  $\beta$ -D-1-thiogalactopyranoside at 4°C for 16 h. The cells were harvested by centrifugation and lysed in B-PER Buffer (Thermo Scientific). The proteins in the lysate were bound to GSH resin (Elpisbio) at 4°C for 1 h and washed three times with TBS buffer. Proteins were purified from glutathione resin by elution buffer (15mM GSH and 50mM Tris, pH 7) at 4°C for 2 h. Pull-down assays were performed using recombinant proteins (GST-fused ARF9, ARF9 $\Delta$ PB1, and SHY2) and the 5'-biotinylated 37-bp ARE probe (ccggtaggTGTCTCccaaaggGAGACA accgtagg, the ARE core is shown in

uppercases). The SHY2 was mixed with the ARF9 or ARF9 $\Delta$ PB1 and probe in the binding buffer (10mM Tris, pH 7.5, and 120mM NaCl) at 25°C for 20 m. The protein complex were loaded to Streptavidin Agarose (Invitrogen; Catalog no. 15942-050). After four time washing, proteins were purified from TBS buffer by boiling 10 min with SDS 10 % solution.

**Table 8.** The primer list

Subject	Primer name	Primer sequence (5' to 3')			
Transgene Construct	ARF1	ARF1_PcF	GTTTTTAATTAATAGAGGAGGATAGGTCC		
		ARF1_AsR	TGCTGGCGCGCCCATATTTCTACGTGGC		
	ARF2	ARF2	ARF2_DBF	ATAGTCGACTAATGGCGAGTTCCGGAG	
			ARF2_BmR	ATAGGATCCTTAAGAGTTCCCAGCGCT	
		ARF2ma	ARF2_DBF	ATAGTCGACTAATGGCGAGTTCCGGAG	
			Mega primer1-maF	CACTCTGGTGCCCTCCGCGAAGGCACATGAATCT	
			Mega primer1-R	ATAGGATCCTTAAGAGTTCCCAGCGCT	
			ARF2_DBF	ATAGTCGACTAATGGCGAGTTCCGGAG	
			ARF2mb	Mega primer1-mbF	GAAGTCAGGTCTCTGGCATT
				Mega primer1-R	ATAGGATCCTTAAGAGTTCCCAGCGCT
		ARF2_DBF		ATAGTCGACTAATGGCGAGTTCCGGAG	
		ARF2mab	Mega primer2-maF	CACTCTGGTGCCCTCCGCGAAGGCACATGAATCT	
			Mega primer1-mbF	GAAGTCAGGTCTCTGGCATT	
			Mega primer1-MD-R	GCAGTCGACACTCTACTTGAGTTGGT	
	ARF3	ARF3	ARF3_PcF	GCTCTTAATTAATCTCTGTTTCTCTCTC	
			ARF3-AsR	AAGCGGCGCGCCAATAAAACACAGAAACC	
		ARF4	ARF4-PcF	GCTCTTAATTAAGAAGCTTTTCAATGGA	
			ARF4-AsR	CTTTGGCGCGCCAAACACACTTTAAACA	
		ARF9	ARF9_PcF	AGAGTTAATTAATGTTTTGGTGTGACTGAT	
			ARF9-AsR	GGATGGCGCGCCTTTGTTAAGCCATGCGC	
		ARF10	ARF10_PcF	CAACTTAATTAAGATGGAGCAAGAGAAA	
			ARF10-AsR	AAAGGGCGCGCCTTATTCCTCAATATGCT	
		ARF11	ARF11_PcF	ATTTTTAATTAATAATCATGAGCCAACAAGCTTAG	
			ARF11-AsR	AATTGGCGCGCCTTGAGAGAGTCTCCAAG	
		ARF16	ARF16_PcF	TTTCTTAATTAACGGTCACAAAAAAATG	
			ARF16-AsR	CTTCGGCGCGCCAACAAAACACTCTGCCA	
		ProARF2	pARF2_H3F	ATCAAGCTTACACAAGAAAATAGAAGAG	
			pARF2_SIR2	ATGTCGACACCTTCCGAAGCTCAGACT	
		ARF9 mKmOPCA	A9mK527A-Fg	CTACAAGAAGCCGTACCCTGtatatatagcctac	
			A9mOPCA-R	CACCGACAAGCATCATAGCTCCCTCATCAGCTGTGAACACTATTTTC	
Y2H assay constructs		TPL	TPL_SIF	GGAGTCGACAGAAAACATGTCTTCTCTTA	
			TPL_XmR	TATCCCGGGTCATCTCTGAGGCTGATCAGATG	
	TPR1	TPR1_SIF	CTTGTCGACACTGAGTGGCAAATCAATC		
		TPR1_SIR	CACTGCAGATCATCTCTGAGGCTGGTC		
	TPR2	TPR2_SmF	TAGCCCGGATGTCTCTTTGAGCAGAG		
		TPR2_SmR	TCACCCGGGTGTCAACTAACTTAAGTACGACAT		
	TPR3	TPR3_SmF	AGACCCGGGGAGAATGTCGTGTTGAGTC		
		TPR3_SmR	ATCGCCCGGGCTGGTTTGTTCATCTTTGTAA		
	TPR4	TPR4_BmF	ACGAGGATCCGAGGATATGTCGTCACCTCAG		
		TPR4_BmR	ATCAGGATCCCTGCTTCCATCTCCAACACTAC		
	ARF2 full	ARF2_DBF	ATAGTCGACTAATGGCGAGTTCCGGAG		
		ARF2_BmR	ATAGGATCCTTAAGAGTTCCCAGCGCT		
	DBD	ARF2_DBD_F	ATAGTCGACTAATGGCGAGTTCCGGAG		
		ARF2_DBD_R	ATAGTCGACTGGCTCTACTTTCCACGG		
	MD	MD_SmF	GCAGTCGACTAATGAGATTTGAAGGC		
		MD_R	GCAGTCGACACTCTACTTGAGTTGGT		
	MDma	MD_SmF	GCAGTCGACTAATGAGATTTGAAGGC		
		Mega primer1-maF	CACTCTGGTGCCCTCCGCGAAGGCACATGAATCT		
		Mega primer1-MD-R	GCAGTCGACACTCTACTTGAGTTGGT		
	MDmb	MD_SmF	GCAGTCGACTAATGAGATTTGAAGGC		
		Mega primer1-mbF	GAAGTCAGGTCTCTGGCATT		
		Mega primer1-MD-R	GCAGTCGACACTCTACTTGAGTTGGT		
	MDmab	MD_SmF	GCAGTCGACTAATGAGATTTGAAGGC		
		Mega primer2-maF	CACTCTGGTGCCCTCCGCGAAGGCACATGAATCT		
		Mega primer1-mbF	GAAGTCAGGTCTCTGGCATT		
		Mega primer1-MD-R	GCAGTCGACACTCTACTTGAGTTGGT		
	PB1	ARF2_PB1_F	ATAGTCGACTAATGAATGGACAGACTCA		
		ARF2_PB1_R	ATAGTCGACTAAGAGTTCCCAGCGCT		

**Table 8.** The primer list (continued)

Subject	Primer name	Primer sequence (5' to 3')	
Y2H assay constructs	TPL	TPL_SIF	GGAGTCGACAGAAAACATGTCTTCTCTTA
		TPL_XmR	TATCCCGGGTCATCTCTGAGGCTGATCAGATG
	TPR1	TPR1_SIF	CTTGTCGACACTGAGTGGCAAATCAATC
		TPR1_SIR	CACTGCAGATCATCTCTGAGGCTGGTC
	TPR2	TPR2_SmF	TAGCCCGGGATGTCGCTTTTGAGCAGAG
		TPR2_SmR	TCACCCGGGTGTCAACTAACTTAACTGACAT
	TPR3	TPR3_SmF	AGACCCGGGGAGAATGTCGTCGTTGAGTC
		TPR3_SmR	ATCGCCCGGGCTGGTTTGTTCATCTTTGTAA
	TPR4	TPR4_BmF	ACGAGGATCCGAGGATATGTCGTCACCTCAG
		TPR4_BmR	ATCAGGATCCCTGCTTCCATCTCCAACCTAC
	ARF2 full	ARF2_DBF	ATAGTCGACTAATGGCGAGTTCGGAG
		ARF2_BmR	ATAGGATCCTTAAGAGTTCCAGCGCT
	DBD	ARF2_DBD_F	ATAGTCGACTAATGGCGAGTTCGGAG
		ARF2_DBD_R	ATAGTCGACTGGCTCTACTTTCCACGG
	MD	MD_SmF	GCAGTCGACTAATGAGATTTGAAGGC
		MD_R	GCAGTCGACACTCCTACTTGAGTTGGT
	MDma	MD_SmF	GCAGTCGACTAATGAGATTTGAAGGC
		Mega primer1-maF	CACTCTGGTGCCTCCGCGAAGGCACATGAATCT
		Mega primer1-MD-R	GCAGTCGACACTCCTACTTGAGTTGGT
	MDmb	MD_SmF	GCAGTCGACTAATGAGATTTGAAGGC
		Mega primer1-mbF	GAAGTCAGGTCTCTGGCATT
		Mega primer1-MD-R	GCAGTCGACACTCCTACTTGAGTTGGT
	MDmab	MD_SmF	GCAGTCGACTAATGAGATTTGAAGGC
		Mega primer2-maF	CACTCTGGTGCCTCCGCGAAGGCACATGAATCT
Mega primer1-mbF		GAAGTCAGGTCTCTGGCATT	
PB1	Mega primer1-MD-R	GCAGTCGACACTCCTACTTGAGTTGGT	
	ARF2_PB1_F	ATAGTCGACTAATGAATGGGACAGACTCA	
	ARF2_PB1_R	ATAGTCGACTTAAGAGTTCCAGCGCT	
QRT-PCR	RSL4	RSL4_qF842	GTGCCAAACGGGACAAAAGT
		RSL4_qR1097	TTGTGATGGAACCCCATGTC
	ARF2	ARF2_qF3471	TGGAGAGTTGATGGCTCCTA
		ARF2_qR3735	CTCGCTCCTACAGCTTAAAGTC
	ACT7	ACT7-rt-F	TCCCTCAGCACCTTCCAACAG
		ACT7-rt-R	CAATTCCCATCTCAACTAGGG
	GH3.6	GH3.6-rt-F	GGACTTTCGATAAGCTCATGGATTATGCG
		GH3.6-rt-R	GTTTCCTCTTTAGTTACTCCCCCATTGC
Pull-down	pGEX-4t-1(ARF9)	GST-A9-EcF	TAAAGAATTCAATCAGCTGATGGCAAATCG
		GST-A9-XhR	TTTTCTCGAGGTTGGAATGATTATCTGTTTTG
	pGEX-4t-1(ARF9-DI,II)	GST-A9-DI,II-XhR	TTTTCTCGAGCACCTTGGTACGGCTTCTTG

## 3.4 Results I

### 3.4.1 In the root hair system, rARFs facilitate repression activity, and specifically overexpressed rARF results in short root hair phenotypes

Since auxin and auxin-signaling components positively affected root hair cell growth (Cho et al., 2007a; Cho et al., 2007b; Ganguly et al., 2010; Lee et al., 2010; Lee and Cho, 2006; Mangano et al., 2017), the root hair system can be used to determine the role of rARFs as a repressor in auxin signaling. To establish if rARFs are linked to root hair growth, we expressed eight rARFs (ARF1, 2, 3, 4, 9, 10, 11, and 16) in the root hair cell using the root hair-specific *EXPANSIN A7* promoter (*ProE7*; Cho and Cosgrove, 2002, Kim et al., 2006, Lin et al., 2011). All of the rARF overexpressed lines decreased root hair length to 20–54% of the control lines (Cont, *ProE7:GFP*), whereas overexpressed ARF5 (activator ARF) resulted in longer root hair than the root hair length of the control lines (Figure 23). These results indicated that rARFs are negative effectors for root hair growth and auxin signaling.

### 3.4.2 ARF2 has two putative TPL/TPR binding motifs in the middle domain

As previously reported (Lee et al., 2016), the interaction between TPL/TPRs and IAA7 contributes to the transcriptional repression function of IAA7 in auxin

signaling. TPL-binding motifs (LxLxL and R/K-LFG-V/I/F motif) were reported in

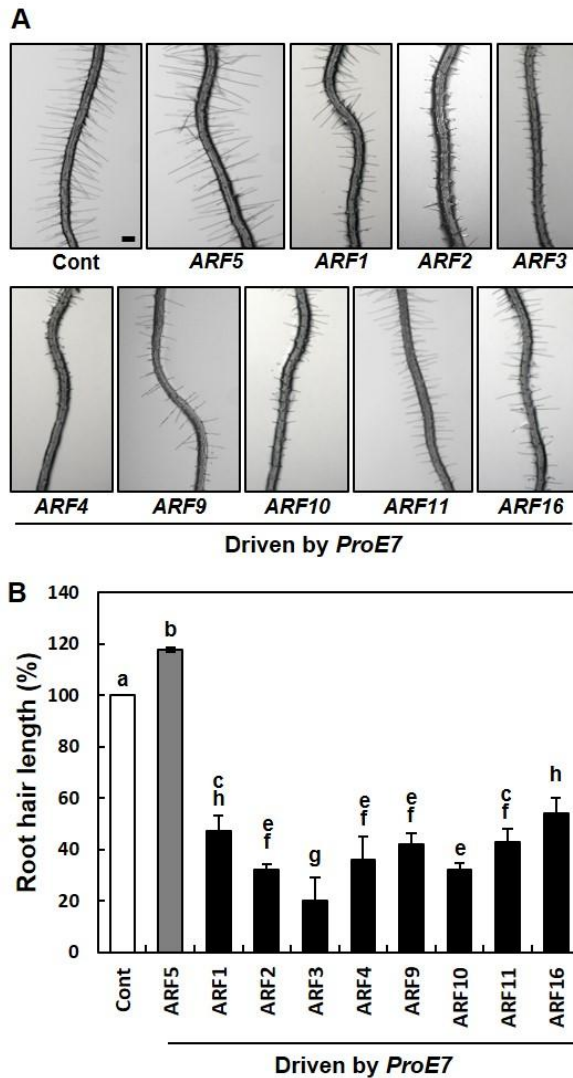


**Figure 23. Repressor ARFs inhibit root hair growth.** (A) Root hair phenotypes of control (Cont; *ProE7:YFP*) and root hair-specific *ARF*-overexpressing lines (*ProE7:ARFs*) in the wild-type background. Scale bar is 100  $\mu$ m. (B) Root hair length of control and *ARF*-overexpressing lines. Error bars indicate  $\pm$  s.e. ( $n = 163$ – $1,482$  root hairs from 12–78 plants from 4–6 independent transgenic lines). Statistically significant differences are denoted with different letters (one-way ANOVA with Tukey's unequal N HSD *post hoc* test,  $P < 0.05$ ).

ARFs. Only one of the activator ARFs, ARF19, has the LxLxL motif. Several rARFs include these TPL-binding motifs in their amino acids (Lokerse and Weijers, 2009). To examine whether the interaction between TPL/TPRs and rARF provides the repressive function to rARFs, we searched for TPL-binding motifs in rARF and marked where TPL-binding motifs are located. We found EAR-like and RLFV-like motifs (Figure 21). The sequences of these motifs are listed in Figure 22. The EAR-like motif was previously reported as a PpTPL-interacting motif in *Physcomitrella* (Paponov et al., 2009). The LxLxL motifs are located in DBD for ARF11, in MD for ARF2 and 19, and in PB1 for ARF12, 14, 15, 20, 21, and 22. The R/K-LFG-V/I/F motifs are located in MD of ARF1, 2, 3, 4, 9, 11, 12, 14, 15, 18, 20, 21, and 22. Recent structural studies have found that DBD and PB1 are homo- or heterodimeric protein-binding domains with ARFs or Aux/IAAs (Boer et al., 2014; Korasick et al., 2014). Thus, we focused only on the TPL-binding motifs in MD for rARFs. In particular, ARF2 has EAR, LxLxL and RLFV (RLFV in ARF2) motifs in MD and clear mutant phenotypes, as mentioned previously. I expected that these noteworthy characteristics of ARF2 (Okushima et al., 2005a; Okushima et al., 2005b; Schruoff et al., 2006; Smyth et al., 1990) would make it easier to investigate the function of TPL-binding motifs.

### 3.4.3 The repressive function of ARF2 in root hair growth

To check the repression activity of TPL-binding motifs in ARF2, three mutant forms of ARF2 were generated (*ma*, the substitution of amino acid residue L to R in EAR motif; *mb*, the substitution of amino acid residue L and F to S in RLFV

motif; *mab*, both mutations in the EAR and RLFGI motifs; Figure 24A).

The *ARF2* and three mutated genes were root hair specifically overexpressed by *ProE7*. I measured the root hair length of transgenic lines and found that the *ProE7:ARF2* seedling grew root hairs that were an average of 20% the length of the control (Figure 24B and C). This is an expected result, indicating that ARF2 negatively regulates root hair growth. *ProE7:ma* showed considerably longer root hair length than *ProE7:ARF2*. This means that the mutation of the EAR motif decreased the repression activity of ARF2 in root hair growth. *ProE7:mb* also showed longer root hair length than *ProE7:ARF2* and the root hair length of *ProE7:mb* was longer than *ProE7:ma*. Both TPL-binding motifs of ARF2 provide repression activity in root hair growth, but the functionality of RLFGI motif is relatively stronger than EAR motif. ARF2 mutated both TPL-binding motifs, and *mab* resulted in much lower repression activity in root hair growth than overexpressed ARF2, *ma*, and *mb*. Thus, both TPL-binding motifs are important for the normal behavior of ARF2 repression.

#### 3.4.4 Mutations of the putative TPL/TPR-binding motifs suppress ARF2-mediated inhibition of root hair growth and *RSL4* expression

To determine whether the transcript level of *ARF2* affects repressive function, I calculated the total *ARF2* and *ARF2* mutant transcript level. First, I confirmed the expression level of *ARF2* in *ProE7:ARF2* independent lines. The root hair length is

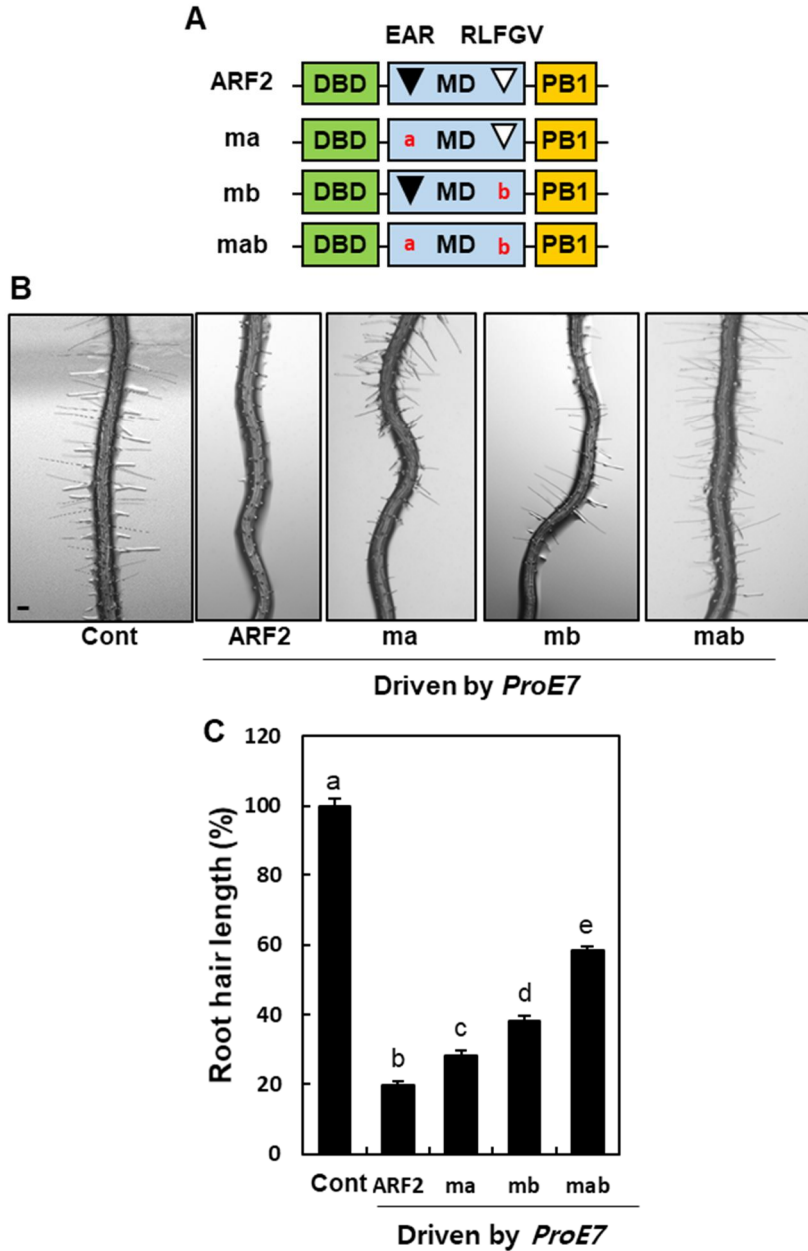


**Figure 24. Mutations of TPL-binding motifs suppress the ARF2-mediated inhibition of root hair growth.** (A) The schematic structures of wild-type (ARF2) and mutant (ma, mb, and mab) ARF2 where ma includes L-to-R substitutions in the

EAR motif (LxLxL), mb includes LF to SS substitution in the RLFGV motif, and mab includes both mutations in EAR and RLFGV motifs. (B) Root hair phenotypes of the control (Cont, *ProE7:GEP*) and overexpressed lines for wild-type or mutant *ARF2* genes (ma, mb, and mab) under the *EXPA7* promoter (*ProE7*) in the wild-type background. Scale bar is 100  $\mu$ m. (C) Root hair length of Cont and overexpressing lines of wild-type and mutant *ARF2* genes under *ProE7*. The root hair length is relative to the control value. Error bars indicate  $\pm$  s.e. (n = 597–3,318 root hairs from eight independent lines for transformants). Statistically significant differences are denoted with different letters (one-way ANOVA with Tukey's unequal N HSD *post hoc* test,  $P < 0.05$ ).

inversely proportional to the *ARF2* expression level (Figure 25). This indicated that repression activity depends on the dose of the repressor in root hair cells. Thus, we selected independent lines from each *ARF2* mutant-overexpressed line with a similar transcript level of *ARF2* (Figure 26A). Even though they expressed a similar level of total *ARF2* transcripts, each line was significantly different in *RSL4* expression, which is a key transcriptional factor for root hair growth (Hwang et al., 2017; Yi et al., 2010) and the direct target of activator ARF (Mangano et al., 2017; Figure 26B). *ARF2* #26 and *ma* #10 represented a similarly low level of *RSL4*. A similar result was obtained with *GH3.6*, another representative auxin-responsive gene (Figure 26B). The degree of the reduced root hair length of *ma* #10 is analogous to the root hair length of *mb* #9 lines. They showed 46–49% of the control root hair length (Figure 26C). However, it is unlikely that *ma* #10 and *mb* #9 did not show significant downregulation of the level of *RSL4* and *GH3.6* expression compared to those of control lines. The root hair that specifically overexpressed the *mab* line (*mab* #28) has an almost indistinguishable *RSL4* level from wild-type plants, but short root hair. This implied that the second TPL-binding motif of ARF2 (RLFGI) is a more powerful motif in transcriptional repression.

### 3.4.5 Both EAR and RLFGI motifs are necessary for ARF2 to interact with TPL

In the whole plant yeast two-hybrid experiments, TPL/TPRs already used ARF2, 9, and 18 as an interacting partner protein (Causier et al., 2012a). However, it is still

not proven whether the TPL-binding motif of ARFs affects the transcriptional

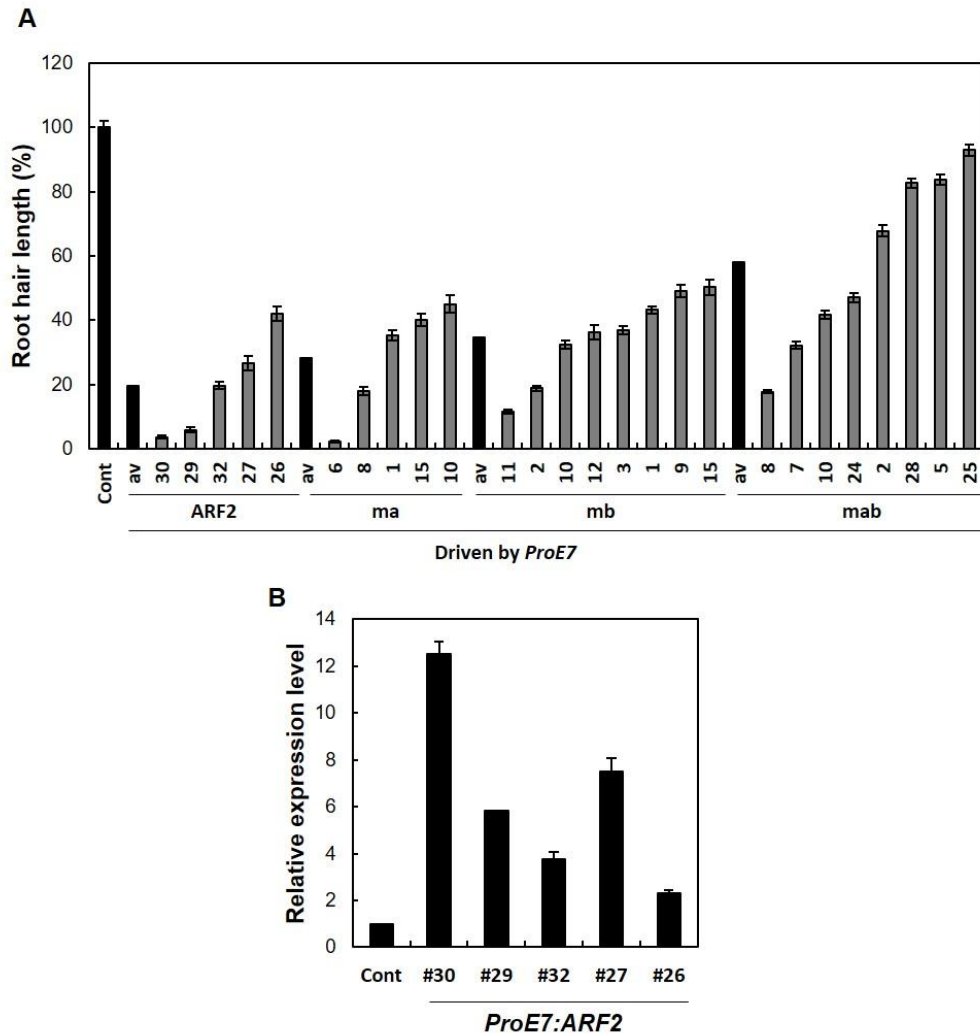


**Figure 25. Root hair length of mutant *ARF2*-overexpressing lines and *ARF2* expression.** (A) Root hair length of control (Cont, *ProE7:YFP*) and independent overexpressing lines of wild-type (*ARF2*) or mutant (ma, mb, and mab) *ARF2* genes under *ProE7*. The root hair length is relative to the control value. Data represent means  $\pm$  s.e. ( $n = 240$ – $597$  root hairs from each line). (B) Transcript levels of Cont and single-overexpressing lines for *ARF2* genes. Data represent means  $\pm$  s.d. from three biological replicates.

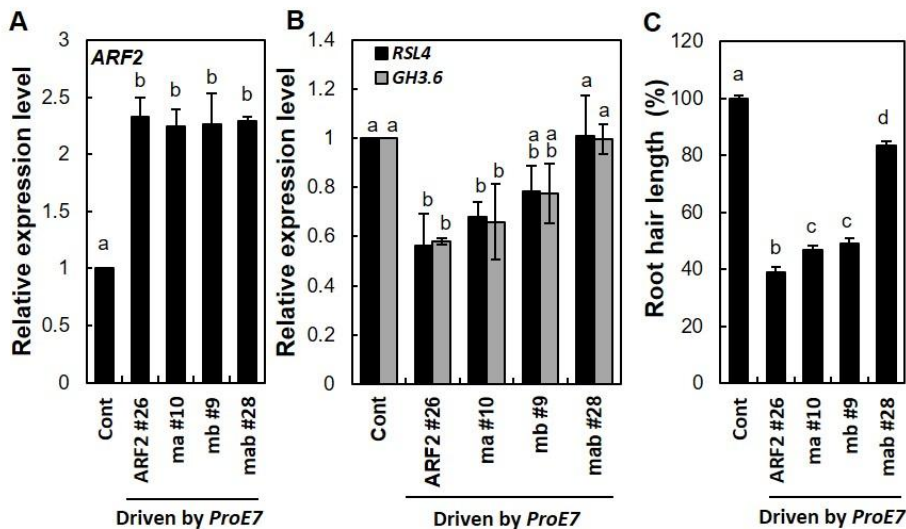


**Figure 26. Transcript levels of *ARF2* and root hair length in single transgenic lines.** (A) Transcript levels of *ARF2* in wild-type (*ARF*) or mutant (*ma*, *mb*, and *mab*) *ARF2*-expressing transformants. Cont is the control line (*ProE7::YFP*) and wild-type and mutant *ARF* were expressed under *ProE7*. Data represent means  $\pm$  s.d. from two biological repeats. (B) Transcript levels of *RSL4* and *GH3.6* of Cont and single overexpressing lines for wild-type or mutant *ARF2* genes. Data represent means  $\pm$  s.d. from three biological replicates. (C) Root hair length of control (Cont) and single overexpression lines of *ARF2* and *ARF2*-mutant forms, respectively. Data represent means  $\pm$  s.e. ( $n = 160$ – $1,429$  root hairs from each line). Statistically significant differences are denoted with different letters (one-way ANOVA with Tukey's unequal N-HSD *post hoc* test,  $P < 0.05$ , C and D).

repressive function in plants. Our data demonstrated that the function of repressor ARF2 significantly originates from interacting with TPL. We conducted a yeast two-hybrid (Y2H) assay to determine whether ARF2 binds to TPL/TRPs. First, we performed an assay to know which domain has TPL protein interacting activity. In the Y2H assay, using GAL4 DNA-binding domain (BD)-tagged TPL and activation domain (AD)-tagged ARF2 full-length, DBD, MD, or the PB1 domain of ARF2 showed that yeast cells were only able to grow with both the TPL as a BD and the protein containing a middle domain as an AD, likely ARF2 or MD (Figure 27A, B). These results suggest that TPL binds to ARF2 in the yeast cell through the MD.

Next, we investigated whether the TPL-binding motifs of ARF2 MD are truly involved in interaction with TPL/TRPs. In the Y2H assay, MD clones were confirmed to interact with TPL (Figure 27A, C). The interaction affinity of MD<sub>ma</sub> decreased the interaction between TPL and MD in the presence of 0.2 mM 3AT in the SD3- medium (Figure 27C). Additionally, *mb #9* decreased root hair length in EAR motif (Figure 26). This indicates that EAR motif is required for full interaction with TPL and has repressive force. However, there is no interaction between TPL and MD<sub>mb</sub> that is analogous to MD<sub>mab</sub> in Y2H (Figure 27C). Thus, we suggest that TPL can bind to MD through both EAR and RLFGI motifs, but RLFGI plays a critical role in the interaction with TPL. These results coincide with our mutated ARF2 overexpressed root hair data.

We continually tested whether the TPL homologs were able to interact with the TPL-binding motifs of ARF2 because Arabidopsis has four homologs of TPL

(TPR1, 2, 3 and 4). In Y2H assay, when using MD as bait, TPL, TPR1, TPR2, and

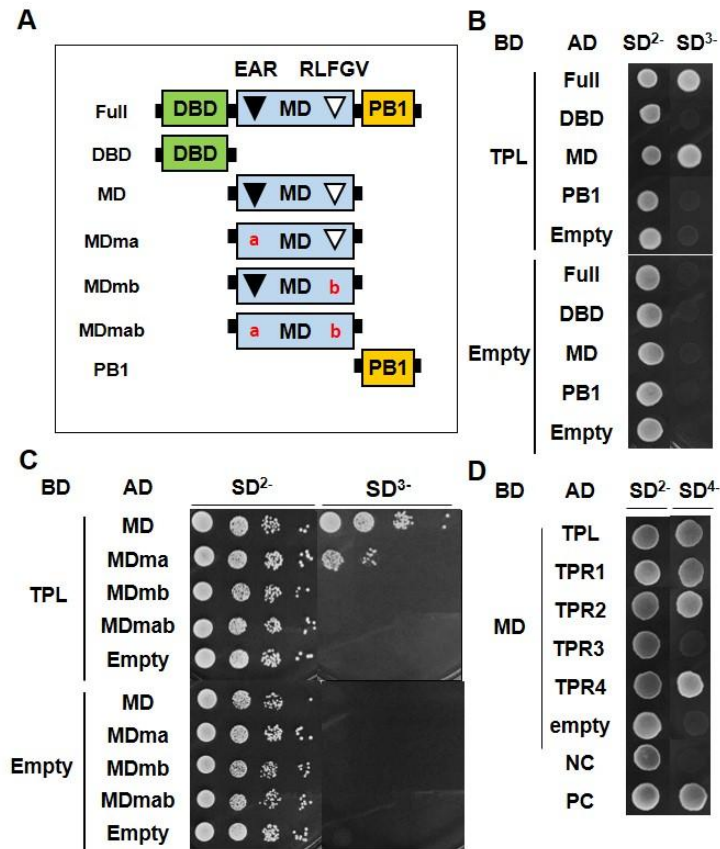


**Figure 27. EAR and RLF RGV motifs are required for the interaction of ARF2 with TPL/TPRs in the yeast cell.** (A) Schematic representations of ARF2 full domains (Full), domain deletions (DBD, MD, PB1), and motif-mutated middle domains (MDma, MDmb, and MDmab). (B) Yeast two-hybrid assay between TPL and ARF2 domains. TPL is fused with GAL4 DNA binding domain (DB), and full length and domain-deleted ARF2 are fused with the GAL4 activation domain (AD). (C) Yeast two-hybrid assay between TPL and mutated ARF2-MD series. TPL is fused with GAL4-BD, and ARF2-MD series are fused with GAL4-AD. (D) Yeast two-hybrid assay between ARF2-MD (MD) and TPL/TPRs. MD is fused with GAL4-BD and TPL/TPRs are fused with GAL4-AD (NC, negative control; PC, positive control as described in Material and Methods). Empty indicates no TPL in the BD-fusion (B and C), and no ARF2 domain (B), no MD (C), or no TPL/TPR

(D) in the AD fusion.

TPR4 were found to bind to MD, but TPR3 did not. This result showed that ARF2 interacts with these co-repressors with different affinities. However, as previously reported, ARF2 interacts with TPL, TPR3, and TPR4, but not TPR1 and TPR2, shown by the Y2H screening of the whole plant library (Causier et al., 2012a). Thus, rARF-TPL/TPRs interaction may be different depending on the cellular conditions. They also showed that ARF9 and ARF18, which contain one RLFGE motif, interact with TPL/TPRs. According to the results, we infer that other repressor ARFs with TPL-binding motifs in the middle domain could bind differently to TPL/TPRs with their own interaction affinity.

### 3.4.6 The repressive motifs of ARF2 are required for the native function of ARF2

To examine the regulatory role of the interaction between TPL and ARF2 in its own expression domain, we confirmed the phenotypes of ARF2 loss-of-function mutants. These *arf2* mutants generate truncated ARF2 transcripts due to T-DNA insertion. We checked the expressed transcript by genotyping PCR (Figure 28). To evaluate the function of TPL-binding motifs, I expressed ARF2 and ARF2 mutant series under the *ARF2* promoter (*ProARF2:ARF2* and *ProARF2:ARF2 mutant* series) in *arf2* plants.

The late flowering phenotype was observed from four ARF2 mutant alleles, *arf2-6* and *arf2-7* (Okushima et al., 2005a), *arf2-8* (Ellis et al., 2005), and *ore14-1* (Lim et al., 2010). We tried to verify the relationship between late flowering

time

and the repressive function of ARF2. To analyze flowering time, we measured the

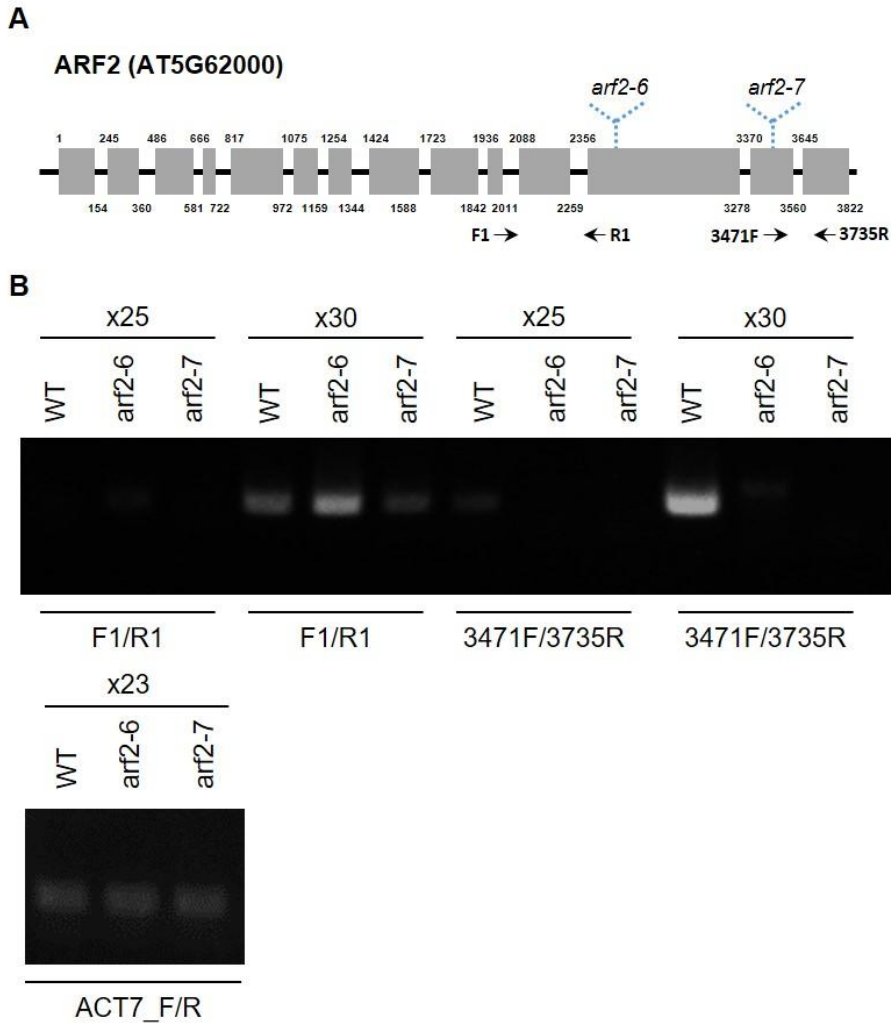


**Figure 28. RT-PCR analysis of the *ARF2* transcript in two *arf2* mutant alleles.** (A) T-DNA insertion positions in the *ARF2* coding region for two *arf2* mutants. Gray boxes represent exons and numbers indicate the nucleotide positions relative to the start codon. Arrows indicate the direction and position of the primers used for RT-PCR analysis in B. (B) RT-PCR analysis of the *ARF2* transcripts from *arf2-6*, *arf2-7*, and wild-type (WT) seedlings. The expression of the *ACTIN7* (*ACT7*) gene was used as a control. Min-Soo Lee contributed to these experiments.

rosette leaf number and days of bolting. Generally, wild-type plants represent an average of 10 rosette leaves and about 23 days of bolting. The *arf2-6* and *arf2-7* showed a relatively late flowering time, producing 19.6 rosette leaves and about 36 days of bolting, that was delayed by two weeks compared to wild-type plants. ARF2 seems to help flowering progress. To demonstrate the function of the TPL-binding motif of ARF2 in regulating flowering time, we observed the phenotype of the ARF2 complemented line (ARF2, *ProARF2:ARF2*) and three types of transgenic lines (*ma*, *ProARF2:ma*; *mb*, *ProARF2:mb*; *mab*, *ProARF2:mab*) in *arf2-6* and *arf2-7* mutant backgrounds (Figure 29A, B). Complemented and transgenic lines in the *arf2-6* mutant background, with the exception of *mab*, showed similar rosette leaf numbers and days of bolting as wild-type plants. The transgenic line-expressed *mab* of *ProARF2* could not recover and delayed flowering time like an *arf2-6* mutant (Figure 29C). ARF2 complemented lines in the *arf2-7* mutant background showed a completely recovered phenotype like a wild-type plant. However, *ma* and *mb* in the *arf2-7* mutant background were significantly different from the wild-type (Figure 29D). The bolting time was moved back by four days in transgenic lines at the *arf2-7* background. In this case, *ma* or *mb* results in the decrease of ARF2 ability. This indicated that ARF2 requires both TPL-binding motifs for normal behavior in plant development. It is assumed that the reason for the difference between transgenic lines in *arf2-6* or *arf2-7* backgrounds is due to the different expression level of the development. It is assumed that the reason for the difference between transgenic lines in *arf2-6* or *arf2-7* backgrounds is due to the different expression level of the

transgene or different residual functionalities of *arf2* mutant proteins. The

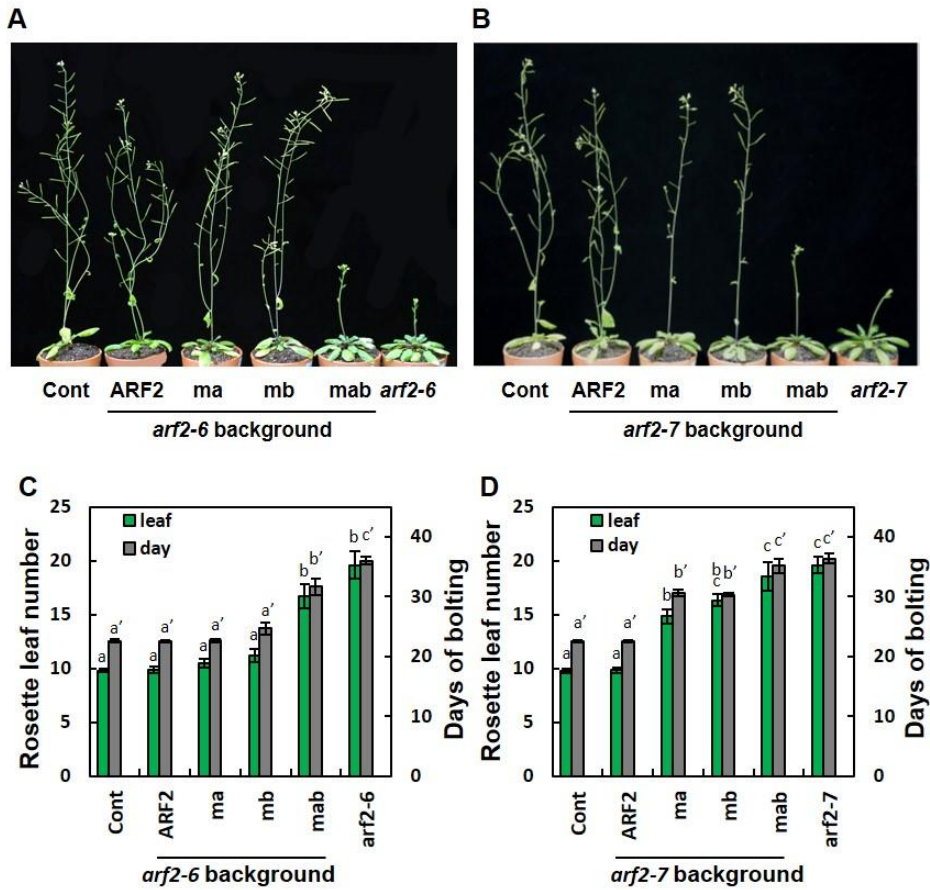


**Figure 29. The repressive motifs are required for the ARF2-mediated regulation of the flowering time.** (A and B) Inflorescence phenotypes of 35-day-old wild-type (Cont), *arf2* mutants, and *arf2* mutants complemented with wild-type (ARF2) or mutated (ma, mb, and mab) *ARF2* under *ProARF2*. (C and D) The flowering times of the lines are as shown in A (C) and B (D) in terms of rosette leaf number at bolting time. Error bars indicate  $\pm$  s.e. ( $n = 7-12$  plants from 2-3 independent lines). Statistically significant differences are denoted with different letters (one-way ANOVA with Tukey's unequal N HSD *post hoc* test,  $P < 0.05$ ).

*ProARF2:mab* in the *arf2-7* background was also unable to recover and experienced delayed flowering time like an *arf2-7* mutant. In other words, TPL-binding motif-mutated ARF2 completely lost function regarding the regulation of flowering time.

I also evaluated the seed sizes. As previously reported (Okushima et al., 2005a; Schruff et al., 2006), the seeds of *arf2-6* and *arf2-7* mutants were ~150% of the size of the control (Figure 30). A complementation of ARF2 under its own promoter fully recovered the seed size of the control. Whereas other mutant gene expressed lines (*ma*, *mb*, and *mab*) showed significantly larger seed sizes than those of the control (wild-type seeds), the larger seed size of transgenic lines indicated that the repressive activity of mutant ARF2 is weaker than wild-type ARF2 in seed growth. In particular, the transformants expressing *mab* produce seeds that are similar in size to the *arf2-6* or *arf2-7* mutant. This means that *mab*, which mutated both TPL-binding ARF2 motifs, experiences complete malfunction in seed growth. The complementation assay suggests that the TPL-binding motifs are essential for the repressive activity of ARF2 in seed growth. However, I expected smaller seeds from the *mab* mutant because *mab* has shown repressive function in the root hair assay of *ProE7:mab*. I carefully reasoned that the *ProE7*, a strongly expressed promoter in root hair cells, caused excessive expression of *ARF2*. However, analysis of seed size is done using *ProARF2*.

Additionally, I gave attention to the root hair length of mutants because root hair specifically overexpressed ARF2 showed root hair-defective phenotypes.

The  
average root hair length of *arf2-6* and *arf2-7* is significantly longer than that

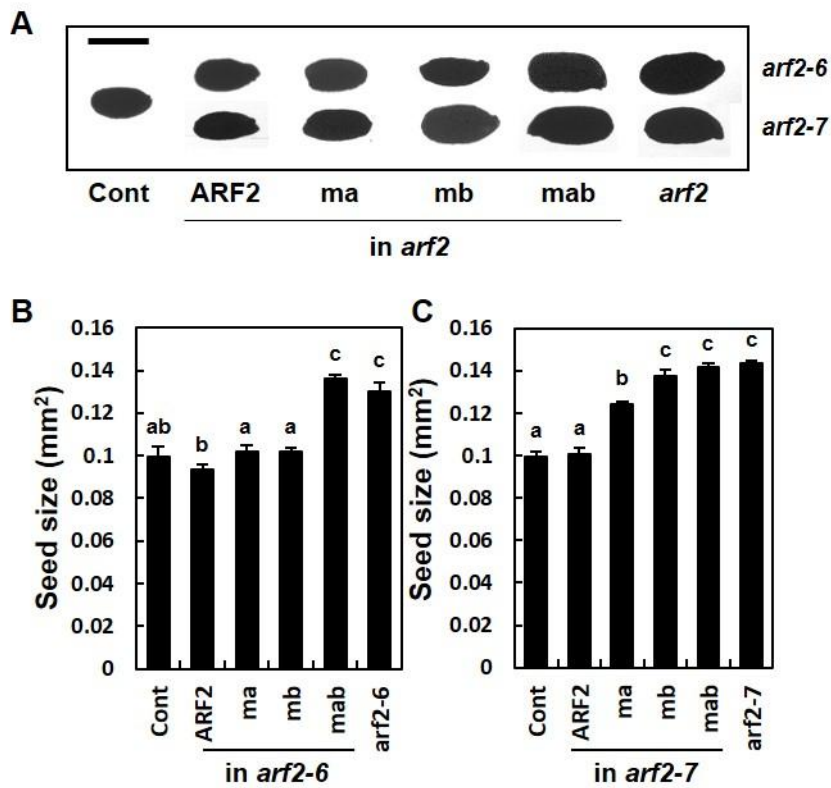


**Figure 30. The determination of seed size by ARF2 requires its TPL/TPR-binding motifs.** (A) Representative seed images of wild-type (Cont), *arf2* mutants, and *arf2* mutants complemented with wild-type (ARF2) or mutated (ma, mb, and mab) *ARF2* under *ProARF2*. Scale bar is 500  $\mu$ m. (B and C) Quantitative seed size analyses of the lines shown in A. Seed size was quantified as the area of a two-dimensional seed image. Data represent means  $\pm$  s.e. ( $n = 24$ – $244$  seeds from 3–7 independent lines for transformants). Statistically significant differences are denoted with different letters (one-way ANOVA with Tukey's unequal N-HSD *post*

*hoc* test,  $P < 0.05$ ).

observed in wild-type plants (113–116% of the control) (Figure 31). Although previous researchers did not report the root hair phenotype of ARF2 mutants, the results indicated that the repression activity of ARF2 is natural in wild-type plants.

In this study, we have demonstrated the molecular interaction between TPL/TPRs and ARF2 EAR/RLFGI motifs, the function of these repressive motifs in ARF2-mediated gene regulation, and three biological processes. The disruption of both TPL-binding motifs fails to recover the function of ARF2 in auxin-related phenotype and molecular interaction. This suggests a possible regulatory role for the interaction of TPL and ARF2. Further studies should follow by extending this view to other rARFs that include these repressive motifs. I suggest a model of the repressor ARF that sets the threshold in auxin-signaling transcription (Figure 42). For a low concentration of auxin, aARF and rARF balance transcription at a low or no expression level. Increases in the auxin level and Aux/IAA degradation cause strong aARF activity in target gene transcription whereas rARF has not changed the activity of transcription. On the other hand, even if there is fluctuation in auxin concentration, increasing the level of rARF could block auxin-responsive transcription. In our root hair assay, all the tested rARFs revealed inhibitory effects for auxin-responsive root hair growth (Figure 23). Since RLFGV- or a RLFGV-like motif is present in most rARFs and located in similar MD regions (Figure 21), this could be a general repressive motif among rARFs.

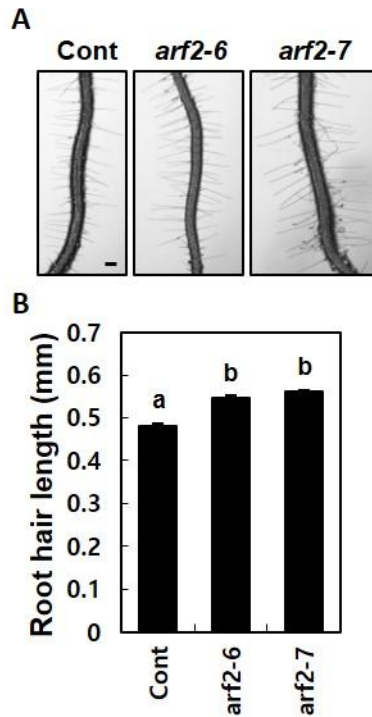


**Figure 31. Root hair phenotypes of *arf2* loss-of-function mutants.** (A and B) Root hair images (A) and length (B) of control (Cont, wild-type), *arf2-6*, and *arf2-7*. Data represent means  $\pm$  s.e. ( $n = 336$ – $608$  root hairs from 21–38 seedlings). Statistically significant differences are denoted with different letters (one-way ANOVA with Tukey’s unequal N HSD *post hoc* test,  $P < 0.05$ ). Scale bar is 100

$\mu\text{m}$ .

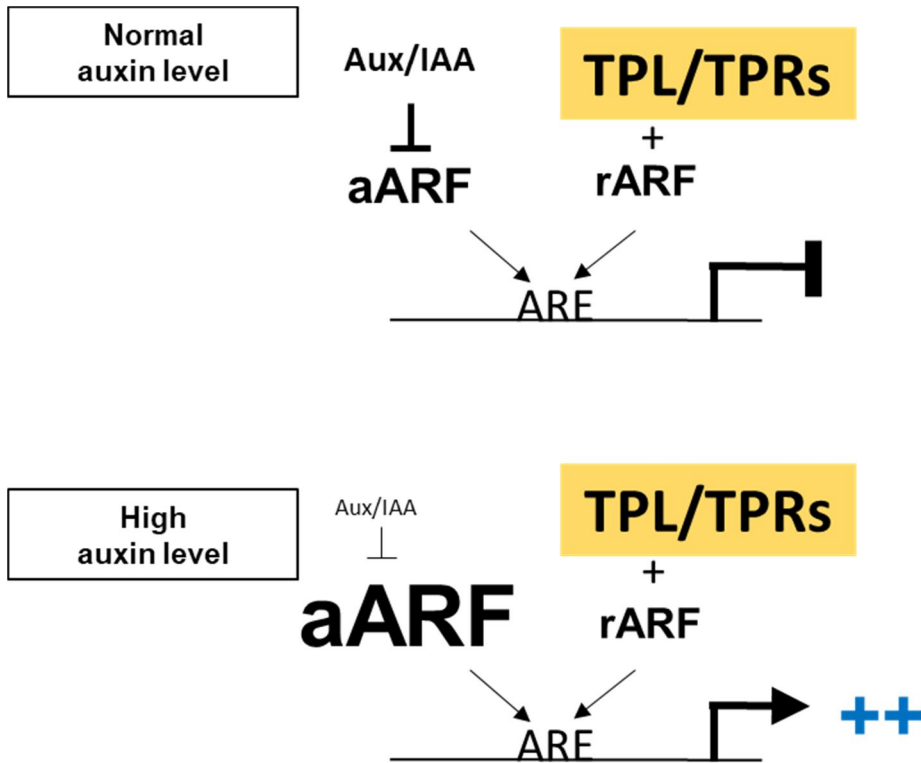


**Figure 32. A model illustrating the repressor ARF sets the threshold in auxin signaling transcription.** A schematic model depicting the role of rARFs interacting with TPL/TPRs in auxin signaling; with a low concentration of auxin, aARF and rARF have balanced transcription activity at low or no expression level. Increasing auxin level, Aux/IAA degradation cause strong activity in aARF with regard to target gene transcription, whereas rARF does not change transcription activity. However, if the level of rARF increases, rARF could block the auxin-responsive transcription in an auxin-independent manner (aARF: activator ARF; rARF: repressor ARF; ARE: auxin-response cis-element; TPL/TPRs: co-repressor in auxin signaling).

## 3.5 Results II

**3.5.1 Auxin does not enhance the rARF activity in root hair growth** Auxin response and signaling are mediated by Aux/IAAs for targeted gene regulation. A certain factor interacting with Aux/IAA indicates that the factor is involved in the auxin-dependent pathway. Generally, the treatment of auxin ranging from 30 nM to 50 nM increases the root hair length of wild-type plants. Even activator ARF8-overexpressed plants grown on auxin media gradually increased their root hair length depending on auxin concentration (Figure 33A). The role of repressor ARFs in an auxin-dependent manner should be elucidated. Only the ARF4 and ARF9 rARFs bind to Aux/IAAs (Piya et al., 2014; Vernoux et al., 2011). To investigate the relationship between auxin and rARFs, I further studied the function of ARF4 and ARF9.

### 3.5.2 The function of PB1 in ARF9

To examine whether ARF4 and ARF9 are dependent on auxin, I expressed them root hair specifically. In addition, I expressed ARF10 as a non-binding rARF to Aux/IAA. Root hair, specifically rARFs overexpressed lines (*ARF4ox*, *ARF9ox*, and *ARF10ox*), showed short root hairs; however, they also showed slightly increased root hair length with auxin treatment (Figure 33B, C, D). This result indicates that auxin could not enhance the natural function of rARFs as expected when following an auxin-dependent manner. For additional analysis of the relationship between rARF and auxin, I deleted ARFs overexpressed lines

(*ARFs* $\Delta$ *PBIox*) from the PBI domain,

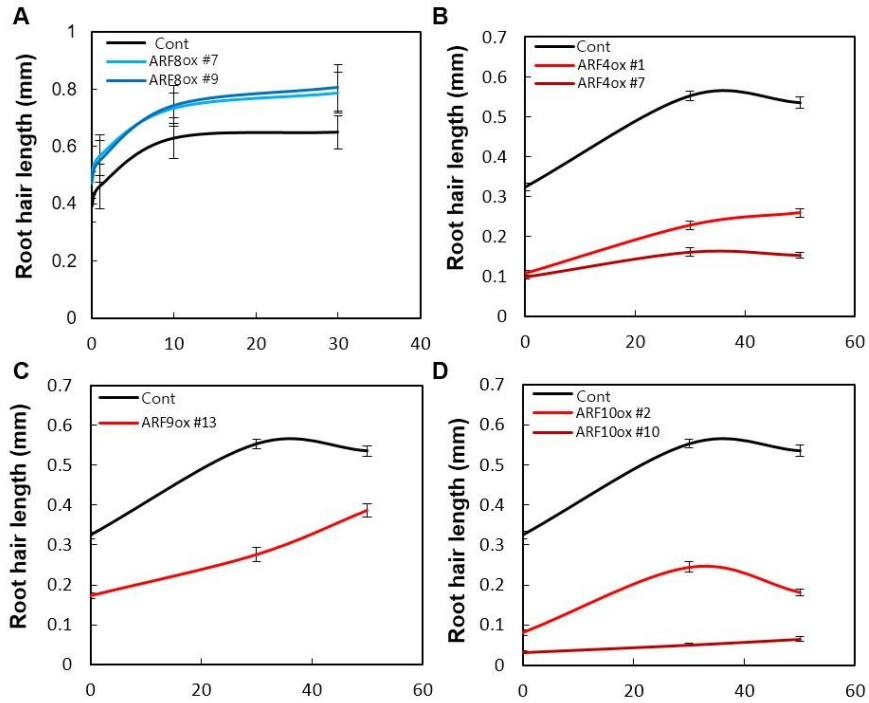


**Figure 33. Root hair length of ARF-overexpressing lines in different auxin concentration media.** (A) Root hair length examined specifically for activator ARF-expressing transgenic lines grown in different concentrations of auxin (IAA) media. The control (*ProE7:YFP*, Cont) and *ProE7:ARF8* (*ARF8ox*) lines. Data represent means  $\pm$  s.e. ( $n = 88$ – $361$  root hairs). (B–D) Root hair length examined specifically for repressor ARFs expressing transgenic lines grown in different concentrations of auxin media. (A) Measuring root hair length of control (*ProE7:YFP*, Cont), *ProE7:ARF4* (*ARF4ox*, B), *ProE7:ARF9* (*ARF9ox*, C), and *ProE7:ARF10* (*ARF10ox*, D). Data represent means  $\pm$  s.e. ( $n = 80$ – $360$  root hairs).

assuming that the auxin signal transmits by Aux/IAA binding to ARFs. Previously, ARF2-overexpressed lines have changed their repressive ability depending on the transgene expression level. I checked the root hair length of independent lines from wild-type ARFs overexpressed plants (*ARF4ox*, *ARF9ox*, *ARF10ox*) and PB1 domain-deleted ARFs overexpressed plants (*ARF4ΔPB1ox*, *ARF9ΔPB1ox*, *ARF10ΔPB1ox*) (Figure 34). All overexpressed lines showed short root hairs. However, several independent lines from *ARF9ox* showed relatively longer root hair compared to the root hair of *ARF9ΔPB1ox* lines, whereas the average root hair length of *ARF4ox* and *ARF10ox* lines are similar to those of the *ARF4ΔPB1ox* and *ARF10ΔPB1ox* lines.

I further confirmed the difference between ARF9 and ARF9ΔPB1. However, there is a possibility of protein structure modification due to PB1 domain deletion. Progressive research of the crystal structure discovered the important protein-interacting motifs of the PB1 domain at ARF C-terminal (Korasick et al., 2014). ARF7 with mutation of the Lysine and OPCA motif in the PB1 domain does not bind to other ARF7 or IAA17. I observed the root hair phenotype from root hair specifically overexpressed in ARF9 lines (*ARF9ox*) and PB1 domain mutated ARF9 lines (*ARF9mKmOPCAox*) (Figure 35A). After measuring the root hair length, the expression level of the transgene was also evaluated using *ARF9ox* or *ARF9mKmOPCAox* independent lines, respectively. I selected two transgenic lines, *ARF9ox* #16 and *ARF9mKmOPCAox* #6, which expressed similar levels of transgenes. Although they have similar transgene expression levels, the root hair length of the two lines is significantly different. The root hair length of *ARF9ox*

#16

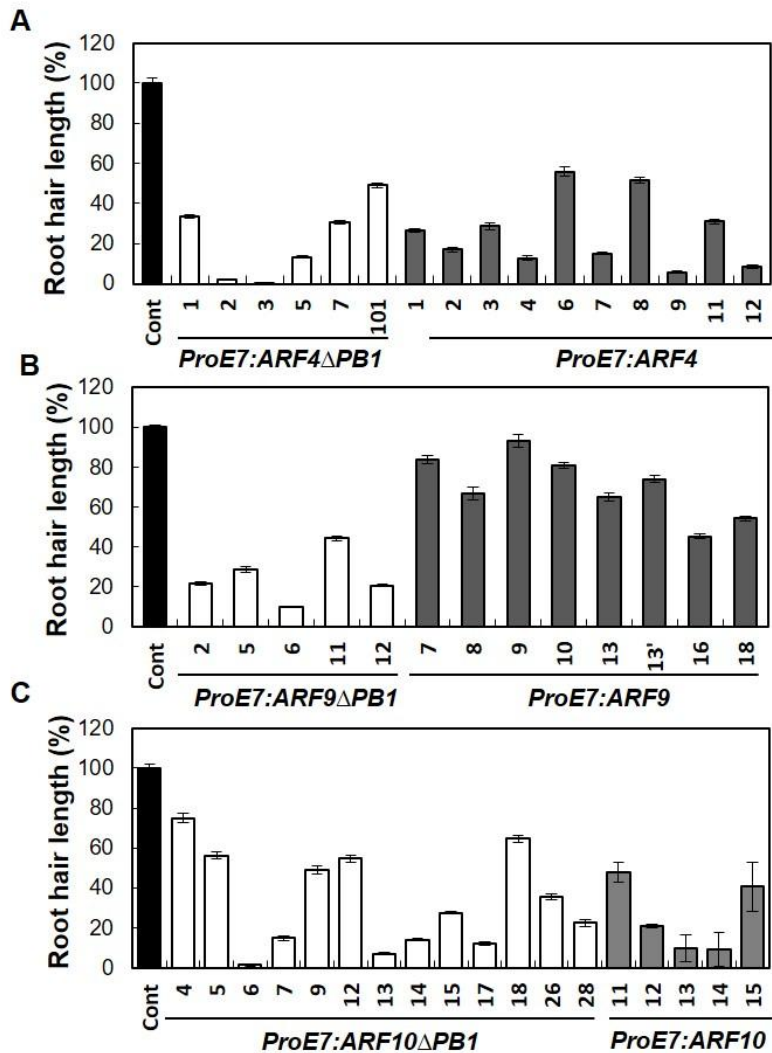


**Figure 34. Root hair length of overexpressing rARFs and PB1 domain-deleted rARFs.** (A) Root hair length of control (*ProE7:YFP*, Cont), *ProE7:ARF4*, and *ProE7:ARF4ΔPB1* T2 lines. Data represent means  $\pm$  s.e. (n = 56–520 root hairs). (B) Root hair length for control (*ProE7:YFP*, Cont), *ProE7:ARF9*, and *ProE7:ARF9ΔPB1* T2 lines. Data represent means  $\pm$  s.e. (n = 94–812 root hairs). (C) Root hair length of control (*ProE7:YFP*, Cont), *ProE7:ARF10*, and *ProE7:ARF10ΔPB1* T2 lines. Data represent means  $\pm$  s.e. (n = 21–889 root hairs).

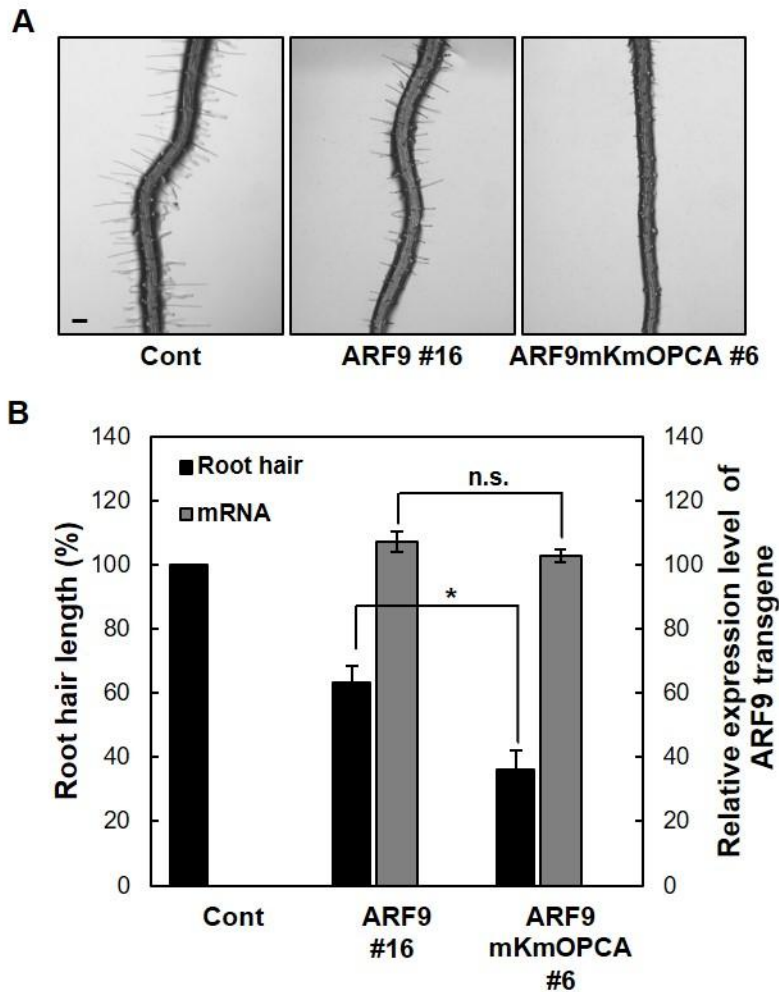


**Figure 35. Transcription levels of *ARF9* and root hair length in single transgenic lines.** (A) Root hair phenotypes of control (*ProE7:YFP*, Cont) and single overexpression lines of *ProE7:ARF9* (ARF9 #16) and *ProE7:ARF9mKmOPCA* (ARF9mKmOPCA #6), respectively. (B) Root hair length and transcript levels of transgene (*ARF9* or ARF9mKmOPCA driven by *ProE7*) expressing transformants. Data represent means  $\pm$  s.e. from three biological replicates. The values are significantly different ( $*P < 0.001$ , Student's *t*-test) from the control value (C and E). Scale bar is 100  $\mu$ m.

is about 64% of the control and that of *ARF9mKmOPCAox #6* is about 27% of the control (Figure 35B). This shorter root hair pattern from the null-function PB1 domain of ARF9 is equal to the results of the PB1 domain-deleted ARF9. ARF9mKmOPCA enables the formation of a homodimer with ARFs by DBD (Boer et al., 2014), but never forms a heterodimer with Aux/IAAs. Therefore, this indicates that the interaction with Aux/IAAs reduces the repression ability of ARF9, at least in root hair growth. I also infer that the repressive transcriptional activity of ARF9 will be enhanced by the high auxin level in a cell. However, the auxin-treatment experiments have previously shown that some lines did not decrease their root hair length, perhaps due to the enhanced function of aARF in hair cells. Thus, ARF9 may be auxin-dependent for the repression of target genes when it is expressed a cell where aARF is not expressed.

To analyze the relationship between ARF9 and Aux/IAAs, I hypothesized that Aux/IAA interrupts the ARF9 DNA binding to suppress the function of ARF9. I expressed GST-tagged ARF9 and ARF9 $\Delta$ PB1 constructs in bacteria and tested the binding ability of biotin-labeled ARE using *in vitro* pull-down assay (Figure 36). Both proteins bound to synthetic DNA, the palindromic sequences of ARE referred to in Boer et al.'s 2014 paper. However, if ARF9 interacts with SHY2 proteins before reacting with the DNA sample, ARF9 did not bind to ARE. There still remains a little ARF9 $\Delta$ PB1 in the DNA. I suggest that heterodimerization with Aux/IAA may negatively influence the DNA binding of ARF9.

### 3.5.3 The phyllotaxis defect in *arf9-1* loss-of-function mutant

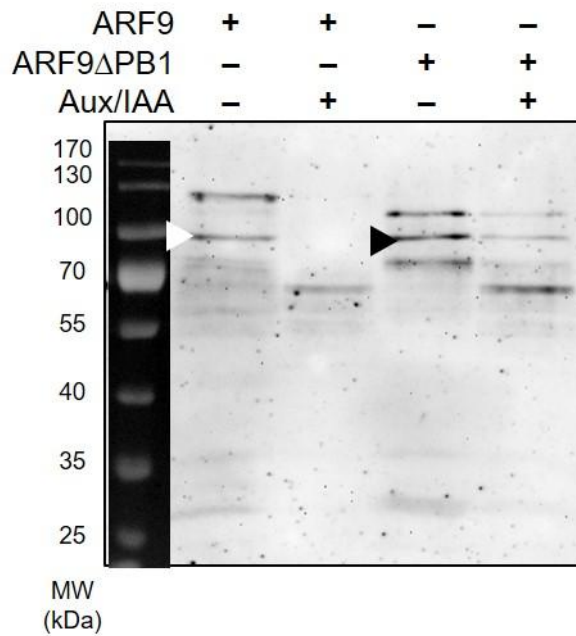


**Figure 36. Effect of PB1 domain in ARF9 binding to ARE.** *in vitro* pull-down assays of ARF9 and PB1 domain deleted ARF9 (ARF9 $\Delta$ PB1). GST-tagged ARF9 and ARF9 $\Delta$ PB1 affinity-purified proteins were used for the pull-down assay with or without SHY2 protein. Arrowheads indicate the GST fusion proteins for ARF9 (white) and ARF9 $\Delta$ PB1 (black), respectively.

I aim to determine the necessity of rARF9 for fine-tuning the transcription of auxin response genes. Most rARFs fail to show the clear phenotypes of mutant plants. However, auxin involves numerous plant patterning processes. There is evidence that auxin-signaling components are important for shoot development. Auxin shows clear differential distribution in the shoot meristem through the distribution of TIR1/AFB activities (Vernoux et al., 2011). ARF5 directly expresses PIN-FORMED (PIN) auxin efflux proteins and controls the patterning in the shoot and root embryos (Krogan et al., 2016). Polar auxin transports attribute plant phyllotaxis by regulating the auxin maxima only at the certain minimal region, where future primordia are expected (Reinhardt et al., 2003). Thus, auxin maxima, auxin signaling, and auxin transport are closely linked to shoot development and phyllotaxis. The systematic RNA *in situ* hybridization showed 13 ARFs and 12 Aux/IAA expressed in the shoot meristem. The only mRNA of ARF9 and ARF10 expressed the whole shoot apical meristem region (Vernoux et al., 2011). Therefore, I anticipate the possibility of ARF9 function in phyllotaxis.

The *arf9-1* mutant line T-DNA was inserted into the first exon of *ARF9* (Figure 37A). I found that the defect of vegetative leaves in phyllotaxis from *arf9-1* caused loss-of-function in the plant. The distribution of graph of *arf9-1* is wider and flatter than that of the wild-type plants (Figure 37B). This indicates that the repression function of ARF9 is necessary for new organ formation, at least in phyllotactic patterning. These genes should be suppressed in the wild-type and may activate because of the loss of ARF9 in the *arf9-1* mutant. However, we still could not solve what the role of ARF9 is. Thus, I have scheduled investigation of the

auxin

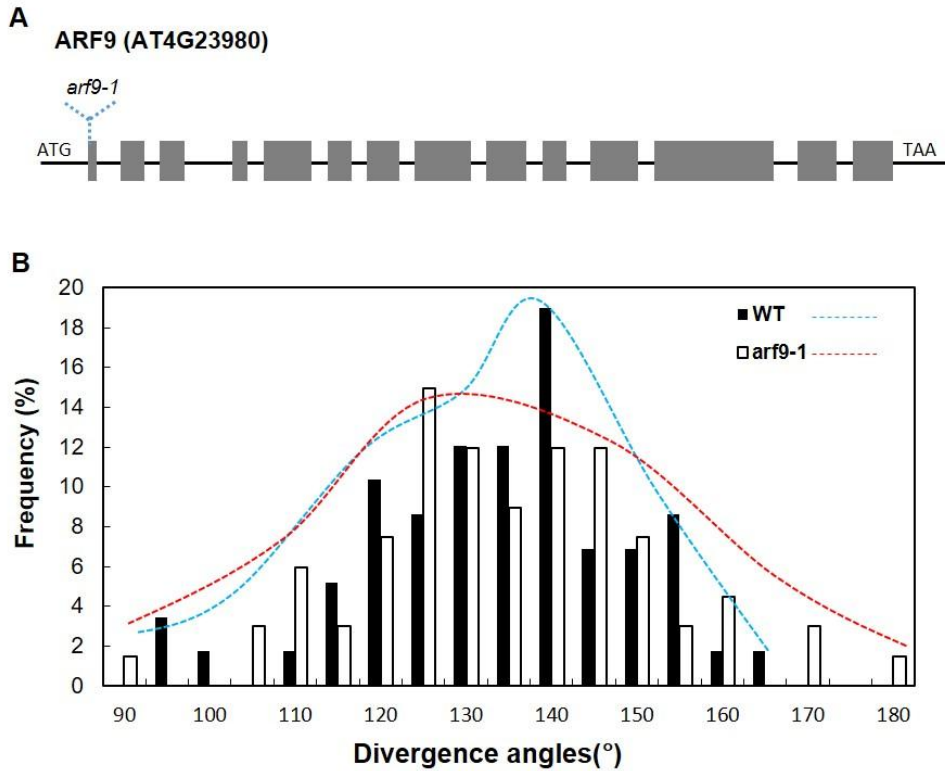


**Figure 37. *arf9* loss-of-function plant affects phyllotaxis change of vegetative leaves.** (A) T-DNA insertion position in the *ARF9* coding region for *arf9-1* mutants. Gray boxes represent the exons, ATG is start codon, and TAA is stop codon. (B) Divergence angles analysis of *arf9-1* mutants. The total number of WT rosette leaf angles is 59, *arf9-1* is 67. (n = 59 from wild-type, 67 from *arf9-1* leaf angles).

distribution, expression pattern of ARF9 and aARF involved in phyllotaxis for comparative analysis.

### **3.6 Discussion**

Auxin distribution and signaling are important for plant organogenesis (Friml et al., 2003; Tanaka et al., 2006). The polar transporter accumulates auxin in a specific cell and then results in an auxin response. These events result in cell division and differentiation. However, if the auxin response generates in unexpected cells owing to a loss of repressors, it inhibits organ development or brings severe defects (Rademacher et al., 2012; Szemenyei et al., 2008), although the other signaling components are normal. Thus, the repression mechanism by rARFs is as important as the activation mechanism by aARFs in auxin signaling. However, it is hard to determine the phenotype from a single mutant of rARFs, except ARF2 and ARF3. In this situation, we showed repression in root hair growth from a single overexpressed rARF (Figure 23).

Our works discover a substantive relationship between the repressor ARF, especially ARF2, and the co-repressor, TPL/TRRs. It is necessary to interact with the co-repressor for the proper function of other rARFs in plant development.

In this study, we conducted Y2H assays to confirm the binding of TPL/TPRs to the EAR motif and the R/K-LFG-I motif of ARF2. To provide further validation for TPL/TPR-mediated ARF2 transcriptional repression in plant

development, we used a root hair system. In the analysis, root hair-specific ARF2 overexpression resulted in short root hair. The disruption of both EAR and RLFGI motifs almost fully abolished the ARF2 functions. These co-repressor-binding motifs are likely to play a major role in the repressive function of ARF2 and probably other rARFs.

However, TPL-binding motifs are not present in all repressor ARFs. In Arabidopsis, ARF10, 16, and 17 do not have these motifs. *Physcomitrella patens* has fifteen PpARFs and two PpTPLs. In addition, Moss TPL bound to Moss ARFs in Y2H experiments (Causier et al., 2012b). They showed that two PpARFs interacted with both PpTPL1 and PpTPL2. PpARFe contained one repression domain, the LxLxL motif. PpARFf had an LxLxL motif and an EAR-like motif (LxLxPP motif). Moss Aux/IAAs used the EAR-like motif (LxLxPP) for interacting with Moss TPL rather than the LxLxL motif (Paponov et al., 2009). Therefore, PpARFf seems to bind to PpTPL1 and PpTPL2 through the EAR-like motif. PpARFs interacting with PpTPLs belonged to the same cluster as AtARF10, 16, and 17 in phylogenetic analyses (Causier et al., 2012b). We could not find both TPL-binding motifs, the LxLxL motif and R/K-LFG-V/I/F motif, in AtARF10, 16, and 17 (Figure 21). Even ARF10 and ARF16 had no EAR and RLFGV motifs; root hair specifically overexpressed ARF10 and ARF16 (*ProE7:ARF10* and *ProE7:ARF16*), resulting in 32% and 54% shorter root hairs than the wild-type plant (Figure 23). Finally, we found the sequence of the LxLxPP motif at AtARF10 (Figure 21, 2). ARF10 may work as a repressor ARF interacting with TPL through the LxLxLPP motif. We could not detect any RD in the amino acid sequence of

ARF16. The rARFs were defined for the amino acid sequence of the middle region. ARF16 is also called the repressor ARF because of its relatively high compositions of Serine, Proline, and Leucine, whereas activator ARFs have Glutamate in the middle region (Guilfoyle and Hagen, 2001). Thus, without typical TPL-binding motifs, ARF16 still plays a repressive role in root hair growth through other uncovered mechanisms.

Additionally, researchers have shown that aARF and rARF share a common binding cis-element. ARF1, 3, and 5 bind to ER7, palindromic ARE (Boer et al., 2014; Ulmasov et al., 1999). ARF2 can also bind to ARE in the promoter *HB33*, the homeodomain gene, and in the promoter *GNC*, the paralogous GATA transcription factor (Richter et al., 2013; Wang et al., 2011). Therefore, aARF and rARF can compete for binding sites in the target promoter region. However, ARF2 and ARF5 showed a lower level of genome-wide binding correlation than that between general transcription factors in the results of DNA affinity purification sequencing (DAP-seq) because of the different protein dimerization properties between ARF2 and ARF5 (O'Malley et al., 2016). Thus, in plants, it seems that ARF2 leaves the target gene of ARF5 and they separately regulate the transcription of their target gene. However, the overexpression of ARF2 (also, other TPL-binding motifs mutated ARF2) have a high chance of binding to the target of aARF. Even if *mab* could not recruit TPL/TPRs, overexpressed *mab* driven by *ProE7* disrupted the binding of aARF to the target promoter and passively repressed transcription.

How auxin-dependent rARF regulates the target genes has still not been determined. ARF9 obviously expressed the suspensor cells of the globular embryo, protoderm cells of the heart embryo, and columella cells of the root (Rademacher et al., 2011). The loss of *ARF9* especially in hypophysis or suspensor cells during embryogenesis disturbed the development of roots (Rademacher et al., 2012). ARF9 may suppress the auxin response in those cells in an auxin-dependent manner. Further investigations will lead to an understanding of the ARF9 function and mechanism to fine-tune transcriptional regulation in the auxin response.

## **Chapter IV.**

### **Transcriptional regulation of *RSL4* through cooperation between RHD6 and aARF**

## 4.1 Abstract

Activator ARF (aARF) specifically binds promoter regions and regulates the expression of auxin-responsive genes to mediate auxin signaling. Although aARF selecting the correct target gene is fundamentally important, the molecular mechanism that controls it remains largely unknown. Here, I tried to uncover a partnership with developmental transcription factors by opening chromatin such that aARF trace exposes ARE on the target promoter in the root hair system. *RSL4* is a major transcription factor for root hair growth and the expression of *RSL4* is regulated in both its developmental and environmental cues by ROOT HAIR DEFECTIVE SIX (RHD6) and auxin, respectively. I confirmed that auxin-related factors elongate root hair length by positively regulating *RSL4* expression. The proximal region of the *RSL4* promoter includes root hair-specific cis-element (RHE) and auxin-response element (ARE). In promoter deletion assay within the 1 kb region, the RHE (RHE3) distally located from the start codon plays a crucial role in *RSL4* expression. The other two RHEs participate in the *RSL4* positive feedback system. RHD6 showed strong association with *RSL4* expression and root hair growth, most probably through binding to RHE3. ChIP assay of the aARFs, particularly ARF5, demonstrated that ARF5 only binds to ARE on the *RSL4* promoter after RHD6 binding. The absence of RHD6 increased the level of trimethylation of lysine 27 on histone 3 (H3K27me3) considering the repressive marker in the *RSL4* promoter region. These results suggest that RHD6 mediates chromatin remodeling to establish aARF binding, at least in part by regulating

RSL4 expression. Finally, further study will determine the molecular link between aARF and developmental transcription factor, regulating the fine-tuning transcription of specific target genes.

## 4.2 Introduction

Auxin response generates reasonable spatiotemporal changes in plant growth and development. The auxin signal is transmitted across to the target gene by ARF, a DNA-binding transcription factor. Thus, activator ARF (aARF) should specifically bind the promoter regions and regulate the expression of auxin-responsive genes to mediate auxin signaling. The ARF-binding sites, the auxin-response element (ARE), were identified from the auxin-responsive promoter of the soybean gene (Liu et al., 1994). The core sequence of ARE has been verified to be TGTCTC (Ulmasov et al., 1997b). Recently, the crystallization of the DNA-binding domain of ARF demonstrated the alteration of ARF-binding sequences (Boer et al., 2014). Advanced analysis has shown the specificity of ARF-binding sites beyond that for the canonical TGTCTC in plants (Brunoud et al., 2012; Liao et al., 2015). In addition, it was revealed that the numerous putative AREs do not have functionality as either ARF-binding sites or auxin-responsive sites in the comparative analysis of microarray data and *in silico* data (Mironova et al., 2014). Therefore, understanding the mechanism of access to ARE will contribute to explaining how aARF controls the specific auxin-responsive genes.

The selectivity of the auxin response through ARF binding involves several barriers. The chromatin status affects aARF to regulate transcription. Histone deacetylase (HDAC) maintains an unpleasant chromatin status for transcription by removing acetyl groups from chromatin. The complex including switching defective/sucrose nonfermenting (SWI/SNF) ATPases performed the remodeling of chromatin (Clapier and Cairns, 2009). This complex cut the interaction between histone and DNA, which resulted in transcriptional activation. In plants, BRAHMA (BRM) and SPLAYED (SYD) showed similar functions and regulatory specificity to SWI/SNF ATPase (Bezhani et al., 2007). The transcriptional activity of ARFs is affected by the chromatin environment. The relationship between the aARF function and chromatin remodeling is well-described in a review paper (Chandler, 2016). Firstly, Aux/IAAs maintain the chromatin in a repressive configuration by recruiting TPL and HDAC to suppress the activity of aARF (Szemenyei et al., 2008). In contrast, if the auxin level increases once without the disturbance of Aux/IAAs, the aARF is exposed to another interacting protein that changes the chromatin opening. ARF5 directly interacts with the complex including BRM or SYD via the middle domain of ARF5. The activity of ARF5 regulating the target gene expression, such as *FIL*, *TMO3*, and *LFY*, depends on BRM and SYD (Wu et al., 2015).

Not only Aux/IAA, but also other tissue-specific transcription factors could operate as a selection barrier. Many types of research have revealed that aARFs physically and genetically interact with other developmental factors for transcriptional activation. Both proteins of ARF8 and BIGPETALp work together

for the repression of cell division and expansion in petal development (Varaud et al., 2011). ARF7 and MYB77 collaborate in the transcriptional promotion of auxin-responsive genes related to lateral root growth (Shin et al., 2007). ARF5 physically interacts with BREVIX RADIX (BRX) and synergistically activates the target genes in the root meristem (Scacchi et al., 2010). ARF6, PIF4, and BZR1 could interact together and bind to nearby sites in similar genes. This complex regulates the target gene transcription involved in hypocotyl elongation (Oh et al., 2014).

However, in a sense, the open chromatin status should precede the aARF regulation of chromatin with other transcription factors because chromatin status allows aARF access to the ARE of target promoter regions. This will operate another barrier mechanism of ARF-binding-site specificity. Thus, the decreasing Aux/IAA concentration, interacting developmental transcription factor, and preceding open chromatin status were all hypothesized to provide selectivity for ARF binding for fine-tuning the auxin response.

To verify our hypothesis, we used the root hair system as a model. Previously, *Arabidopsis* root hair growth was an effective system in confirming the activity of the auxin transporter (Cho et al., 2007a; Cho et al., 2007b; Ganguly et al., 2010; Lee et al., 2010; Lee and Cho, 2006). If the auxin exporter proteins, PIN1,2,3,4, and 7, are root hair specifically expressed driven by *ProE7 (PINsox)*, it decreases the auxin level in hair cells and results in short root hairs (Ganguly et al., 2010). Moreover, when expressed under the root hair-specific *EXPANSIN A7* promoter (*ProE7*) (Cho and Cosgrove, 2002; Kim et al., 2006), one of the auxin-

signaling components, Aux/IAA7(AXR2), showed its own function by inhibiting the root hair growth and suppressing the auxin-responsive genes (Lee et al., 2016; Won et al., 2009). Conversely, the auxin importer protein, AUX1, overexpressed by *ProE7 (AUX1ox)* increased the auxin level in the hair cell and resulted in long root hair. The auxin receptor, TIR1-overexpressed lines (*TIR1ox*), also showed a longer root hair due to promoting Aux/IAA degradation (Ganguly et al., 2010). Thus, we investigated the aARF-binding function and target gene expression in root hair cells.

ROOT HAIR DEFECTIVE SIX-LIKE4 (RSL4) is a key transcription factor for root hair growth, which is a basic helix-loop-helix transcription factor (Datta et al., 2015; Yi et al., 2010). Our lab demonstrated that *Arabidopsis thaliana* RSL4 directly bound to the root hair-specific cis-element (RHE) of the promoter region of *ROOT HAIR SPECIFIC* (RHS) genes and stimulated root hair formation in *Arabidopsis* (Hwang et al., 2017). RSL4 may include the cis-elements to receive ROOT HAIR DEFECTIVE SIX (RHD6) and auxin-mediated signaling because RSL4 is a direct target of these two upstream factors (Yi et al., 2010).

In this study, we conducted the *in vivo* binding assay of aARF to the *RSL4* promoter and examined the relationship with RHD6. Our results will contribute to explaining what affects the aARF access to the AREs of target promoters, inducing a change of chromatin for specific and fine-tuned transcriptional control.

## 4.3 Materials and methods

### 4.3.1 Accession numbers

The accession numbers for the genes analyzed in this study are AT1G12560 (*EXPA7*), AT1G19850 (*ARF5*), At1G27740 (*RSL4*), AT1G70460 (*RHS10*), AT1G73590 (*PIN1*), AT2G38120 (*AUX1*), AT3G62980 (*TIR1*), AT5G20730 (*ARF7*), and AT5G37020 (*ARF8*). *axr2-1* (CS3077) and *rhs10* (SALK 075892) were purchased from the *Arabidopsis* stock center (<http://www.arabidopsis.org/>).

### 4.3.2 Plant materials and growth conditions

*Arabidopsis thaliana*, Columbia ecotype (Col-0), was used as a control and for transformation of transgene constructs unless otherwise stated. *Arabidopsis* plants were transformed using *Agrobacterium tumefaciens* strain C58C1 (pMP90) by the inflorescence-dipping method. Transformed plants were selected on hygromycin-containing plates (30  $\mu\text{g ml}^{-1}$ ). All seeds were grown on agarose plates containing 4.3  $\text{g ml}^{-1}$  Murashige and Skoog (MS) nutrient mix (Duchefa, Netherlands), 1% sucrose, 0.5  $\text{g ml}^{-1}$  MES pH 5.7 with KOH, and 0.8% agarose. Seeds were cold treated before germination at 23°C under a 16 h/8 h light/dark photoperiod. For observation of root hairs, homozygous transformants were planted on antibiotic-free media, and T1 and T2 lines were planted on hygromycin-containing media. Hygromycin did not significantly interfere with root hair development, as shown in the control *ProE7:YFP* (yellow fluorescence protein) transformants. For all estradiol treated experiments, 3-d-old seedlings of homozygous transformants were

transferred to new plates and grown for an additional day, after which root hairs were observed.

Two control lines were adopted; *ProE7:YFP* (Lee and Cho, 2006; Ganguly et al., 2010) for the transformant analysis with hygromycin and *pMDC7-empty* vector line for the transformant analysis with estradiol.

### 4.3.3 Construction of transgenes

The binary vector *pCAMBIA1300-NOS* with modified cloning sites (Lee et al., 2010) was used for transgene construction. The *AtEXPA7* promoter (*ProE7*; Cho and Cosgrove, 2002; Kim et al., 2006) was used for root hair-specific expression. *ProRSL4:RSL4:GFP* (Hwang et al., 2017) and *ProE7:TIR1*, *ProE7:Aux1*, and *ProE7:PINI* (Ganguly et al., 2010) and *ProE7:RHS10* (Won et al., 2009) and *ProE7:ARF5*, *ProE7:ARF7*, *ProE7:ARF8*, *pMDC7:ARF5:GFP*, *pMDC7:ARF7:GFP*, and *ProARF5:GUS* (Mangano et al., 2017) were described previously.

For estradiol-inducible *pMDC7:RHD6-GFP* constructs, *RHD6* coding regions without their stop codon were generated by PCR using the primers listed in Table S1 inserted before the *GFP* fragment of the *ProE7:GFP* construct to make *RHD6-GFP* fusions. To transfer the *RHD6-GFP* fragments to the *pDONR207* vector, the *RHD6-GFP* regions were amplified by PCR using the primers for the site-specific recombination cloning system as listed in Table S1. Each resulting amplified fragment was transferred to *pDONR207* using standard Lambda Integrase (Elpisbio, Korea). After confirmation of the inserts by nucleotide

sequencing, the Lambda Integrase/Excisionase (Elpisbio, Korea) reaction was performed with the resulting *pDONR207-RHD6:GFP* plasmids and the binary vector *pMDC7* (Curtis and Grossniklaus, 2003).

For the deletion analysis of the RSL4 promoter, the serial deletion fragments of promoter (F1 to F5) were generated by PCR using the primers listed in Table S1 and inserted into the *ProRSL4:RSL4:GFP* vector replacing original *RSL4* promoter. For the generating deletion promoters mutated of RHEs, each construct were amplified by mega-pcr method using PCR with the primer set listed in Table S1.

To express RHD6, RSL1, and RSL4 proteins in *Escherichia coli* for the EMSA, the cDNA sequences were amplified by PCR from the *Arabidopsis* seedling cDNA library and cloned into the *EcoRI/XhoI* sites of the *pGEX-4T-1* vector (GE Healthcare), generating fusion proteins with GST at the N termini of RHD6, RSL1, and RSL4 proteins.

#### 4.3.4 Observation of biological parameters

Root hair length was estimated as described in Lee and Cho (2006, 2009) with modifications. The 3-day-old seedling root was digitally photographed using a stereomicroscope (M205 FA, Leica, Heerbrugg, Switzerland) at 40X magnification. The lengths of 9 consecutive hairs protruding perpendicularly from each side of the root, 18 hairs in total, were estimated using ImageJ 1.50b software (National Institutes of Health, United States).

#### 4.3.5 Observation of reporter gene expression and evaluation of promoter activity

The fluorescence from reporter proteins and organelle markers were observed by confocal laser scanning microscopy (LSM 700; Carl Zeiss). GFP was detected using 488/505- to 530-nm. Fluorescence images were digitized using the Zeiss LSM image browser. Promoter activity was evaluated by quantifying the GFP fluorescence using the histogram function of Adobe Photoshop (Adobe Systems) as described by Cho and Cosgrove (2002). For observation of estradiol-inducible proteins of ARF5:GFP in *pMDC7:ARF5:GFP* in wild-type or *rhd6-3* backgrounds and ARF7:GFP in *pMDC7:ARF7:GFP* in wild-type or *rhd6-3* backgrounds, GFP signals in 2-4 nucleus of root hair cell in maturation zone were detected.

#### 4.3.6 RNA isolation and quantitative reverse transcriptase(qRT)-PCR analysis

Total RNA was isolated from the roots of 4-day-old seedlings (25 for each line) using an RNeasy Plant Mini Kit (Qiagen). cDNA was synthesized as described previously (Lee and Cho, 2006). qRT-PCR analyses were performed using an amfiSure qGreen Q-PCR Master mix without ROX (Applied GenDEOT) and a Chromo4™ Four-Color Real-Time Detector (Bio-Rad). Gene specific signals were normalized by the *ACTIN7* transcript level. qRT-PCRs were performed in three technical replications per RNA sample with three independent RNA preparations. Primers used for quantitation were as in Supplementary Table S1.

### 4.3.7 Preparation of fusion proteins and EMSA

To produce RHD6, RSL1, and RSL4 proteins for EMSA, the gene-containing vectors were transformed into *E. coli* strain BL21 and the transgene expression was induced with 0.25mM isopropyl  $\beta$ -D-1-thiogalactopyranoside at 28°C for 4 h. The cells were harvested by centrifugation and lysed in B-PER Buffer (Thermo Scientific). The proteins in the lysate were bound to GSH resin (Elpisbio) at 4°C for 12 h and washed three times with TBS buffer. The bound proteins were eluted in elution buffer (15mM GSH and 50mM Tris, pH 6.17) at 4°C for 3 h. The eluted proteins were confirmed by SDS-PAGE separation and protein blot analysis using anti-GST antibody (GeneScript; catalog no. A00097; 1:10,000 dilution). EMSA was performed using the LightShift Chemiluminescent EMSA kit (Thermo Scientific) following the manufacturer's protocol. The assays were performed using recombinant proteins (GST-fused RHD6, RSL1, and RSL4) and the 5'-biotinylated RHE probes. The biotinylated probe was used at a concentration of 20 fmol/ $\mu$ L, and 20- to 100-fold of nonbiotinylated probe was used as the competitor. The protein was mixed with the probe or the probe and competitor in the binding buffer (10mM Tris, pH 7.5, 50mM KCl, and 1mM DTT) with 50ng $\mu$ L<sup>-1</sup> poly(dI-dC), 0.05% Nonidet P-40, 5 mM MgCl<sub>2</sub>, and 2.5% glycerol. The protein-probe complexes were resolved on an 8% polyacrylamide gel, transferred to a positively charged nylon membrane (Roche), and cross-linked by 254-nm UV for 8 min. The resulting bands were detected using the Chemiluminescent Nucleic Acid Detection Module Kit (Thermo Scientific).

### 4.3.8 ChIP and qPCR analysis

ChIP analysis was performed as previously described (Gendrel et al., 2002; Haring et al., 2007). Four-day-old transgenic seedlings expressing the GFP-fusion proteins were vacuum-infiltrated in 1% formaldehyde solution for cross-linking. After quenching the cross-linking by adding glycine, the seedlings were ground in liquid nitrogen. The chromatin was isolated as described (Moehs et al., 1988), resuspended in nuclei lysis buffer (50 mM Tris-HCl, pH 8.0, 10 mM EDTA, and 1% SDS), and sonicated to obtain 0.5- to 1.0-kb fragments. The chromatin solution was precleared with salmon sperm DNA/Protein-A agarose beads (Millipore) at 4°C for 1 h and immunoprecipitated with anti-GFP antibody beads (MBL; code 598; 1:200 dilution) overnight. The immunocomplex was washed once with each of the following buffers: low-salt buffer (140 mM NaCl, 0.2% SDS, 0.5% Triton X-100, 2 mM EDTA, and 20 mM Tris-HCl, pH 8.0), high-salt buffer (500 mM NaCl, 0.2% SDS, 0.5% Triton X-100, 2 mM EDTA, and 20 mM Tris-HCl, pH 8.0), and LiCl wash buffer (0.25 M LiCl, 0.5% Nonidet P-40, 0.5% sodium deoxycholate, 1 mM EDTA, and 10 mM Tris-HCl, pH 8.0), and twice with TE buffer (10 mM Tris-HCl, pH 8.0, and 1 mM EDTA). Each wash buffer (1 mL) was added to the immunocomplex, mixed by rotating for 5 min, and centrifuged for 2 min at 5900g at 4°C. Chromatin was eluted from the beads by adding 300  $\mu$ L elution buffer (1% SDS and 0.1 M NaHCO<sub>3</sub>) and incubated at 65°C for 15 min. After incubation, the beads were pelleted by a 1 min centrifugation at 16,100g at room temperature and the supernatant was collected. Cross-linking was reversed by adding 5M NaCl (final 200 mM) for 7 h at 65°C and the resulting sample was treated with

proteinase K (final concentration of 40 ng  $\mu\text{L}^{-1}$ ) to remove all the proteins. Antibody untreated samples for estimating input DNA were also treated with the same processes. DNA from the reverse cross-linked samples was purified using the QIAquick PCR purification kit (Qiagen), and input DNA was estimated by PCR using *ACTIN7* primers. The ChIP-qPCR analysis was done using the primer sets listed in Supplemental Table 1 and the amfiSure qGreen Q-PCR Master Mix (2X) without ROX (GenDepot) in the Chromo4 four-color real-time detector (Bio-Rad). The “% of input” value of each ChIP-qPCR fragment was calculated first by normalizing the fragment amount against the input value and then by normalizing the value from the transgenic plants against the value from the control plants. Each ChIP-qPCR reaction was performed in quadruplicate, and each experiment was repeated two to three times using chromatin samples prepared at different times.

#### 4.3.9 GUS histochemical analysis

Histochemical GUS staining was performed by incubating whole seedlings in the staining buffer containing 1 mM 5-bromo-4-chloro-3-indoyl-b-D-glucuronic acid cyclohexyl-ammonium salt (X-Gluc; Glycosynth), 0.1 M  $\text{NaH}_2\text{PO}_4$ , 0.01M EDTA, 0.1 % Triton-X, and 0.5 mM potassium ferri- and ferrocyanide at 37 °C until the blue color appeared (6 to 24 h). Stained seedlings were cleared in 70 % ethanol for 1 h. Seedlings were photographed under a stereomicroscope (Leica MZ FLIII).

**Table 9.** The Primer list

Subject	Primer name	Primer sequence (5' to 3')	
ChIP-qPCR	ChIP-ProRSL4 RHE3r	ChIP-R3-F	AGCGGCATGGATTAAAAGTTTC
		ChIP-R3-R	GAGATTAGTATAATAATGAGAAAGAC
	ChIP-ProRSL4 RHE2r	ChIP-R2-F	TTTAATTAATTGAGATGAATGGATAG
		ChIP-R2-R	CGTTAATTAATAAAGTGAAACGAAGCC
	ChIP-ProRSL4 negative	ChIP-nc1-F	CTTTTCACATGCCATAACTAG
		ChIP-nc1-R	TTCATGTGTTAAAGTGTGAACATTC
		ChIP-nc2-F	ATTCTTGGGATCAAAGTCATCACC
	ChIP -ProRSL4-AuxRE	ChIP-nc2-R	GTAACATTATATATTGGATCTTCCAC
		AxE-1F	TCTTCCCTTCTAGTGTGTATGG
		AxE-1R	AGCTCATTTTAAACACAAAATGTTAC
		AxE-2F	TATATCATGCTGCCTCCAAA
		AxE-2R	CCATGCCGCTTTTTACCTTA
		AxE-3F	GAGATGAATGGATAGTTATAAATAAGAAT
		AxE-3R	GATGAACACGATCAGTCAAC
		AxE-4F	TGGCTTCGTTTCACTTATTT
		AxE-4R	AGAGATCAAGAGATTCTTAAACTG
		AxE-5F	AAATCTTCCTTGAGAAAATTTCTCT
		AxE-5R	TTCTTGAACCTTGTCAACTATAT
		nc1R	GGTATTGTAGTTGTATACTTGTATGTA
		nc2F	ACAGCTGTATGTTTTGGTATC
		nc2R	ACTCATTTCGTAAGAGAGTGATC
nc3F		TTGCGATAATGATTCCACAA	
nc3R	TTTACATTGGCCACACAAGAG		
Transgene constructions	RHD6	pMDC7-RHD6-1F	GGGGACAAGTTTGTACAAAAAAGCAGGCT TAATGGCACTCGTTAATGAC
		pMDC7-GFP-720R	GGGGACCACCTTTGTACAAAGAAAGCTGGGTATTACTTGTACAGCTCGTCC
	Promoter RSL4 deletion	F1	GGAAGCTTCAAGTATATAACAAAAGAATG
		F1.5	TCTTGTTAAACTAGTGTGTGTTGA
		F2	CGCTAAGCTTGTGTGGCCAATGT
		F3	GCCTAAGCTTGTGACCCCCAAGTTG
		F4	TGCAAAGCTTCGTTTCACTTATTTAATT
		F5	CTCCAAGCTTTATATATATATATAGTTGCACAAG
		pRSL4-reverse	ACGTGGATCCCTCTAACTGATCAAC
		F1 mRHE3f(RP)	AATCGTGCATTGGATGTGCCATATTTTATAC
		F2 mRHE1r (RHE2 mutation)	GCTTTGTTCCCTTACATACACATTAACAT
		F2 mRHE2r (RHE1 mutation)	ATGATGATGAAACATATCAGTCAACTT
		qRT-PCR	RSL4
RSL4_qR1097	TTGTGATGGAACCCCATGTC		
ACT7	ACT7-rt-F		TCCCTCAGCACCTTCCAACAG
	ACT7-rt-R		CAATTCCCATCTCAACTAGGG
ARF5	ARF5-qRT-F		TGAACAGCGCAGGCATTAAC
	ARF5-qRT-R		TACAGGCGCGCCGTTTCTCCTCTACCAGTTGG
ARF7	ARF7-qRT-F		CGGAGTTCCTGCAGCTGCAG
	ARF7-qRT-R		CACCAGCAGCTGACTCATCC
ARF8	ARF8-qRT-F	GATCATGGAGAAGGCAGTGG	
	ARF8-qRT-R	GAATGGCGCGCCAAGATGAGTGGAAACGA	
EMSA	RHD6	cRHD6S11-F	A GTCGAC TC ATGGCACTCGTTAATG
		cRHD6N11-R	A GCGGCCGC TTAATTGGTGATCAG
	RSL1	cRSL1 EcR1-F	AAGAATTCTATATGTCACTCATTAACG
		cRSL1 Xh1-R	AACTCGAGTTATTCTGCTATACTTG
RSL4	cR4Ec_0F	ATATGAATTCATGGACGTTTTTGTGTGATGGTGAA	
	cR4Xh_0R	AATTCTCGAGTCACATAAGCCGAGACAAA	

## 4.4 Results

### 4.4.1 The relationship between root hair growth and *RSL4* expression

*RSL4* is a key transcription factor for root hair growth. *RHD6* is a direct upstream factor of *RSL4*, which regulates the expression of *RSL4* in root hair cells (Yi et al., 2010). Both T-DNA insertion mutants, *rsl4-1* and *rhd6-3*, showed short root hair. Overexpressed *RSL4* lines by promoter *RSL4* in wild-type plants showed longer root hair length, as expected (Hwang et al., 2017).

In our root hair system using *ProE7*, auxin response-related factors represented their own function through root hair length. To confirm the relationship between the root hair phenotypes that caused auxin factors and *RSL4*, we re-analyzed the root hair length and *RSL4* transcript level from these lines (Figure 38). Long-root-hair lines, *ProRSL4:RSL4*, *TIR1ox*, and *AUX1ox*, represented an increased *RSL4* level compared to the *RSL4* level of wild-type plants. Short-root-hair lines, *rsl4-1*, *rhd6-3*, *axr2-1*, and *PIN1ox* showed a very low level of *RSL4*. *RSL4*-downstream genes, *RHS10*, also changed the root hair length; however, they did not significantly affect *RSL4* expression. This data indicated that auxin controls *RSL4*-mediated root hair growth.

### 4.4.2 Root hair specifically overexpressed *aARFs* promote root hair growth by activating *RSL4* expression

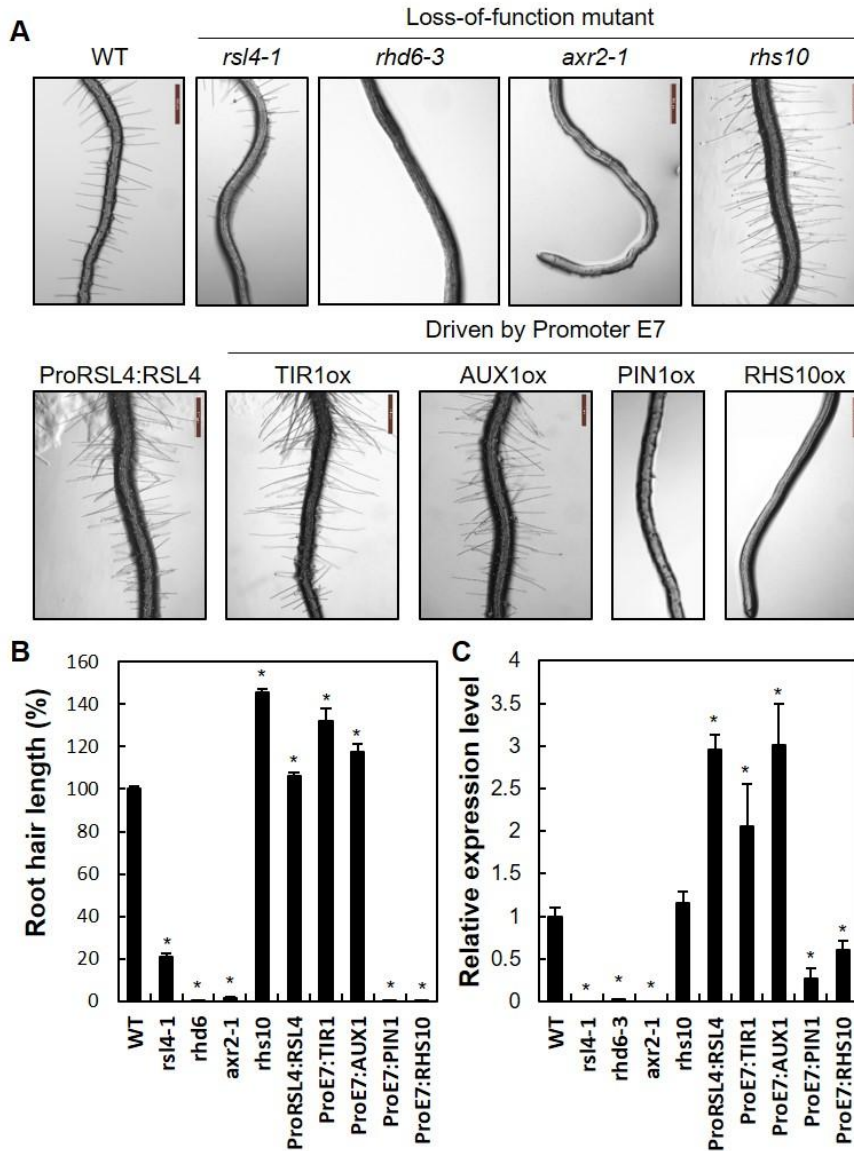


**Figure 38. Relative root hair length and *RSL4* expression level of various lines that have short, normal, or long root hair phenotypes.** (A) Root-hair phenotypes of wild-type plant (WT), loss-of-function mutants (*rsl4-1*, *rhd6-3*, *axr2-1*, and *rhs10*), *RSL4*-expressed lines by *RSL4* promoter (*ProRSL4:RSL4*), and overexpressed lines for root hair- and auxin-related genes (*TIR1*, *AUX1*, *PIN1*, and *RHS10*) under the *EXPA7* promoter (*ProE7*) in the wild-type background. Scale bar

is 100  $\mu\text{m}$ . (B) Root hair length of WT, loss-of-function mutants, and overexpressing lines. Data represent means  $\pm$  s.e. (n = 200–601 root hairs from independent transgenic lines). (C) The transcript level of *RSL4* of the above lines. Total RNA was isolated from each plant and transcript levels for *RSL4* and actin were estimated by qRT-PCR using gene-specific primers. The values are significantly different ( $*P < 0.01$ , Student's *t*-test) from the control value (B and C). Scale bar is 100  $\mu\text{m}$ .

To identify the activity of aARF in root hair growth, we expressed aARFs with *ProE7* (*ARF5ox*, *ARF7ox*, and *ARF8ox*). All of the overexpressing lines showed increased root hair length (Figure 39). The *ARF5ox*, *ARF7ox*, *ARF8ox* seedlings grew root hairs that were on average 129%, 118%, and 122% of the length of the control, respectively. As expected, they increased the RSL4 expression level (Figure 39C). The increased RSL4 level of each line was proportional to the expressed ARF level (Figure 39D). These root hair and qRT-PCR analyses demonstrated that RSL4 is regulated by aARFs.

However, when we directly expressed *RSL4* under *ProE7*, the root hair grew by up to 131% of the control length (Hwang et al., 2017). This is a longer root hair length than the hair length of *aARFox*. ARFs prefer to make a homodimer for binding to palindromic DNA because of the DNA-binding domain of aARF (Boer et al., 2014; Ulmasov et al., 1997a). They also bind to each aARF (Vernoux et al., 2011). Thus, we thought that single aARF overexpression may not be sufficient to drive maximum expression. I crossed the *aARFox* lines and observed the root hair phenotypes from the double *aARFox* lines (Figure 39E). The double *aARFox* lines did not show longer root hair than the single *aARFox* lines. Sometimes, single *aARFox* had longer root hair. The dose of aARF is considered more important for root hair growth rather than the type of aARF. In addition, simply increasing the expression level of aARF is limited for achieving maximum root hair growth.

#### 4.4.3 Overexpressed *aARFs* in *rhd6-3* mutant could not resotre

root hair growth

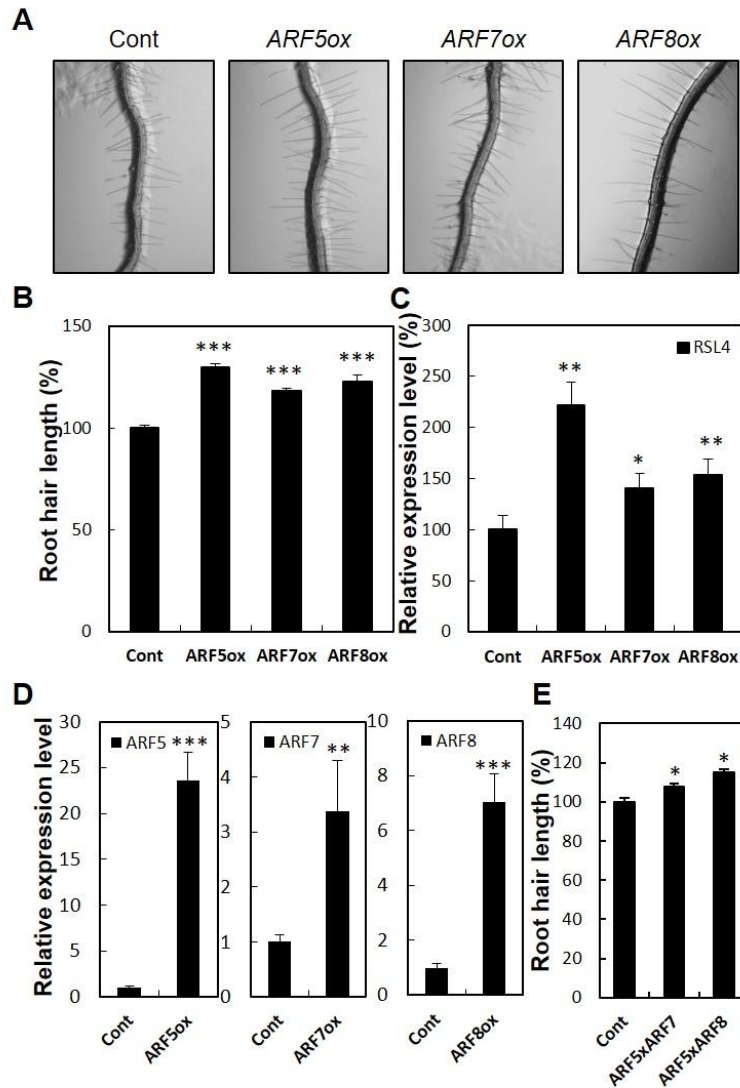


**Figure 39. Root hair-specific overexpression of *ARFs* enhances root hair growth and the *RSL4* expression.** (A) Root hair phenotypes of control (Cont, *ProE7:GFP*) and *ARF*-overexpressing transformants (*ARF<sub>ox</sub>*, *ProE7:ARFs*). (B) Root hair length of Cont and *ARF<sub>ox</sub>* lines. Error bars indicate  $\pm$  s.e. (n=355–1,283 root hairs from independent transgenic lines). The values are relative to the Cont value and significantly different (\*\*\*)  $P < 0.001$ ; *t*-test) from the Cont value.

(C) Relative *RSL4* mRNA levels of Cont and ARFox lines. Error bars indicate  $\pm$  s.d. Results were from three biological samples for qRT-PCR. The values are relative to the Cont value and are significantly different (\*\*  $P < 0.01$ ; \* $P < 0.05$ ;  $t$ -test) from the Cont value. (D) Transcript levels of each *ARF* in ARFox lines. Error bars indicate  $\pm$  s.d. Results were from two biological samples for qRT-PCR. The values are relative to the Cont value and significantly different (\*\* $P < 0.001$ ; \*\* $P < 0.01$ ;  $t$ -test) from the Cont value. (E) Root hair length of Cont (Col-0) and ARFox-crossing lines. *ProE7:ARF5* was crossed with *ProE7:ARF7* (*ARF5xARF7*) or *ProE7:ARF8* (*ARF5xARF8*). Data represent means  $\pm$  s.e. ( $n = 452$ – $477$  root hairs). The values are relative to the Cont value and are significantly different (\* $P < 0.05$ ;  $t$ -test) from the Cont value.

Auxin treatment of *rhd6-3 rsl1-1* mutant recovered the root hair defect (Yi et al., 2010). To further verify aARF function in root hair growth, I made estradiol-inducible aARF-fused GFP constructs (*ARF5:GFP* and *ARF7:GFP*) and transformed wild-type plant and *rhd6-3* mutant. The transgenic lines of the wild-type background (*ARF5:GFP* #1-5 and *ARF7:GFPs*) had longer root hair than the control lines (Cont, transformed empty vector to wild-type plant) with an ARFs:GFP signal in the root hairs (Figure 40). In some transgenic lines without a GFP signal (*ARF5:GFP* #4-1 or #5-1), a difference in root hair length compared to the controls was not observed. However, I could not detect any recovery from *rhd6-3* mutants that induced *ARF5:GFP* or *ARF7:GFP* in root hair growth as well as the *RSL* level (Figure 41B, C) even though they showed obvious GFP signals in the root hair cells (Figure 41A). This result disagrees with the previous auxin treatment data.

To examine whether these transgenic lines respond to auxin, I treated auxin and estradiol together. The seedlings were grown in MS media for 3 days and transferred to pharmacological media, and then the root hair phenotypes were observed after 24 h. Firstly, I observed the root hair length from mutants with only IAA treatment ranged from 0 to 100 nM. The *rhd6-3* mutants, not inducing any ARFs:GFP, generated root hairs with more than 50-nM IAA (Figure 42). In the treatment of both auxin and estradiol, ARF7:GFP-induced *rhd6-3* mutants also generated root hairs with 50-nM IAA, although we confirmed the ARF expression by observing the GFP signals. I could only detect root hair from ARF5-induced *rhd6-3* mutants with 100-nM IAA (Figure 43). This data means *rhd6-3* mutants

showed recovery from the root hair defect with auxin, but not by means of ARFs.

From the

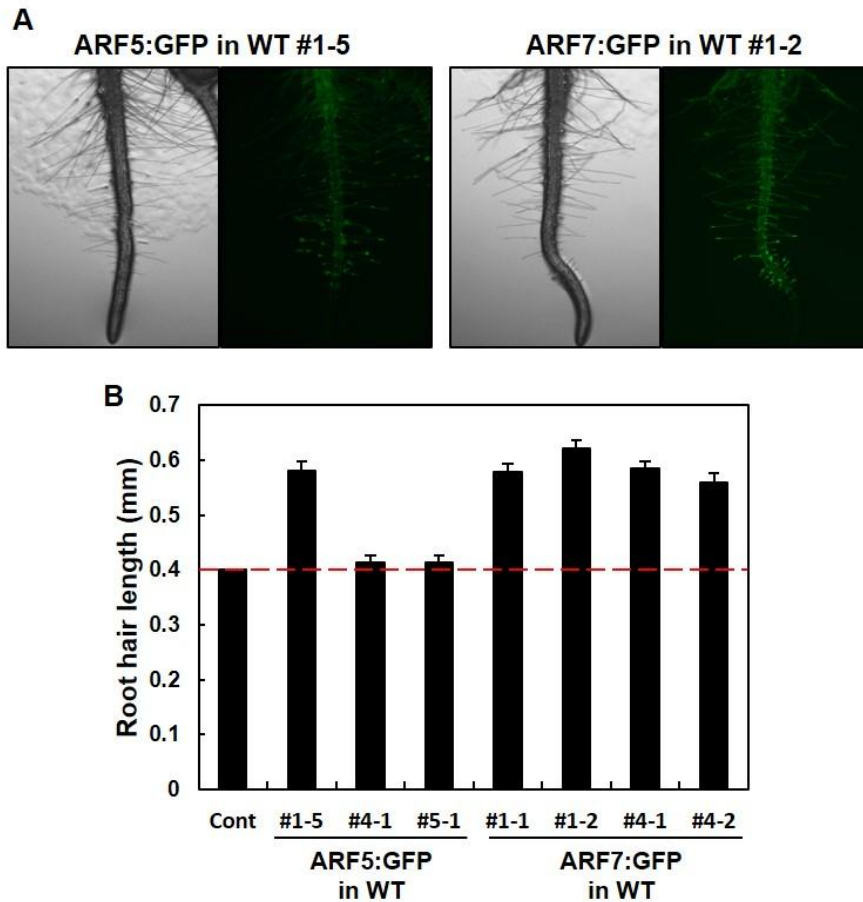


**Figure 40. Overexpression of ARFs enhances root hair growth in wild-type background in estradiol inducible system.** (A) Root hair phenotypes of estradiol inducible ARF-overexpressing transformants in wild-type background (*pMDC7-ARF5:GFP* in wild-type background, *ARF5:GFP* in *WT*; *pMDC7-ARF7:GFP* in wild-type background, *ARF7:GFP* in *WT*). (B) Root hair length of control (Cont, *pMDC7-Empty*) and *ARF-GFP* in *WT* transformants. Error bars indicate  $\pm$  s.e. (n = 83–163 root hairs from independent transgenic lines). Seedlings were grown on MS media with 10  $\mu$ M estradiol.

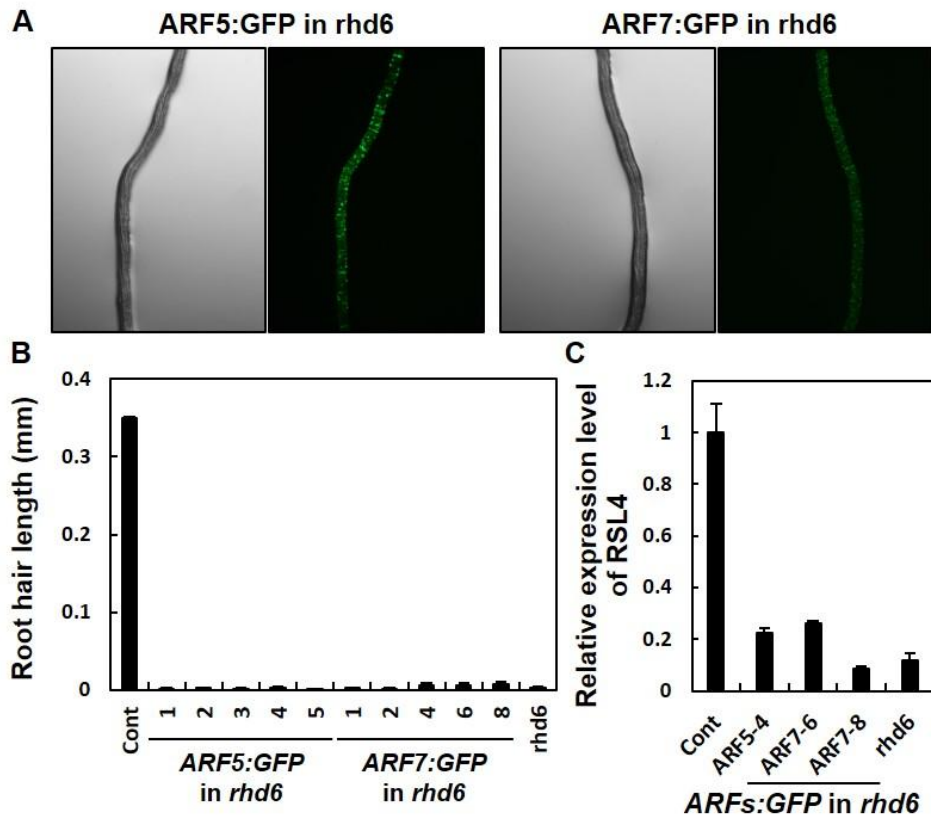


**Figure 41. Overexpression of ARFs could not enhance root hair growth in the *rh*d6-3 mutant background.** (A) Root hair phenotypes of ARF-overexpressing transformants in *rh*d6-3 mutant background (*pMDC7-ARF5:GFP* in *rh*d6-3 mutant, *ARF5:GFP* in *rh*d6; *pMDC7-ARF7:GFP* in *rh*d6-3 mutant, *ARF7:GFP* in *rh*d6); (B) Root hair length of control (Cont, *pMDC7-Empty*) and *ARF-GFP* in *rh*d6 transformants. Error bars indicate  $\pm$  s.e. (n = 136–426 root hairs from independent transgenic lines). (C) RSL4 expression level pattern of Cont, independent *pMDC7-*

*ARFs:GFP* lines in *rhb6-3* mutant background (*ARFs:GFP* in *rhb6*), and *rhb6-3* mutant. Seedlings were grown on MS media with 10  $\mu$ M estradiol.

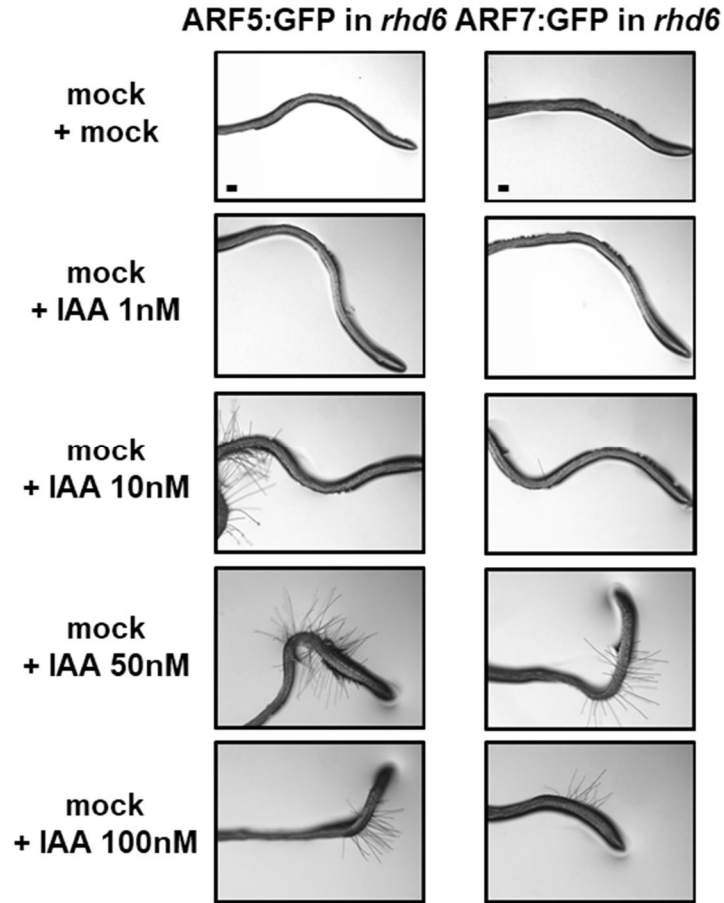


**Figure 42. Root hair images of *ARFs:GFP* in *rhd6* lines under auxin-treated conditions.** Root hair images of *ARFs:GFP* in *rhd6-3* lines with different concentrations of auxin. These seedlings were grown in MS media for three days and then transferred to MS media with IAA (0–100 nM). The root images were taken after 24 hours of auxin treatment. Scale bar is 100  $\mu$ m for all.

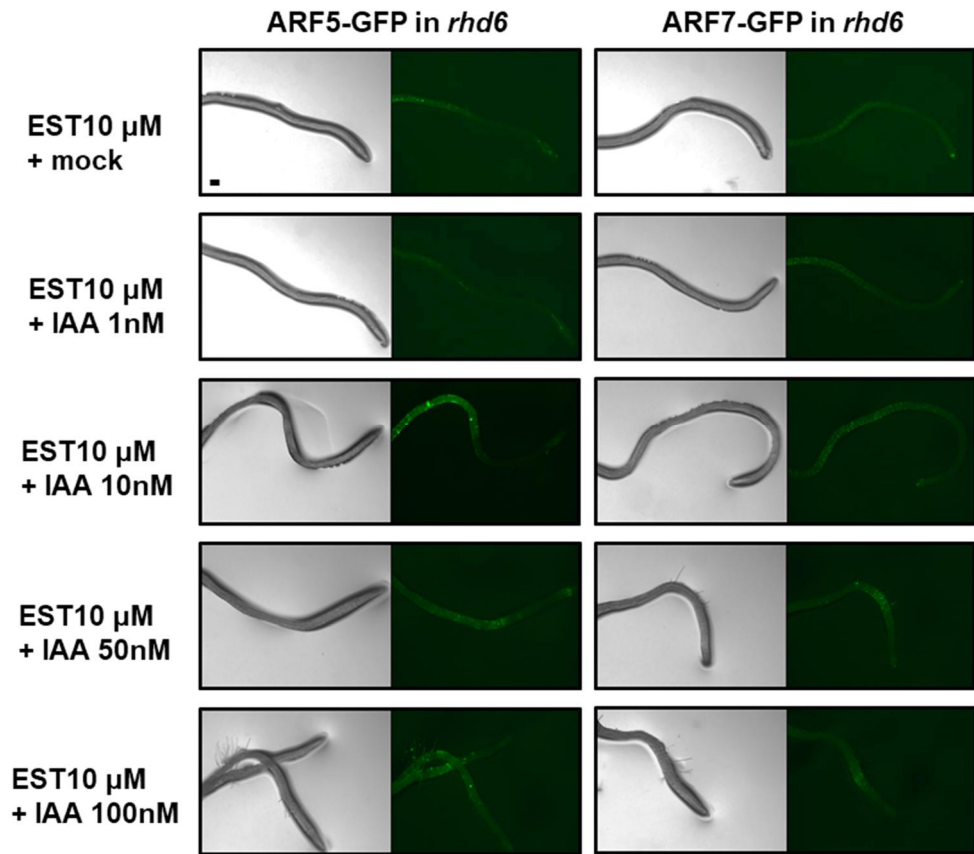


**Figure 43. Root hair images of *pMDC7-ARFs:GFP* in *rhid6* lines under estradiol- and auxin-treated conditions.** Root hair images and GFP images of *pMDC7-ARFs:GFP* lines in *rhid6-3* mutant background (*ARFs:GFP* in *rhid6*) from estradiol 10  $\mu$ M and different concentrations of auxin-treated samples. These seedlings were grown in MS media for three days and then transferred to MS media within estradiol 10  $\mu$ M and IAA (0–100 nM). The root images were taken after 24 hours of treatment. Scale bar is 100  $\mu$ m for all.

root hair assays, I hypothesized that exogenously treated auxin removed Aux/IAAs, resulting in the chromatin status activating transcription in the promoter *RSL4* regions. However, simply overexpressed ARFs themselves could not change the closed chromatin status repressing transcription in the *rh6-3* mutant.

#### 4.4.4 Overexpressed *RHD6* in the auxin-defect mutant (*axr2-1* GOF) recovered root hair growth

Conversely, to investigate the ability of RHD6 with auxin signaling interrupting conditions, I transformed RHD6-fused GFP into *axr2-1* gain-of-function mutants. When RHD6:GFP was expressed by the estradiol-inducible promoter, the transgenic lines generated and increased root hairs compared with *axr2-1* mutants (Figures 43 and 44). I measured the root hair length of several lines from three independent experiments. The length of each line was not consistent; however, there were patterns in increased root hair length following dependence on RHD6:GFP expression levels (Figure 45). I suggest that the RHD6 function to grow root hair is upstream of the auxin function.

#### 4.4.5 Key cis-elements in the *RSL4* promoter

To analyze how *RSL4* promoter received both of the signals from RHD6 and auxin, we performed promoter deletion assay on the proximal *RSL4* promoter. I referenced the papers of Boer et al. (2014) and Won et al. (2009) to select putative AREs and RHEs, respectively. There were eight putative AREs and three putative RHEs in the promoter region of 1kb from the starting codon site (Figure 46A). I

named the

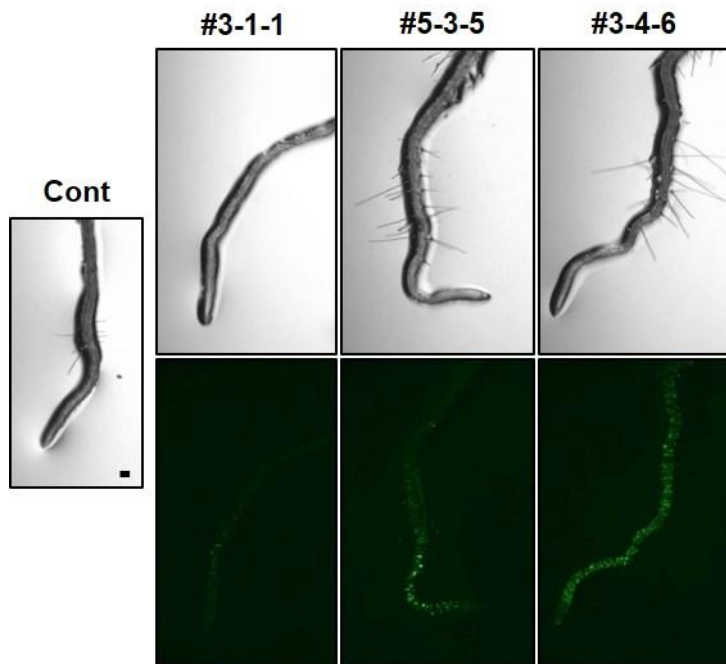


**Figure 44. Root hair images of *pMDC7-RHD6:GFP* transgenic lines in *axr2-1* background.** Root hair images of *pMDC7-RHD6:GFP* in *axr2-1* and GFP expression images from each roots. Scale bar is 100  $\mu$ m for all. Equally, the exposure time is three seconds for all GFP fluorescence pictures. These seedlings were grown in MS media for three days and then transferred to 0.1  $\mu$ M estradiol MS media. The root images were taken after 24 hours of estradiol treatment.

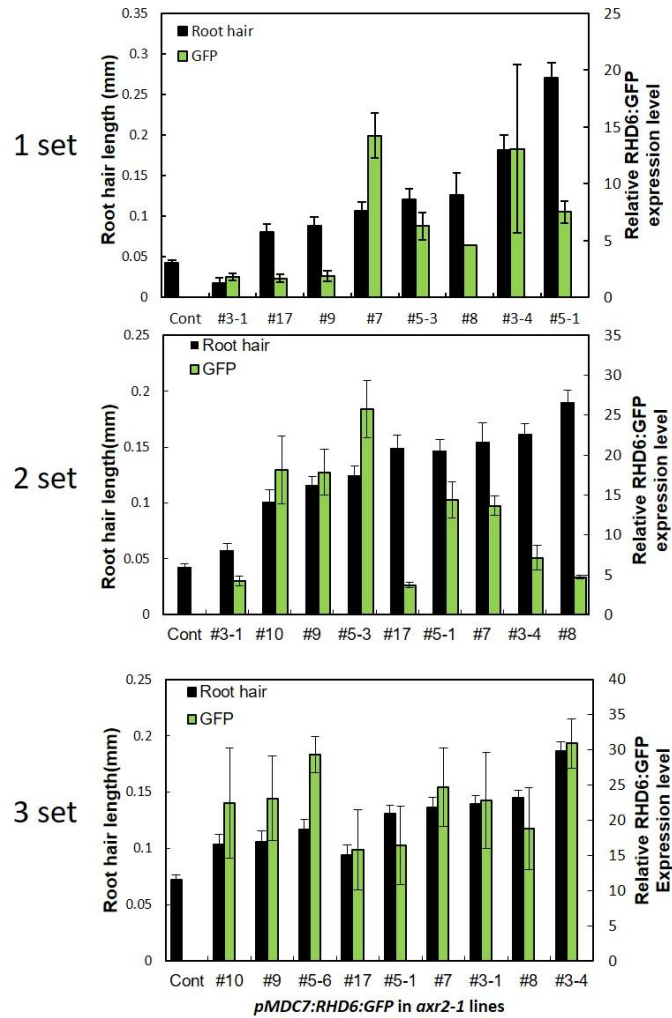


**Figure 45. Root hair lengths of *pMDC7-RHD6:GFP* under *axr2-1* transgenic lines.** Root hair lengths and the relative RHD6:GFP expression level of control (Cont, *pMDC7-empty* in *axr2-1*) and *pMDC7-RHD6:GFP* in *axr2-1* transformants. These seedlings were grown in MS media for three days and then transferred to 10  $\mu$ M estradiol MS media. The root hairs' lengths were measured after 24 hours of estradiol treatment. Data represent means  $\pm$  s.e. (n = 90–452 root hairs from each transgenic line). Data were not merged because these results were not perfectly identical in 1, 2, and 3 sets. However, I infer that the expressed RHD6 could increase the root hair growth.

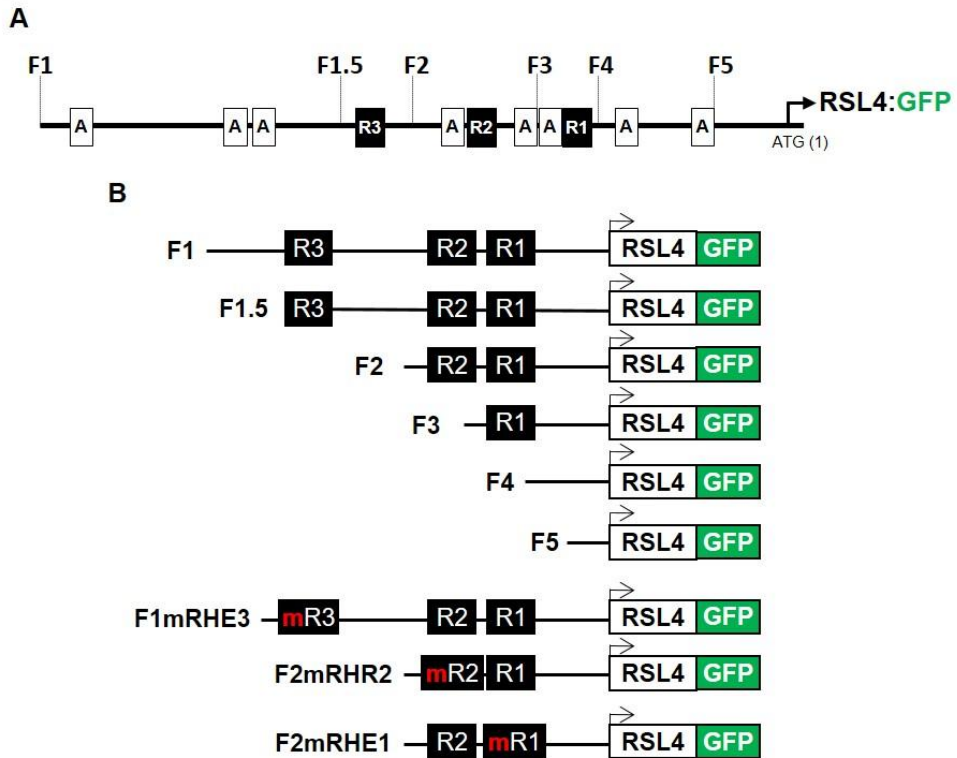


**Figure 46. Deletion analysis of the promoter region of *RSL4* for *RSL4* expression.** (A) Locations of the putative root hair-specific cis-element (RHE) and auxin-response element (ARE) in the promoter region of *RSL4*. The RHE (black boxed, R) and ARE (white boxed, A) positions are indicated by the number relative to the start codon (ATG); promoter deletion sites are marked (F1–F5). (B) Promoter deletion construction of promoter *RSL4* fused to the *RSL4* gene and *GFP*. Each construct contains deleted promoter fragments (F1 and F1mRHE3 = 993 bp, F1.5 = 506 bp, F2 = 430 bp, F3 = 288 bp, F4 = 243 bp, and F5 = 106 bp). An “m” indicates a muted sequence in the core region of RHEs; this was changed from CACG to ACAT.

further distally located RHE RHE3, the middle one RHE2, and the proximal one RHE1. To determine which region of the RSL4 promoter is necessary for RHD6 and ARF function in terms of root hair growth, we generated serial deletion constructs based on the RHEs anticipating they would recruit root hair-specific transcription factors. Each deleted promoter was fused RSL4 and GFP proteins (F1 to F5) (Figure 46B). The final constructs expressed RSL4-fused GFP proteins in the root hair cell using this truncated-form RSL4 promoter and the estimated GFP signal and root hair length of independent transformant lines to reflect the promoter activity.

The F1 and F2 lines in wild-type backgrounds showed GFP signals in root hair cells specifically. F1 had a strong signal, and F2 had a weak signal; however, a shorter promoter length than F2, such as those in the F3, F4, and F5 lines, did not show any signal likely negative control lines, which plant did not produce GFP protein (Figures 46A and 47A). F1 included all three RHEs, but F2 included RHEs except for RHE3. Thus, it seems that RHE3 and the only remaining sequences of F1 (563 bp) are important for the normal expression intensity of RSL4. Nevertheless, RHE2 and the sequences between F2 and F3 (142 bp) are critical for expressing the mRNA of RSL4.

However, in unlikely wild-type backgrounds, I failed to observe an RSL4:GFP signal from F2 in *rsl4-1* mutant lines. Only the F1 lines among all of the truncated promoter lines in *rsl4-1* mutant backgrounds showed a GFP signal (Figures 46B and 47B). This event appeared repeatedly in the root hair

complementary experiments. The F1 in the *rs14-1* mutant backgrounds fully complemented the root

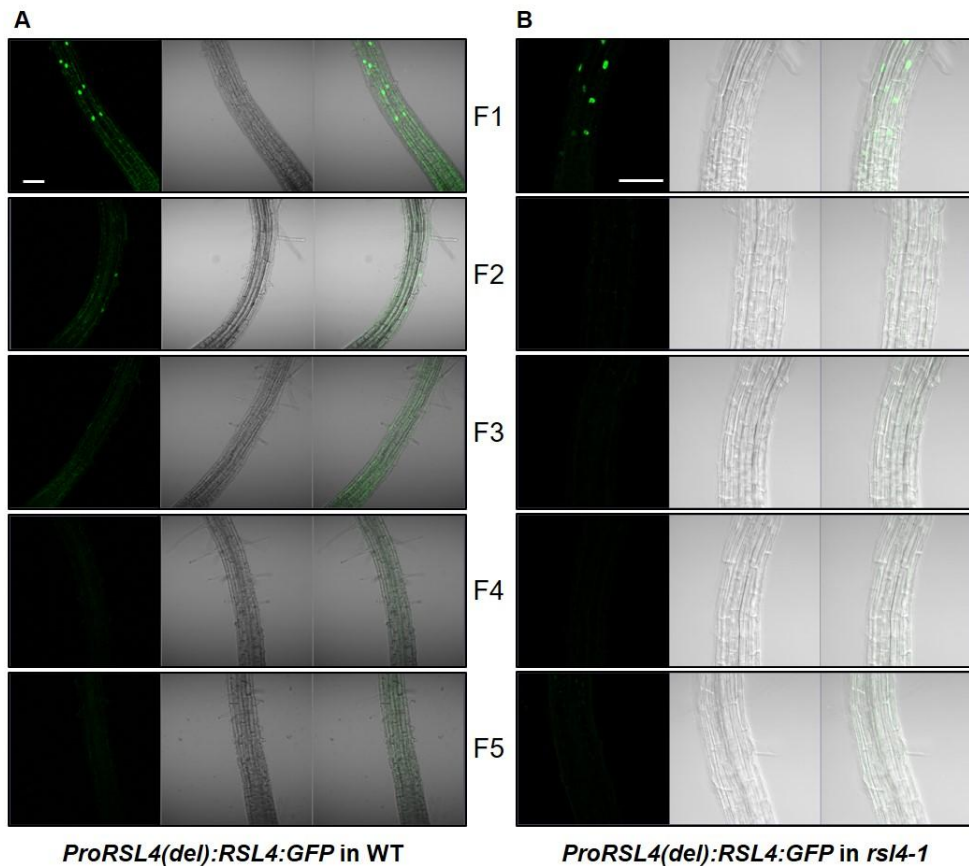


**Figure 47. Different expression intensities from sequentially deleted *RSL4* promoters in Arabidopsis.** (A and B) Confocal microscopy images show RSL4:GFP signals in the nuclei of root hair cells of promoter deleted transgenic lines [*pRSL4(del):RSL4:GFP* in the wild-type (A) or *rsI4-1* mutant (B) backgrounds]. Each construct contained deleted promoter fragments (F1 = 993 bp, F2 = 430 bp, F3 = 288 bp, F4 = 243 bp, and F5 = 106 bp). Scale bar is 100  $\mu$ m.

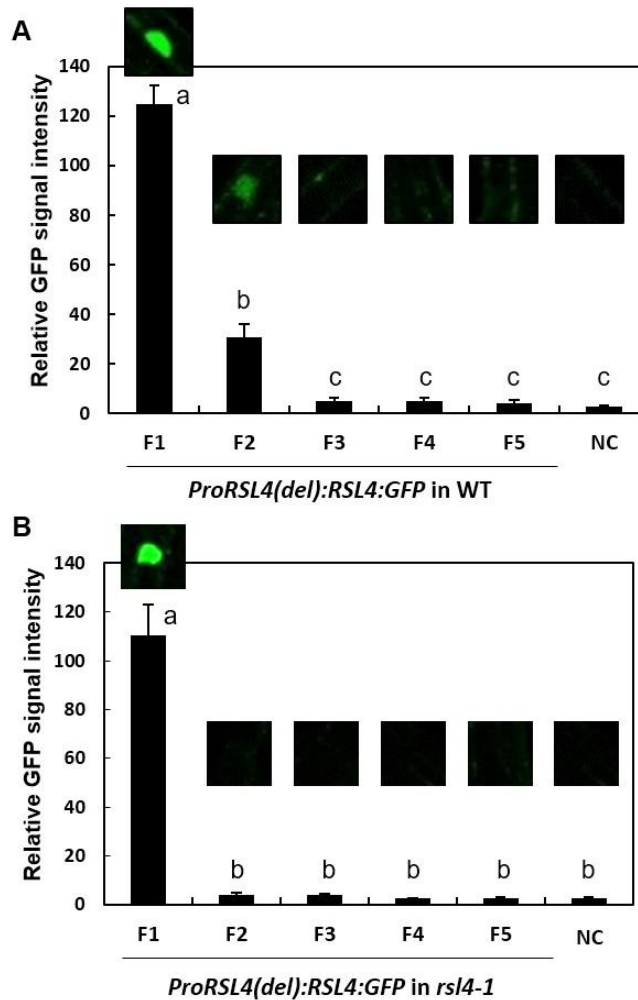


**Figure 48. Relative activities of deleted *RSL4* promoters by comparing GFP expression.** (A and B) Relative signal intensities and images of GFP signal in the nucleus. *ProRSL4(deleted):RSL4:GFP* (F1, F2, F3, F4, and F5) in the wild-type background or *rsl4-1* mutant background. Wild type plants used for GFP signal-negative control (NC). Data represent means  $\pm$  s.e. (n = 30–78 hair cells, A; n = 18–72 hair cells, B; from independent T1 seedlings). GFP signals were observed in the elongation zone hair cell. Statistically significant differences are denoted with different letters (one-way ANOVA with Tukey's unequal N HSD post hoc test,  $P < 0.05$ ).

hair that was the same length as the control. The others from the *F2* to *F5* lines could not elongate the root hair cells (Figure 49B). In the promoter deletion assays, the biggest difference was existence or nonexistence of *RSL4* depending on the background plants. *F2* in wild-type plants had natural *RSL4*, which was generated from its own genome sequences. *RSL4* may positively regulate its own transcription owing to *RSL4*, which could directly bind to RHE (Hwang et al., 2017). Thus, I altered our previous assumption. The critical promoter region for *RSL4* expression was in the *F1*, not in the *F2* following *rsl4-1* background data. All transgenic lines in the wild-type backgrounds increased root hair length compared to the control lines (Figure 49A). Unfortunately, I could not interpret the root hair length data of deletion lines.

Because the region between *F1* and *F2* turned out to be critical for root hair growth through the expression of *RSL4*, I made one more deletion-construct in this region (*F1.5*) that excluded three AREs and before the sequences of RHE3 from *F1*. Both the *F1.5* deletion-construct in the wild-type and *rsl4-1* mutant backgrounds showed a similar intensity of *RSL4*:GFP to *F1* (Figure 50 B, C). The *F1.5* lines showed slightly weak GFP signals suggesting that deleted sequences were helpful for expressing *RSL4*, but not critical. To discover the function of RHE3, the only difference between *F2* and *F1.5*, I made RHE3 mutation *F1* constructs (*F1mRHE3*) that had the same promoter length as *F1*, but non-functional RHE3. These RHE3-mutated promoter deletion lines in the *rsl4-1* mutant background showed few or no GFP signals. Although *F1mRHE3* in wild-type plants showed some GFP signals, this was considered a result of the remaining

RHEs in the promoter (Figure 50). To

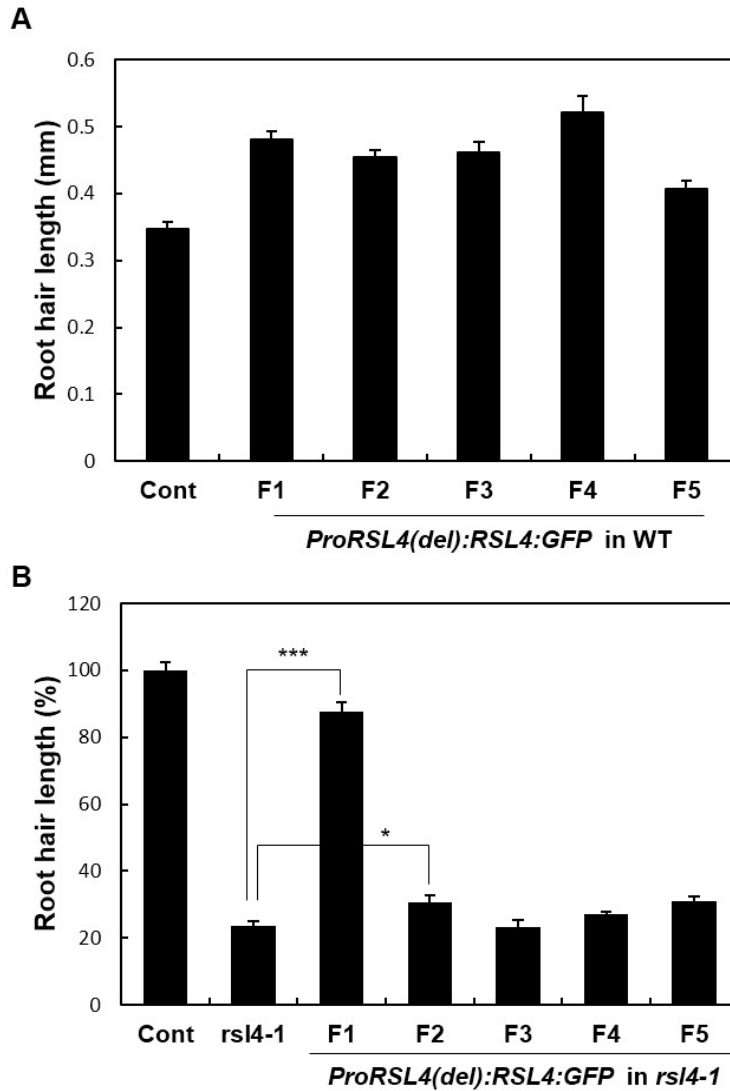


**Figure 49. Root hair length of RSL4 complementation lines.** (A and B) Root hair lengths of control (Cont, *ProE7:GFP*) and *ProRSL4(deletion):RSL4:GFP* transgenic lines in wild-type (A) or in *rsl4-1* (B). Data represent means  $\pm$  s.e. (n = 121–1,931 root hairs, A; 130–799, B). The values are relative to the Cont value and

significantly different ( $***P < 0.001$ ;  $*P < 0.05$ ;  $t$ -test) from the Cont value.

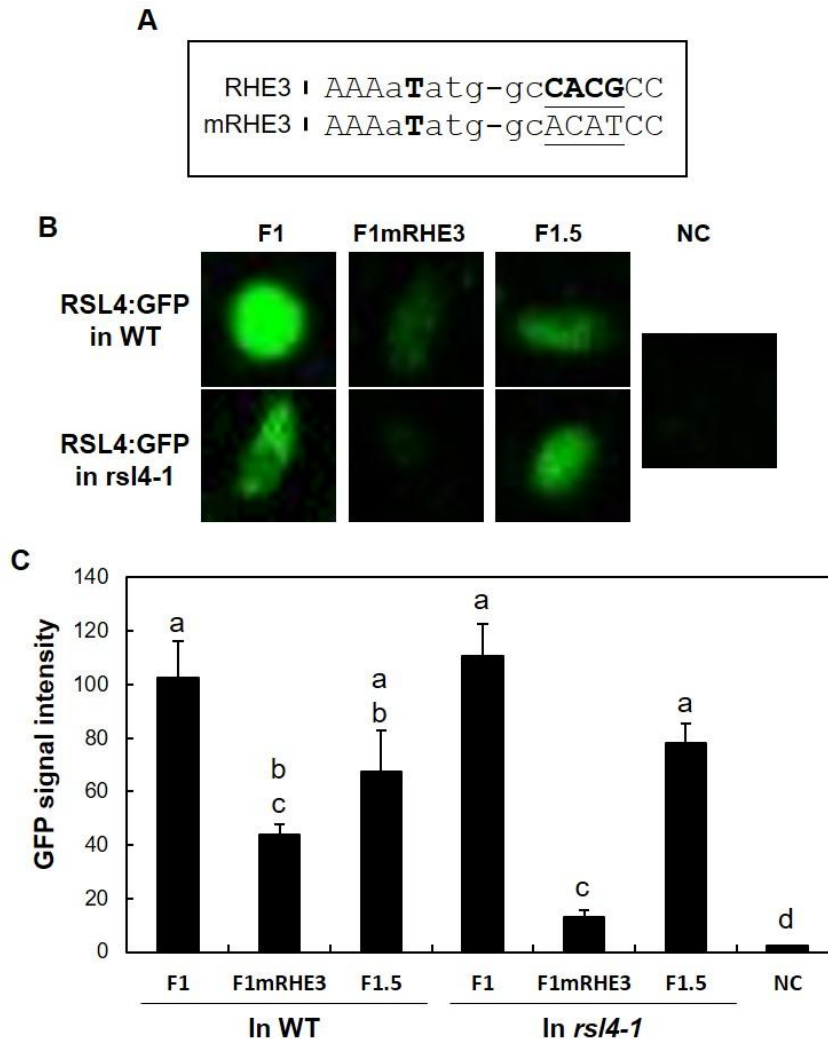


**Figure 50. Analyses of *RSL4* promoter region.** (A) Sequences of three RHE3 from the *RSL4* promoter and mutated RHE3; it was changed from CACG to ACAT. The strictly conserved nucleotides are in bold. (B and C) GFP images and relative activities of deleted *RSL4* promoters in Arabidopsis by comparing GFP expression. Deleted promoter fragments of *RSL4* were fused to the *RSL4* gene and *GFP* was analyzed in root hair cells. *F1mRHE3* promoter has mutated RHE in the F1 sequence. Each construct contained deleted promoter fragments (F1, F1mRHE3 = 991 bp, and F1.5 = 506 bp) and wild-type was used for negative control (NC) in

GFP images.

characterize the function of other RHEs in RSL4 expression, I mutated the RHE2 and RHE1 of the RSL4 promoter in the ordering (F2mRHE1, F2mRHE2, and F2mRHE1,2) (Figure 51A). All the mutated promoters of the *F2* lines decreased the GFP signal compared to the signal of *F2*. The GFP signal of the *F2mRHE2* lines was of a lower intensity than those of the *F2mRHE1* lines, but had a stronger intensity than those of the *F2mRHE1,2* lines, which lost the functionality of both RHE1 and RHE2. This deletion analysis suggests that the promoter including RHE3 is critical for RSL4 transcription. Moreover, the two proximal RHEs of the RSL4 promoter (RHE2 and RHE1) cooperated with the regulation of RSL4 expression. I infer that transcription factor binding to RHE3 is important for driving RSL4 expression and transcription factor binding to RHE2 and RHE1 is involved in positive feedback to amplify RSL4 expression.

#### 4.4.6 RSL1, RSL4, and RHD6 bind to RHE in the *RSL4* promoter

In the previous study, the RSL transcription factors were grouped into two classes. Class I RSLs, including RHD6 and RSL1, regulated class II RLSs (RSL2-5) (Pires et al., 2013). RSL4 was directly regulated by RHD6 (Yi et al., 2010). To examine the class I RSLs and RSL4 binding ability to the RHEs of the *RSL4* promoter, I performed an electrophoresis mobility shift assay (EMSA) using each 30-bp promoter region, including a single RHE from the *RSL4* promoter as the probe (Figure 52C). All heterologously expressed RSL1, RSL4, and RHD6 caused a mobility shift of the probe band including the RHE1 and RHE2 promoter region.

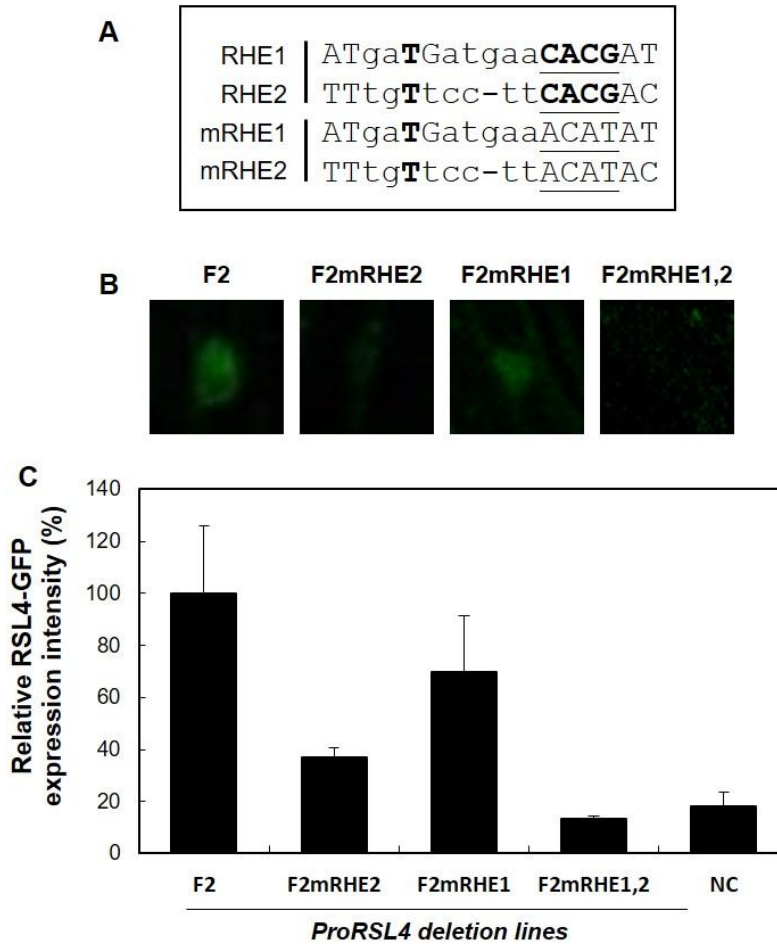


**Figure 51. Relative activities of deleted *RSL4* promoters by comparing GFP expression.** (A) Sequences of two RHEs (RHE1 and RHE2) from the *RSL4* promoter and mutated RHEs (mRHE1 and mRHE2). This was changed from CACG to ACAT; strictly conserved nucleotides are in bold. (B and C) Insets are fluorescence images of the root containing designated promoter constructs. Each construct contained deleted and RHE-mutated promoter fragments (Promoter lengths were all 430 bp) (B). Relative signal intensities of *pRSL4(deleted):RSL4:GFP* (F2, F2mRHE1, F2mRHE2, and F2mRHE1,2) T1 lines and negative control lines were observed in the root hair nucleus (C). Data

represent means  $\pm$  s.e. (n = 6–42 root hairs).

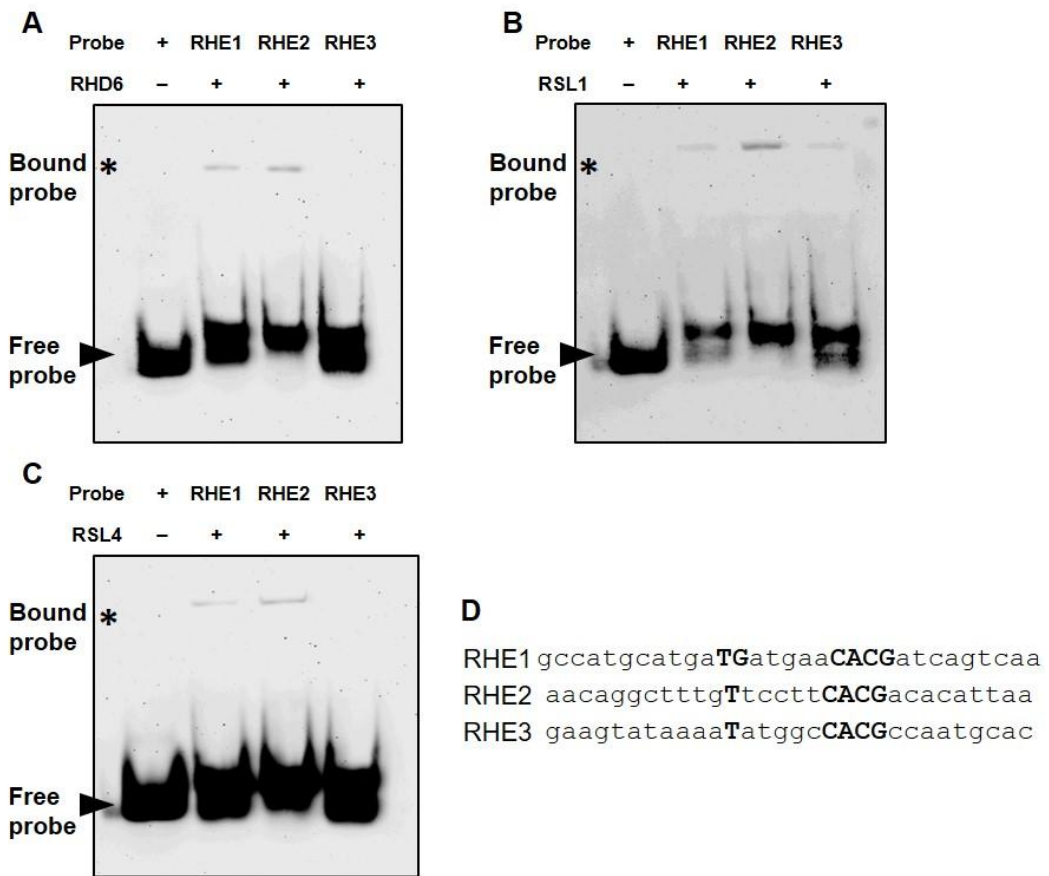


**Figure 52. RSL1, RHD6, and RSL4 bind to the RHE.** (A–C) EMSA showing RHD6, RSL1, and RSL4 binding to each type of RHE of the promoter *RSL4* gene. GST-tagged proteins and biotinylated RHE probe were used. (D) EMSA showing the effect of the RHE sequence on RSLs binding. In each length (bp) of probe, the RHE core (17 bp) was located at the probe's center. The sequences of each RHE were used for the EMSA in (A, B, C). The RHE consensus sequences are

shown in bold.

This result indicates that class I RSLs and RSL4 bind to RHE1 and RHE2 *in vitro* (Figure 52), whereas only RSL1 protein caused a mobility shift of the probe band of the RHE3 promoter region (Figure 52B), indicating that RSL1 binds to RHE3, but RSL4 and RHD6 do not prefer to bind to RHE3 *in vitro*. However, RSL1 never showed a defect of root hair growth (Menand et al., 2007). Thus, an *in vivo* binding assay is required to elucidate the binding ability of RSL1, RSL4, and RHD6 to the RHEs of the *RSL4* promoter.

To investigate the binding ability of RSL4 to RHE *in vivo*, I performed chromatin immunoprecipitation (ChIP) analyses with the promoter region of the RHEs. The ChIP-PCR regions were divided into two sites, R3 for RHE3 and R2 for RHE2 with RHE1. Because RHE2 and RHE1 were physically close, they were merged into one PCR region (Figure 53A). The binding of RSL4 to both RHE regions was significantly higher than the binding to negative sites located distally from the RHE3 and exon parts (Figure 53B). RSL4 bound to RHE3 in the *in vivo* binding assay unlikely *in vitro* data (Figure 52C). There is a chance that RSL4 interacted with another transcription factor binding to RHE3 *in vivo*. This result suggests that RHE3 is also used as a positive feedback cis-element for RSL4 expression because of the coincidence of RSL4 binding to the R2 site *in vivo*. I am still preparing an RHD6 construct for ChIP analysis and expecting RHD6 to bind to RHE3, likely RSL4.

#### 4.4.7 RHD6 is required for aARF's binding to ARE

Next, to investigate the relationship between auxin and *RSL4* promoter, I treated

the

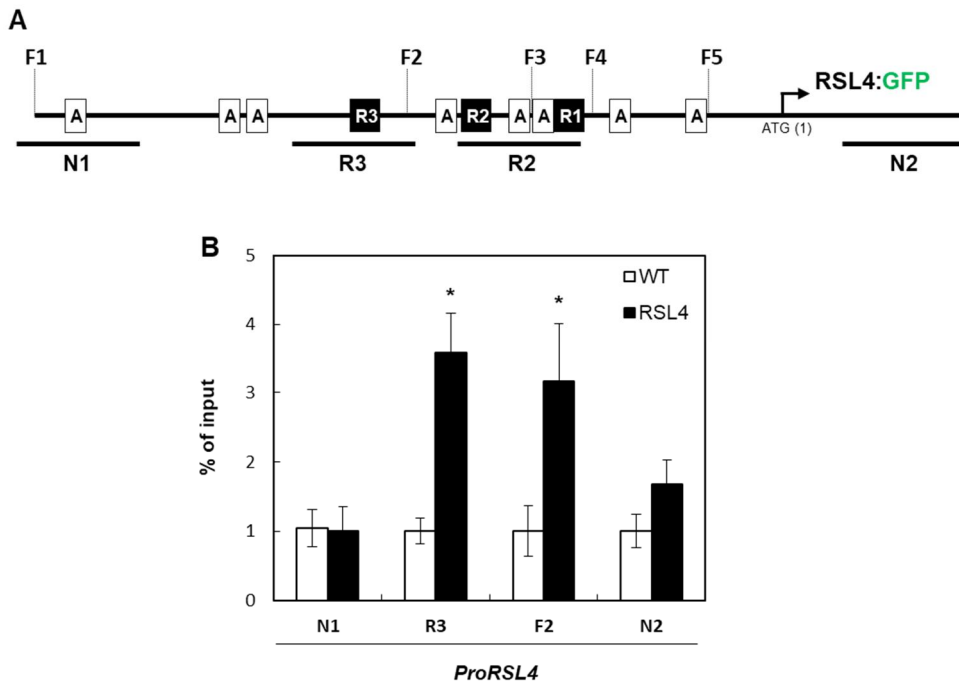


**Figure 53. ChIP analysis of RSL4:GFP binding to the RHE on the *RSL4* promoter region in four-day-old seedling roots.** (A) Schematic diagram of the *RSL4* promoter region (*pRSL4*) and relative positions of the primer binding sites that were used for ChIP qRT-PCR (Negative region 1: N1 = 211 bp; ChIP RHE3 region: R3 = 164 bp; ChIP RHE2 region: R2 = 145 bp; Negative region 2: N2 = 141 bp). (B) The enrichment fold of RSL4:GFP in the ChIP per of each region was as shown in (A). ChIP analysis was done with wild-type (Cont) and *pRSL4:RSL4:GFP* (RSL4) transformant plants. Error bars indicate  $\pm$  s.e. for two biological replicates. Values are relative to each control value and significantly different (\* $P < 0.05$ ; Student's *t* test) from the control value.

*RSL4* promoter-deleted lines with exogenous auxin. The *F1* lines clearly showed an increased intensity of GFP signal from the response to auxin (Figure 54A). Although the construct of F1.5 removed three AREs and the upstream part of RHE3 (Figure 46A), it also responded to auxin, showing an increased GFP signal compared to those of the *F1.5* lines without auxin treatment (Figure 54B). Interestingly, the promoter of the *F1mRHE3* lines, which had eight normal AREs but only mutated RHE3, showed a similar expression level of *RSL4:GFP* with and without auxin conditions (Figure 54C). The construct of F2 also did not respond to auxin (Figure 54D). This result suggests that the function of RHE3 recruiting a specific transcription factor is required for not only *RSL4* expression, but also the response to auxin. Even RHE3 is more important for promoting *RSL4* expression with auxin than the AREs specifically located upstream of RHE3.

The last step of auxin signaling is ARF binding to the promoter of the target genes, but we do not have evidence of which AREs in the *RSL4* promoter recruit aARFs *in vivo* and in practice. Furthermore, to demonstrate how RHE is more critical than AREs for the response to auxin in root hair cells, firstly, I tested aARF binding to the *RSL4* promoter. When the root hair was expressed specifically, ARF5 resulted in the most up-regulated *RSL4* expression among the tested aARFs (Figure 39C). Thus, I used GFP-tagged ARF5 (ARF5:GFP) driven by estradiol-inducible 35s promoters operating ubiquitously and strongly for ChIP assay in wild-type plants. ChIP-qPCR

primers were designed to amplify the ARE or non-ARE regions, as shown in

Figure

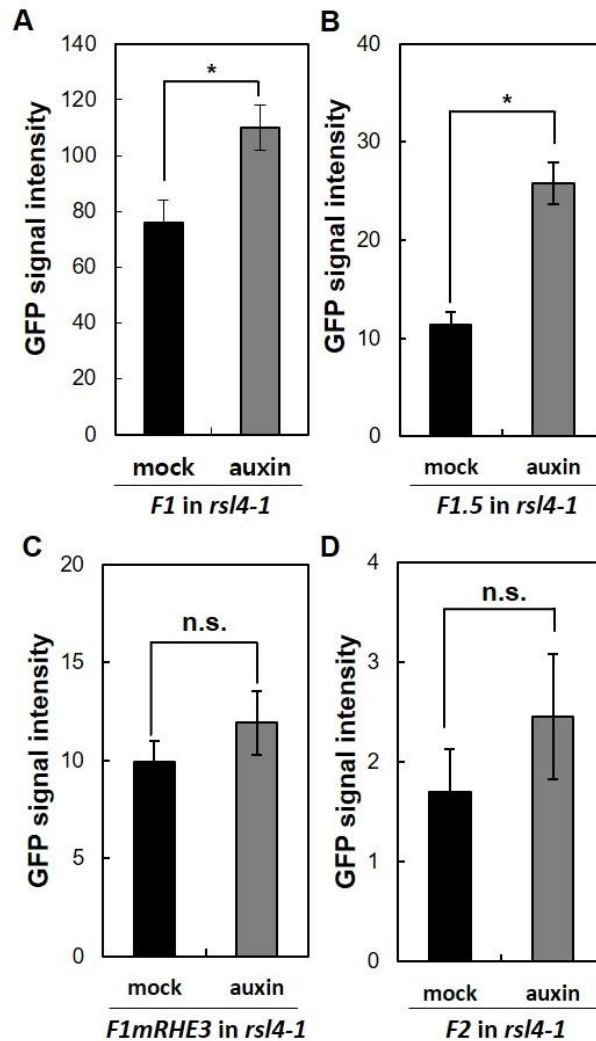


**Figure 54. Analyses of auxin response to the *RSL4* promoter region.** (A–D) *pRSL4(F1):RSL4:GFP* (A), *pRSL4(F1.5):RSL4:GFP* (B), *pRSL4(F1mRHE3):RSL4:GFP* (C), and *pRSL4(F2):RSL4:GFP* (D) activity in the root hair cells with auxin or without auxin. Data represent means  $\pm$  s.e. (n = 20–47 hair cells). Auxin treatment (IAA 100 nM). Values are relative to each control value and significantly different ( $*P < 0.001$ ; Student's *t*-test) from the control value. The GFP signal intensities were observed in the root hair nucleus and analyzed using Adobe Photoshop CS6, The scale box size is 3 x 3 mm.

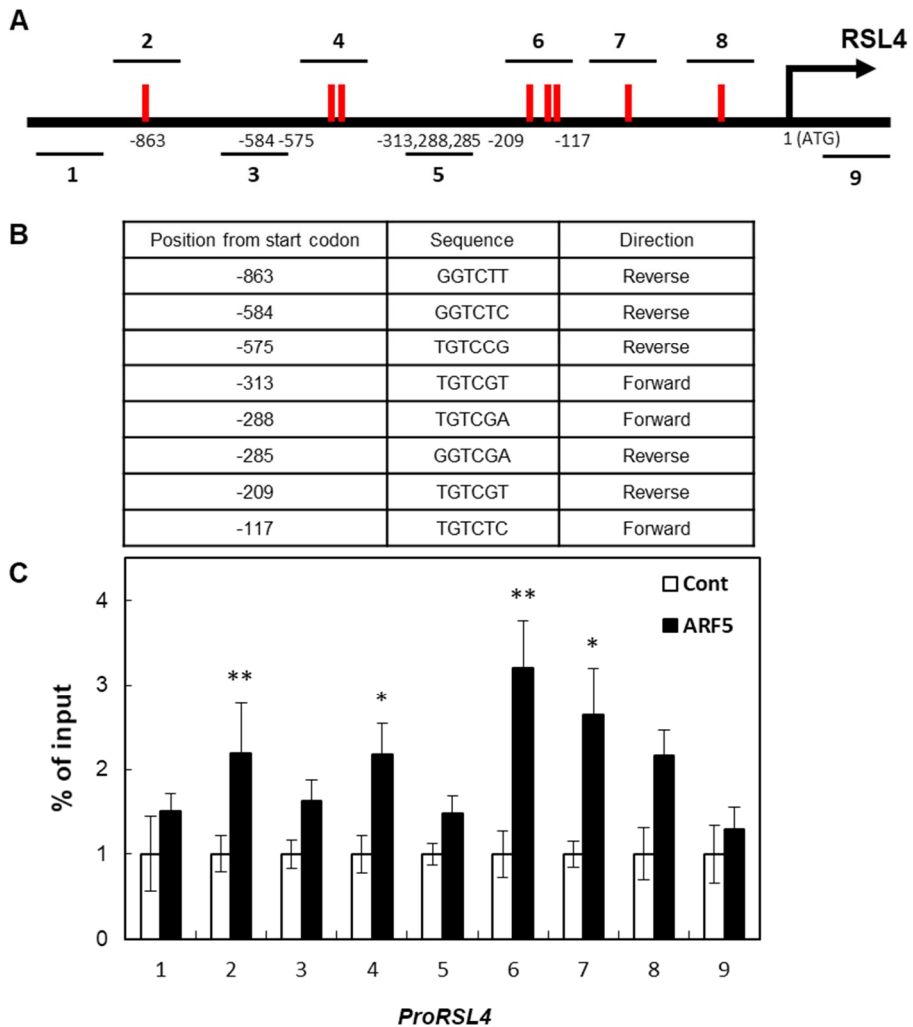


**Figure 55. Chromatin immuno-precipitation (ChIP) analysis showing ARF5-binding to auxin response elements (AREs) on the *RSL4* promoter region.** (A) The *RSL4* promoter region (*ProRSL4*) with relative positions of putative AREs (red bars) and ChIP-PCR regions (lines with #1–9). Positions are relative to the start codon. (B) Information of putative AREs in (A). (C) % of input value of ARF5:GFP in ChIP-PCR on each region shown in (A). Cont, *pMDC7*-empty control line; ARF5, *pMDC7-ARF5:GFP*; dexamethasone-inducible ARF5:GFP line. ChIP assay was performed using anti-GFP antibody. Error bars indicate  $\pm$  s.d. from three biological replicates. The values are relative to each Cont value and significantly different (\*\* $P < 0.001$ ; \* $P < 0.005$ ; *t*-test) from each Cont value.

65A. The ChIP data demonstrated that the input percentage of ChIP-qPCR was significantly higher in the ARE-containing regions than in the non-ARE regions (Figure 55C). In particular, PCR site 6, including three AREs between -313 and -285, showed the strongest interaction with ARF5:GFP (Figure 55). This data suggests that ARF5 preferentially binds to the ARE of the *RSL4* promoter region *in vivo*. However, in the promoter deletion assay, the *F3* promoter including PCR site 6 could not express *RSL4*:GFP (Figure 48). Considering the result of the promoter deletion assay, I suggest ARF prefers binding to the *RSL4* promoter; however, ARF binding to ARE has to be preceded by certain events related to the RHE3 region.

My results demonstrated that RHE3 is required for the expression of *RSL4* in auxin response. In addition, I have assumed that RHD6 and RSL1 may bind to RHE3, although *RSL4* also binds to its own promoter. I questioned whether RHD6 affects ARF5 binding to the *RSL4* promoter. To test this possibility, I transformed estradiol-inducible ARF5:GFP into the *rhdb6-3* mutant and carried out ChIP analysis using *ARF5:GFP*-bound chromatin from the *rhdb6-3* background plant. In this case, the ChIP analysis of ARF5:GFP in the *rhdb6-3* mutant showed that the fold-enrichment levels were not increased in the positive region. However, the ChIP analysis of ARF5:GFP in wild-type plants of the same region showed a 4.3-fold increase compared to the level of the control (Figure 56). Overall, these findings suggest that RHD6 binding to RHE3 of the *RSL4* promoter plays a key role in the ARF-mediated *RSL4* transcription in root hairs.

#### 4.4.8 RHD6 affects the chromatin status of the proximal region

of

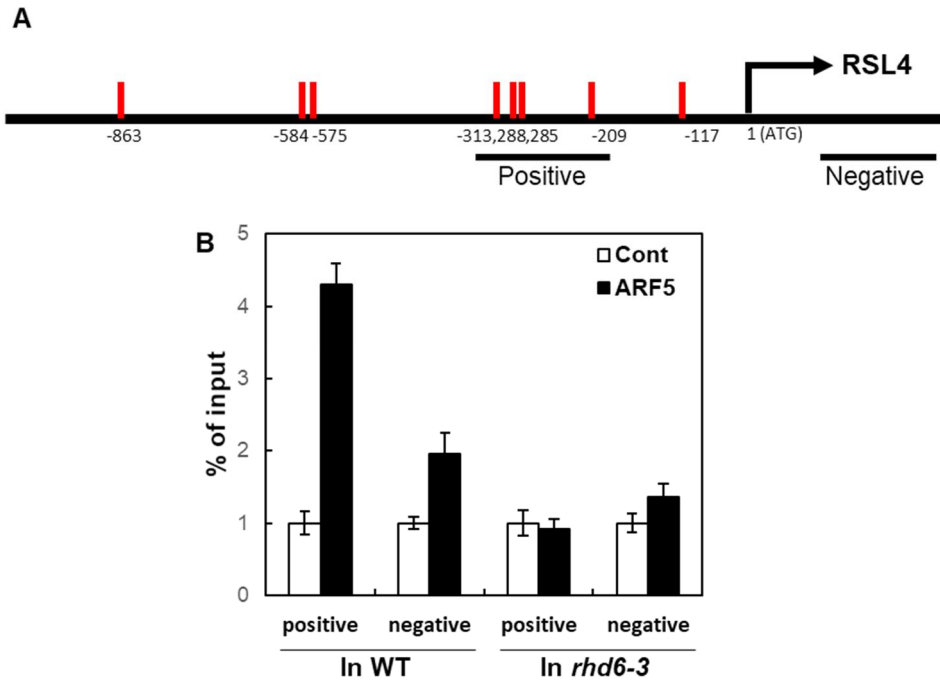


**Figure 56. ChIP analysis at the *RSL4* promoter region showed that ARF5 binding to AREs is interrupted in *rhd6-3* mutant.** (A) The *RSL4* promoter region (*ProRSL4*) with the relative positions of putative AREs (red bars) and ChIP-PCR regions (lines with positive or negative); positions are relative to the start codon. (B) % of input value of ARF5:GFP in ChIP-PCR on each region in (A). Cont,

*pMDC7*-empty control line; ARF5, *pMDC7-ARF5:GFP*; dexamethasone-inducible ARF5:GFP line. ChIP assay was performed using anti-GFP antibody. Error bars indicate  $\pm$  s.d. from two technical replicates.

## the *RSL4* promoter

The gene activity is considered by the chromatin structure-consisting nucleosome. The decreased nucleosome density on the chromosome results in a relaxed structure and transcriptional activation (Clark and Felsenfeld, 1991). In addition, histone modification provides the genome with access to the regulatory proteins in plants (reviewed in Pfluger and Wagner, 2007). Aux/IAAs repress the activity of DNA-bound aARFs by recruiting TPL and the resultant crowding chromatin remodelers, such as HDAC. These histone modifications are required not only for gene repression, but also gene activation by controlling more closed or open chromatin configurations, respectively. Several data showed the inducing trimethylated pattern of lysine 27 on histone H3 (H3K27me3) at the closed chromatin in the plant (Makarevich et al., 2006; Schubert et al., 2006; Turck et al., 2007).

To elucidate the reason for the decrease in ARF5 binding to the *RSL4* promoter without RHD6, I hypothesize that RHD6 binding to the promoter causes a change of chromatin status that is favorable to aARF binding. I referenced the published database of chromatin components. The nucleosome density and methylation density of H3K27 is only displayed in the UCSC genome browser (<http://epigenomics.mcdm.ucla.edu>), which allows the easy visualization of chromosomal status through the *Arabidopsis* genome (Figure 57A). I tested the chromatin status of the *RSL4* promoter in *rh6-3* mutant through ChIP assay using antibodies specific to H3K27me3. For this ChIP analysis, I used eight primers to

cover 1,000 base pairs of the proximal promoter region and one primer for the exon

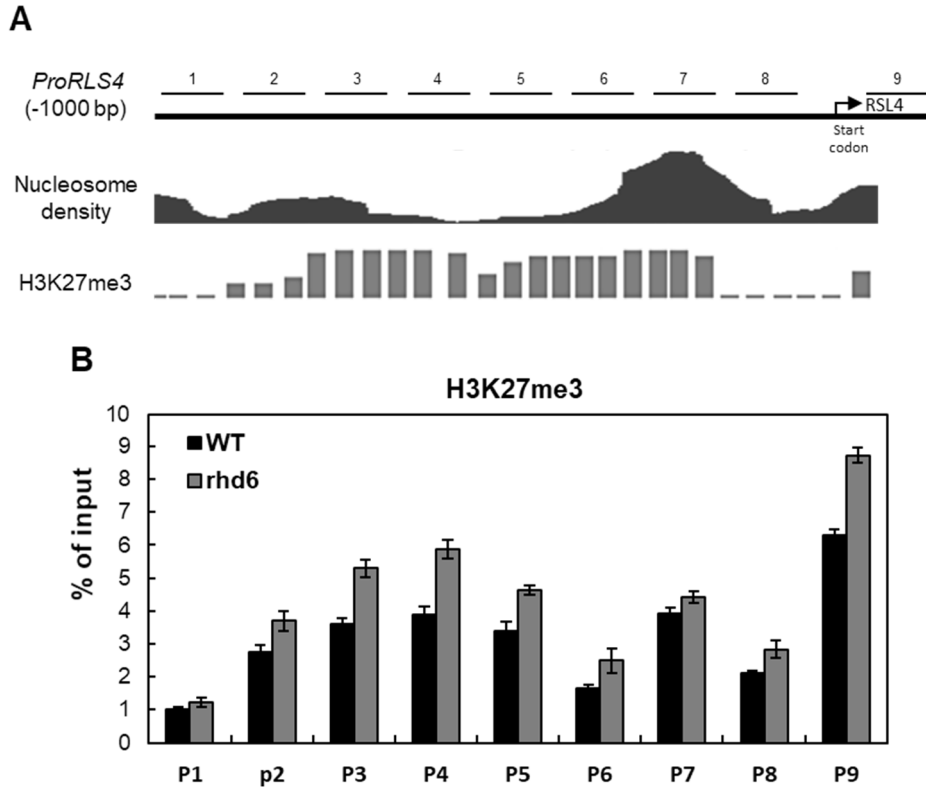


**Figure 57. ChIP analysis showing the level of H3K27me3 in the *RSL4* promoter region.** (A) The *RSL4* promoter region (*ProRSL4*) with ChIP-PCR regions (lines with #1–9). Positions are relative to the start codon. Representative UCSC Browser screenshot of an *RSL4* promoter showing calculated nucleosome densities and the level of H3K27me3. (B) % of input value of H3K27me3 in ChIP-PCR on each region shown in (A) of WT and *rhd6-3* mutant. ChIP assay was done using anti-H3K27me3 antibody. Error bars indicate  $\pm$  s.d. from two biological replicates. The values are relative to the Cont value of P1.

region (Figure 57A). The pattern of H3K27me3 is similar to the data in the UCSC genome browser. This means that our ChIP assay is reliable. However, the results showed that the *RSL4* promoter region within 1kb in the *rhdl6-3* mutant underwent increasing histone methylation compared to the level in wild-type plants (Figure 57B). Thus, the ChIP assay indicates that RHD6 binding to the promoter of *RSL4* is involved in the opening chromatin and initiating auxin response.

## 4.5 Discussion

Transcription causes critical changes in plant development. It should be strictly managed. In particular, the expression of regulatory protein-related morphogenesis is comprehensively controlled by environmental and developmental cues. Auxin is a plant hormone and morphogen. aARFs regulate the expression of the target gene as a transcription factor in auxin signaling. In the previous concept, the repression mechanism of heterodimerization with Aux/IAAs is a major system for determining the activity of aARFs. However, the target-selection mechanism of mediating ARF binding AREs to activation could not cover the whole auxin response because of the short and variable sequence of ARE. I suggest an activation mechanism interacting with a developmental factor on the target promoter in auxin signaling (Figure 58).

Transcription factors bind to specific DNA sequences and cis-elements and regulate the target genes for correct transcription in response to developmental

and

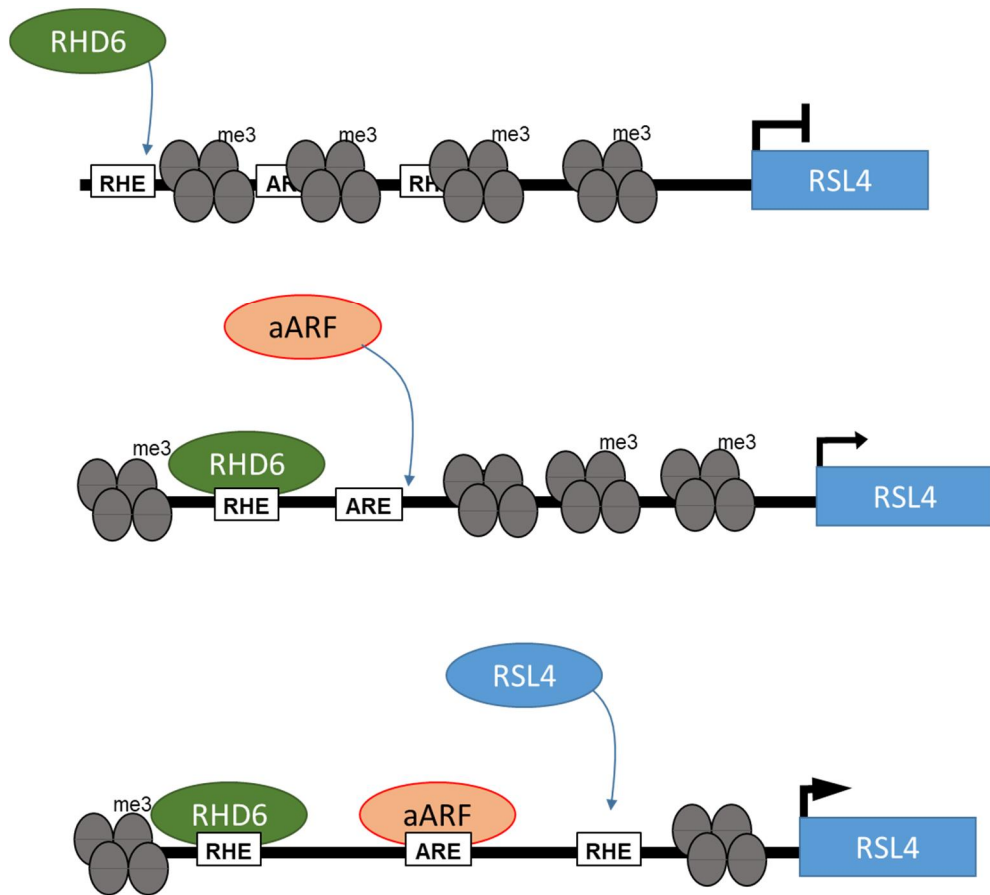


**Figure 58. A model illustrating the developmental factor affects aARF's binding to ARE on the target gene promoter.** A schematic model depicting the role of aARFs related with developmental transcription factors in auxin signaling; The proximal region of the *RSL4* promoter includes two representative cis-elements, such as root hair-specific cis-element (RHE) and auxin signal-specific cis-element (ARE) but they were hidden by histone. The level of H3K27me3 is mainly enriched in the promoter of the repressed gene. However, binding RHD6 to RHE results in chromatin status and expose ARE. aARF binds to ARE and induces *RSL4* expression. (me3: Trimethylation on lysine of Histone 3).

environmental cues. The presence of variable cis-elements in the promoter region to respond to different signals provides a prospective molecular link between diverse metabolic pathways. The proximal region of the RSL4 promoter includes two representative cis-elements, such as root hair-specific cis-element and auxin signal-specific cis-element. Thus, it is ready to express development and environment specifically. The remaining problem is how to control the exposure level of the cis-element to transcription factors.

It has been shown that the environmental or developmental cues induce histone modification patterns, resulting in target gene expression (reviewed in Pfluger and Wagner, 2007). H3K27me3 is usually associated with multigene-silenced domains instead of single genes in metazoans through POLYCOMB REPRESSIVE COMPLEX 1 (PRC1). However, plants are absent from PRC1 complex. In plants, in *in vivo* binding assay, HETEROCHROMATIN PROTEIN (HP1) homolog, LHP1/TFL2, binds to H3K27me3 for the repressive gene. LHP1/TFL2 only suppresses genes located in the euchromatin region, but not genes in heterochromatin, unlikely PRC1 in metazoans (Libault et al., 2005; Nakahigashi et al., 2005). In addition, TFL2/LHP1 specifically binds to H3K27me3 in a repression mechanism (Turck et al., 2007). The level of H3K27me3 is mainly enriched in the promoter of the repressed gene, especially transcription factors and developmental regulators, by ChIP in chip assay (Zhang et al., 2007). This suggests that H3K27me3 affects the exposure of cis-elements in the proximal promoter (Turck et al., 2007). The result of ChIP assay showed the

change of the H3K27me3 level in RSL4 the promoter region depending on RHD6 (Figure 57B), and the qRT-PCR data showed that the RSL4 expression level significantly decreased without RHD6 (Figure 39). This indicated that RHD6 regulated the expression level of RSL4 through histone modification, especially H3K27me3, as discussed above. In addition, aARF binding to the *RSL4* promoter was affected by RHD6. Taking these results together, I suggest RHD6 may permit aARF access to DNA by regulating histone modification. The combination of a sequence-specific developmental factor, likely RHD6, and histone modifiers will provide an accurate recruitment mechanism for aARFs in auxin signaling.

RSL4 positive feedback regulation plays a pivotal role in the RSL4 expression mechanism. I assumed that RHD6 and RSL1 bind to the RHE3 of the *RSL4* promoter. Thus, the *rh6-3 rsl1-1* mutant should not respond to auxin in RSL4 expression. However, the *rh6-3 rsl1-1* double mutant recovered the root hair growth and RSL4 expression after auxin treatment (Yi et al., 2010). This is in conflict with my data. I may solve this problem by suggesting RSL4 positive feedback. Auxin treatment in the *rh6-3 rsl1-1* mutant could express RSL4 from the transgene and natural genome at once; then, the newly generated RSL4 binds to RHE3 to turn on the positive feedback transcription because of the possibility that RSL4 regulates its own expression by binding to the RHE3 and RHE2 region following ChIP assay. In our case, auxin treatment in the *rsl4-1* mutant could generate RSL4 only from the transgene, not the genome; moreover, RSL4 could not bind to RHE3, resulting in difficulty regarding positive feedback regulation. These results indicated that enhancing *RSL4* expression with an RSL4 positive

feedback system is necessary for a normal level of *RSL4* expression and auxin promotes positive feedback.

Finally, to correct the expression of target genes in auxin signaling, this study suggests a transcriptional activation system including cooperation with sequence-specific developmental factors, histone modification, and a feedback system.

For further analysis of *RSL4* expression in transcriptional activation complex, I am considering additional experiments. Firstly, the acetylation of lysine 4 on histone 3 (H3K4ac) has been extensively researched and shown to mark genes for active expression. To define the relative role of H3K27me3 and H3K4ac in the transcription of *RSL4*, I will observe the acetylation pattern of H3K4.

For reference, I were interested in whether wild-type (natural) ARF5 works for root hair growth because the function of ARF5 in root hair development has not been reported. I checked the expression of GUS:GFP with the *ARF5* promoter. It expressed in the root, hypocotyl-root junction, primary root, root tip, and root hairs (Figure 59). Thus, ARF5 may promote the RSL4 level in necessary root hair growth. We are preparing a ChIP assay of aARF7, which is one of the aARFs. ARF7 is usually involved in the root developmental process and expressed in the root hair cells according to the eFP browser.

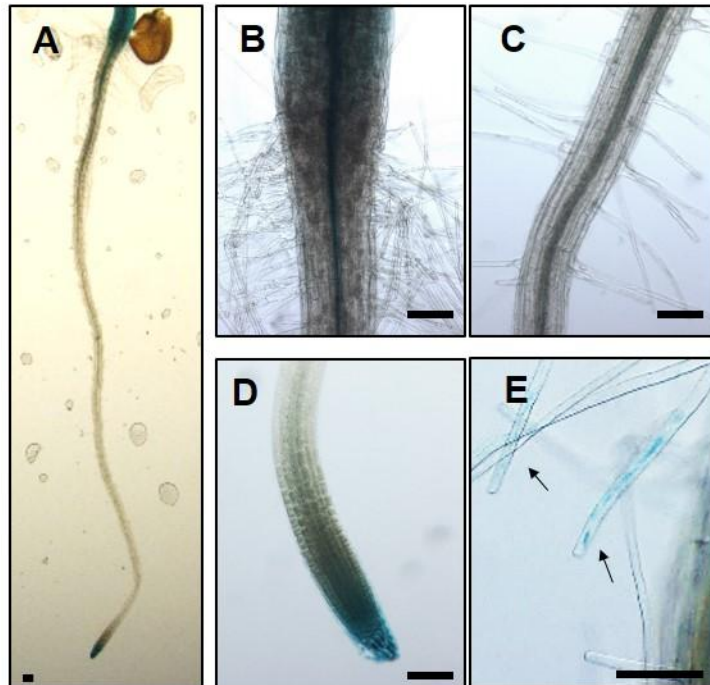


**Figure 59. Expression pattern of *ProARF5:GUS*.** (A–F) Expression pattern of GUS driven by promoter *ARF5* (*ProARF5*) in the root of a four-day-old seedling (A), hypocotyl-root junction (B), primary root (C), root tip (D), and root hairs (E). The arrow indicates GUS expression in the root hair (D). Scale bars are 100 μm.

## **Conclusions of chapter I ~ IV**

In this study, taking advantage of the auxin-responsive root hair system, I addressed the interacting dynamics between transcription factors that are implicated in auxin signaling and responses (Figure 60). First, I elucidated the mechanism how auxin induces root hair growth by demonstrating that aARFs directly target AREs on the promoter region of *RSL4* that encodes the master modulator for root hair growth. Second, I identified functionally distinctive two Aux/IAA subgroups; RG-Aux/IAs with a lower affinity and CG-Aux/IAs with a higher affinity to TPL/TPRs. In a (root hair) cell with a pool of these two Aux/IAA variants, the increase of RG-Aux/IAA doses revealed a transient transcriptional activation of *RSL4* and root hair growth most likely by altering the density of TPL/TPRs on the regulatory region of *RSL4*. Third, I addressed the molecular and biological function of a rARF (ARF2). I demonstrated that ARF2, by way of its interacting motifs, recruits TPL/TPRs so as to inhibit auxin-responsive root hair growth. Forth, I found that aARFs cooperatively work with RHD6 to activate *RSL4* transcription and root hair growth, indicating that both the developmental cue (via RHD6) and the auxin signaling are required for full root hair growth. In conclusion, this study demonstrates the interaction dynamics between transcriptional factors such as competition (aARFs vs. rARFs and RG-Aux/IAA vs. CG-Aux/IAA) and cooperation with the developmental factor (aARFs vs. RHD6). My study suggests that diverse molecular homologs of auxin-signaling components provide the opportunity for diversification and fine-tuning of auxin responses, which could not be explained by the simple canonical auxin signaling pathway. This discovery in the root hair system should expand to the auxin responses in

other cell types and organs.



TPL/TPR co-repressor to the target gene. RG-motif Aux/IAA can result in a transient repressor-to-activator activity switch most likely by altering the TPL/TPR density in a dose-dependent manner. DNA-binding transcriptional repressor, rARF, represses the auxin-responsive genes by directly recruiting TPL/TPR. RHD6 as a developmental transcription factor promotes *RSL4* expression. RSL4 gives positively feedback on its expression.

## **Chapter V.**

### **Ecological roles of root hairs**

## 5.1 Abstract

Root hairs on the epidermal cells of the root effectively uptake water and nutrients by increasing the surface area. However, the relationship between root hairs and root anchorage to the ground remains unresolved. This paper assessed whether the ability of root hairs to hold water and soil improves the survival ratio of particular seedlings. In the sink part of the root, the length of root hairs has an important role in deciding the contact surface with water or soil. I analyzed the effect of root hair length through the root hair-specifically overexpressed transgenic lines, which are different in root hair length. Seedlings pulled-off from media or soil were able to sustain their life depending on the root hair length. Moreover, root hair was apparently advantageous for anchoring the plant in the soil in conditions that mimicked a landslide. These results suggest that root hairs are necessary for seedling's survival by increasing the surface area of the root with water and soil.

## 5.2 Introduction

The overall developmental process of the study of root hair formation has progressed since the beginning from cell-fate determination to tip growth (reviewed in Grierson and Schiefelbein, 2008). *Arabidopsis* root hairs form from root epidermal cells, which are two intact cortical cells in a position-dependent manner (Dolan et al., 1994; Galway et al., 1994). Tip growth results in a tubular-

shaped epidermal cell. This shape increases the volume of soil in contact with the root. Root hairs enlarge the surface area of the root ranging from by none to twice as much depending on the hair length and number (Jungk, 2001). Therefore, root hairs have been considered essential for absorbing nutrients and plant anchorage to the soil (Peterson and Farquhar, 1996). There is evidence that root hair increases the efficiency of nutrient-absorbing from the soil. For more effective nutrient uptake, some plant species regulate root hair development in response to nutrient stress (reviewed in Gilroy and Jones, 2000). Recently, it has been reported that plant–soil interaction accumulates soil and protects soil from erosion. The thallus and rhizoids of liverwort attached to fine grains and increased the soil-stabilizing effects (Mitchell et al., 2016). The rhizomes of the basal lycopsid *Drepanophycus* conferred erosion resistance to floodplains (Xue et al., 2016). However, it remains unknown whether the interaction with soil is beneficial to plant survival. I examined the role of root hairs in holding soil and water to increase the survival rate of seedlings.

## **5.3 Materials and methods**

### **5.3.1 Accession numbers**

The accession numbers for the genes analyzed in this study are AT1G12560 (*EXPA7*), At1G27740 (*RSL4*), AT1G70460 (*RHS10*), AT3G23030 (*IAA2*), and AT3G23050 (*IAA7*).

### 5.3.2 Plant materials and growth conditions

*Arabidopsis* (*Arabidopsis thaliana*), Columbia ecotype, was used as the wild-type plant in this study. All T2 generation seeds for the measurement of root hair length were grown on agarose plates containing 4.3 g/L Murashige and Skoog (MS) nutrient mix (Sigma-Aldrich), 1 % Suc, 0.5 g/L MES (pH 5.7), KOH, and 0.8 % agarose. All T2 generation seeds for the measurement of soil-holding ability were grown on agarose plates and the seedlings were transferred to the soil after three days after germination. All T2 generation seeds for the measurement of water-retention ability were grown on agarose plates containing 4.3 g/L Murashige and Skoog (MS) nutrient mix (Sigma-Aldrich), 1 % Suc, 0.5 g/L MES (pH 5.7), KOH, and 0.3 % agarose. All seeds were cold treated (4 °C) for 3 d and germinated at 23 °C under 16-h-light/8-h-dark photoperiods.

### 5.3.3 Observation of biological parameters

Root hair length was estimated as described in Lee and Cho (2006, 2009) with modifications. The lengths of 9 consecutive hairs protruding perpendicularly from each side of the root, 18 hairs in total, were estimated. Primary root width was estimated at three point of a root. The 3-day-old seedling root was digitally photographed using a stereomicroscope (M205 FA, Leica, Heerbrugg, Switzerland) at 40X magnification. All measuring experiment were used ImageJ 1.50b software (National Institutes of Health, United States).

### 5.3.4 Measurements of root dehydration and soil holding

For quantitative of root dehydrating, pulled out seedlings from 0.3 % agarose-MS media were put on the glass. The root was digitally photographed using a stereomicroscope (M205 FA, Leica, Heerbrugg, Switzerland) at 40X magnification. The widest possible length of retained water of root images was measured every 15 sec. For quantitative of root holding soil, pulled out seedlings from soil were measured the total weight of soil and seedling. Then, the weight of seedling was removed after washing out the soil. For evaluate survival ability in landslide conditions, water was poured onto four-day-grown seedlings grown on the slope of the land. After two days, the number of remained seedlings were counted.

## 5.4 Results and discussion

To examine the function of root hair, I selected long and short-root-hair plants. To reduce prejudice regarding genotype and focus only on root hair length, we used root hair-specific overexpressed transgenic lines by *ProE7* and seedlings before producing lateral roots. I selected root hair development-related genes and auxin signal-related genes. Two of them had longer root hair (*RSL4ox*, *ProE7:RSL4*; *IAA2mImIlox*, *ProE7:IAA2mImII*) and the other two had shorter root hair (*RHS10ox*, *ProE7:RHS10*; *axr2-1ox*, *ProE7:axr2-1*) than that of the control plants (Cont, *ProE7:YFP*) (Hwang et al., 2017; Hwang et al., 2016; Won et al., 2009, Chapter II) (Figure 61A, B). The *RHS10ox* and *axr2-1ox* seedling grew root hairs that were on average ~1% of the length of the control and most of the seedlings could not even produce root hairs. In particular, these two lines did not have collet hairs. The *RSL4ox* seedling showed a root hair length that was 120% of that of the control. The overexpression *IAA2mImII* constructs, enhancing auxin response, greatly increased root hair growth by up to 215% of the control length (Figure 61B). However, they all showed a similar primary root width (Figure 61C). The improved root surface enhanced adhesion to soil or water. The character of both the root and root hair determines the surface area of the root. In this case, only the root hair was a variable of the sink surface area in these lines due to the equal radius of the roots.

I measured the water-retention ability. Pulled seedlings out of 0.3% agarose media were observed the dehydrating process. The control, *RSL4ox*, and *IAA2mImIlox* lines retained water for longer than the *RHS10ox* and *axr2-1ox* lines

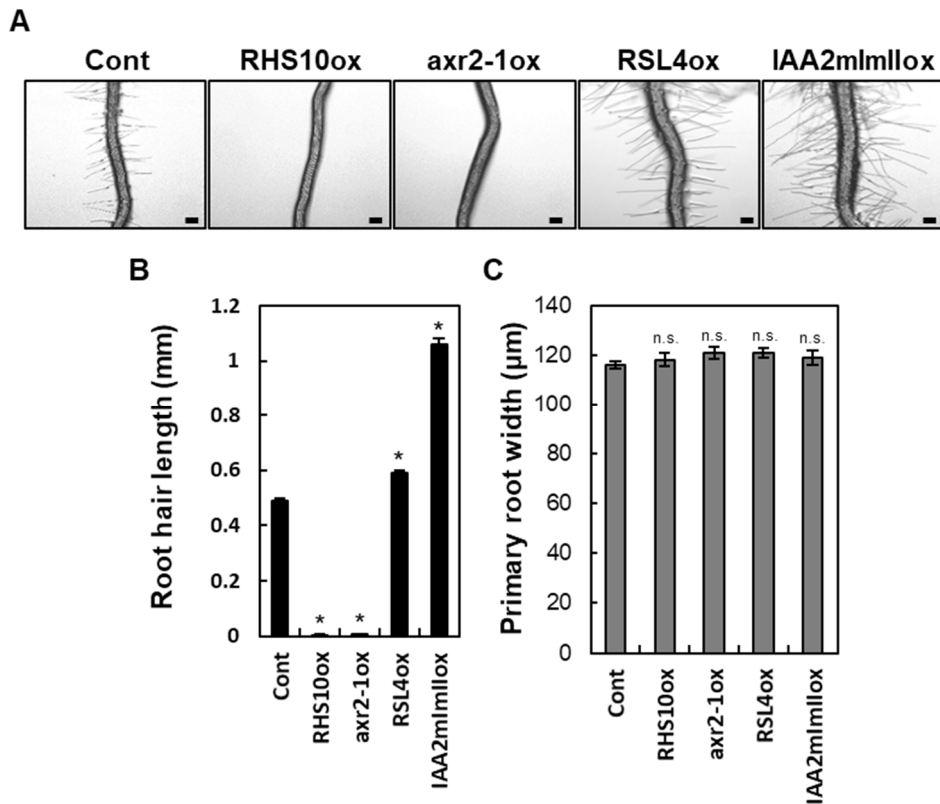


**Figure 61. Root phenotypes of transgenic lines.** (A) Representative root phenotypes of the control (Cont; *ProE7:YFP*) and overexpressed lines-driven promoter *EXPANSIN A7* (*RHS10ox*, *ProE7:RHS10*; *axr2-1ox*, *ProE7:axr2-1*; *RSL4ox*, *ProE7:RSL4*; and *IAA2mImIlox*, *ProE7:IAA2mImII*) in wild-type background growing in MS media at four days after germination. Scale bars are 100  $\mu\text{m}$ . (B) Root hair length of control and overexpressed lines. Error bars indicate  $\pm$  s.e. ( $n = 151\text{--}203$  root hairs from each transgenic line). Asterisks indicate that differences in the value between control and transgenic lines are statistically significant ( $*P < 0.001$ , Student's *t*-test). (C) Primary root width of the control and overexpressed lines. Error bars indicate  $\pm$  s.e. ( $n = 9\text{--}15$  roots from each transgenic line; n.s. indicates that differences in the value between control and transgenic lines are not statistically significant).

(Figure 62). The short- or no-root-hair seedlings of *RHS10ox* and *axr2-1ox* showed water-holding times (an average of ~146.7 sec) that were less than half of those of the long-root-hair seedlings of *RSL4ox* and *IAA2mImIlox* (as average of ~365.9 sec). In particular, the dehydrating speed is similar of all seedlings but the water volume is obviously larger in hairy root seedlings at initial time point. This result indicates that the existence of root hairs is beneficial for retaining water in the root regions. I anticipate that the water-retention ability could sustain the seedlings.

Next, to analyze the soil-holding ability, I rooted up seedlings and measured the weight of the soil attached to the root. In addition, the soil weight was normalized by the primary root length to reduce bias. The soil-holding ability also depends on root hair length. The roots of the *RSL4ox* and *IAA2mImIlox* lines held much more soil than the other lines. The roots of the *RHS10ox*, *axr2-1ox*, and Cont lines sometimes could not hold the soil at all (Figure 63). These results showed that the holding ability of the root was significantly increased by the root hairs.

That much of the soil attached to the hairy roots indicates that the plants also embed into land depending on the root hairs. To investigate the holding ability of seedlings to the soil, I simulated a landslide situation (Figure 64A). I poured 2 liters of water onto the seedlings that were found on sloping land. After two days, I counted the seedlings that were not swept away by the “flood” (Figure 64B). The seedlings of Cont, *RSL4ox*, and *IAA2mImIlox* with the hairy roots survived at rates

of 68.7%, 63.7%, and 78%, respectively. Only 18% and 40% of the seedlings of *RHS10ox* and *axr2-1ox* without root hair remained, respectively. Although the long

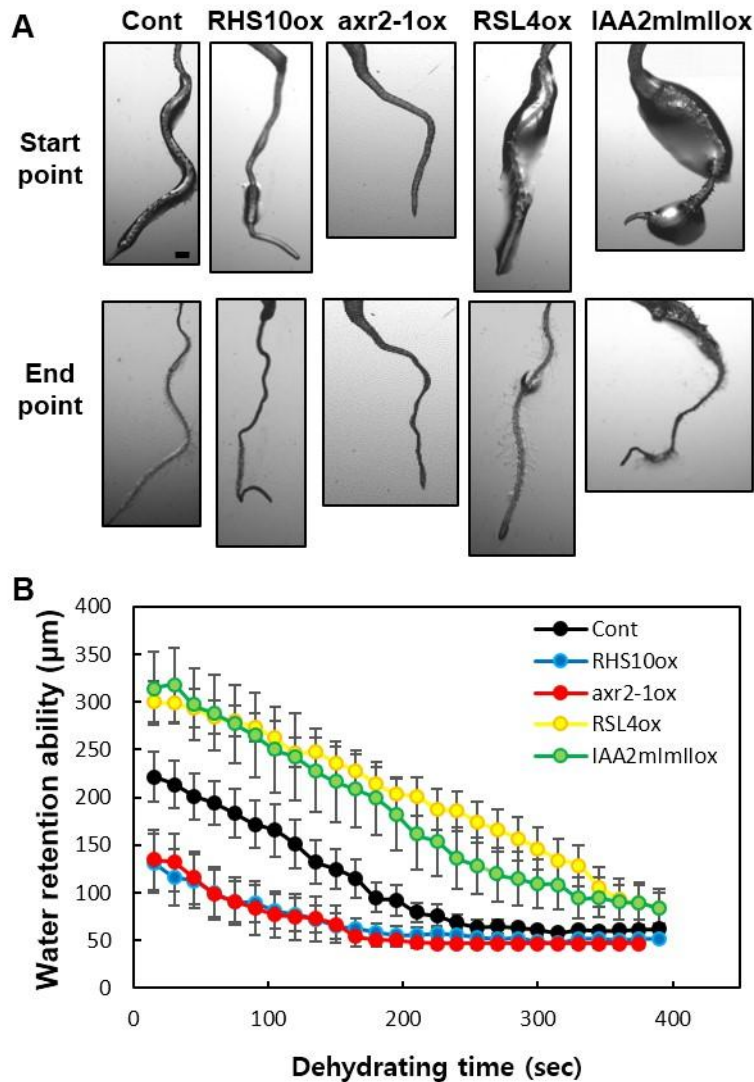


**Figure 62. Seedlings' water retention ability depends on root hair length.** (A) The water-loss root images of Cont, *RHS10ox*, *axr2-1ox*, *RSL4ox*, and *IAA2mlmllox* seedlings pulled off from 0.3% agarose MS media. The start points are right after they were pulled off within 15 s. The end points differ depending on independent lines. Scale bars = 100  $\mu\text{m}$ . (B) The water retention time was measured when the roots were totally dried. (n = 6–17 from each transgenic line).

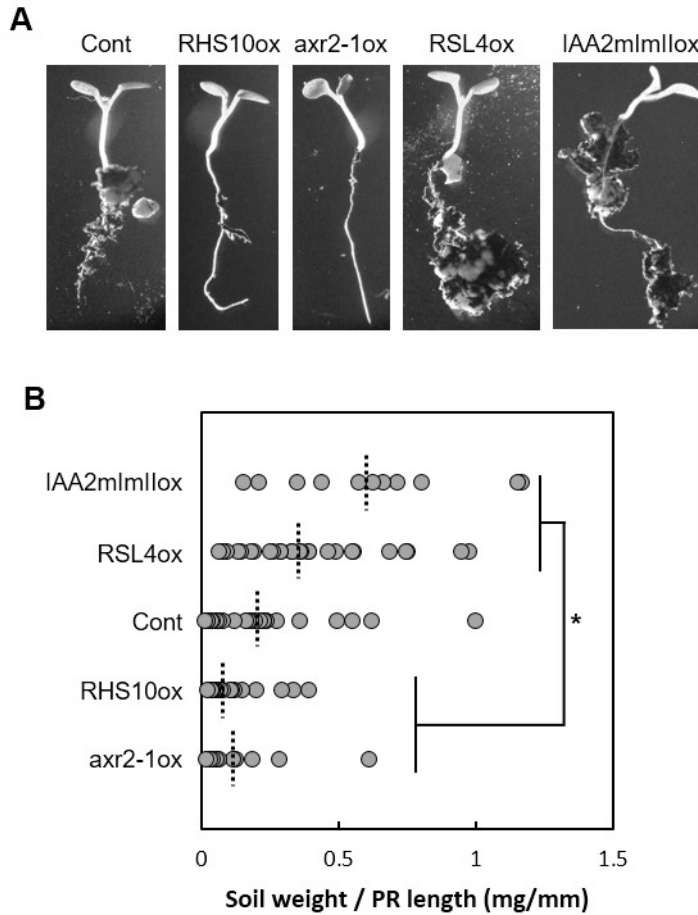


**Figure 63. Soil holding ability of seedlings depends on root hair length.** (A) The images of soil fixed roots of control (Cont, *ProE7:YFP*) and overexpressed lines (*RHS10ox*, *axr2-1ox*, *RSL4ox*, and *IAA2mImIlox*) pulled off from soil at five days after germination. Scale bar is 1 mm. (B) Soil weight per primary root (PR) length of control and transgenic lines. Error bars indicate  $\pm$  s.e. ( $n = 10\text{--}27$  roots from each transgenic line). Dashi lines are mean values. Asterisks indicate where differences in the values between transgenic lines are statistically significant ( $*P < 0.001$ , Student's *t*-test).

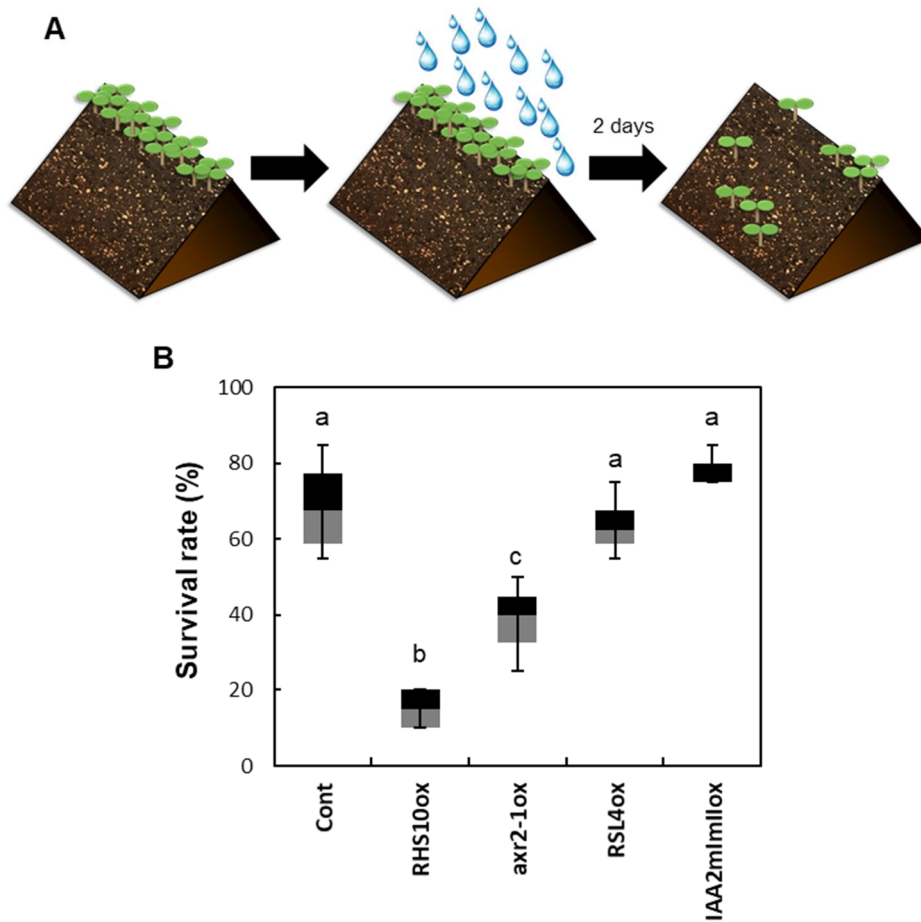


**Figure 64. The survival ratio is high for hairy root lines.** (A) Schematic images of an imitation landslide in a laboratory for analyzing seedlings' soil retention capabilities. I poured water onto four-day-grown seedlings and counted how many seedlings remained after two days. (B) Box-plot of the effect of different root hair lengths on the survival of seedlings in a landslide. Control (Cont, *ProE7:YFP*) and overexpressed lines (*RHS10ox*, *axr2-1ox*, *RSL4ox*, and *IAA2mImIlox*) were counted after the landslide. (Box: interquartile range; whiskers: lower and upper quartiles; boundary lines within boxes: median), [four independent experiments, n = 80 (Cont), 80 (*RHS10ox*), 60 (*axr2-1ox*), 60 80 (*RSL4ox*), and (*IAA2mImIlox*) number of seedlings]. Statistically significant differences are denoted with different letters (one-way ANOVA with Tukey's unequal N-HSD *post hoc* test,  $P < 0.05$ )

hair lines were not superior at survival, the survival ratio of short- or no-root-hair lines showed a sharp decrease. Consistent with the previous results, these data showed that root hair is critical for the survival of seedlings.

The data clearly showed the function of root hair in holding water and soil as a part of the root. The holding ability of root hair may differ depending on the soil type, particle size, and moisture level. Further research that aims to enlarge the effects of root hair will provide information on how plants develop root hair to survive.

## References

- Abel, S., Oeller, P.W., and Theologis, A. (1994). Early auxin-induced genes encode short-lived nuclear proteins. *Proceedings of the National Academy of Sciences of the United States of America* *91*, 326-330.
- Abel, S., and Theologis, A. (1996). Early genes and auxin action. *Plant Physiology* *111*, 9-17.
- Aichinger, E., Villar, C.B., Farrona, S., Reyes, J.C., Hennig, L., and Köhler, C. (2009). CHD3 proteins and polycomb group proteins antagonistically determine cell identity in Arabidopsis. *PLoS genetics* *5*, e1000605.
- Benková, E., Michniewicz, M., Sauer, M., Teichmann, T., Seifertová, D., Jürgens, G., and Friml, J. (2003). Local, efflux-dependent auxin gradients as a common module for plant organ formation. *Cell* *115*, 591-602.
- Bennett, M.J., Marchant, A., Green, H.G., May, S.T., Ward, S.P., Millner, P.A., Walker, A.R., Schulz, B., and Feldmann, K.A. (1996). Arabidopsis AUX1 gene: a permease-like regulator of root gravitropism. *Science* *273*, 948-950.
- Berendzen, K.W., Weiste, C., Wanke, D., Kilian, J., Harter, K., and Dröge-Laser, W. (2012). Bioinformatic cis-element analyses performed in Arabidopsis and rice disclose bZIP-and MYB-related binding sites as potential ARE-coupling elements in auxin-mediated transcription. *BMC plant biology* *12*, 125.
- Bezhani, S., Winter, C., Hershman, S., Wagner, J.D., Kennedy, J.F., Kwon, C.S., Pfluger, J., Su, Y., and Wagner, D. (2007). Unique, shared, and redundant roles for the Arabidopsis SWI/SNF chromatin remodeling ATPases BRAHMA and SPLAYED. *The Plant Cell* *19*, 403-416.
- Blakeslee, J.J., Bandyopadhyay, A., Lee, O.R., Mravec, J., Titapiwatanakun, B., Sauer, M., Makam, S.N., Cheng, Y., Bouchard, R., and Adamec, J. (2007). Interactions among PIN-FORMED and P-glycoprotein auxin transporters in Arabidopsis. *The Plant Cell* *19*, 131-147.
- Boer, D.R., Freire-Rios, A., van den Berg, W.A., Saaki, T., Manfield, I.W., Kepinski, S., Lopez-Vidrieo, I., Franco-Zorrilla, J.M., de Vries, S.C., Solano, R., *et al.* (2014). Structural basis for DNA binding specificity by the auxin-dependent ARF transcription factors. *Cell* *156*, 577-589.
- Brunoud, G., Wells, D.M., Oliva, M., Larrieu, A., Mirabet, V., Burrow, A.H., Beekman, T., Kepinski, S., Traas, J., and Bennett, M.J. (2012). A novel sensor to map auxin response and distribution at high spatio-temporal resolution. *Nature* *482*, 103-106.
- Calderon Villalobos, L.I., Lee, S., De Oliveira, C., Ivetac, A., Brandt, W., Armitage, L., Sheard, L.B., Tan, X., Parry, G., Mao, H., *et al.* (2012). A combinatorial

- TIR1/AFB-Aux/IAA co-receptor system for differential sensing of auxin. *Nature Chemical Biology* 8, 477-485.
- Cambridge, A.P., and Morris, D.A. (1996). Transfer of exogenous auxin from the phloem to the polar auxin transport pathway in pea (*Pisum sativum* L.). *Planta* 199, 583-588.
- Causier, B., Ashworth, M., Guo, W., and Davies, B. (2012a). The TOPLESS interactome: a framework for gene repression in *Arabidopsis*. *Plant Physiol* 158, 423-438.
- Causier, B., Lloyd, J., Stevens, L., and Davies, B. (2012b). TOPLESS co-repressor interactions and their evolutionary conservation in plants. *Plant Signaling Behavior* 7, 325-328.
- Chandler, J.W. (2016). Auxin response factors. *Plant, Cell & Environment* 39, 1014-1028.
- Chapman, E.J., and Estelle, M. (2009). Mechanism of auxin-regulated gene expression in plants. *Annual Review of Genetocs* 43, 265-285.
- Cho, H.-T., and Cosgrove, D.J. (2002). Regulation of root hair initiation and expansin gene expression in *Arabidopsis*. *The Plant Cell* 14, 3237-3253.
- Cho, M., Lee, O.R., Ganguly, A., and Cho, H.T. (2007a). Auxin-signaling: short and long. *Journal of Plant Biology* 50, 79-89.
- Cho, M., Lee, S.H., and Cho, H.T. (2007b). P-glycoprotein4 displays auxin efflux transporter-like action in *Arabidopsis* root hair cells and tobacco cells. *The Plant Cell* 19, 3930-3943.
- Chung, Y., Maharjan, P.M., Lee, O., Fujioka, S., Jang, S., Kim, B., Takatsuto, S., Tsujimoto, M., Kim, H., and Cho, S. (2011). Auxin stimulates DWARF4 expression and brassinosteroid biosynthesis in *Arabidopsis*. *The Plant Journal* 66, 564-578.
- Clapier, C.R., and Cairns, B.R. (2009). The biology of chromatin remodeling complexes. *Annual review of biochemistry* 78, 273-304.
- Clark, D.J., and Felsenfeld, G. (1991). Formation of nucleosomes on positively supercoiled DNA. *The EMBO journal* 10, 387-395.
- Coulon, A., Chow, C.C., Singer, R.H., and Larson, D.R. (2013). Eukaryotic transcriptional dynamics: from single molecules to cell populations. *Nature Reviews Genetocs* 14, 572-584.
- Curtis, M.D., and Grossniklaus, U. (2003). A gateway cloning vector set for high-throughput functional analysis of genes in *planta*. *Plant physiology* 133, 462-469.
- Darwin, C. (1880). The power of movements in plants.
- Datta, S., Prescott, H., and Dolan, L. (2015). Intensity of a pulse of RSL4 transcription factor synthesis determines *Arabidopsis* root hair cell size. *Nature Plants* 1, 15138.
- Davies, P.J. (2010). The plant hormones: their nature, occurrence, and functions. In

- Plant hormones (Springer), pp. 1-15.
- Dharmasiri, N., Dharmasiri, S., and Estelle, M. (2005). The F-box protein TIR1 is an auxin receptor. *Nature* *435*, 441-445.
- Dion, M.F., Kaplan, T., Kim, M., Buratowski, S., Friedman, N., and Rando, O.J. (2007). Dynamics of replication-independent histone turnover in budding yeast. *Science* *315*, 1405-1408.
- Dolan, L., Duckett, C.M., Grierson, C., Linstead, P., Schneider, K., Lawson, E., Dean, C., Poethig, S., and Roberts, K. (1994). CLONAL RELATIONSHIPS AND CELL PATTERNING IN THE ROOT EPIDERMIS OF ARABIDOPSIS. *Development* *120*, 2465-2474.
- Dreher, K.A., Brown, J., Saw, R.E., and Callis, J. (2006). The Arabidopsis Aux/IAA protein family has diversified in degradation and auxin responsiveness. *The Plant Cell* *18*, 699-714.
- Ellis, C.M., Nagpal, P., Young, J.C., Hagen, G., Guilfoyle, T.J., and Reed, J.W. (2005). AUXIN RESPONSE FACTOR1 and AUXIN RESPONSE FACTOR2 regulate senescence and floral organ abscission in Arabidopsis thaliana. *Development* *132*, 4563-4574.
- Finet, C., Berne-Dedieu, A., Scutt, C.P., and Marlétaz, F. (2012). Evolution of the ARF gene family in land plants: old domains, new tricks. *Molecular Biology and Evolution* *30*, 45-56.
- Friml, J., Vieten, A., Sauer, M., Weijers, D., Schwarz, H., Hamann, T., Offringa, R., and Jürgens, G. (2003). Efflux-dependent auxin gradients establish the apical-basal axis of Arabidopsis. *Nature* *426*, 147-153.
- Friml, J., Wiśniewska, J., Benková, E., Mendgen, K., and Palme, K. (2002). Lateral relocation of auxin efflux regulator PIN3 mediates tropism in Arabidopsis. *Nature* *415*, 806-809.
- Fukaki, H., Tameda, S., Masuda, H., and Tasaka, M. (2002). Lateral root formation is blocked by a gain-of-function mutation in the SOLITARY-ROOT/IAA14 gene of Arabidopsis. *The Plant Journal* *29*, 153-168.
- Galinha, C., Hofhuis, H., Luijten, M., Willemsen, V., Blilou, I., Heidstra, R., and Scheres, B. (2007). PLETHORA proteins as dose-dependent master regulators of Arabidopsis root development. *Nature* *449*, 1053.
- Gallavotti, A., Long, J.A., Stanfield, S., Yang, X., Jackson, D., Vollbrecht, E., and Schmidt, R.J. (2010). The control of axillary meristem fate in the maize ramosa pathway. *Development* *137*, 2849-2856.
- Galway, M.E., Masucci, J.D., Lloyd, A.M., Walbot, V., Davis, R.W., and Schiefelbein, J.W. (1994). The TTG gene is required to specify epidermal cell fate and cell patterning in the Arabidopsis root. *Developmental biology* *166*, 740-754.
- Ganguly, A., Lee, S.H., and Cho, H.T. (2012). Functional identification of the

- phosphorylation sites of Arabidopsis PIN-FORMED3 for its subcellular localization and biological role. *The Plant Journal* *71*, 810-823.
- Ganguly, A., Lee, S.H., Cho, M., Lee, O.R., Yoo, H., and Cho, H.-T. (2010). Differential auxin-transporting activities of PIN-FORMED proteins in Arabidopsis root hair cells. *Plant physiology* *153*, 1046-1061.
- Gaudinier, A., and Brady, S.M. (2016). Mapping Transcriptional Networks in Plants: Data-Driven Discovery of Novel Biological Mechanisms. *Annual Review of Plant Biology* *67*, 575-594.
- Geisler, M., Blakeslee, J.J., Bouchard, R., Lee, O.R., Vincenzetti, V., Bandyopadhyay, A., Titapiwatanakun, B., Peer, W.A., Bailly, A., and Richards, E.L. (2005). Cellular efflux of auxin catalyzed by the Arabidopsis MDR/PGP transporter AtPGP1. *The Plant Journal* *44*, 179-194.
- Ghaemmaghami, S., Huh, W.-K., Bower, K., Howson, R.W., Belle, A., Dephoure, N., O'shea, E.K., and Weissman, J.S. (2003). Global analysis of protein expression in yeast. *Nature* *425*, 737.
- Gilkerson, J., Hu, J., Brown, J., Jones, A., Sun, T.-p., and Callis, J. (2009). Isolation and characterization of cull-7, a recessive allele of CULLIN1 that disrupts SCF function at the C terminus of CUL1 in Arabidopsis thaliana. *Genetics* *181*, 945-963.
- Gilroy, S., and Jones, D.L. (2000). Through form to function: root hair development and nutrient uptake. *Trends in plant science* *5*, 56-60.
- Goda, H., Sasaki, E., Akiyama, K., Maruyama-Nakashita, A., Nakabayashi, K., Li, W., Ogawa, M., Yamauchi, Y., Preston, J., Aoki, K., *et al.* (2008). The AtGenExpress hormone and chemical treatment data set: experimental design, data evaluation, model data analysis and data access. *The Plant Journal* *55*, 526-542.
- Goda, H., Sawa, S., Asami, T., Fujioka, S., Shimada, Y., and Yoshida, S. (2004). Comprehensive comparison of auxin-regulated and brassinosteroid-regulated genes in Arabidopsis. *Plant physiology* *134*, 1555-1573.
- Gray, S., and Levine, M. (1996). Short-range transcriptional repressors mediate both quenching and direct repression within complex loci in Drosophila. *Genes & development* *10*, 700-710.
- Gray, W.M. (2004). Hormonal regulation of plant growth and development. *PLOS Biology* *2*, E311.
- Gray, W.M., del Pozo, J.C., Walker, L., Hobbie, L., Risseuw, E., Banks, T., Crosby, W.L., Yang, M., Ma, H., and Estelle, M. (1999). Identification of an SCF ubiquitin–ligase complex required for auxin response in Arabidopsis thaliana. *Genes & development* *13*, 1678-1691.
- Gray, W.M., Hellmann, H., Dharmasiri, S., and Estelle, M. (2002). Role of the Arabidopsis RING-H2 protein RBX1 in RUB modification and SCF function.

- The Plant Cell *14*, 2137-2144.
- Gray, W.M., Kepinski, S., Rouse, D., Leyser, O., and Estelle, M. (2001). Auxin regulates SCF TIR1-dependent degradation of AUX/IAA proteins. *Nature* *414*, 271-276.
- Greenham, K., Santner, A., Castillejo, C., Mooney, S., Sairanen, I., Ljung, K., and Estelle, M. (2011). RETRACTED: the AFB4 auxin receptor is a negative regulator of auxin signaling in seedlings (Elsevier).
- Grierson, C., and Schiefelbein, J. (2008). Genetics of root hair formation.
- Guilfoyle, T.J., and Hagen, G. (2001). Auxin Response Factors. *Journal of Plant Growth Regulation* *20*, 281-291.
- Guilfoyle, T.J., and Hagen, G. (2007). Auxin response factors. *Current Opinion in Plant Biology* *10*, 453-460.
- Guilfoyle, T.J., and Hagen, G. (2012). Getting a grasp on domain III/IV responsible for Auxin Response Factor-IAA protein interactions. *Plant Science* *190*, 82-88.
- Han, M., Park, Y., Kim, I., Kim, E.H., Yu, T.K., Rhee, S., and Suh, J.Y. (2014). Structural basis for the auxin-induced transcriptional regulation by Aux/IAA17. *Proceedings of the National Academy of Sciences of the United States of America* *111*, 18613-18618.
- Harrison, M.R., Georgiou, A.S., Spink, H.P., and Cunliffe, V.T. (2011). The epigenetic regulator Histone Deacetylase 1 promotes transcription of a core neurogenic programme in zebrafish embryos. *BMC genomics* *12*, 24.
- Hwang, Y., Choi, H.-S., Cho, H.-M., and Cho, H.-T. (2017). Tracheophytes contain conserved orthologs of a basic helix-loop-helix transcription factor that modulate ROOT HAIR SPECIFIC genes. *The Plant Cell* *29*, 39-53.
- Hwang, Y., Lee, H., Lee, Y.-S., and Cho, H.-T. (2016). Cell wall-associated ROOT HAIR SPECIFIC 10, a proline-rich receptor-like kinase, is a negative modulator of Arabidopsis root hair growth. *Journal of experimental botany* *67*, 2007-2022.
- Ikeda, M., and Ohme-Takagi, M. (2009). A novel group of transcriptional repressors in Arabidopsis. *Plant Cell Physiol* *50*, 970-975.
- Johnson, A.D. (1995). The price of repression. *Cell* *81*, 655-658.
- Jungk, A. (2001). Root hairs and the acquisition of plant nutrients from soil. *Journal of Plant Nutrition and Soil Science* *164*, 121-129.
- Kagale, S., Links, M.G., and Rozwadowski, K. (2010). Genome-wide analysis of ethylene-responsive element binding factor-associated amphiphilic repression motif-containing transcriptional regulators in Arabidopsis. *Plant Physiology* *152*, 1109-1134.
- Kato, H., Ishizaki, K., Kouno, M., Shirakawa, M., Bowman, J.L., Nishihama, R., and Kohchi, T. (2015). Auxin-mediated transcriptional system with a minimal set of components is critical for morphogenesis through the life cycle in *Marchantia polymorpha*. *PLoS genetics* *11*, e1005084.

- Kaufmann, K., Pajoro, A., and Angenent, G.C. (2010). Regulation of transcription in plants: mechanisms controlling developmental switches. *Nature Reviews Genetics* *11*, 830-842.
- Ke, J.Y., Ma, H.L., Gu, X., Thelen, A., Brunzelle, J.S., Li, J.Y., Xu, H.E., and Melcher, K. (2015). Structural basis for recognition of diverse transcriptional repressors by the TOPLESS family of corepressors. *Science Advances* *1*.
- Kepinski, S., and Leyser, O. (2005). The Arabidopsis F-box protein TIR1 is an auxin receptor. *Nature* *435*, 446-451.
- Kieffer, M., Stern, Y., Cook, H., Clerici, E., Maulbetsch, C., Laux, T., and Davies, B. (2006). Analysis of the transcription factor WUSCHEL and its functional homologue in *Antirrhinum* reveals a potential mechanism for their roles in meristem maintenance. *The Plant Cell* *18*, 560-573.
- Kim, D.W., Lee, S.H., Choi, S.-B., Won, S.-K., Heo, Y.-K., Cho, M., Park, Y.-I., and Cho, H.-T. (2006). Functional conservation of a root hair cell-specific cis-element in angiosperms with different root hair distribution patterns. *The Plant Cell* *18*, 2958-2970.
- Knox, K., Grierson, C.S., and Leyser, O. (2003). AXR3 and SHY2 interact to regulate root hair development. *Development* *130*, 5769-5777.
- Korasick, D.A., Westfall, C.S., Lee, S.G., Nanao, M.H., Dumas, R., Hagen, G., Guilfoyle, T.J., Jez, J.M., and Strader, L.C. (2014). Molecular basis for AUXIN RESPONSE FACTOR protein interaction and the control of auxin response repression. *Proceedings of the National Academy of Sciences of the United States of America* *111*, 5427-5432.
- Krogan, N.T., Marcos, D., Weiner, A.I., and Berleth, T. (2016). The auxin response factor MONOPTEROS controls meristem function and organogenesis in both the shoot and root through the direct regulation of PIN genes. *New Phytologist* *212*, 42-50.
- Lavy, M., Prigge, M.J., Tao, S., Shain, S., Kuo, A., Kirchsteiger, K., and Estelle, M. (2016). Constitutive auxin response in *Physcomitrella* reveals complex interactions between Aux/IAA and ARF proteins. *Elife* *5*.
- Lee, D.J., Park, J.W., Lee, H.W., and Kim, J. (2009). Genome-wide analysis of the auxin-responsive transcriptome downstream of *iaa1* and its expression analysis reveal the diversity and complexity of auxin-regulated gene expression. *Journal of experimental botany* *60*, 3935-3957.
- Lee, M.-S., An, J.-H., and Cho, H.-T. (2016). Biological and molecular functions of two EAR motifs of Arabidopsis IAA7. *Journal of plant biology* *59*, 24-32.
- Lee, N., Park, J., Kim, K., and Choi, G. (2015). The transcriptional coregulator LEUNIG\_HOMOLOG inhibits light-dependent seed germination in Arabidopsis. *The Plant Cell* *27*, 2301-2313.
- Lee, O.R., Kim, S.J., Kim, H.J., Hong, J.K., Ryu, S.B., Lee, S.H., Ganguly, A., and

- Cho, H.-T. (2010). Phospholipase A2 is required for PIN-FORMED protein trafficking to the plasma membrane in the Arabidopsis root. *The Plant Cell* *22*, 1812-1825.
- Lee, S.H., and Cho, H.-T. (2006). PINOID positively regulates auxin efflux in Arabidopsis root hair cells and tobacco cells. *The Plant Cell* *18*, 1604-1616.
- Leopold, A.C. (1955). *Auxins and plant growth* (Univ of California Press).
- Leyser, H., Pickett, F.B., Dharmasiri, S., and Estelle, M. (1996). Mutations in the AXR3 gene of Arabidopsis result in altered auxin response including ectopic expression from the SAUR-AC1 promoter. *The Plant Journal* *10*, 403-413.
- Li, H., Johnson, P., Stepanova, A., Alonso, J.M., and Ecker, J.R. (2004b). Convergence of signaling pathways in the control of differential cell growth in Arabidopsis. *Developmental cell* *7*, 193-204.
- Liao, C.-Y., Smet, W., Brunoud, G., Yoshida, S., Vernoux, T., and Weijers, D. (2015). Reporters for sensitive and quantitative measurement of auxin response. *Nature methods* *12*, 207-210.
- Libault, M., Tessadori, F., Germann, S., Snijder, B., Fransz, P., and Gaudin, V. (2005). The Arabidopsis LHP1 protein is a component of euchromatin. *Planta* *222*, 910-925.
- Licht, J.D., Grossel, M.J., Figge, J., and Hansen, U.M. (1990). Drosophila Krüppel protein is a transcriptional repressor. *Nature* *346*, 76-79.
- Lim, P.O., Lee, I.C., Kim, J., Kim, H.J., Ryu, J.S., Woo, H.R., and Nam, H.G. (2010). Auxin response factor 2 (ARF2) plays a major role in regulating auxin-mediated leaf longevity. *Journal of Experiment Botany* *61*, 1419-1430.
- Lin, C., Choi, H.-S., and Cho, H.-T. (2011). Root hair-specific EXPANSIN A7 is required for root hair elongation in Arabidopsis. *Molecules and cells* *31*, 393-397.
- Liu, Z.-B., Ulmasov, T., Shi, X., Hagen, G., and Guilfoyle, T.J. (1994). Soybean GH3 promoter contains multiple auxin-inducible elements. *The Plant Cell* *6*, 645-657.
- Lloyd, A., Schena, M., Walbot, V., and Davis, R. (1994). Epidermal cell fate determination in Arabidopsis: patterns defined by a steroid-inducible regulator. *Science* *266*, 436-439.
- Lokerse, A.S., and Weijers, D. (2009). Auxin enters the matrix--assembly of response machineries for specific outputs. *Current Opinion in Plant Biology* *12*, 520-526.
- Lu, P., Vogel, C., Wang, R., Yao, X., and Marcotte, E.M. (2007). Absolute protein expression profiling estimates the relative contributions of transcriptional and translational regulation. *Nature biotechnology* *25*, 117-124.
- Luschnig, C., Gaxiola, R.A., Grisafi, P., and Fink, G.R. (1998). EIR1, a root-specific protein involved in auxin transport, is required for gravitropism in Arabidopsis thaliana. *Genes & development* *12*, 2175-2187.

- Makarevich, G., Leroy, O., Akinci, U., Schubert, D., Clarenz, O., Goodrich, J., Grossniklaus, U., and Kohler, C. (2006). Different Polycomb group complexes regulate common target genes in Arabidopsis. *EMBO Reports* 7, 947-952.
- Mangano, S., Denita-Juarez, S.P., Choi, H.-S., Marzol, E., Hwang, Y., Ranocha, P., Velasquez, S.M., Borassi, C., Barberini, M.L., and Apteckmann, A.A. (2017). Molecular link between auxin and ROS-mediated polar growth. *Proceedings of the National Academy of Sciences*, 114, 5289-5294..
- Masucci, J.D., and Schiefelbein, J.W. (1994). The *rhd6* mutation of Arabidopsis thaliana alters root-hair initiation through an auxin-and ethylene-associated process. *Plant Physiology* 106, 1335-1346.
- Masucci, J.D., and Schiefelbein, J.W. (1996). Hormones act downstream of TTG and GL2 to promote root hair outgrowth during epidermis development in the Arabidopsis root. *The Plant Cell* 8, 1505-1517.
- Mattsson, J., Ckurshumova, W., and Berleth, T. (2003). Auxin signaling in Arabidopsis leaf vascular development. *Plant Physiology* 131, 1327-1339.
- McNally, J.G., Muller, W.G., Walker, D., Wolford, R., and Hager, G.L. (2000). The glucocorticoid receptor: rapid exchange with regulatory sites in living cells. *Science* 287, 1262-1265.
- Menand, B., Yi, K., Jouannic, S., Hoffmann, L., Ryan, E., Linstead, P., Schaefer, D.G., and Dolan, L. (2007). An ancient mechanism controls the development of cells with a rooting function in land plants. *Science* 316, 1477-1480.
- Mironova, V.V., Omelyanchuk, N.A., Wiebe, D.S., and Levitsky, V.G. (2014). Computational analysis of auxin responsive elements in the Arabidopsis thaliana L. genome. *BMC genomics* 15, S4.
- Mitchell, R.L., Cuadros, J., Duckett, J.G., Pressel, S., Mavris, C., Sykes, D., Najorka, J., Edgecombe, G.D., and Kenrick, P. (2016). Mineral weathering and soil development in the earliest land plant ecosystems. *Geology* 44, 1007-1010.
- Mockaitis, K., and Estelle, M. (2008). Auxin receptors and plant development: a new signaling paradigm. *Annual Review of Cell and Developmental Biology* 24, 55-80.
- Moss, B.L., Mao, H., Guseman, J.M., Hinds, T.R., Hellmuth, A., Kovenock, M., Noorassa, A., Lanctot, A., Villalobos, L.I., Zheng, N., *et al.* (2015). Rate Motifs Tune Auxin/Indole-3-Acetic Acid Degradation Dynamics. *Plant Physiology* 169, 803-813.
- Muto, H., Watahiki, M.K., Nakamoto, D., Kinjo, M., and Yamamoto, K.T. (2007). Specificity and similarity of functions of the Aux/IAA genes in auxin signaling of Arabidopsis revealed by promoter-exchange experiments among MSG2/IAA19, AXR2/IAA7, and SLR/IAA14. *Plant physiology* 144, 187-196.
- Nagpal, P., Walker, L.M., Young, J.C., Sonawala, A., Timpote, C., Estelle, M., and Reed, J.W. (2000). AXR2 encodes a member of the Aux/IAA protein family.

- Plant physiology *123*, 563-574.
- Nakahigashi, K., Jasencakova, Z., Schubert, I., and Goto, K. (2005). The Arabidopsis heterochromatin protein1 homolog (TERMINAL FLOWER2) silences genes within the euchromatic region but not genes positioned in heterochromatin. *Plant and cell physiology* *46*, 1747-1756.
- Nemhauser, J.L., Hong, F., and Chory, J. (2006). Different plant hormones regulate similar processes through largely nonoverlapping transcriptional responses. *Cell* *126*, 467-475.
- Nemhauser, J.L., Mockler, T.C., and Chory, J. (2004). Interdependency of brassinosteroid and auxin signaling in Arabidopsis. *PLoS biology* *2*, e258.
- O'Malley, R.C., Huang, S.C., Song, L., Lewsey, M.G., Bartlett, A., Nery, J.R., Galli, M., Gallavotti, A., and Ecker, J.R. (2016). Cistrome and Epicistrome Features Shape the Regulatory DNA Landscape. *Cell* *165*, 1280-1292.
- Oh, E., Kang, H., Yamaguchi, S., Park, J., Lee, D., Kamiya, Y., and Choi, G. (2009). Genome-wide analysis of genes targeted by PHYTOCHROME INTERACTING FACTOR 3-LIKE5 during seed germination in Arabidopsis. *The Plant Cell* *21*, 403-419.
- Oh, E., Zhu, J.-Y., Bai, M.-Y., Arenhart, R.A., Sun, Y., and Wang, Z.-Y. (2014). Cell elongation is regulated through a central circuit of interacting transcription factors in the Arabidopsis hypocotyl. *Elife* *3*.
- Ohta, M., Matsui, K., Hiratsu, K., Shinshi, H., and Ohme-Takagi, M. (2001). Repression domains of class II ERF transcriptional repressors share an essential motif for active repression. *The Plant Cell* *13*, 1959-1968.
- Okushima, Y., Mitina, I., Quach, H.L., and Theologis, A. (2005a). AUXIN RESPONSE FACTOR 2 (ARF2): a pleiotropic developmental regulator. *The Plant Journal* *43*, 29-46.
- Okushima, Y., Overvoorde, P.J., Arima, K., Alonso, J.M., Chan, A., Chang, C., Ecker, J.R., Hughes, B., Lui, A., Nguyen, D., *et al.* (2005b). Functional genomic analysis of the AUXIN RESPONSE FACTOR gene family members in Arabidopsis thaliana: unique and overlapping functions of ARF7 and ARF19. *The Plant Cell* *17*, 444-463.
- Paponov, I.A., Paponov, M., Teale, W., Menges, M., Chakrabortee, S., Murray, J.A.H., and Palme, K. (2008). Comprehensive transcriptome analysis of auxin responses in Arabidopsis. *Molecular Plant* *1*, 321-337.
- Paponov, I.A., Teale, W., Lang, D., Paponov, M., Reski, R., Rensing, S.A., and Palme, K. (2009). The evolution of nuclear auxin signalling. *BMC Evolutionary Biology* *9*, 126.
- Park, J.Y., Kim, H.J., and Kim, J. (2002). Mutation in domain II of IAA1 confers diverse auxin-related phenotypes and represses auxin-activated expression of Aux/IAA genes in steroid regulator-inducible system. *The Plant Journal* *32*,

669-683.

- Pauwels, L., Barbero, G.F., Geerinck, J., Tilleman, S., Grunewald, W., Pérez, A.C., Chico, J.M., Bossche, R.V., Sewell, J., and Gil, E. (2010). NINJA connects the co-repressor TOPLLESS to jasmonate signalling. *Nature* *464*, 788-791.
- Payankulam, S., Li, L.M., and Arnosti, D.N. (2010). Transcriptional repression: conserved and evolved features. *Current Biology* *20*, R764-771.
- Peterson, R.L., and Farquhar, M.L. (1996). Root hairs: specialized tubular cells extending root surfaces. *The Botanical Review* *62*, 1-40.
- Petrasek, J., Mravec, J., Bouchard, R., Blakeslee, J.J., Abas, M., Seifertova, D., Wisniewska, J., Tadele, Z., Kubes, M., Covanova, M., *et al.* (2006). PIN proteins perform a rate-limiting function in cellular auxin efflux. *Science* *312*, 914-918.
- Pfluger, J., and Wagner, D. (2007). Histone modifications and dynamic regulation of genome accessibility in plants. *Current Opinion in Plant Biology* *10*, 645-652.
- Pires, N.D., Yi, K., Breuninger, H., Catarino, B., Menand, B., and Dolan, L. (2013). Recruitment and remodeling of an ancient gene regulatory network during land plant evolution. *Proceedings of the National Academy of Sciences of the United States of America* *110*, 9571-9576.
- Pitts, R.J., Cernac, A., and Estelle, M. (1998). Auxin and ethylene promote root hair elongation in Arabidopsis. *The Plant Journal* *16*, 553-560.
- Piya, S., Shrestha, S.K., Binder, B., Stewart, C.N., Jr., and Hewezi, T. (2014). Protein-protein interaction and gene co-expression maps of ARFs and Aux/IAAs in Arabidopsis. *Frontiers in Plant Science* *5*, 744.
- Ploense, S.E., Wu, M.F., Nagpal, P., and Reed, J.W. (2009). A gain-of-function mutation in IAA18 alters Arabidopsis embryonic apical patterning. *Development* *136*, 1509-1517.
- Rademacher, E.H., Lokerse, A.S., Schlereth, A., Llavata-Peris, C.I., Bayer, M., Kientz, M., Rios, A.F., Borst, J.W., Lukowitz, W., and Jürgens, G. (2012). Different auxin response machineries control distinct cell fates in the early plant embryo. *Developmental cell* *22*, 211-222.
- Rademacher, E.H., Möller, B., Lokerse, A.S., Llavata-Peris, C.I., van den Berg, W., and Weijers, D. (2011). A cellular expression map of the Arabidopsis AUXIN RESPONSE FACTOR gene family. *The Plant Journal* *68*, 597-606.
- Ramos, J.A., Zenser, N., Leyser, O., and Callis, J. (2001). Rapid degradation of auxin/indoleacetic acid proteins requires conserved amino acids of domain II and is proteasome dependent. *The Plant Cell* *13*, 2349-2360.
- Reed, J.W. (2001). Roles and activities of Aux/IAA proteins in Arabidopsis. *Trends in plant science* *6*, 420-425.
- Reinhardt, D., Mandel, T., and Kuhlemeier, C. (2000). Auxin regulates the initiation and radial position of plant lateral organs. *The Plant Cell* *12*, 507-518.
- Reinhardt, D., Pesce, E.-R., Stieger, P., Mandel, T., Baltensperger, K., Bennett, M.,

- Traas, J., Friml, J., and Kuhlemeier, C. (2003). Regulation of phyllotaxis by polar auxin transport. *Nature* *426*, 255-260.
- Reynolds, N., O'Shaughnessy, A., and Hendrich, B. (2013). Transcriptional repressors: multifaceted regulators of gene expression. *Development* *140*, 505-512.
- Richter, R., Behringer, C., Zourelidou, M., and Schwechheimer, C. (2013). Convergence of auxin and gibberellin signaling on the regulation of the GATA transcription factors GNC and GNL in *Arabidopsis thaliana*. *Proceedings of the National Academy of Sciences of the United States of America* *110*, 13192-13197.
- Rogg, L.E., Lasswell, J., and Bartel, B. (2001). A gain-of-function mutation in IAA28 suppresses lateral root development. *The Plant Cell* *13*, 465-480.
- Rouse, D., Mackay, P., Stirnberg, P., Estelle, M., and Leyser, O. (1998). Changes in auxin response from mutations in an AUX/IAA gene. *Science* *279*, 1371-1373.
- Ryu, H., Cho, H., Bae, W., and Hwang, I. (2014). Control of early seedling development by BES1/TPL/HDA19-mediated epigenetic regulation of ABI3. *Nature Communication* *5*, 4138.
- Sachs, T. (1981). The control of the patterned differentiation of vascular tissues. In *Advances in botanical research* (Elsevier), pp. 151-262.
- Salehin, M., Bagchi, R., and Estelle, M. (2015). SCFTIR1/AFB-based auxin perception: mechanism and role in plant growth and development. *The Plant Cell* *27*, 9-19.
- Sauer, F., Fondell, J.D., Ohkuma, Y., Roeder, R.G., and Jäckle, H. (1995). Control of transcription by Krüppel through interactions with TFIIB and TFIIE $\beta$ . *Nature* *375*, 162-164.
- Sauer, F., and Jäckle, H. (1993). Dimerization and the control of transcription by Krüppel. *Nature* *364*, 454.
- Scacchi, E., Salinas, P., Gujas, B., Santuari, L., Krogan, N., Ragni, L., Berleth, T., and Hardtke, C.S. (2010). Spatio-temporal sequence of cross-regulatory events in root meristem growth. *Proceedings of the National Academy of Sciences* *107*, 22734-22739.
- Schena, M., Lloyd, A.M., and Davis, R.W. (1991). A steroid-inducible gene expression system for plant cells. *Proceedings of the National Academy of Sciences* *88*, 10421-10425.
- Schermer, U.J., Korber, P., and Horz, W. (2005). Histones are incorporated in trans during reassembly of the yeast PHO5 promoter. *Molecular Cell* *19*, 279-285.
- Schruff, M.C., Spielman, M., Tiwari, S., Adams, S., Fenby, N., and Scott, R.J. (2006). The AUXIN RESPONSE FACTOR 2 gene of *Arabidopsis* links auxin signalling, cell division, and the size of seeds and other organs. *Development* *133*, 251-261.

- Schubert, D., Primavesi, L., Bishopp, A., Roberts, G., Doonan, J., Jenuwein, T., and Goodrich, J. (2006). Silencing by plant Polycomb-group genes requires dispersed trimethylation of histone H3 at lysine 27. *The EMBO Journal* 25, 4638-4649.
- Shin, R., Burch, A.Y., Huppert, K.A., Tiwari, S.B., Murphy, A.S., Guilfoyle, T.J., and Schachtman, D.P. (2007). The Arabidopsis transcription factor MYB77 modulates auxin signal transduction. *The Plant Cell* 19, 2440-2453.
- Smyth, D.R., Bowman, J.L., and Meyerowitz, E.M. (1990). Early flower development in Arabidopsis. *The Plant Cell* 2, 755-767.
- Soh, M.S., Hong, S.H., Kim, B.C., Vizir, I., Park, D.H., Choi, G., Hong, M.Y., Chung, Y.-Y., Furuya, M., and Nam, H.G. (1999). Regulation of both light-and auxin-mediated development by the Arabidopsis IAA3/SHY2 gene. *Journal of Plant Biology* 42, 239.
- Szemenyei, H., Hannon, M., and Long, J.A. (2008). TOPLESS mediates auxin-dependent transcriptional repression during Arabidopsis embryogenesis. *Science* 319, 1384-1386.
- Tan, X., Calderon-Villalobos, L.I.A., Sharon, M., Zheng, C., Robinson, C.V., Estelle, M., and Zheng, N. (2007). Mechanism of auxin perception by the TIR1 ubiquitin ligase. *Nature* 446, 640-645.
- Tanaka, H., Dhonukshe, P., Brewer, P.B., and Friml, J. (2006). Spatiotemporal asymmetric auxin distribution: a means to coordinate plant development. *Cellular and Molecular Life Science* 63, 2738-2754.
- Tatematsu, K., Kumagai, S., Muto, H., Sato, A., Watahiki, M.K., Harper, R.M., Liscum, E., and Yamamoto, K.T. (2004). MASSUGU2 encodes Aux/IAA19, an auxin-regulated protein that functions together with the transcriptional activator NPH4/ARF7 to regulate differential growth responses of hypocotyl and formation of lateral roots in Arabidopsis thaliana. *Plant Cell* 16, 379-393.
- Tian, Q., and Reed, J.W. (1999). Control of auxin-regulated root development by the Arabidopsis thaliana SHY2/IAA3 gene. *Development* 126, 711-721.
- Tiwari, S.B., Hagen, G., and Guilfoyle, T. (2003). The roles of auxin response factor domains in auxin-responsive transcription. *Plant Cell* 15, 533-543.
- Tiwari, S.B., Hagen, G., and Guilfoyle, T.J. (2004). Aux/IAA proteins contain a potent transcriptional repression domain. *The Plant Cell* 16, 533-543.
- Tiwari, S.B., Wang, X.-J., Hagen, G., and Guilfoyle, T.J. (2001). AUX/IAA proteins are active repressors, and their stability and activity are modulated by auxin. *The Plant Cell* 13, 2809-2822.
- Turck, F., Roudier, F., Farrona, S., Martin-Magniette, M.L., Guillaume, E., Buisine, N., Gagnot, S., Martienssen, R.A., Coupland, G., and Colot, V. (2007). Arabidopsis TFL2/LHP1 specifically associates with genes marked by trimethylation of histone H3 lysine 27. *PLOS Genetics* 3, e86.

- Ulmasov, T., Hagen, G., and Guilfoyle, T.J. (1997a). ARF1, a transcription factor that binds to auxin response elements. *Science* 276, 1865-1868.
- Ulmasov, T., Hagen, G., and Guilfoyle, T.J. (1999). Activation and repression of transcription by auxin-response factors. *Proceedings of the National Academy of Sciences* 96, 5844-5849.
- Ulmasov, T., Liu, Z.-B., Hagen, G., and Guilfoyle, T.J. (1995). Composite structure of auxin response elements. *The Plant Cell* 7, 1611-1623.
- Ulmasov, T., Murfett, J., Hagen, G., and Guilfoyle, T.J. (1997b). Aux/IAA proteins repress expression of reporter genes containing natural and highly active synthetic auxin response elements. *The Plant Cell* 9, 1963-1971.
- Varaud, E., Brioudes, F., Szécsi, J., Leroux, J., Brown, S., Perrot-Rechenmann, C., and Bendahmane, M. (2011). AUXIN RESPONSE FACTOR8 regulates Arabidopsis petal growth by interacting with the bHLH transcription factor BIGPETALp. *The Plant Cell* 23, 973-983.
- Vernoux, T., Brunoud, G., Farcot, E., Morin, V., Van den Daele, H., Legrand, J., Oliva, M., Das, P., Larrieu, A., Wells, D., *et al.* (2011). The auxin signalling network translates dynamic input into robust patterning at the shoot apex. *Molecular Systems Biology* 7, 508.
- Vijayakumar, P., Datta, S., and Dolan, L. (2016). ROOT HAIR DEFECTIVE SIX□ LIKE4 (RSL4) promotes root hair elongation by transcriptionally regulating the expression of genes required for cell growth. *New Phytologist* 212, 944-953.
- Wang, L., Hua, D., He, J., Duan, Y., Chen, Z., Hong, X., and Gong, Z. (2011). Auxin Response Factor2 (ARF2) and its regulated homeodomain gene HB33 mediate abscisic acid response in Arabidopsis. *PLOS Genetics* 7, e1002172.
- Wang, L., Kim, J., and Somers, D.E. (2013). Transcriptional corepressor TOPLESS complexes with pseudoresponse regulator proteins and histone deacetylases to regulate circadian transcription. *Proceedings of the National Academy of Sciences of the United States of America* 110, 761-766.
- Weijers, D., Benkova, E., Jäger, K.E., Schlereth, A., Hamann, T., Kientz, M., Wilmoth, J.C., Reed, J.W., and Jürgens, G. (2005). Developmental specificity of auxin response by pairs of ARF and Aux/IAA transcriptional regulators. *The EMBO journal* 24, 1874-1885.
- Weijers, D., and Wagner, D. (2016). Transcriptional Responses to the Auxin Hormone. *Annual Review Plant Biology* 67, 539-574.
- Wenzel, C.L., Schuetz, M., Yu, Q., and Mattsson, J. (2007). Dynamics of MONOPTEROS and PIN-FORMED1 expression during leaf vein pattern formation in Arabidopsis thaliana. *The Plant Journal* 49, 387-398.
- Wilson, A.K., Pickett, F.B., Turner, J.C., and Estelle, M. (1990). A dominant mutation in Arabidopsis confers resistance to auxin, ethylene and abscisic acid. *Molecular & General Genetics MGG* 222, 377-383.

- Won, S.-K., Lee, Y.-J., Lee, H.-Y., Heo, Y.-K., Cho, M., and Cho, H.-T. (2009). Cis-element-and transcriptome-based screening of root hair-specific genes and their functional characterization in *Arabidopsis*. *Plant physiology* *150*, 1459-1473.
- Wu, M.-F., Yamaguchi, N., Xiao, J., Bargmann, B., Estelle, M., Sang, Y., and Wagner, D. (2015). Auxin-regulated chromatin switch directs acquisition of flower primordium founder fate. *Elife* *4*.
- Xu, J., Hofhuis, H., Heidstra, R., Sauer, M., Friml, J., and Scheres, B. (2006). A molecular framework for plant regeneration. *Science* *311*, 385-388.
- Xue, J., Deng, Z., Huang, P., Huang, K., Benton, M.J., Cui, Y., Wang, D., Liu, J., Shen, B., Basinger, J.F., *et al.* (2016). Belowground rhizomes in paleosols: The hidden half of an Early Devonian vascular plant. *Proceedings of the National Academy of Sciences of the United States of America* *113*, 9451-9456.
- Yang, X., Lee, S., So, J.H., Dharmasiri, S., Dharmasiri, N., Ge, L., Jensen, C., Hangarter, R., Hobbie, L., and Estelle, M. (2004). The IAA1 protein is encoded by AXR5 and is a substrate of SCF(TIR1). *The Plant Journal* *40*, 772-782.
- Yi, K., Menand, B., Bell, E., and Dolan, L. (2010). A basic helix-loop-helix transcription factor controls cell growth and size in root hairs. *Nature Genetics* *42*, 264-267.
- Zhang, J., Kalkum, M., Yamamura, S., Chait, B.T., and Roeder, R.G. (2004). E protein silencing by the leukemogenic AML1-ETO fusion protein. *Science* *305*, 1286-1289.
- Zhang, J.Y., He, S.B., Li, L., and Yang, H.Q. (2014). Auxin inhibits stomatal development through MONOPTEROS repression of a mobile peptide gene STOMAGEN in mesophyll. *Proceedings of the National Academy of Sciences of the United States of America* *111*, E3015-3023.
- Zhang, X., Clarenz, O., Cokus, S., Bernatavichute, Y.V., Pellegrini, M., Goodrich, J., and Jacobsen, S.E. (2007). Whole-genome analysis of histone H3 lysine 27 trimethylation in *Arabidopsis*. *PLoS biology* *5*, e129.
- Zhao, Z., Andersen, S.U., Ljung, K., Dolezal, K., Miotk, A., Schultheiss, S.J., and Lohmann, J.U. (2010). Hormonal control of the shoot stem-cell niche. *Nature* *465*, 1089-1092.
- ZhiMing, Y., Bo, K., XiaoWei, H., ShaoLei, L., YouHuang, B., WoNa, D., Ming, C., HyungTaeg, C., and Ping, W. (2011). Root hair-specific expansins modulate root hair elongation in rice. *The Plant Journal* *66*, 725-734.
- Zhu, Y., Qian, W., and Hua, J. (2010). Temperature modulates plant defense responses through NB-LRR proteins. *PLoS pathogens* *6*, e1000844.

## 초 록

식물은 발달 및 환경 적응 과정에서 호르몬을 신호전달 물질로 이용한다. 옥신은 핵심 호르몬 중 하나로, 신호전달 과정을 통해 최종적으로 옥신 반응 유전자들의 전사를 조절한다. 옥신 신호전달은 단일 과정으로 구성되어 있다. 옥신은 전사억제인자의 분해를 유도하는데, SCF-복합체의 F-box 단백질에 그들을 부착시키는 풀처럼 이용된다. 그 결과 옥신 반응 유전자들의 전사가 촉진된다. 신호전달 과정은 단순하지만, 옥신은 다양한 범위에 걸쳐 식물의 발달과 반응 과정에 관여한다. 즉, 옥신이 매개하는 다양한 발달과정에는 더욱 다양한 신호전달 메커니즘이 존재할 것이다. 각각의 옥신 신호전달 구성요소에는 다수의 기능적 유사체가 존재한다. 이번 연구의 목적은 신호전달 구성 요소들의 다양한 기능적 유사체와 옥신 반응의 다양성 및 세밀한 조절의 관계를 전사수준에서 검증하는 것이다.

본 연구에서는 옥신 신호전달 구성요소의 능력을 생물학적으로 정량 할 수 있는 단일 세포 시스템으로 애기장대 뿌리털을 채택하였다. 뿌리털은 뿌리의 표피세포에서 돌출되며, 뿌리털의 생장이 내부의 옥신 농도나 신호전달 정도와 비례하기 때문에, 옥신 신호전달과정을 확인할 수 있는 세포 자율적인 시스템이다. 게다가, 뿌리털 표현형은 눈에 쉽게 띄고 일차원적 성장을 하기 때문에 정량 하기 용이하다.

Auxin/Indole-Acetic Acids (Aux/IAAs)는 옥신 신호전달 과정의 주요 전사억제인자로 TOPLESS(TPL)/TPL-Related(TPR) 보조 전사억제인자를 Auxin Response Factor (ARF)로 불러들여서 옥신 반응 유전자의 전사를 억제한다. 그러나 옥신 반응을 지속적으로 억제할 것이라 여겨지는 aux/iaa 기능획득돌연변이에 의해 오히려 옥신 반응이 촉진되는 현상이 나타나는 경우가 있다. 본 연구의 첫 번째 주제는 이와 같은 옥신 신호전달 과정의 수수께끼를 해결하는 것이다. 본 연구에서는 Aux/IAA가 TPL/TPR과의 결합력에 따라 두 그룹으로 나뉘어짐을 밝혔다. 그리고 TPL/TPR과 결합력이 낮은 Aux/IAA는 양적 변화를 통해 타겟 유전자 주변의 TPL/TPR 밀도를 변화시키는, 일시적으로 전사억제인자에서 전사촉진인자로 역할이 변환될 수 있음을 밝혔다. 이 연구는 전사억제인자의 양-의존성(dose-dependent) 전사조절능력 전환이라는 독특한 전사조절 모델을 제안한다. Aux/IAA의 양-의존성 행동은 옥신 반응과 옥신 반응 전사조절을 섬세하게 조절하는데 기여할 것이다.

ARF는 DNA에 결합하는 전사조절인자로 activator (aARF)와 repressor (rARF)로 나뉘어진다. 현재 알려진 옥신 신호전달 과정과 규명되어 있는 aARF의 역할이 잘 부합하는 반면, rARF의 메커니즘은 명확하지 않다. 두번째 파트에서는 rARF (ARF2)에 존재하는 예상 TPL/TPR 결합 모티브의 분자적, 생물학적 역할을 규명한다. ARF2의 두 TPL/TPR 결합 모티브는 TPL/TPR과의 결합에 필요하고, 옥신 반

응에서 ARF2의 기능에 필요함이 밝혀졌다.

비록 옥신이 뿌리털 생장에 관여하지만, 그 분자메커니즘은 아직 드러나지 않은 부분이 있다. 세번째 파트에서는 aARF가 어떻게 직접적으로 그리고 협력적으로 뿌리털 발달 핵심 전사조절인자에 관여하는지 확인한다. 본인이 속한 실험실은 이전 연구에서 뿌리털 특이적 유전자의 발현을 직접 조절하고 뿌리털 생장 및 형태 형성에 연관 있는 ROOT HAIR DEFECTIVE SIX-LIKE 4 (RSL4)를 규명하였다. 여기에서는 aARF가 *RSL4* 프로모터의 auxin-response elements (AREs)에 직접 결합하고, 발달과정 상 *RSL4*의 상위 전자조절인자인 RHD6와 협력하여 뿌리털 생장을 촉진하는 것을 밝혔다.

뿌리털은 유용한 모델 시스템으로 세포 운명 결정, 형태 형성, 극성 생장, 그리고 영양 흡수의 연구에 이용되었다. 그러나 뿌리털의 생태학적인 또는 물리적인 역할은 연구가 부족하다. 뿌리털이 물과 토양에 흡착함으로써 유식물의 생존에 관여하는 역할을 규명하기 위해, 뿌리털의 길이와 뿌리의 물리적 능력을 비교하였다. 뿌리의 물, 토양 흡착 능력 및 유식물의 생존률은 뿌리털의 길이와 비례한다는 결과를 얻었고, 이것은 뿌리털이 뿌리의 토양 흡착과 수분 유지를 돕고, 토양 붕괴 상황에서 유식물의 생존에 기여한다는 것을 의미한다.

이상의 결과를 요약하면, 본인의 박사학위 논문은 옥신 신호전달 과정에서 전사억제인자의 독특한 전사조절 메커니즘(양-의존적 전사 능

력 변환)과, 신호전달 요소(rARF)의 기능 규명, 뿌리털 발달에서 옥신의 분자메커니즘, 그리고 뿌리털의 생태적인 역할에 관하여 고찰하였다. 이 연구는 단순히 옥신 신호전달 과정뿐만 아니라 일반적인 전사조절 연구에서도 유전자 발현 조절의 이해 범위를 확장시키고, 또한, 식물 주변의 물리적 환경 속에서 뿌리털 역할에 관한 새로운 관점 생성에 도움이 될 것으로 기대된다.

주요어: 단백질 상호작용, 뿌리털, 에기장대, 옥신, 옥신 신호전달, 전사 조절, 전사조절인자, Auxin/Indole-Acetic Acid (Aux/IAA), Auxin Response Factor (ARF)

학번: 2010-23127